TRANSMISSION AND RADIATION OF ELECTROMAGNETIC WAVES

IN HOLLOW-PIPES AND HORNS

by

LAN JEN CHU

B.S., Chiao Tung University
1934

S.M., Massachusetts Institute of Technology
1935

SUBMITTED IN PARTIAL FULFILLMENT OF THE
REQUIREMENTS FOR THE DEGREE OF

DOCTOR OF SCIENCE

from the
MASSACHUSETTS INSTITUTE OF TECHNOLOGY
1938

Signature of Author _____

Department of Electrical Engineering, January 10, 1938.

Signature of Professor
in Charge of Research _

Signature of Chairman of Department
Committee on Graduate Students

ACKNOWLEDGMENTS

TABLE OF CONTENTS

I. INTRODUCTION

The application of electromagnetic wave theory to engineering problems involving low frequencies and the frequencies used in radio communition has been in an advanced stage for some time. Such theory has not been applied as frequently to problems involving the ultra-high-frequencies. Particularly in the last few years, following the advancement of technique in the generation and application of the ultra-high-frequency waves, the problems concerning transmission, radiation and circuits have been actively studied from a theoretical basis. One instance where an exact analysis on an electromagnetic basis has been very valuable is the case of transmission inside of conducting pipes.

The pioneer paper in this field was published by Lord Rayleigh in 1897. In this paper[1], he discussed the possibility of transmiting electromagnetic waves of sufficiently high frequency inside a perfectly conducting uniform tube of either circular or rectangular cross-section. He discovered that theoretically two types of waves may exist inside tubes of any cross-section, one without

---

[1]Lord Rayleigh: "Scientific Papers" Vol. IV pp227-280
   (1897)

the longitudinal component of magnetic field, and the other
without the longitudinal component of electric field. Inci-
dently, he determined the critical frequencies for waves
inside ideal non-dissipative tubes of circular and
rectangular cross section, ie., the frequencies below
which they cannot exist. In 1898, R. C. Maclaurin[1] obtained
the natural frequencies of oscillation for tubes of
elliptical cross section, but he did not treat the case
of transmitted waves. In the years that follows, very
little can be found in the literature that related to this
problem, until 1910, when Hondros and Debye[2] described
theoretically the transmission of electromagnetic waves
along a dielectric wire. A recent paper by Schelkunoff[3]
is confined to problems associated with coaxial conductors
which is still another type of system.

The recent interest in the transmission of Ultra-
high-frequency electromagnetic waves inside hollow conducting
pipes started apparently with papers by W. L. Barrow[4] of
M. I. T. and by G. C. Southworth[5], J. R. Carson, S. P. Mead,
and S. A. Schelkunoff[6] of the Bell Telephone Laboratories.

[1]R.C.Maclaurin, Cambridge Philosophical Transactions,
 Vol. XVII, Part I, pp. 5-100, (1898).
[2]D.Hondros and P.Debye, Ann. d. Phys. Vol.32, pp. 465-476,
 (1910)
[3]S.A.Schelkunoff, Bell Sys. Tech. Jour. Vol. 13, p. 533
(1934)
[4]W.L.Barrow, Proc. I.R.E. Vol. 24, No. 10, pp.1298-1328,
 (1936)
[5]G.C.Southworth, Bell Sys. Tech. Jour. Vol. 15, pp. 284-309,
 (1936)
[6]J.R.Carson, S.P.Mead, and S.A.Schelkunoff, Bell Sys. Tech.
 Jour. Vol. 15, pp. 310-333. (1936).

In these papers, special attention was given to pipes made of finitely conducting materials filled with low-dissipative dielectrics such as air or vacuum.

The pipe they considered has a circular cross section. The wave, generated by an antenna placed at one end of the pipe or by some other means of excitation, propagates along the pipe. If the conductor had an infinitely high conductivity, the waves would confine themselves within the dielectric and no energy could be absorbed by the conductor. Otherwise, the absorption of energy by the conductor causes the attenuation of the wave. It has been reported that the phase velocity of the waves inside the circular pipe is greater than the light velocity and the attenuation of one type of the waves decreases with increasing frequency. Both phenomena are quite extraordinary to the ordinary experience of guided waves.

After the presentation of the above three papers, Léon Brillouin immediately published a paper[1], in which he studied the problem from an entirely different angle, giving a clear physical picture of the nature of the waves inside a non-dissipative pipe of rectangular cross-section. The waves are constructed by projecting the ordinary plane waves into a rectangular pipe at an appropriate angle with respect

---

[1] Léon Brillouin, Revue Generale de E'lectricité, Vol.XL
pp 227-239. (1936)

to the axis of the pipe. The multiple reflections, caused by the four perfectly conducting walls, transform the plane wave into a composite wave which acts like a standing wave in the transverse direction and like a traveling wave in the longitudinal direction. That the original wave does not travel in the axial direction explains the phenomenon of the increasing of phase velocity of the wave in the pipes as compared to their free-space velocity. He also tried to explain the peculiar behavior of the attenuation for the afore-mentioned type of wave by pointing out that waves possessing this property can only exist inside the tubes having perfect symmetrical cross-section like a circle or a square. This, however, does not seem to be so.

Following Brillouin's paper, L. Page and N. I. Adams Jr.[1] mathematically constructed the waves in circular pipes from plane waves by a similar method as for the rectangular pipe. The last paper on this subject appeared on the November 1937 issue of the Proceedings of the Institute of Radio Engineers, by S. A. Schelkunoff[2]. In this paper, he presented a general theory of hollow-pipe waves including the attenuation, and as a special example, treated the rectangular pipe in detail.

The radiation of electromagnetic waves from the

---

[1]L.Page and N.I.Adams Jr., Phy. Rev. Vol. 52, pp. 647-651 (1937)
[2]S.A.Schelkunoff, Proc. I.R.E. Vol.25, pp. 1457-1493. (1937)

open end of a hollow pipe or from a horn goes hand-in-hand with the hollow-pipe transmission problem. Bergmann and Kruegel[1] reported in 1934, the experiment of measuring the radiation from the open end of a very short hollow metal cylinder in which a half-wave coaxial antenna was properly excited. Schelkunoff[2], in his paper titled"Some Equivalent Theorems of Electromagnetics and their Application to Radiation Problems", calculated the radiation loss from the open end of a coxial tube. No papers dealing with the electromagnetic horns are known to exist, although their use for directive radiation has been suggested in several papers in the last two years.

My work during the past year and a half, has concerned mainly for aspects of these problems, namely: (1) the transmission characteristics of waves in rectangular pipes; (2) the transmission characteristics of waves in elliptical pipes; (3) the radiation from the open end of rectangular pipes; and (4) the transmission and radiation characteristic of a special type of the electromagnetic horn. The natures and the backgrounds of the problems and the results obtained during my research are summarized as follows.

In the fall of 1936, Professor Barrow, after he has concluded his research on transmission of waves in

---

[1]Bergmann and Kruegel, Ann. der Phys. Vol. 21, pp113-138. (1934)
[2]S.A.Schelkunoff, Bell Sys. Tech. Jour. Vol.15,pp. 92-112 (1936)

circular pipes, turned to the study of rectangular pipes.
Some of his work will be summarized at the begining of
the second chapter. I took over the problem and tried to
calculate the attenuations of waves in the finitely con-
ducting rectangular pipe as a boundary-value preblem.
Difficulty was encountered in trying to find a wave fun-
ction which would represent the fields inside the metal,
on account of the discontinuity of curvature at the four
corners of the rectangular pipe. The possibility of
resolving the waves in a rectangular pipe into ordinary
plane waves, as suggested by Brillouin, inspired the idea
that the problem might be treated in a way similar to the
reflection of light by an imperfect reflector. In this
respect, A. Sommerfeld[1] has treated the problem of travel-
ing electromagnetic waves along a finitely conducting sur-
face. In our problem it was found that the best way of
presentation was probably to resolve the waves inside a rec-
tangular pipe into waves which exist between two parallel con-
ducting surfaces of infinitely large area. In the Appendix,
the solution of waves between two parallel and finitely con-
ducting surfaces is given. The attenuation and the loss in
the conductor were calculated under the assumption of a rea-
sonably high conductivity ($|\sigma| >> |\omega \varepsilon|$), a condition usually
satisfied in practical problems. In Chapter II, the attenua-

---

[1]P.Frank and R.Mises, die Differential und Integralgleichun-
gen. pp 876. (1935)

tions of waves in a rectangular pipe are calculated by uti-
liaing the results obtained in the Appendix. Comparisons
are made for a given wave inside pipes of different ratios
of dimensions but of equal peripheries; and also for dif-
ferent waves in a square pipe and a circular pipe of equal
peripheries. None of the waves in a rectangular pipe pos-
sesses the peculiar characteristic of attenuation which
decreases with increasing frequency, except for the degen-
erate rectangular pipe which results when one of the trans-
verse dimensions is extended to infinity.

A   circular pipe is a degenerate form of
the pipes of elliptical cross-section. In order to study
the effects of deformation of the circular cross-section
on the properties, especially the attenuation,of the waves
in a circular pipe, the waves in the elliptical pipes were
studied. Maclaurin has treated the problem of standing-
waves in an ideally conducting elliptical pipe. Of course,
this solution is not exactly of the same nature as the
present problem which deals with traveling waves. The
treatment of waves in elliptical pipes required the use
of elliptical coordinates. The solutions of the wave
equation in elliptical coordinates are the Mathieu fun-
ctions. For the non-dissipative case, the general expres-
sions for the fields in the dielectric, the phase constants,
the critical frequencies and the other constants for

various types of waves in the elliptical pipe, have been
obtained. I am much indebted to Prof. P. M. Morse for the
use of his "Tables of Mathieu Function", to calculate the
numerical values of critical frequencies and later on, the
attenuation constants. To calculate the attenuation of the
waves in elliptical pipes as a boundary-value problem, the
same difficulty occurs as in case of waves in rectangular pi-
pes, i.e., the choice of a proper wave function for the fields
in the conductor. This is overcome by using the asymptotic
forms of the Mathieu functions derived by Prof. J. A. Stratton[1].
The attenuation constants, thus obtained, are illustrated by
laborous numerical calculations, and comparisons are made for
various types of waves in elliptical pipes of different
eccentricities but equal peripheries. The transmission
characteristics, including the attenuation, for waves in a
circular pipe are partly duplicated here, as they represent a
degenerate case of an elliptical pipe, and comparisons are
made with the general cases. It is discovered in this
chapter that, so far attenuation is concerned, a circular
pipe is inferior to an elliptical pipe with small eccentricity
except for the waves whose fields have a circular symmetry in
the circular pipe. It is also discovered that no wave in
an elliptical pipe can have a decreasing attenuation with
increasing frequency. This exceptional attenuation can only

---

[1] J.A.Stratton, Proceedings of the National Academy of Sciences.
Vol.21,No.1,pp 51-62.(1935) Vol.21,No.6,pp 316-321.(1935)

occur when the pipe degenerates into a circular one.

As a conclusion to the work on hollow pipes, the anomalous phenomenon of the decreasing attenuation with increasing frequency is explained in terms of the absorption coefficient of metal and a general theorem is deduced. After the completion of the work cited above,S. A. Schelkunoff's paper appeared in the Proceedings of I. R. E. Although this paper represents a valuable contribution from the mathematical aspect, he failed to emphasize the most important type of wave in a rectangular pipe ———— the $H_{o,1}$-wave ———— for which, the attenuation was not even given. Very little effort has been made by him to clear up the question of the anomalous attenuation phenomenon reported by Carson, Mead and Schelkunoff in their first paper on hollow-pipe waves.

The theoretical work on the calculations of the radiation from the open end of rectangular pipes and horns has been collaborated with the experimental work on the same subjects carried on by Messrs. F. M. Green and F. D. Lewis under Prof. Barrow. In the calculations of the radiations from the open end of rectangular pipes, the waves inside the pipes are represented by the vector potentials. By means of Huygens' principle[1] the vector potentials, and consequently the fields too, in the outside space are calculated. Special attention is paid to the $H_{o,1}$-wave, which

---

[1]K.Försterling,"Lehrbuch der Optik" (1928)

has the electric field everywhere parallel inside the rectangular pipes and gives a single-beam directive pattern. In agreement with the experimental work and a rough theory, it is found that the sharpness of the beam depends upon the ratios of the linear demensions of the pipes to the wavelength. A sharper beam may be obtained by increasing the ratios. The effects of the high order $H_{o,m}$-waves (m = odd) in the pipe is studied. Other types of waves than the $H_{o,m}$-wave (m = odd), do not give single-beam radiation.

The horn that was actually studied, is, in a sense, an extension of a rectangular pipe, with the side walls only turned outward at a certain angle. Since the horizontal cross-section of the horn (Fig. 5.1) is a sector of a circle, we will call this the "Sectoral Horn". The measurements made during the last summer[1] on this shape of horn revealed amazingly good results. With the proper angle between the sides of the horn, the radiated energy can be concentrated within a very sharp beam. This horn may find an immediate application in ultra-high- frequency directive transmission, particularly to the blind landing of airplanes. Later mesaurements have shown that the rectangular pipe is not essential for proper functioning of the horn, as had been earlier suggested, and an antenna with a simple plane reflector or a parabolic reflector, properly shielded at the throat of the horn may serve equally well.

---

[1] F.M.Green, E.E.Thesis, M.I.T. (1937)

Most of the essentials of a rigorous treatment for the horn has been obtained by starting from Maxwell equations and using the proper boundary conditions. The problem is similar to the transmission of waves along a circular pipe. In the sectoral horn, the wave propagates in the radial direction, which is represented by the Bessel function of the third kind, i.e., the Hankel function. Only one type of wave, in which the electric fields are everywhere parallel to the divergent sides of the horn, has been analyzed. This wave can be most conveniently produced experimentally, and it alone has the possibility of radiating a single-beam pattern. Based upon the property of the Hankel functions, the transmission characteristics of waves inside a horn are determined. It is found that the waves are highly attenuated at the small end of the horn and are freely transmitted beyond a certain distance from the hypothetic center of the horn. The radiation patterns are calculated in a way similar to that used for the rectangular pipe, but more approximations must be imposed because of the difficulties of integration.

Units and Definitions.

A practical system of units will be used in which:

$\bar{E}$ = electric field intensity in volts per cm.

$\bar{H}$ = magnetic field intensity in amperes per cm^2.

σ = conductivity in mhos per cm.

μ = permeability in henrys per cm. (for air $\mu = \mu_o = 4\pi \times 10^{-9}$)

ζ = dielectric constant in farads per cm. (for air

$\zeta = \zeta_o = 10^{-11}/36\pi$)

The quantity $\bar{E}$ and $\bar{H}$ are real. For convenience in analysis, the complex field intensities E and H will be employed throughout, but it should be kept in mind that, in the end, the real part of E and H must be taken. Similarly the vector potential used here-after will be a complex quantity. The complex vector quantities are usually expressed in terms of their components, and the directional unit vectors of the coordinate system. The components are therefore complex scalar quantities and will be hereafter indicated by a subscript to denote the direction of the component. The conjugate of a complex quantity is denoted by a ∧ under the letter representing the quantity. For example, the conjugate of E_x is $E_{\wedge x}$.

In the treatment of electromagnetic waves, the Maxwell equations will be frequently used. Although they were originally derived for real quantities, they can also be used for complex quantities. The wave equations are usually derived vectorially from the Maxwell equations. Therefore, the wave equations for the component fields in curvilinear orthogonal coordinates, do not necessarily

have the same form. The wave constant k which appears in the wave equation is defined as $\sqrt{\omega^2 \varepsilon \mu - i\omega \mu \sigma}$. In a dielectric having negligible conductivity, the wave constant is simply equal to $\omega\sqrt{\varepsilon \mu}$. The constant $1/\sqrt{\varepsilon \mu}$ for air is equal to the light velocity in air, and for a dielectric having other values of ε and μ, it is equal to the light velocity in that medium. Hence it is convenient to let c represent the light velocity in that medium. The constant ω has its usual meaning and is equal to $2\pi f$. Sometimes, the frequency of a wave will be expressed in the equivalent form $f = \dfrac{c}{\lambda}$, and it will be sometimes convenient to speak of wave length alone. Unless otherwise specified, it will be understood that the wave length is to be measured in the dielectric considered. The following expressions are therefore identical:

$$k = \omega\sqrt{\varepsilon \mu} = \omega/c = 2\pi f/c = 2\pi/\lambda$$

and will be used interchangeably hereafter.

In calculating the attenuation of waves in pipes, the fields in the metal and the constants of the metal will also be encountered. In order to make the nomenclatures unique throughout the present work, we will use primed letters to indicate constants or functions in the metal and leave the unprimed letters exclusively for constants or functions in the dielectric. The wave constant in the metal is defined as $k' = \sqrt{-i\omega\mu'\sigma'}$

The electromagnetic waves in a sufficiently long non-dissipative hollow pipe can be classified into two main types. They have been defined in various ways according to the properties of the waves. The more exact one was given by Prof. Barrow as follows:

> "All waves that may be propagated within any hollow conducting pipe or tube will be called hollow- pipe waves."
>
> "Any hollow-pipe wave having both a longitudinal and a transverse component of magnetic field but only a transverse component of electric field will be called an H-wave."
>
> "Any hollow-pipe wave having both a longitudinal and a transverse component of electric field but only a transverse component of magnetic field will be called E-wave."

If the wall of a pipe is finitely conducting, it is sometimes misleading to consider that one of the longitudinal fields may be set arbitrarily to zero, since the finiteness of the conductivity requires different boundary conditions. The difficulties of the mathematics obscure the actual situation in the pipe. However, if the conductivity of the conducting wall is very large but finite, the electromagnetic waves inside a dissipative pipe may be considered as either a modified H-wave or a modified E-wave. The following definitions will introduce the correct idea when we discuss the attenuations of the hollow-pipe waves.

> An H-wave or an E-wave in a slightly dissipative hollow-pipe is one which would degenerate into the H-wave or the E-wave respectively in a non-dissipative hollow-pipe, were the conductivity to approach infinity as a limit.

Inside a straight hollow-pipe of sufficiently great length, the waves propagate along the longitudinal or axial direction. Let the X-axis be in the axial direction of the pipe and consider only the waves having simple sinusoidal time variation. The propagation of the waves along the axial direction may be described by the factor $e^{i\omega t - hx}$, where h is the propagation constant. By substituting this factor into the Maxwell or the wave equations, they are reduced to the partial differential equations of the two remaining coordinates, and the factor $e^{i\omega t - hx}$ remains as a constant in these equations.

For a non-dissipative pipe, the propagation constant h is zero when the frequency is equal to a critical value. Below that frequency, the propagation constant is a real quantity. This frequency is defined as the critical frequency, and the corresponding wave length λ and wave constant k are defined as the critical wave length and the critical wave constant of the wave respectively, and they will be denoted by a subscript "$_o$".

The transmission and radiation of electromagnetic waves of ultra-high-frequency by means of the horns is but little explored, and their general properties are still to be determined. In the Chapter V only one type of wave in a particular shape of horn has been investigated. The horn is named the "sectoral horn" on account of its geometrical shape, which resembles a sector slice of a cylinder.

Inside the horn, two types of waves may exist, one without the
radial component of electric field and the other without the
radial component of magnetic field. Only the first type has
been preliminarily investigated. Another condition has been
imposed that the waves are independent of the coordinate y of
cylindrical coordinate system $(r, \emptyset, y)$, r being the direction
of transmission. This type of wave will be refered in the
text as "horn waves".

II TRANSMISSION CHARACTERISTICS

OF WAVES IN RECTANGULAR PIPE

The transmission characteristic of waves inside a non-dissipative pipe of rectangular cross-section have been studied by various authors. In the present work, it is intended to study the transmission characteristic, principally the attenuation of dissipative rectangular pipes. A summary of the results of non-dissipative pipe is given here with the courtesy of Prof. W. L. Barrow[1].

Non-dissipative Case——Summary.

In Fig. 2.1, a section of a rectangular pipe is shown. The X-axis of the Cartesian coordinates (x,y,z) is chosen to coincide with one of inner corners of the pipe. Thus the dielectric is bounded by conducting walls, $y = 0$, $y = a$, $z = 0$ and $z = b$. The pipe is sufficiently long that the end effects may be neglected. The conductivity of the conducting walls is assumed infinity for the present, and the dielectric,which fills the inside, is assumed to be a perfect insulator.

---

[1] A paper titled "Electromagnetic Waves in Hollow Metal Tubes of Rectangular Cross Section" jointly by W.L.Barrow and L.J.Chu was sent to the Institute of Radio Engineering for consideration for publication in their Journal.
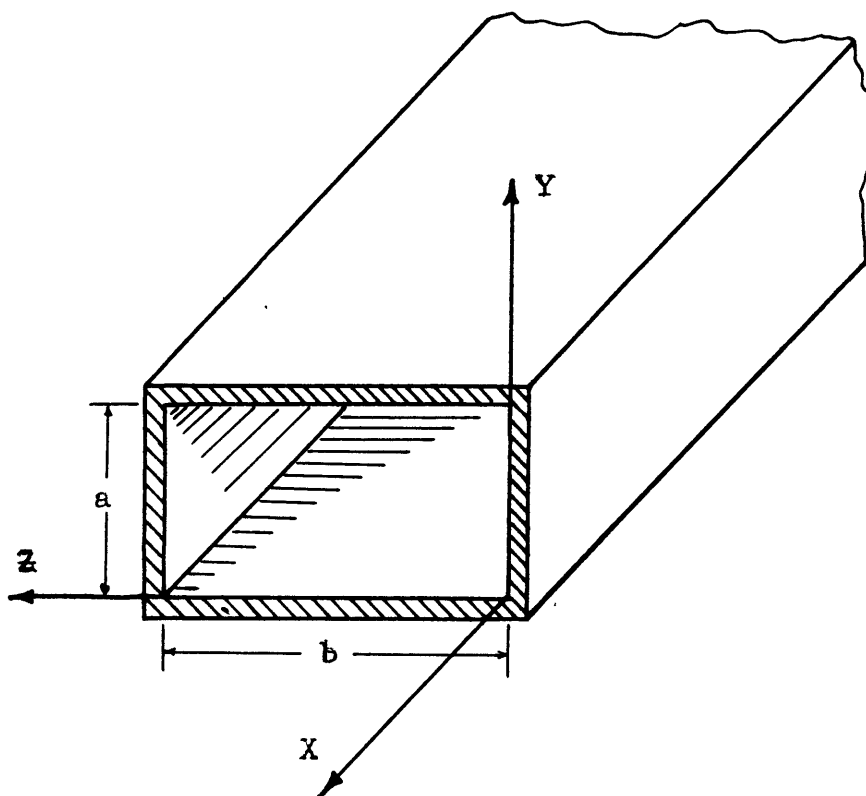
Fig. 2.1

Two types of waves may exist inside such a non-dissipative pipe. The H-waves have only transverse electric intensity and both longitudinal and transverse components of magnetic intensity. The E-waves have only transverse magnetic intensity and both longitudinal and transverse components of electric intensity.

The double subscripts n,m are used to denote the order of harmonics of the waves along the two linear dimensions (y and z) in the cross-section of the pipe. All the waves are assumed to propagate in the positive x direction and to have a sinusoidal time variation. Therefore the variation in X-axis and also the time variation can be discribed by the exponential factor $e^{i\omega t - i\beta x}$

The fields of the $H_{n,m}$-waves in the dielectric are following:

$$H_x = B \cos\left(\frac{n\pi}{a} y\right) \cos\left(\frac{m\pi}{b} z\right) e^{i(\omega t - \beta x)}$$

$$H_y = B \frac{i\beta}{K_0^2} \cdot \frac{n\pi}{a} \sin\left(\frac{n\pi}{a} y\right) \cos\left(\frac{m\pi}{b} z\right) e^{i(\omega t - \beta x)}$$

$$H_z = B \frac{i\beta}{K_0^2} \cdot \frac{m\pi}{b} \cos\left(\frac{n\pi}{a} y\right) \sin\left(\frac{m\pi}{b} z\right) e^{i(\omega t - \beta x)}$$

2.1

$$E_y = B \frac{i\omega\mu}{K_0^2} \cdot \frac{m\pi}{b} \cos\left(\frac{n\pi}{a} y\right) \sin\left(\frac{m\pi}{b} z\right) e^{i(\omega t - \beta x)}$$

$$E_z = -B \frac{i\omega\mu}{K_0^2} \cdot \frac{n\pi}{a} \sin\left(\frac{n\pi}{a} y\right) \cos\left(\frac{m\pi}{b} z\right) e^{i(\omega t - \beta x)}$$

$$E_x = 0$$

where $\qquad \kappa_o^2 = \kappa^2 - \beta^2 = \left(\frac{n\pi}{a}\right)^2 + \left(\frac{m\pi}{b}\right)^2 = \left(\frac{\omega_o}{c}\right)^2$ $\qquad$ 2.2

k_o is defined as the critical wave constant.

All combinations of n and m are possible except the one, n = m = 0 . The $H_{o,o}$-wave has only a transverse component of magnetic intensity H_x, which of course has no physical meaning. For n = 0, the $H_{o,m}$-waves have only these components of fields, H_x, H_z and E_y:

$$H_x = B \qquad \cos\left(\frac{m\pi}{b}z\right) e^{i(\omega t - \beta x)}$$

$$H_z = B \frac{i\beta}{m\pi/b} \sin\left(\frac{m\pi}{b}z\right) e^{i(\omega t - \beta x)} \qquad 2.3$$

$$E_y = B \frac{i\omega\mu}{m\pi/b} \sin\left(\frac{m\pi}{b}z\right) e^{i(\omega t - \beta x)}.$$

The vector electric intensity of the $H_{o,m}$-wave is every where parallel to the Y-axis. All the fields are independent of the variable y.

The field expressions of the $E_{n,m}$-waves are as following:

$$E_x = B \qquad \sin\left(\frac{n\pi}{a}y\right)\sin\left(\frac{m\pi}{b}z\right) e^{i(\omega t - \beta x)}$$

$$E_y = -B \frac{i\beta}{\kappa_o^2}\frac{n\pi}{a} \cos\left(\frac{n\pi}{a}y\right)\sin\left(\frac{m\pi}{b}z\right) e^{i(\omega t - \beta x)}$$

$$E_z = -B \frac{i\beta}{\kappa_o^2}\frac{m\pi}{b} \sin\left(\frac{n\pi}{a}y\right)\cos\left(\frac{m\pi}{b}z\right) e^{i(\omega t - \beta x)} \qquad 2.4$$

$$H_y = B \frac{i\omega\varepsilon}{\kappa_o^2}\frac{m\pi}{b} \sin\left(\frac{n\pi}{a}y\right)\cos\left(\frac{m\pi}{b}z\right) e^{i(\omega t - \beta x)}$$

$$H_z = -B \frac{i\omega\varepsilon}{\kappa_o^2}\frac{n\pi}{a} \cos\left(\frac{n\pi}{a}y\right)\sin\left(\frac{m\pi}{b}z\right) e^{i(\omega t - \beta x)}$$

$$H_x = 0$$

The $E_{n,m}$-wave with n or m or both equal zero is not possible since all the six components of fields vanish. Thus the lowest order of the $E_{n,m}$-wave is $E_{1,1}$-wave.

For all the waves in a rectangular pipe, the rôles of y and z are interchangable with appropriate changes of sign. The indices n,m have the physical significance that the fields have n half-periods of sinusoidal variation along Y-axis from 0 to a, and m half-periods of sinusoidal variation along Z-axis from 0 to b.

The expressions for the constants of the waves are the same for both the $H_{n,m}$-and the $E_{n,m}$-waves and are as follows:

Phase constant:

$$\beta = \sqrt{(\frac{\omega}{c})^2 - (\frac{n\pi}{a})^2 - (\frac{m\pi}{b})^2} = \frac{\omega}{c}\sqrt{1 - (\frac{f_o}{f})^2}. \qquad 2.5a$$

Critical frequency:

$$f_o = \frac{c}{2}\sqrt{(\frac{n}{a})^2 + (\frac{m}{b})^2}. \qquad 2.5b$$

Critical wave length:

$$\lambda_o = 2\left[(\frac{n}{a})^2 + (\frac{m}{b})^2\right]^{-\frac{1}{2}}. \qquad 2.5c$$

Wave length in pipe:

$$\lambda = 2\pi/\beta. \qquad 2.5d$$

Phase velocity:

$$V_p = \omega/\beta .$$

2.5e

Group velocity:

$$V_g = 1 \Big/ \frac{d\beta}{d\omega} = \frac{\beta c}{\omega} .$$

2.5f

The field distribution diagrams may be calculated by a procedure similar to that used for circular pipe[1]. The differential equations for the lines of constant H and constant E can be solved since they involve only sine or cosine funtions. In Fig. 2.2 the field distributions of $H_{o,1}$-, $H_{1,1}$ - and $E_{1,1}$ -waves in a square pipe are plotted. We must remember that three dimensional fields can not be represented by a two dimensional diagram. Thus in the transversal cross-sectional view of the $H_{1,1}$ -wave, the electric lines, which have only transversal components, end normally on the conducting walls, while the magnetic lines, which have both longitudinal and transversal components end irregularly nearly the corner, where the magnetic lines seem apparently crowded. Actually the magnetic lines near the corner turn gradually into the x dimension. There seems no means to represent the magnitude of the magnetic fields by the concentration of the lines.
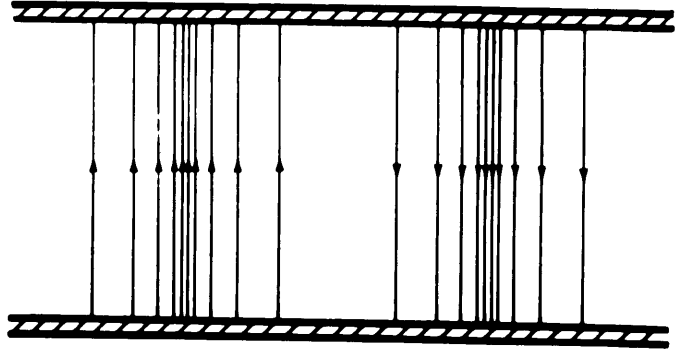

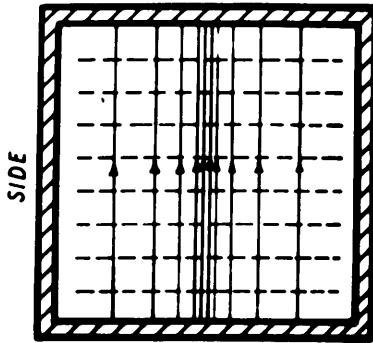[1] W. L. Barrow, Proc. I.R.E., Vol. 24, pp.1298-1329,(1936)
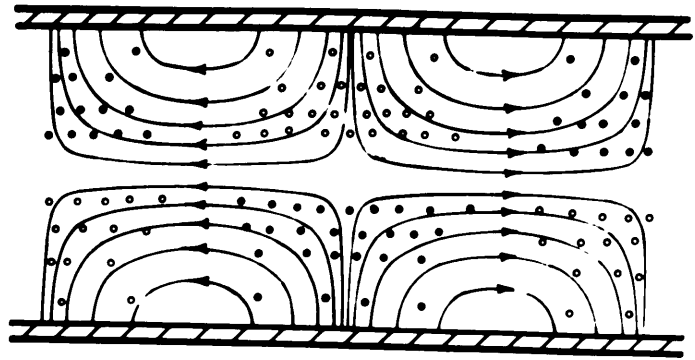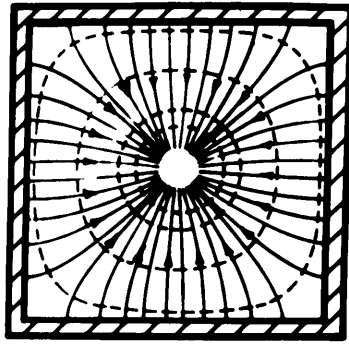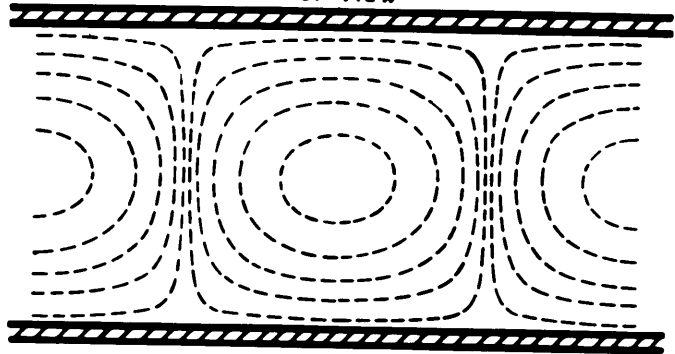
E₁,₁- wave

H₀,₁- wave

SIDE VIEW

TOP

SIDE

—— ELECTRIC INTENSITY
--- MAGNETIC INTENSITY

TOP VIEW

H₁,₁- wave

TOP VIEW ON SECTION a-a'

a ———— a'
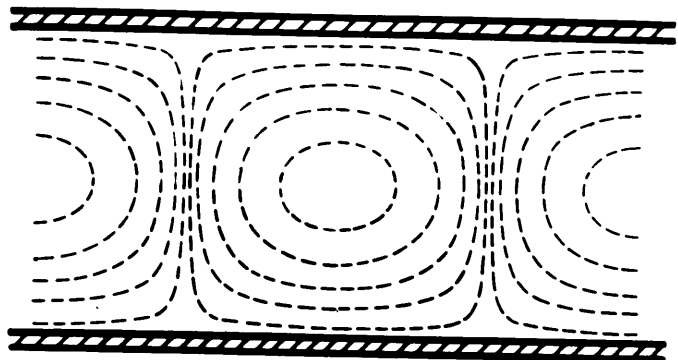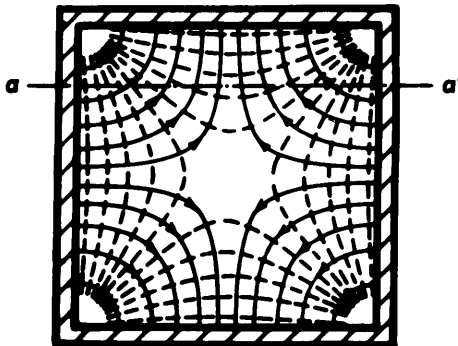
Fig. 2.2

Dissipative Case ―― General Considerations.

While the waves inside a nondissipative rectangular pipe have simple analytic solution, there is doubt whether the problem of a dissipative rectangular pipe has a rigorous mathematic solution or not. In a dissipative pipe, the waves no longer confine themselves to the dielectric. The conductor is no longer a perfect reflector and absorbs energy. There seems no mathematical solution that may take care of the discontinuity of curvature at the four corners. Therefore, we have to use the approximate perturbation method, based upon some assumptions which are justified within the practical range of frequency and conductivity. The method will be explained in the following pages.

The principal task is to calculate the attenuation constant of the waves. For a pipe made of a conductor of finite conductivity filled with a dissipative dielectric, the attenuation constant may be assumed to consisted of two terms, one caused by the conductor and the other by the dielectric. Therefore, we shall be able to treat them separately. The attenuation caused by the conductor will be treated first.

In Appendix , we have solved the attenuation of waves between two parallel conducting planes in a rigorous straight forward manner. We may consider it as a degenerate

case of the rectangular pipe waves, with the dimension a
extended to infinity in both directions. There is no ques-
tion of the soundness of the solution. Therefore we may
pickup a few facts from there, which will be useful to
make assumptions in calculation the attenuation of waves
in rectangular pipe.

First, the waves do not penetrate any consider-
able distance into the conductor. The propagation constant
of waves inside the metal in the direction normal to the
boundary is r'_g

$$r'_g = \sqrt{i \omega \mu' \sigma'} = \sqrt{\pi f \mu' \sigma'} + i \sqrt{\pi f \mu' \sigma'} .$$

Its real part is the attenuation constant in that direc-
tion. With commercial coper and at a frequency of 3×10^9
c.p.s. ($\lambda = 1$ m), the attenuation constant is 8300 nepers
per cm. That is to say, the field intensity drops to
0.1% within a distance of .0008cm. For a pipe of practical
dimension, the effect of the discontinuity of the curvature
at the four corners extends to only a negligible distance
from the corners as compared with the periphery of the pipe.
Therefore, this effect can be neglected.

Second, the finite but large conductivity of the
conducting wall does not distort appreciably the field dis-
tribution within the dielectric. The constant r_g, which
controls the distribution in tranverse direction, appears
in Eq. A.12 and A.26b as a complex number with an imaginary

part of insignificant magnitude. If again we use commer-
cial copper as the conductor, at a wave length of one meter
or less, the maximum possible distorsion of field from the
the fields of the non-dissipative case is not more than
0.1%.

The pipe now considered is the same as shown
in Fig. 2.1. The conductor has a finite conductivity
and the dielectric is assumed to be a perfect insulator.
The walls are so thick that no energy may exist at the
outer surface. The waves in the dielectric, strictly speak-
ing, do not have the form of either the H- or E-wave as
previously defined. We are not able to impose again the
condition that one of the longitudinal components of field
intensity identically vanishes everywhere inside the pipe,
since the boundary conditions do not permit so, except
in some special cases. We will find it convenient to define
an H- or E-wave of a dissipative pipe as one, which would
degenerate into the H- or E-wave of non-dissipative pipe, were
the conductivity of the conducting walls to be increased
indefinitely.

It has been an established fact that the waves
inside a non-dissipative rectangular pipe may be resolved
into ordinary planes waves with conjugate directions of
propagation[1]. It is from this idea that we are able to

[1] Léon Brillouin: Revue Generale de E'lectricité Vol. XL,
1936 pp 227-239.
L. Page and N.I.Adams,Jr. Physical Review, Vol. 52, 1937
pp 647-651.

calculate the attenuation of waves inside a dissipative
rectangular pipe as a boundary problem. However, we may
find it more convenient to resolve the waves inside a non-
dissipative rectangular pipe into components of parallel-
plane waves, which exist between two parallel conducting plan-
es as discussed in the Appendix.

The attenuation constant is equal to half the
ratio of power loss per unit length of the pipe to the power
transmitted through the pipe. If the field inside the pipe
is not appreciably distorted by the finite conductivity of
the metal, the power transmitted is just the summation of
the longitudinal Poynting's vector calculated from the field
expressions of a non-dissipative pipe.

To calculate the loss, we start also with the
non-dissipative field expressions, and see what would be
the loss, were the pipe dissipative, but not sufficiently
so to disturb appreciably the field adjacent to the wall.
The loss may be divided into two parts, (A) the loss
dissipated into the set of walls $z = 0$, b and (B) the
loss into the set of walls $y = 0$, a . To calculate (A)
the loss into the walls $z = 0$, b , we resolve the complete
field expressions in the non-dissipative rectangular pipe
into component parallel-plane waves between walls $z = 0$
and $z = b$. The effects of the two side walls are now
neglected. Each component wave would be modified in the
manner we discussed in the Appendix, if the walls $z = 0$

and $z = b$ were dissipative. This loss in the walls $z = 0, b$
can be calculated from Eq. A.17 and A.32. Similarly the loss
in the walls $y = 0$, a, may be calculated. The total loss
is the sum of loss of each component parallel-plane waves
between $z = 0$, b planes and $y = 0$, a planes.

It can be proven that the total losses into the
walls $z = 0$, b of the pipe is the sum of loss of each com-
ponent parallel plane waves as follows. The fields in a
non-dissipative rectangular pipe have a general form as below,

$$\frac{\cos}{\sin}\left(\frac{n\pi}{a}y\right)\frac{\cos}{\sin}\left(\frac{m\pi}{b}z\right)e^{i(\omega t - \beta x)} .$$

By spliting the sine or cosine of y into exponentials, the
fields expressions separate into two groups (G_1 and G_2),
one having the exponential $e^{i(\omega t - \beta x + \frac{n\pi}{a}y)}$ and the other
having the exponential $e^{i(\omega t - \beta x - \frac{n\pi}{a}y)}$. In each group, we may
replace x and y by new coordinates x' and y' such that the
fields are independent of y'. According to Eq. A.1 and
A.2, the fields of each group fall into two subgroups, one
having $E_{y'}$, $H_{x'}$ and H_z (H_g-wave) and the other having
$H_{y'}$, $E_{x'}$ and E_z (E_g-wave). These two subgroups have abso-
lutely no interaction between them at the boundary, since
the magnetic field of one is always parallel to the elec-
tric field of the other.

There is interaction between the two groups,
(G_1 abd G_2). Suppose we take a component of electric field
of G_1 tangential to the boundary surface

$$K_1 \, e^{i\omega t \, - \, i\beta x \, - \, i\frac{n\pi}{a}y}$$

and a component of magnetic field of G_2 also tangential to the boundary surface

$$K_2 \, e^{i\omega t \, - \, i\beta x \, + \, i\frac{n\pi}{a}y} \qquad .$$

If the two are normal to each other, the power transmitted per unit area in the normal direction of the surface is half the conjugate product of the two:

$$\frac{1}{2} \, K_1 K_2 \, e^{i\frac{2n\pi}{a}y} \qquad \text{(real part)}.$$

That is, at any point y, there will be an interaction between the two groups. However, if we integrate the exponential from y = 0 to y = a, the result is zero. It proves that the average interaction between two groups is zero. Even if the factor $\frac{n\pi}{a}$ is modified by adding a small imaginary part to it, as it ought to be in the case of dissipative pipe, the integral of the exponential is still negligible as compared to unity.

The $H_{o,m}$-wave is a special case of the $H_{n,m}$-waves. Its attenuation can not be deduced from general formula of attenuation constant of the $H_{n,m}$-wave. Hence, we shall treat it separately.

Attenuation of $H_{o,m}$-wave in a Rectangular Pipe

The expressions for fields of the $H_{o,m}$-wave in the dielectric bounded by perfect conducting rectangular pipe are

given by Eq. 2.3 . The power loss dissipated into the walls, if they are finitely conductive may be divided into two parts: (A), the loss into the walls $z = 0$ and $z = b$ and (B), the loss into the wall $y = 0$ and $y = a$. The two will be treated separately.

(A) <u>Loss into walls $z = 0$ abd $z = b$</u>

Between the metallic walls $z = 0$ and $z = b$, the field expressions look exactly like Eq. A.36, the H_g-wave between the two non-dissipative conducting planes $z = 0$ and $z = d$, treated in the Appendix. The corresponding constants are tabulated below:

H_g-wave	$H_{0,m}$-waves between walls $z = 0$ and $z = b$
B_g	$B \dfrac{i\,\omega\mu}{m\pi/b}$
m	m
d	b
β_g	β

Were the pipe dissipative, there would be loss into the walls considered and the field would be distorted by the two side walls $y = 0$ and $y = a$. This effect of the side walls is of secondary order and will not be considered. The power loss per unit area of H_g-wave is given by Eq. A.17. Since the two waves behave exactly in the same way we may obtain the power loss of the $H_{0,m}$-wave per sq. cm. of the walls $z = 0$ and $z = b$, by substituting the constant into Eq. A.17. Multiplying it by an area 2a, we have the total loss (A)

per cm. length of the pipe.

$$\text{Loss (A)} = \left|B\right|^2 a \sqrt{\frac{\omega\mu'}{2\sigma}} \qquad \text{per cm length of the pipe}$$

$$2.6$$

(B) <u>Loss into walls y = 0 and y = a</u>

The fields of the $H_{o,m}$ -wave between the side walls y = 0 and y = a may be resolved into the form of parallel-plane wave by spliting the sine and cosine functions of z into exponentials as follows:

$$\cos\left(\frac{m\pi}{b}z\right) = \frac{1}{2}\left(e^{i\frac{m\pi}{b}z} + e^{-i\frac{m\pi}{b}z}\right)$$

$$\sin\left(\frac{m\pi}{b}z\right) = \frac{i}{2}\left(-e^{i\frac{m\pi}{b}z} + e^{-i\frac{m\pi}{b}z}\right).$$

Substituting them into Eq. 2.3, we may separate the Eq. 2.3 into two groups of expressions characterized by different exponentials as follows:

$$\text{Group 1.} \begin{cases} H_x = \dfrac{B}{2} \, e^{i\left(\omega t - \beta x - \frac{m\pi}{b}z\right)} \\[2mm] H_z = -\dfrac{B}{2}\dfrac{\beta b}{m\pi} \, e^{i\left(\omega t - \beta x - \frac{m\pi}{b}z\right)} \\[2mm] E_y = -\dfrac{B}{2}\dfrac{\omega\mu b}{m\pi} \, e^{i\left(\omega t - \beta x - \frac{m\pi}{b}z\right)} \end{cases} \quad 2.7a$$

$$\text{Group 2.} \begin{cases} H_x = \dfrac{B}{2} \, e^{i\left(\omega t - \beta x + \frac{m\pi}{b}z\right)} \\[2mm] H_z = \dfrac{B}{2}\dfrac{\beta b}{m\pi} \, e^{i\left(\omega t - \beta x + \frac{m\pi}{b}z\right)} \\[2mm] E_y = \dfrac{B}{2}\dfrac{\omega\mu b}{m\pi} \, e^{i\left(\omega t - \beta x + \frac{m\pi}{b}z\right)} \end{cases} \quad 2.7b$$

The first group travels in a direction normal to Y-axis with directional cosines

$$\cos \theta_x = \frac{\beta}{K} \quad , \quad \cos \theta_z = \frac{m\pi/b}{K} \qquad 2.8$$

where $K = \sqrt{\beta^2 + \left(\frac{m\pi}{b}\right)^2} = \frac{\omega}{c}$ for the $H_{0,m}$-wave

and the second group travels in a conjugate direction with respect to X-axis. Let us consider the group 1 first. Rotate the XZ-plane by an angle $-\theta_x$, so that the new X'-axis coincides with the direction of propagation:

$$x = x' \cos \theta_x - z' \sin \theta_x$$

$$z = x' \sin \theta_x + z' \cos \theta_x \qquad 2.9$$

Substituting these x and z in Eq. 2.7a, and resolving E_y, H_x and H_z into $E_{y'}$, $H_{x'}$ and $H_{z'}$, by means of Eq. 2.9, we find that

$$E_y = -B \frac{\omega\mu}{\frac{2m\pi}{b}} e^{i\left(\omega t - \frac{\omega}{c}x'\right)}$$

$$H_{x'} = 0 \qquad 2.10$$

$$H_{z'} = -B \frac{\omega\sqrt{\epsilon\mu}}{2 \frac{m\pi}{b}} e^{i\left(\omega t - \frac{\omega}{c}x'\right)}$$

These fields belong to a plane wave traveling in the x'-direction. Such a wave can only exist between the walls y = 0 and y = a when the conductor is perfectly conductive. When the conductor is finitely conductive, however, the electric field normal to the surface tends to tilt over

against or toward the direction of propagation by an infinitesimal complex angle. Thus, besides E_y and $H_{z'}$, there will be an $E_{x'}$ component which causes the power dissipation into the metal walls.

If we put m = 0 in Eq. A.37, we may see that the group 1 wave is just a special case of the E_g-wave for m = 0 , with equivalent constants tabulated below.

E_g-wave (m=0)	Group 1 of the $H_{o,m}$-wave
H_y	$H_{z'}$
E_z	$- E_y$
B_g	$- B\, \dfrac{k}{2\frac{m\pi}{b}}$
$\beta_g = \dfrac{\omega}{c}$	$\dfrac{\omega}{c}$

The power loss per sq. cm. is given by Eq. A.32. Substituting the equivalent constants of Group 1 of the $H_{o,m}$-wave and multiplying the result by the area 2b , we have the power loss per cm. length of the pipe into the walls y = 0 and y = a caused by the Group 1 of $H_{o,m}$-wave. Since the behavior of group 2 is exactly the same as that of group 1 , except for the direction of propagation, it must cause same amount of loss. Hence the total loss (B) per cm. of the pipe into the wall y = 0 and y = a is

$$\text{Loss (B)} = \frac{1}{2}\left| B \right|^2 \left(\frac{\omega b}{c m \pi} \right)^2 b \sqrt{\frac{\omega \mu}{2\sigma}} \qquad \text{per cm of the pipe.}$$

$$2.11$$

The total loss per cm. of the pipe is the sum
of (A) (Eq. 2.6) and (B) (Eq. 2.11)

$$ L = |B|^2 \sqrt{\frac{\omega\mu'}{2\sigma'}} \left[a + \frac{\omega^2 b^2}{2 c^2 m^2 \pi^2} \right]. $$

The power transmitted along the pipe in the X-
direction is equal to the integral over the cross-section of
the Poynting's vector in X-direction. Using the E_y and H_z
of Eq. 2. we have

$$ S = |B|^2 \frac{\omega\mu\beta a b^3}{4 (m\pi)^2}. $$

The attenuation constant of $H_{o,m}$-wave are there-
fore as following.

$$ \alpha = \frac{1}{2} \frac{L}{S} $$

$$ = \sqrt{\frac{2\pi\mu'\xi c}{\sigma'\mu}} \frac{\sqrt{m}}{b^{3/2}} \frac{(f_o/f)^{3/2} + \frac{b}{2a}(f/f_o)^{1/2}}{\sqrt{1 - (f_o/f)^2}} \quad \text{nepers per cm.} \quad 2.12 $$

Attenuation of $H_{n,m}$-wave in a Rectangular Pipe.

The fields of the $H_{n,m}$-wave in a non-dissipative
rectangular pipe are given by Eq. 2.1 . The power loss dissi-
pated into the metal, if the walls are finitely conductive
may be divided into two parts: (A) loss into the wall z=0
and z = b and (B) loss into the wall y = 0 and y = a.

(A) Loss into walls z = 0 and z = b

Between the walls z = 0 and z = b, x and y are

tangential to the boundary and z is normal to it. Expressing $\cos(\frac{n\pi}{a} y)$ and $\sin(\frac{n\pi}{a} y)$ in exponnential forms and substituting them into Eq. 2.1 , the latter may be split into two groups according to the exponentials. The expressions for the group 1 are:

$$H_x = \frac{B}{2} \cos\left(\frac{m\pi}{b} z\right) e^{i\left(\omega t - \beta x - \frac{n\pi}{a} y\right)}$$

$$H_y = -\frac{B}{2} \frac{\beta}{\kappa_o^2} \frac{n\pi}{a} \cos\left(\frac{m\pi}{b} z\right) e^{i\left(\omega t - \beta x - \frac{n\pi}{a} y\right)}$$

$$H_z = \frac{B}{2} \frac{i\beta}{\kappa_o^2} \frac{m\pi}{b} \sin\left(\frac{m\pi}{b} z\right) e^{i\left(\omega t - \beta x - \frac{n\pi}{a} y\right)}$$

Group 1

$$E_y = \frac{B}{2} \frac{i\omega\mu}{\kappa^2} \frac{m\pi}{b} \sin\left(\frac{m\pi}{b} z\right) e^{i\left(\omega t - \beta x - \frac{n\pi}{a} y\right)}$$

$$E_z = \frac{B}{2} \frac{\omega\mu}{\kappa^2} \frac{n\pi}{a} \cos\left(\frac{m\pi}{b} z\right) e^{i\left(\omega t - \beta x - \frac{n\pi}{a} y\right)}$$

$$E_x = 0$$

2.13

The expressions for the group 2 are the same as those of group 1 except for the replacing of $\frac{n\pi}{a}$ by $\frac{-n\pi}{a}$. The group 1 wave propagates parallel to the XY-plane, having the directional cosines

$$\cos\theta_x = \frac{\beta}{\sqrt{\beta^2 + \left(\frac{n\pi}{a}\right)^2}} \quad , \quad \cos\theta_y = \frac{n\pi/a}{\sqrt{\beta^2 + \left(\frac{n\pi}{a}\right)^2}} \qquad 2.14$$

and the group 2 wave travels in the conjugate direction with respect to X-axis. We shall consider the group 1 wave only.

Rotating the XY-plane through an angle $-\theta_x$ by using Eq. 2.9 into the new Cartesian coordinates (x', y' and z) such that the direction of propagation coincides with X'-axis, the component fields become

$$\text{Subgroup H} \begin{cases} E_{y'} = B_1 \qquad \sin\left(\frac{m\pi}{b}z\right) e^{i\left(\omega t - \sqrt{\beta^2 + \left(\frac{n\pi}{a}\right)^2}\, x'\right)} \\[3mm] H_{x'} = B_1 \frac{m\pi}{i\omega\mu b} \quad \cos\left(\frac{m\pi}{b}z\right) e^{i\left(\omega t - \sqrt{\beta^2 + \left(\frac{n\pi}{a}\right)^2}\, x'\right)} \qquad \text{2.15a} \\[3mm] H_z = B_1 \frac{\sqrt{\beta^2 + \left(\frac{n\pi}{a}\right)^2}}{\omega\mu} \sin\left(\frac{m\pi}{b}z\right) e^{i\left(\omega t - \sqrt{\beta^2 + \left(\frac{n\pi}{a}\right)^2}\, x'\right)} \end{cases}$$

$$\text{Subgroup E} \begin{cases} H_{y'} = B_2 \qquad \cos\left(\frac{m\pi}{b}z\right) e^{i\left(\omega t - \sqrt{\beta^2 + \left(\frac{n\pi}{a}\right)^2}\, x'\right)} \\[3mm] E_{x'} = B_2 \frac{m\pi}{i\omega\mu b} \quad \sin\left(\frac{m\pi}{b}z\right) e^{i\left(\omega t - \sqrt{\beta^2 + \left(\frac{n\pi}{a}\right)^2}\, x'\right)} \qquad \text{2.15b} \\[3mm] E_z = -B_2 \frac{\sqrt{\beta^2 + \left(\frac{n\pi}{a}\right)^2}}{\omega\epsilon} \cos\left(\frac{m\pi}{b}z\right) e^{i\left(\omega t - \sqrt{\beta^2 + \left(\frac{n\pi}{a}\right)^2}\, x'\right)} \end{cases}$$

where

$$B_1 = \frac{B}{2} \frac{i\omega\mu\beta\, m\pi/b}{\sqrt{\beta^2 + \left(\frac{n\pi}{a}\right)^2}\, K_0^2}$$

$$B_2 = -\frac{B}{2} \frac{n\pi/a \quad K^2}{\sqrt{\beta^2 + \left(\frac{n\pi}{a}\right)^2}\, K_0^2}$$

After the rotation of XY-plane, the fields become independent of the variable y'. It is shown in the Appendix that under such condition, the Maxwell Equations fall into two independent groups, defined as the H_g-wave and the E_g-waves. Thus, we may separate Eq. 2.15 into two subgroup as indicated. The subgroup H consists of three component fields, $E_{y'}$, $H_{x'}$ and H_z and the subgroup E consists of three other component fields $H_{y'}$, $E_{x'}$ and E_z.

Sub-group H

Comparing the Eq 2.15a with Eq. A.26, shows that the two are similar with the following corresponding terms:

H_g-wave	Subgroup H
B_g	B_1
β_g	$\sqrt{\beta^2 + (\frac{n\pi}{a})^2}$
$\frac{m\pi}{d}$	$\frac{m\pi}{b}$

Both waves are for non-dissipative case. If the walls are dissipative, the loss of the H_g-wave is given by Eq. A.17 . The power loss per cm. of pipe at the walls $z = 0$ and $z = b$ caused by the subgroup H of group 1 may be obtained by substituting the constants into Eq. A.17 and multiplying the results by the area 2a

$$= |B|^2 \frac{\beta^2 (\frac{m\pi}{b})^4 a}{4 \kappa_0^4 [\beta^2 + (\frac{n\pi}{a})^2]} \sqrt{\frac{\omega\mu'}{2\sigma'}} . \qquad 2.16$$

Sub-group -E

Except for the following tabulated constants, the subgroup -E-wave (Eq. 2.15b) and the E_g-wave (Eq. A.37) are identical.

E_g-wave	Subgroup E
B_g	B_1
β_g	$\sqrt{\beta^2 + (\frac{n\pi}{a})^2}$
$\frac{m\pi}{d}$	$\frac{m\pi}{b}$

Substituting the corresponding constants of subgroup E wave into Eq. A.32 and multiplying the result by the area 2a , we have the power loss per cm of pipe at walls $z = 0$

and z = b caused by the sub-group E is following.

$$= |B|^2 \frac{(\frac{n\pi}{a})^2 K^4 a}{4 K_o^4 [\beta^2 + (\frac{n\pi}{a})^2]} \sqrt{\frac{\omega\mu'}{2\sigma'}} \,.$$ 2.17

The total loss caused by group 1 is the sum of losses caused by the subgroup H and subgroup E. Since the group 2 wave differs from group 1 wave only in the direction of propagation and otherwise they are same, the group 2 wave must have the same amount of loss as group 1 wave. Hence the total loss (A) into the wall z = 0 and z = b is

$$= |B|^2 \frac{a}{2 K_o^4 [\beta^2 + (\frac{n\pi}{a})^2]} \sqrt{\frac{\omega\mu'}{2\sigma'}} \left[(\frac{n\pi}{a})^2 K^4 + \beta^2 (\frac{m\pi}{b})^4 \right]$$

$$= |B|^2 \frac{a}{2} \sqrt{\frac{\omega\mu'}{2\sigma'}} \left[1 + \frac{\beta^2}{K_o^4} (\frac{n\pi}{a})^2 \right] \,.$$ 2.18

(B) Loss into the wall y = 0 and y = a

By changing the constants n, m, a, and b of Eq. 2.18 into m, n, b and a respectively, we have the total power loss into the walls y = 0 and y = b

$$= |B|^2 \frac{b}{2} \sqrt{\frac{\omega\mu'}{2\sigma'}} \left[1 + \frac{\beta^2}{K_o^4} (\frac{n\pi}{a})^2 \right] \,.$$ 2.19

The total power loss into four walls per cm. of the pipe is

$$L = \frac{|B|^2}{2} \sqrt{\frac{\omega\mu'}{2\sigma'}} \left\{ a + b + \frac{\beta^2 \pi^2}{K_o^4} \left[\frac{n^2}{a} + \frac{m^2}{b} \right] \right\}$$

The power transmitted through the pipe is cal-
culated from the field expressions of non-dissipative pipe
(Eq. 2.1)

$$S = \frac{1}{2} \int_0^b \int_0^a \left[E_y \hat{H}_z - E_z \hat{H}_y \right] dy \, dz$$

$$= |B|^2 \frac{\omega\mu\, ab\beta}{8\, K_0^2}.$$

The attenuation constant of $H_{n,m}$-wave is

$$\alpha = \frac{1}{2} \frac{L}{S}$$

$$= \sqrt{\frac{2\pi\mu'\xi c}{\sigma'\mu}} \frac{\sqrt{m}}{b^{3/2}} \frac{\frac{b}{a}\left[1+(\frac{n}{m})^2\frac{b}{a}\right](\frac{f}{f_0})^{\frac{1}{2}} + \left[1+(\frac{n}{m})^2(\frac{b}{a})^3\right](\frac{f_0}{f})^{3/2}}{\left[1+(\frac{b}{a})^2(\frac{n}{m})^2\right]^{3/4} \sqrt{1-(f_0/f)^2}}.$$

$$2.20$$

For a square pipe and n = m

$$\alpha = \sqrt{\frac{2\pi\mu'\xi c}{\sigma'\mu}} \frac{\sqrt{m}}{b^{3/2}} 2^{\frac{1}{4}} \frac{(\frac{f}{f_0})^{\frac{1}{2}} + (\frac{f_0}{f})^{3/2}}{\sqrt{1-(f_0/f)^2}}.$$

nepers per cm.
2.21

Attenuation of the $E_{n,m}$-wave in Rectangular Pipe

The precedure for the calculation of attenua-
tion constant the $E_{n,m}$-wave is the same as that for the
$H_{n,m}$-wave. In the following, the results at various stages
will be given without detail explanation.

The field expressions for the $E_{n,m}$-wave are gi-
ven by Eq. 2.4 . Consider the loss into walls z = 0 and
z = b. By replacing the $\cos(\frac{n\pi}{a} y)$ and $\sin(\frac{n\pi}{a} y)$ by
exponentials and separating the fields into two groups
according to the exponentials, the fields of the group 1

wave are

$$E_x = B \frac{1}{2} \sin\left(\frac{m\pi}{b} z\right) e^{i\left(\omega t - \beta x - \frac{n\pi}{a} y\right)}$$

$$E_y = -B \frac{i\beta n\pi}{2K_0^2 a} \sin\left(\frac{m\pi}{b} z\right) e^{i\left(\omega t - \beta x - \frac{n\pi}{a} y\right)}$$

$$E_z = B \frac{\beta m\pi}{2K_0^2 b} \cos\left(\frac{m\pi}{b} z\right) e^{i\left(\omega t - \beta x - \frac{n\pi}{a} y\right)}$$

$$H_y = -B \frac{\omega \epsilon m\pi}{2K_0^2 b} \cos\left(\frac{m\pi}{b} z\right) e^{i\left(\omega t - \beta x - \frac{n\pi}{a} y\right)}$$

$$H_z = -B \frac{i\omega \epsilon n\pi}{2K_0^2 a} \sin\left(\frac{m\pi}{b} z\right) e^{i\left(\omega t - \beta x - \frac{n\pi}{a} y\right)}$$

$$H_x = 0$$

2.22

The field expressions of the group 2 wave are
the same except for the change of A and $\frac{n\pi}{a}$ into -A and
- $\frac{n\pi}{a}$. The group 1 wave travels in a direction parallel
to the z = 0 and z = b walls and with the directional co-
sines:

$$\cos \theta_x = \frac{\beta}{\sqrt{\beta^2 + \left(\frac{n\pi}{a}\right)^2}} \quad , \quad \cos \theta_y = \frac{n\pi/a}{\sqrt{\beta^2 + \left(\frac{n\pi}{a}\right)^2}} \quad 2.23$$

Rotate the XY-plane through an angle $-\theta_x$ so that the X'
axis is in the direction of propagation. The fields in the
new system of coordinates are

$$\text{Subgroup H} \begin{cases} E_{y'} = B_1 \sin\left(\frac{m\pi}{b} z\right) e^{i\left(\omega t - \sqrt{\beta^2 + \left(\frac{n\pi}{a}\right)^2}\, x'\right)} \\[2mm] H_{x'} = B_1 \frac{m\pi}{i\omega\mu b} \cos\left(\frac{m\pi}{b} z\right) e^{i\left(\omega t - \sqrt{\beta^2 + \left(\frac{n\pi}{a}\right)^2}\, x'\right)} \quad 2.24a \\[2mm] H_z = B_1 \frac{\sqrt{\beta^2 + \left(\frac{n\pi}{a}\right)^2}}{\omega\mu} \sin\left(\frac{m\pi}{b} z\right) e^{i\left(\omega t - \sqrt{\beta^2 + \left(\frac{n\pi}{a}\right)^2}\, x'\right)} \end{cases}$$

Subgroup E :

$$H_{y'} = B_2 \cos\left(\frac{m\pi}{b}z\right) e^{i\left(\omega t - \sqrt{\beta^2 + \left(\frac{n\pi}{a}\right)^2}\, x'\right)} \qquad 2.24b$$

$$E_{x'} = B_2 \frac{m\pi}{i\omega\varepsilon b} \sin\left(\frac{m\pi}{b}z\right) e^{i\left(\omega t - \sqrt{\beta^2 + \left(\frac{n\pi}{a}\right)^2}\, x'\right)}$$

$$E_z = -B_2 \frac{\sqrt{\beta^2 + \left(\frac{n\pi}{a}\right)^2}}{\omega\varepsilon} \cos\left(\frac{m\pi}{b}z\right) e^{i\left(\omega t - \sqrt{\beta^2 + \left(\frac{n\pi}{a}\right)^2}\, x'\right)}$$

where

$$B_1 = -\frac{B}{2} \frac{i K^2 n\pi}{\sqrt{\beta^2 + \left(\frac{n\pi}{a}\right)^2}\, K_o^2 a}$$

and

$$B_2 = -\frac{B}{2} \frac{\omega\varepsilon \beta m\pi}{\sqrt{\beta^2 + \left(\frac{n\pi}{a}\right)^2}\, K_o^2 b} \quad .$$

The fields are separated into two subgroups as indicated. By comparing the constants in above equations with those in Eq. A.36 abd A.27 , the total power loss for Group 1 may be determined by means of Eq A.32 and subsequent summations. The group 2 wave causes exactly the same amount of loss. Thus,

Total loss/cm. of pipe on walls z = 0 and z = b is

$$= |B|^2 \frac{\omega^2 \varepsilon^2 m^2 \pi^2 a}{2 K_o^4 b^2} \sqrt{\frac{\omega\mu}{2\sigma'}} \quad .$$

Similarly, the total loss/ cm of pipe on walls y = 0 and y = a is

$$= |B|^2 \frac{\omega^2 \varepsilon^2 n^2 \pi^2 b}{2 K_o^4 a^2} \sqrt{\frac{\omega\mu}{2\sigma'}} \quad .$$

The total power loss per cm. of pipe on four walls is

$$L = |B|^2 \frac{\omega^2 \varepsilon^2 \pi^2}{2 K_o^4} \sqrt{\frac{\omega\mu}{2\sigma'}} \left[\frac{n^2 b}{a^2} + \frac{m^2 a}{b^2} \right] \quad .$$

The power transmitted through the pipe is

$$S = \frac{1}{2} \int_o^b \int_o^a \left[E_y H_z - E_z H_y \right] dy \, dz$$

$$= |B|^2 \frac{\beta \omega \varepsilon a b}{8 K_o^2} \quad .$$

The attenuation constant is equal to

$$\alpha = \sqrt{\frac{2\pi\mu'\mathcal{E}c}{\sigma'\mu}}\ \frac{\sqrt{m}}{b^{3/2}}\ \frac{\left[1+\left(\frac{n}{m}\right)^2\left(\frac{b}{a}\right)^3\right]}{\left[1+\left(\frac{n}{m}\right)^2\left(\frac{b}{a}\right)^2\right]^{3/4}}\ \frac{\left(\frac{f}{f_0}\right)^{1/2}}{\sqrt{1-\left(\frac{f_0}{f}\right)^2}}$$ nepers per cm.
2.25

For a square pipe and n=m,

$$\alpha = \sqrt{\frac{2\pi\mu'\mathcal{E}c}{\sigma'\mu}}\ \frac{\sqrt{m}}{b^{3/2}}\ 2^{1/4}\ \frac{\left(\frac{f}{f_0}\right)^{1/2}}{\sqrt{1-\left(\frac{f_0}{f}\right)^2}}$$ nepers per cm.
2.26

General Discussion

The expressions for attenuation constants
(Eq. 2.12, 2.20 and 2.25) caused by the absorpsion by
conductor have been arranged in three factors. The first
factor for all waves

$$\sqrt{\frac{2\pi\mu'\mathcal{E}c}{\sigma'\mu}} = \sqrt{\frac{2\pi\mu'}{\sigma'\mu}\sqrt{\frac{\mathcal{E}}{\mu}}}$$ 2.27

depends only upon the electric and magnetic properties
of the materials. The attenuation is inversely proportion-
al to the square root of the conductivity of the conductor.
Were the conductivity infinitely great, the wave would
be unattenuated. The permeabilities of most dielectrics
are arround unity in e.m.u. Metals of high permeability and
dielectrics of high dielectric constant would be useful in
the experiment of testing the attenuation, since a shorter
pipe may be used to give measurable attenuation than the

materials of low permeability or dielectric constant.

The second factor $\sqrt{\frac{m}{b^3}}$ depends upon the order (m or n) of harmonic and one of the linear dimensions of the cross-section of the pipe. For waves of constant n/m in pipes of constant a/b , the attenuation is proportional to the square root of m and inversely proportional to the three-halves power of the linear dimension. Thus for a given pipe, the $E_{2,2}$-wave has an attenuation $\sqrt{2}$ time as great as the $E_{1,1}$-wave.

The remaining factor depends upon the ratio n/m , a/b, and f/f_o of the waves and pipes. The expressions are different for the $H_{o,m}$-, $H_{n,m}$- and $E_{n,m}$-waves and will be discussed separately. This factor will be abbreviated as F hereafter.

$H_{o,m}$-wave

The factor F for $H_{o,m}$-wave is

$$ F = \frac{\left(\frac{f_o}{f}\right)^{3/2} + \frac{b}{2a}\left(\frac{f}{f_o}\right)^{1/2}}{\sqrt{1 - \left(\frac{f_o}{f}\right)^2}} \qquad 2.28 $$

At the critical frequency, the attenuation of the $H_{o,m}$-wave like all other hollow-pipe waves, is infinity. However, above the critical frequency, the denominator increases rapidly to unity. At sufficiently high frequency, the two terms of F behave in opposite ways. The first

term decreases with the increase of frequency and vanishes at infinitely high frequency. The second term is proportional to the square root of frequency, and therefore is responsible for the attenuation of the $H_{0,1}$-wave at high frequencies. This term is caused by the dissipation of power into the walls $y = 0$ and $y = a$, where there is a transversal component of magnetic field tangential to the two walls.

If the pipe is degenerated by moving the two walls to infinity, the ratio b/a becomes negligible, and the factor F becomes

$$ F = \left(\frac{f_0}{f} \right)^{\frac{3}{2}} \Big/ \sqrt{1 - \left(\frac{f_0}{f} \right)^2} \qquad\qquad 2.29 $$

and at sufficient high frequency, $F = \left(\frac{f_0}{f} \right)^{\frac{3}{2}}$. The attenuation decreases with increasing frequency. A similar phenomenon for the H_0-wave in a circular pipe has been discovered by Carson and his co-workers. The general discussion of this type of attenuation is defered to the end of the next chapter.

Brillouin has pointed out in his paper that the peculiar property of attenuation such as possessed by the H_0-wave in a circular pipe is attributed to the symmetrical cross-section like a circle or a square. Then he proceeded to construct the wave of similar properties in a square pipe by superposing a $H_{0,2}$-wave and a $H_{2,0}$-wave together. Although a part of configuration of the resultant field is similar to that of the H_0-wave (Footnote, p.3)

the constructed wave does not possess the peculiar property of the H_o-wave. We may judge from the general field expressions of the Ho,m-waves, that the $H_{o,2}$-wave has two transverse. fields E_y and H_z and that the $H_{2,o}$-wave has two other transverse. fields E_z and H_y. A linear superposition by no means eliminates any particular component of field. The magnetic field H_y of the $H_{o,2}$-wave will cause the same amount of less on the walls $y = 0$ and $y = a$ whether the $H_{2,0}$-wave is present or not. The attenuation of the constructed wave is just the same as that of the $H_{o,2}$ - or $H_{2,o}$ - wave. The wave in rectangular pipe similar to the H_0-wave of circular pipe, is the degenerate $H_{o,m}$-wave or the H_g-wave so far as the attenuation is concerned.

By equating to zero the derivative of the factor F with respect to f/f_o, we find that for a given pipe, the $H_{o,m}$-wave has a minimum attenuation at the optimum frequency

$$\left(\frac{f}{f_o}\right)_{opt.} = \sqrt{3\left(\frac{a}{b} + \frac{1}{2}\right) + \sqrt{9\left(\frac{a}{b}\right)^2 + 7\frac{a}{b} + \frac{9}{4}}} \qquad 2.30$$

For a square pipe, this ratio is 2.96. If the dimension a is extended to infinity, the ratio becomes infinity, i.e., the attenuation always decrease with the increase of frequency. In Fig. 2.3, the curves show the variation of critical and optimum wave lengths with the ratio a/b , for the $H_{o,m}$-wave.

Perhaps the most reasonable comparison of

Fig. 2.3 $H_{0,1}$-wave in Rectangular Pipe
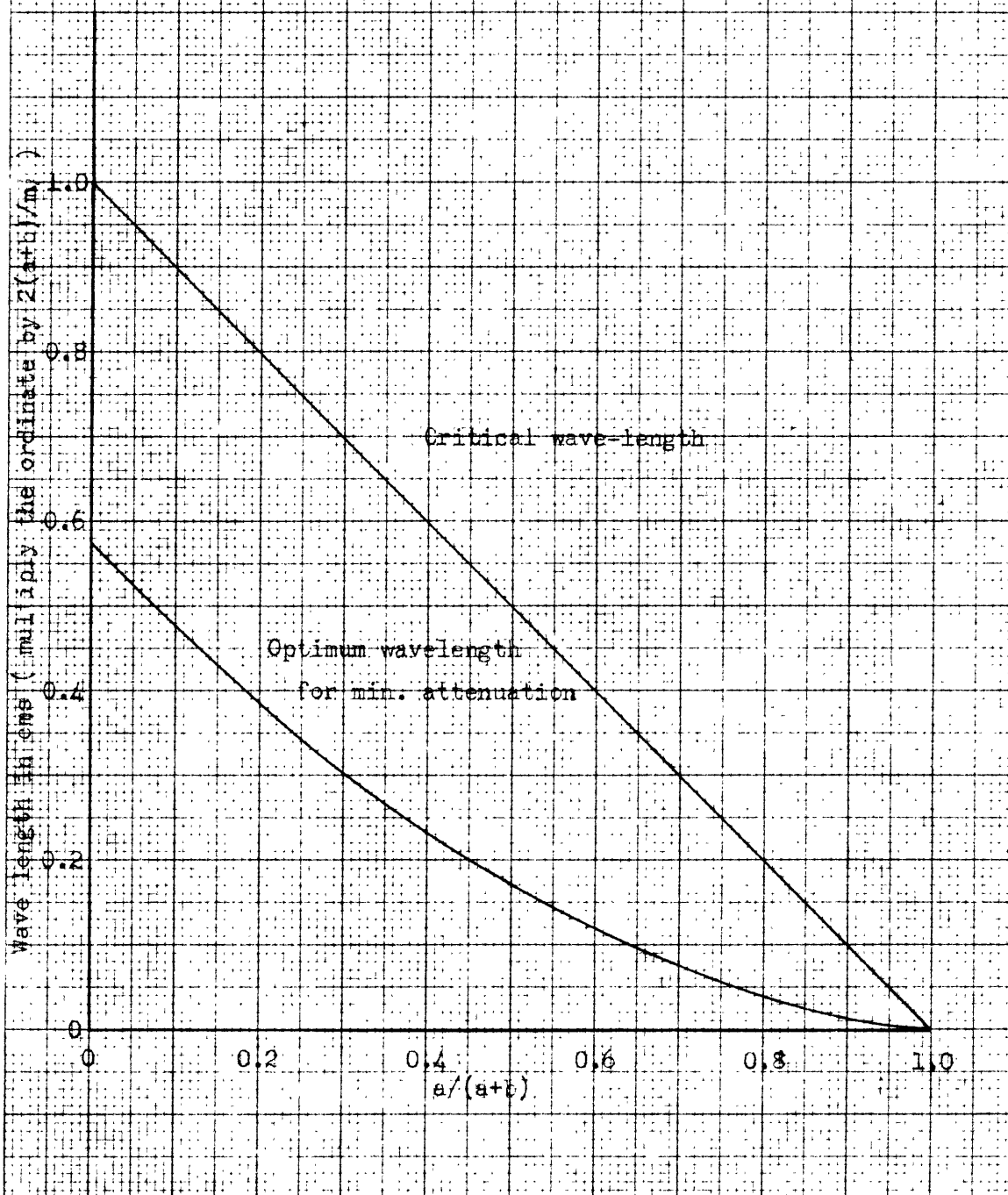
Critical wave-length

Optimum wavelength
for min. attenuation

Wave length in cms (multiply the ordinate by $2(a+b)/m_i$)

$a/(a+b)$

FORM 4T

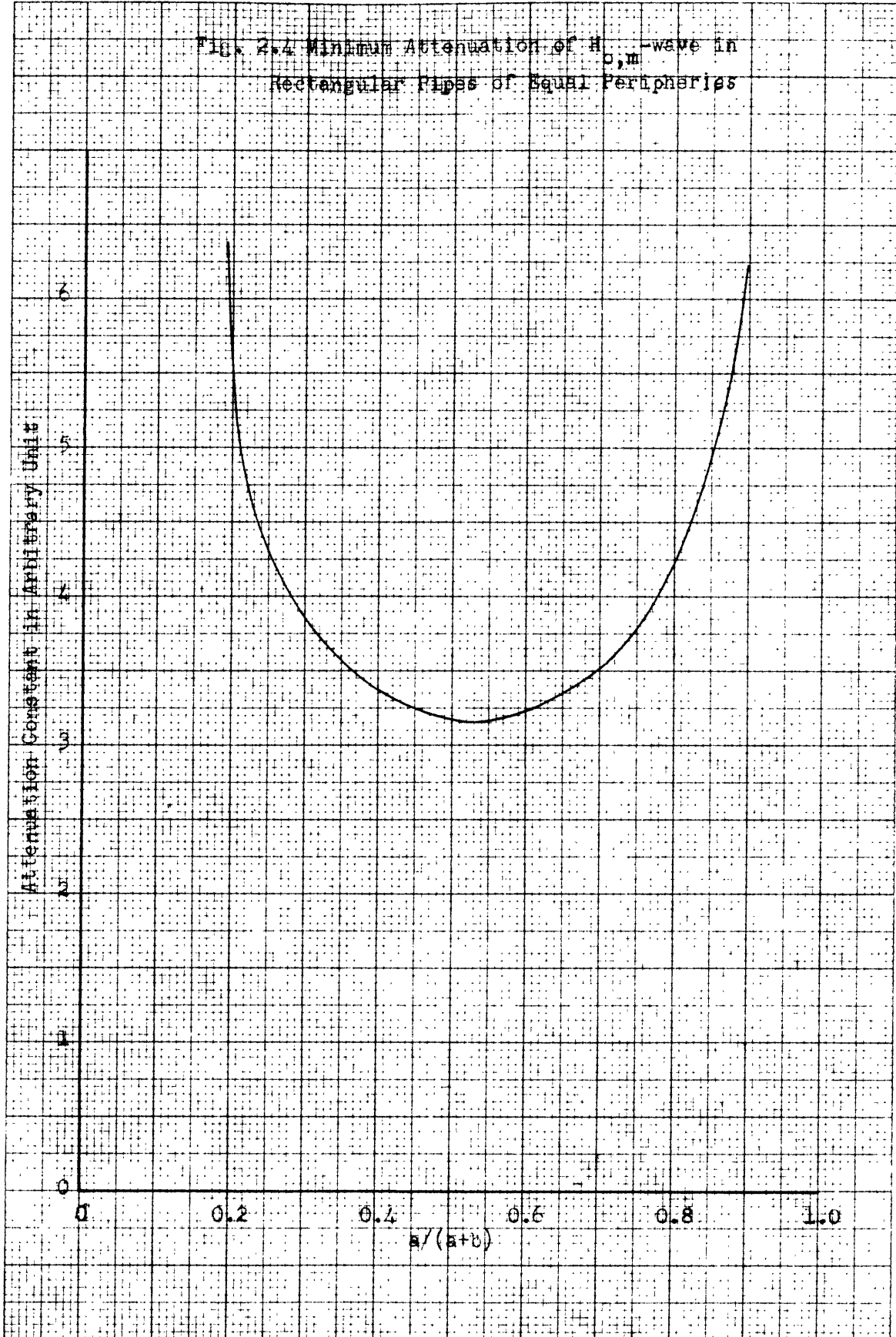Fig. 2.4 Minimum Attenuation of $H_{o,m}$-wave in Rectangular Pipes of Equal Peripheries

FORM 4 T

Fig. 2.5 $H_{0,1}$-wave in air-filled Copper Pipe of
Rectangular Cross Section for different
a/b Ratio

Periphery = 40cm.
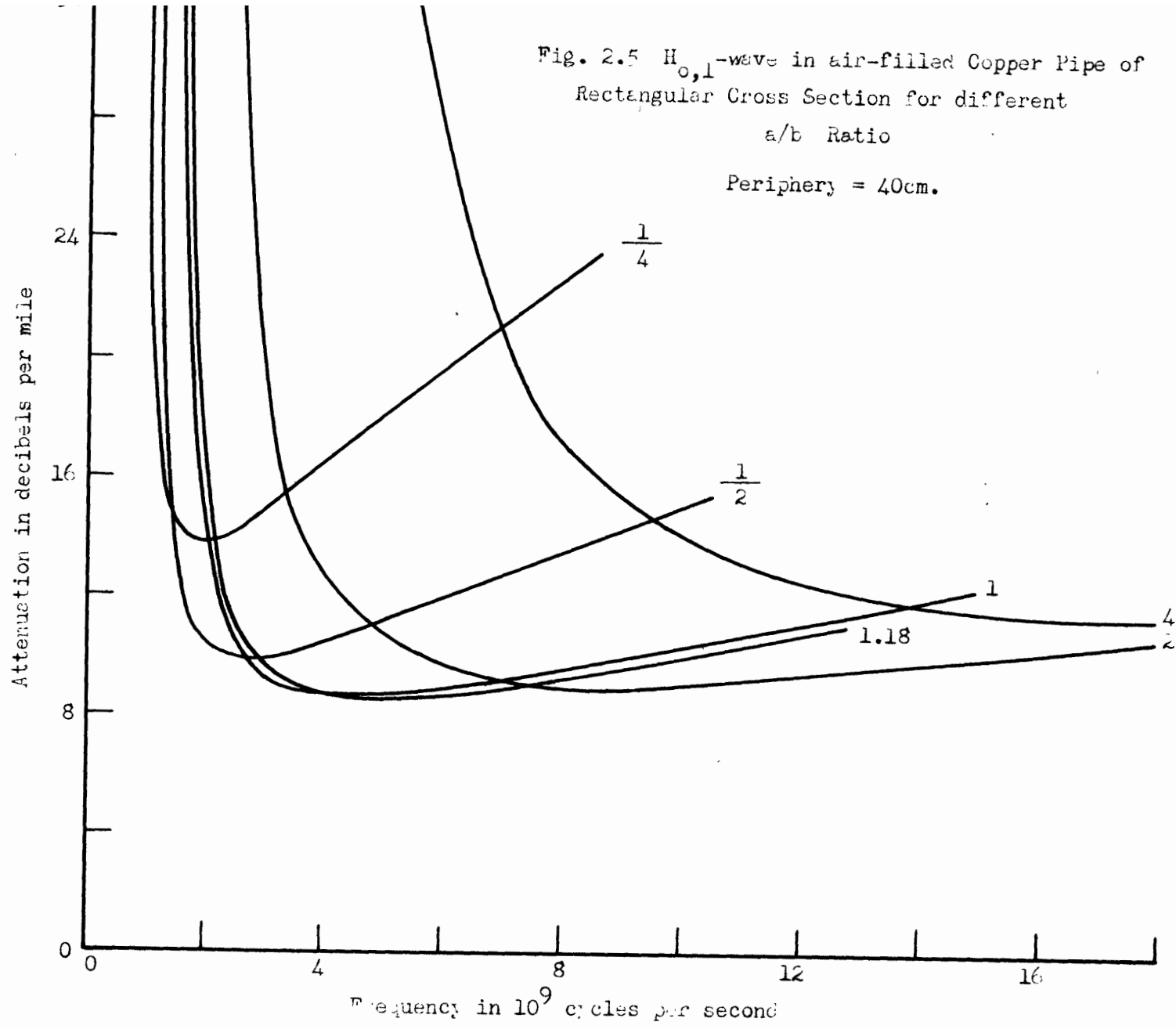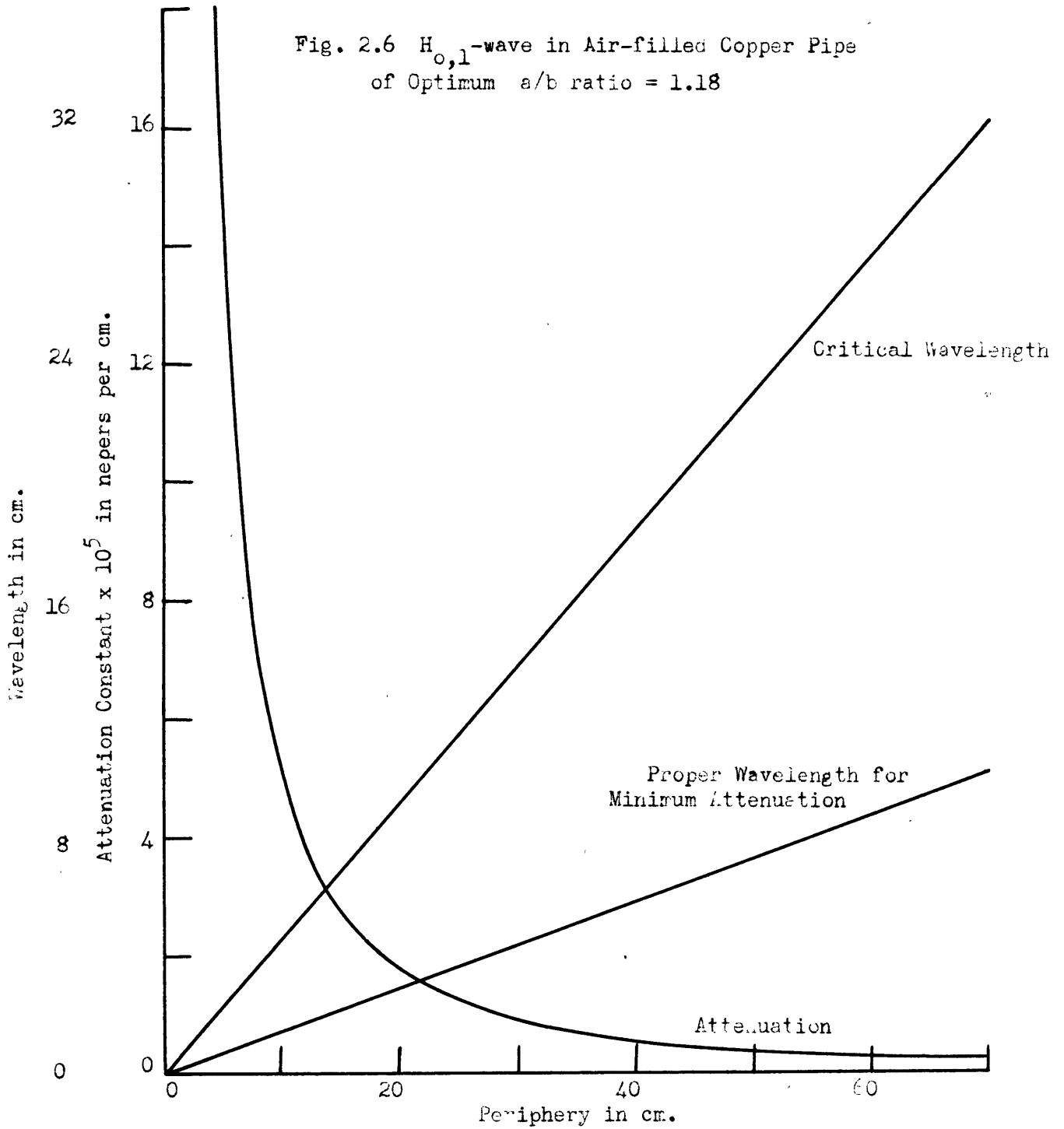
Fig. 2.6 $H_{o,1}$-wave in Air-filled Copper Pipe
of Optimum a/b ratio = 1.18

Critical Wavelength

Proper Wavelength for
Minimum Attenuation

Attenuation

Wavelength in cm.

Attenuation Constant x 10^5 in nepers per cm.

Periphery in cm.

rectangular pipes is one in which the shape is changed, but keeping the periphery and so also the amount of metal used in the construction and the cost at some constant value, while the range of the frequency is disregarded. To obtain the most favorable ratio of a/b, for pipes of constant periphery, the optimum attenuation constant in arbitrary units, of pipes, having $a + b$ = Constant, are plotted against the ratio $\frac{a}{a+b}$ in Fig. 2.4. The curve is fairly flat around $\frac{a}{a+b} = .5$. The most favorable ratio of a/b is found to be 1.18. Of course this value is not very critical. In Fig. 2.5, the attenuation constant of the $H_{o,1}$-wave is plotted against the operating frequency for pipes having $\frac{a}{b} = .25, .5,$ 1,1.18,2 and 4, the periphery being 40 cm. for all pipes. From these curves, we may see that for a square pipe, the optimum attenuation is only 1% greater than for the pipe of ratio 1.175, however, the corresponding wave length is greater by 17%. While the generation of ultra-high frequency power is still in the experimental stage, pipes having ratio $\frac{a}{b} = 1$ or even smaller may be the most economical ones. We may also see that the larger the ratio a/b the flatter the curve.

Fig. 2.6 shows the optimum attenuation, critical wave enough, and optimum wave length of $H_{o,1}$-waves, in pipes having ratio $\frac{a}{b} = 1.18$ and variable periphery. It indicates the part which the factor $b^{-3/2}$ plays in the expression for attenuation.

$H_{n,m}$-wave

The factor F of the attenuation constant for the $H_{n,m}$ - wave in a rectangular pipe is the following:

$$F = \frac{\frac{b}{a}\left[1 + (\frac{n}{m})^2\frac{b}{a}\right](\frac{f}{f_0})^{\frac{1}{2}} + \left[1 + (\frac{n}{m})^2(\frac{b}{a})^3\right](\frac{f_0}{f})^{\frac{3}{2}}}{\left[1 + (\frac{na}{mb})^2\right]^{\frac{3}{4}}\sqrt{1 - (\frac{f_0}{f})^2}} \qquad 2.31$$

For a square pipe, a = b and n = m, it is

$$F = \sqrt[4]{2}\,\frac{(\frac{f}{f_0})^{\frac{1}{2}} + (\frac{f_0}{f})^{\frac{3}{2}}}{\sqrt{1 - (\frac{f_0}{f})^2}} \qquad 2.32$$

If n = m, a square pipe has a lower attenuation constant for the $H_{n,m}$-wave than pipes having other ratio of a/b but the same periphery. This fact is attributable to symmetry. By comparing expression Eq. 2.32 with expression Eq. 2.28, in which a/b is put equal to unity, we see that in a square pipe, the $H_{n,m}$-wave of n = m always has greater attenuation than the $H_{o,m}$-wave. At sufficiently high frequency, the ratio of the two is 2.83 for same frequency. The $H_{n,m}$-wave has $\sqrt{2}$ time higher critical frequency than the $H_{o,m}$-wave. The minimum attenuation of $H_{n,m}$-wave occurs in a square pipe and n = m, when

$$f/f_0 = 2.415$$

If one set of the opposite walls of the rectangular pipe is moved to negative and positive infinity, that is, a/b or b/a equal to infinity, then within a finite

portion of the cross-section the $H_{n,m}$-waves are degenerated

into the degerate $H_{o,m}$-wave, and have the same anomalous

attenuation function (Eq. 2.29).

$E_{n,m}$ -wave

The factor F of the attenuation constant for

the $E_{n,m}$ -wave in a rectangular pipe has only a single term

as follows

$$ F = \frac{\left[1 + \left(\frac{n}{m} \right)^2 \left(\frac{b}{a} \right)^3 \right]}{\left[1 + \left(\frac{n}{m} \right)^2 \left(\frac{b}{a} \right)^2 \right]^{\frac{3}{4}}} \frac{\left(f/f_o \right)^{\frac{1}{2}}}{\sqrt{1 - \left(f_o/f \right)^2}} \qquad 2.33 $$

Unlike the $H_{o,m}$-wave or the $H_{n,m}$-wave, the attenuation of

the $E_{n,m}$ -wave consists of only a single term and therefore

there is no possibly for obtaining a decreacing attenuation

with increasing frequency by degenerating the shape of the

pipe. For a given pipe, the minimum attenuation occurs at

$f/f_o = \sqrt{3}$.

For a square pipe of $\frac{a}{b} = 1$ and n = m, the

factor F becomes

$$ F = \sqrt[4]{2} \; \frac{\left(f/f_o \right)^{\frac{1}{2}}}{\sqrt{1 - \left(f_o/f \right)^2}} \qquad 2.34 $$

It has a lower attenuation than pipes having other value

of the ratio a/b and same periphery. It may be recognized

that it is the same as the first term of F for the $H_{n,m}$ -

wave in a square pipe. At sufficiently high frequency,

the two will have same attenuation which is 2.83 times greater than that of the $H_{o,m}$-wave for same frequency.

In Fig. 2.7 are shown curves of attenuation constant vs. frequency for the three lowest order waves the $H_{o,1}$ -, $H_{1,1}$ - and $E_{1,1}$ in an air filled square pipe of copper, 10 cm. on a side. For these cases, we find the following values:

Table 2.1

Wave type	$H_{o,1}$	$H_{1,1}$	$E_{1,1}$
Critical freq.(c.p.s.)	1.5×10^9	2.12×10^9	2.12×10^9
Freq. for min.atten.(c.p.s.)	4.44×10^9	5.18×10^9	3.67×10^9
Min. atten. db./mile	8.55	18.1	14.6

Comparison of Attenuations in Square and Cicular Pipes

The expressions for attenuation constants for different types of waves in a circular pipe have been presented by Carson, Mead, and Schelkunoff and for the E_o-wave by Prof. Barrow. All these values have been checked in Chapter III by degenerating an elliptical pipe into a circular one. Those expressions are rewritten here in terms of a square pipe b centimeters on a side having the same periphery:
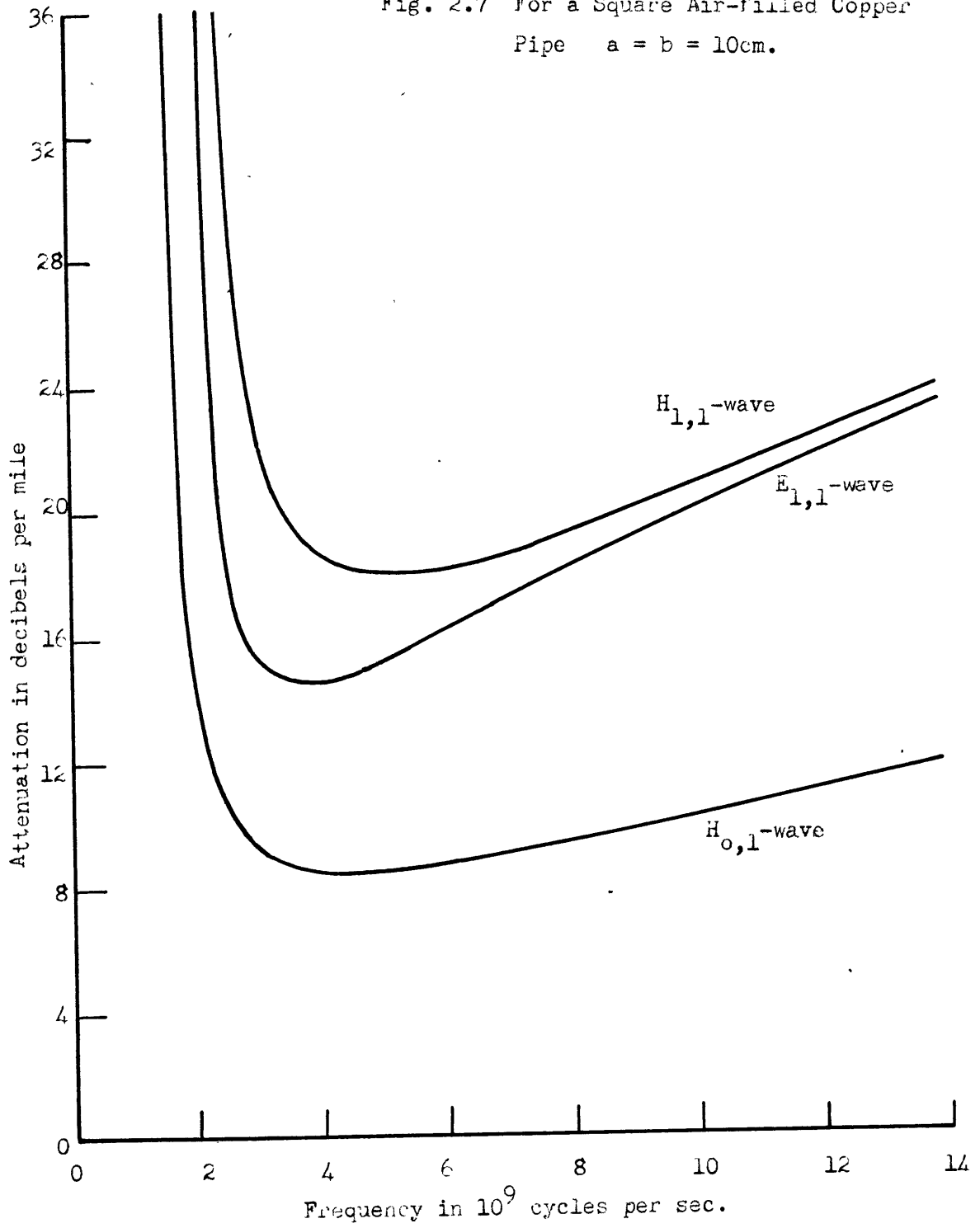
E_o-wave

$$\alpha = K\, b^{-\frac{3}{2}} \times 0.862\, \frac{(f/f_o)^{\frac{1}{2}}}{\sqrt{1 - (f_o/f)^2}}.$$

E_1-wave

$$\alpha = K\, b^{-\frac{3}{2}} \times 1.087\, \frac{(f/f_o)^{\frac{1}{2}}}{\sqrt{1 - (f_o/f)^2}}.$$

Fig. 2.7 For a Square Air-filled Copper Pipe   a = b = 10cm.

H_o-wave

$$\alpha = K \, b^{-\frac{3}{2}} \times 1.087 \frac{(f_o/f)^{\frac{3}{2}}}{\sqrt{1 - (f_o/f)^2}} \; . \qquad\qquad 2.35$$

H_1-wave

$$\alpha = K \, b^{-\frac{3}{2}} \times 0.753 \frac{(f_o/f)^{\frac{3}{2}} + 0.419 \, (f/f_o)^{\frac{1}{2}}}{\sqrt{1 - (f_o/f)^2}}$$

where

$$K = \sqrt{\frac{2\pi\mu'\iota_c}{\sigma'\mu}} \; .$$

Except for the H_o-wave in circular pipe, whose attenuation decreases with increasing frequency, the attenuation in a circular pipe passes through a minimum value. The following table shows the relative magnitudes of the minimum attenuations, the critical wave lengths, and the optimum wave lenghths, for waves in circular and square pipes of equal peripheries.

Table 2.2

Shape of pipe	Wave type	$\dfrac{\alpha_{mn} b^{\frac{3}{2}}}{K}$	Critical Wave length/b	Wave length for min. atten./b
Circular cross-section	H_1 E_o E_1	0.597 1.203 1.518	2.174 1.622 1.041	0.690 0.960 0.602
Square Cross-section	$H_{o,1}$ $H_{1,1}$ $E_{1,1}$	1.12 2.375 1.917	2.00 1.414 1.414	0.676 0.579 0.817

For air-filled copper pipe

On the basis of attenuation, none of the waves in a square pipe is as good as the corresponding wave in a circular pipe. The H_o-wave requires an excessively high operating frequency for sufficiently low attenuation. Although, the critical wave length of the H_1-wave, which is the longest of all, is only a little above that for the

$H_{o,1}$-wave, the attenuation of the H_1-wave is less than one half of that of the $H_{o,1}$-wave in a square type. Unless the generation of very high frequency power is made commercially possible, it would appear that the H_1-wave in a circular pipe is the most promising one for hollow pipe transmission for long distances. On the other hand, the $H_{o,1}$-wave in a square or rectangular pipe will, because of its appropriate field pattern, probably find early application to radiation problems.

Attenuation Caused by the Conductivity of Dielectric

Consider a cylindrical pipe of any geometrical cross-section. The conductor is assumed to have infinitely large conductivity. For all types of waves, the propagation constant h is determined from the expression

$$k^2 + h^2 = k_o^2$$

where k is the wave constant and is equal to $-i\omega\mu(i\omega\xi + \sigma)$ and k_o is the critical wave constant corresponding to the critical frequency and is a real quantity for a perfect conducting pipe. We may write k_o as $\omega_o\sqrt{\xi\mu}$. Thus,

$$h = i\sqrt{\omega^2\xi\mu - i\omega\mu\sigma - \omega_o^2\xi\mu}$$

$$\doteq i\sqrt{\omega^2\xi\mu\left[1 - \left(\frac{\omega_o}{\omega}\right)^2\right]} - i\omega\mu\sigma \quad . \tag{2.36}$$

Expanding the square root by the Binomial Theorem, and neglecting high order terms of σ , we have

$$h = i\beta + \alpha$$

$$= i\omega \sqrt{\epsilon\mu}\left[1- \left(\frac{f_0}{f}\right)^2\right]^{\frac{1}{2}} + \frac{\sigma}{2}\sqrt{\frac{\mu}{\epsilon}}\left[1-\left(\frac{f_0}{f}\right)^2\right]^{-\frac{1}{2}} .$$

The real part

$$\alpha = \frac{\sigma}{2}\sqrt{\frac{\mu}{\epsilon}}\left[1-\left(\frac{f_0}{f}\right)^2\right]^{-\frac{1}{2}} \quad \text{nepers per cm.} \quad 2.37$$

This expression is valid for all types of hollow pipe waves if the appropriate value of critical frequency f_0 is used. At the critical frequency, the attenuation caused by the conductivity of the dielectric is infinitely great but it decreases rapidly with increasing frequency, and approaches a constant value $\frac{\sigma\sqrt{\mu}}{2\sqrt{\epsilon}}$. Such a variation is shown in Fig. 2.8.

This phenomenon may be explained pictorially and particularly for the waves in a rectangular pipe, for the $H_{o,m}$-wave. We have learned while calculating the loss of the $H_{o,m}$-wave into the walls $y = 0$ and $y = a$, that the wave may be resolved into components waves traveling in a direction at an angle θ_x with the X-axis which is the longitudinal axis of the pipe

$$\cos\theta_x = \frac{\beta}{k} = \sqrt{1-\left(\frac{f_0}{f}\right)^2} .$$

Fig. 2.8 Attenuation Caused by Dielectric

$$\alpha = \frac{g}{2}\sqrt{\frac{\mu}{\epsilon}}\left[1 - \left(\frac{f_0}{f}\right)^2\right]^{-\frac{1}{2}}$$

For All Hollow-Pipe Waves
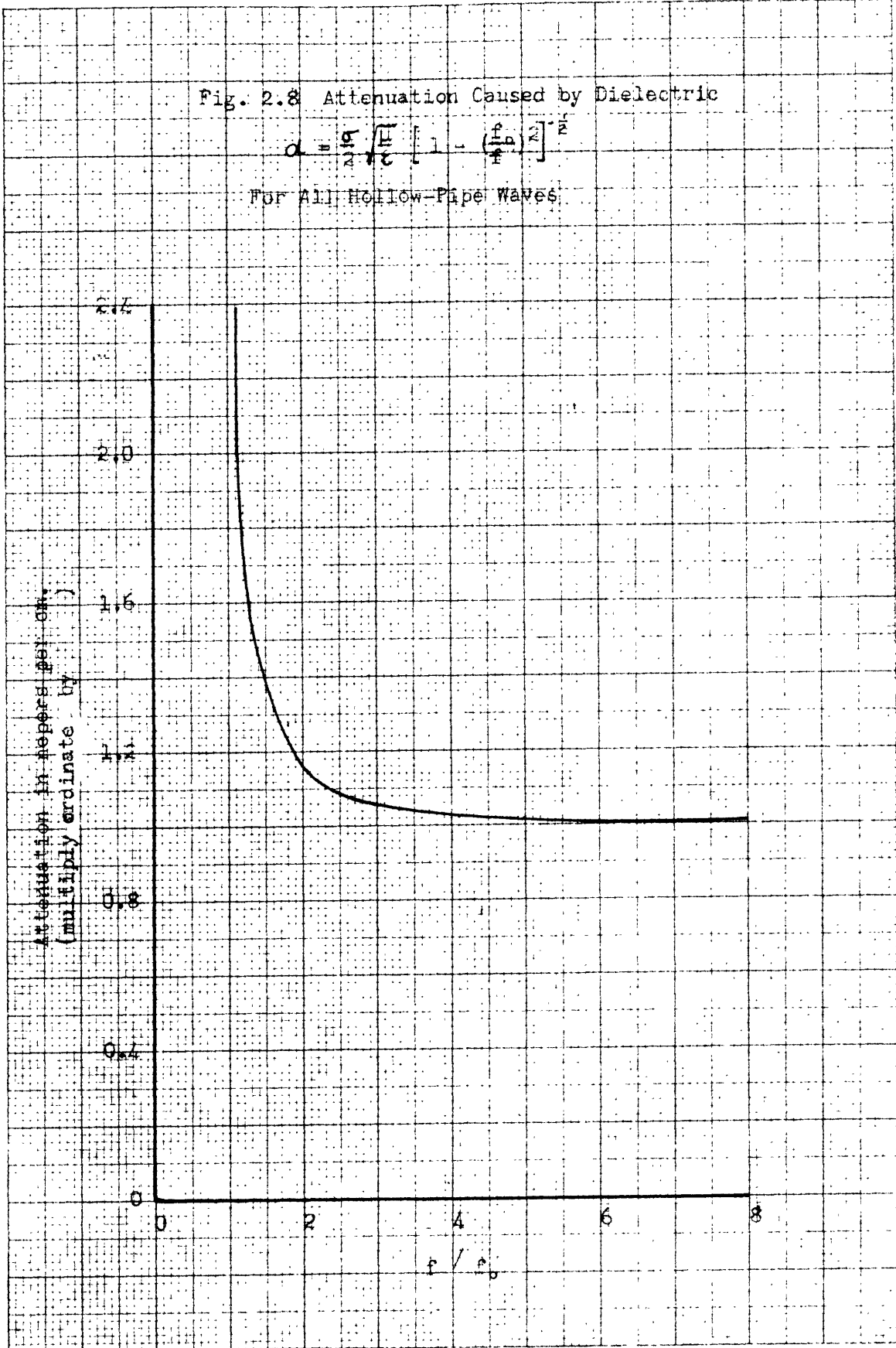
Although the apparent distance traveled by the wave along the pipe is $\triangle x$, the actual distance travels by its component waves is $\triangle x/\cos\theta_x$. Since the component waves are equevalent to plane waves traveling in free space, their attenuation caused by the conductivity of the dielectric is given by $\frac{\sigma\sqrt{\mu}}{2\sqrt{\varepsilon}}$. The expression 2.37 may be obtained by multiplying $\frac{\sigma\sqrt{\mu}}{2\sqrt{\varepsilon}}$ by the ratio of the distance actually traveled to the distance apparently traveled along the pipe.

Summary of Equations

Non-dissipative Case

Fields in the dielectric:

$$H_{n,m}\text{-waves}$$

$$H_x = B \cos\left(\frac{n\pi}{a}y\right)\cos\left(\frac{m\pi}{b}z\right)e^{i(\omega t - \beta x)}$$

$$H_y = B \frac{i\beta}{K_o^2}\frac{n\pi}{a}\sin\left(\frac{n\pi}{a}y\right)\cos\left(\frac{m\pi}{b}z\right)e^{i(\omega t - \beta x)}$$

$$H_z = B \frac{i\beta}{K_o^2}\frac{m\pi}{b}\cos\left(\frac{n\pi}{a}y\right)\sin\left(\frac{m\pi}{b}z\right)e^{i(\omega t - \beta x)}$$

$$E_y = B \frac{i\omega\mu}{K_o^2}\frac{m\pi}{b}\cos\left(\frac{n\pi}{a}y\right)\sin\left(\frac{m\pi}{b}z\right)e^{i(\omega t - \beta x)} \quad 2.1$$

$$E_z = -B \frac{i\omega\mu}{K_o^2}\frac{n\pi}{a}\sin\left(\frac{n\pi}{a}y\right)\sin\left(\frac{m\pi}{b}z\right)e^{i(\omega t - \beta x)}$$

$$E_x = 0$$

$H_{0,m}$-waves

$$H_x = B \quad \cos \left(\frac{m\pi}{b} z \right) e^{i(\omega t - \beta x)}$$

$$H_z = B \frac{i\beta b}{m\pi} \sin \left(\frac{m\pi}{b} z \right) e^{i(\omega t - \beta x)}$$

$$E_y = B \frac{i\omega\mu b}{m\pi} \sin \left(\frac{m\pi}{b} z \right) e^{i(\omega t - \beta x)} \qquad 2.3$$

$E_{n,m}$-waves

$$E_x = B \quad \sin \left(\frac{n\pi}{a} y \right) \sin \left(\frac{m\pi}{b} z \right) e^{i(\omega t - \beta x)}$$

$$E_y = -B \frac{i\beta}{k_o^2} \frac{n\pi}{a} \cos \left(\frac{n\pi}{a} y \right) \sin \left(\frac{m\pi}{b} z \right) e^{i(\omega t - \beta x)}$$

$$E_z = -B \frac{i\beta}{k_o^2} \frac{m\pi}{b} \sin \left(\frac{n\pi}{a} y \right) \cos \left(\frac{m\pi}{b} z \right) e^{i(\omega t - \beta x)}$$

$$H_y = B \frac{i\omega\varepsilon}{k_o^2} \frac{m\pi}{b} \sin \left(\frac{n\pi}{a} y \right) \cos \left(\frac{m\pi}{b} z \right) e^{i(\omega t - \beta x)} \quad 2.4$$

$$H_z = -B \frac{i\omega\varepsilon}{k_o^2} \frac{n\pi}{a} \cos \left(\frac{n\pi}{a} y \right) \sin \left(\frac{m\pi}{b} z \right) e^{i(\omega t - \beta x)}$$

$$H_x = 0$$

The constants for above three types of waves:

Phase constant:

$$\beta = \sqrt{(\tfrac{\omega}{c})^2 - (\tfrac{n\pi}{a})^2 - (\tfrac{m\pi}{b})^2} = \tfrac{\omega}{c}\sqrt{1 - (f_o/f)^2} \qquad 2.5a$$

Critical frequency

$$f_o = \tfrac{c}{2}\sqrt{(\tfrac{n}{a})^2 + (\tfrac{m}{b})^2} \qquad 2.5b$$

Critical wave length:

$$\lambda = 2\left[(\tfrac{n}{a})^2 + (\tfrac{m}{b})^2\right]^{-\frac{1}{2}} \qquad 2.5c$$

Dissipative Case

The attenuation constants of the waves inside the rectangular pipe caused by the finite conductivity of the metal (the dielectric is assumed absolutely non-conductive):

$$H_{o,m}\text{-waves}$$

$$\alpha = \sqrt{\frac{2\pi\mu'\varepsilon c}{\sigma'\mu}}\;\frac{\sqrt{m}}{b^{3/2}}\;\frac{(f_o/f)^{3/2} + \tfrac{b}{2a}(\tfrac{f}{f_o})^{1/2}}{\sqrt{1 - (f_o/f)^2}} \qquad 2.12$$

nepers per cm.

$$H_{n,m}\text{-waves}$$

$$\alpha = \sqrt{\frac{2\pi\mu'\varepsilon c}{\sigma'\mu}}\;\frac{\sqrt{m}}{b^{3/2}}\;\frac{\tfrac{b}{a}\left[1 + (\tfrac{n}{m})^2\tfrac{b}{a}\right](\tfrac{f}{f_o})^{1/2} + \left[1 + (\tfrac{n}{m})^2(\tfrac{b}{a})^3\right](\tfrac{f_o}{f})^{3/2}}{\left[1 + (\tfrac{b}{a})^2(\tfrac{n}{m})^2\right]^{3/4}\;\sqrt{1 - (\tfrac{f_o}{f})^2}} \qquad 2.20$$

nepers per cm.

$E_{n,m}$-waves

$$\alpha = \sqrt{\frac{2\pi\mu'\xi c}{\sigma'\mu}} \; \frac{\sqrt{m}}{b^{3/2}} \; \frac{[1 + (\frac{b}{a})^3 (\frac{n}{m})^2]}{[1 + (\frac{nb}{ma})^2]^{3/4}} \; \frac{(f/f_0)^{1/2}}{\sqrt{1 - (f_0/f)^2}} \qquad 2.25$$

nepers per cm.

For a square pipe a = b and n = m:

$H_{o,m}$-waves

$$\alpha = \sqrt{\frac{2\pi\mu'\xi c}{\sigma'\mu}} \; \frac{\sqrt{m}}{b^{3/2}} \; \frac{\frac{1}{2}(\frac{f}{f_0})^{1/2} + (\frac{f_0}{f})^{3/2}}{\sqrt{1 - (\frac{f_0}{f})^2}} \qquad$$ nepers per cm.

$H_{n,m}$-waves

$$\alpha = \sqrt{\frac{2\pi\mu'\xi c}{\sigma'\mu}} \; \frac{\sqrt{m}}{b^{3/2}} \; \sqrt[4]{2} \; \frac{(\frac{f}{f_0})^{1/2} + (\frac{f_0}{f})^{3/2}}{\sqrt{1 - (\frac{f_0}{f})^2}} \qquad \begin{matrix} 2.21 \\ \text{nepers per cm.} \end{matrix}$$

$E_{n,m}$-waves

$$\alpha = \sqrt{\frac{2\pi\mu'\xi c}{\sigma'\mu}} \; \frac{\sqrt{m}}{b^{3/2}} \; \sqrt[4]{2} \; \frac{(f/f_0)^{1/2}}{\sqrt{1 - (f_0/f)^2}} \qquad \begin{matrix} 2.26 \\ \text{nepers per cm.} \end{matrix}$$

The Attenuation constant of waves inside any hollow-pipe, caused by the conductivity of the dielectric (the conductor is assumed absolutely conductive)

$$\alpha = \frac{\sigma}{2}\sqrt{\frac{\mu}{\xi}} \; [1 - (f_0/f)^2]^{-1/2} \qquad \begin{matrix} \text{nepers per cm.} \\ 2.37 \end{matrix}$$

III. TRANSMISSION CHARACTERISTICS
OF WAVES IN ELLIPTICAL PIPES

We will now consider waves in elliptical conducting pipes, i.e., pipes the inner boundary of which forms an elliptical cylinder. Inside the pipes, the space is filled with a dielectric, which is assumed to be a perfect insulator throughout this chapter. The effects of a small conductivity of the dielectric have been discussed in the last chapter. The conductor may be either non-dissipative or it may have a finite but large conductivity. In either case, the conductor is assumed to be thick enough to prevent the currents from reaching the outside surface. A perspective view of such a pipe is shown in Fig. 3.1.

Maxwell and Wave Equations

In dealing with waves in elliptical pipes, we use the elliptical coordinate system (x, ξ, η). They are defined in terms of a Cartesian system by the equations:

$$x = x$$
$$y = q \cosh \xi \cos \eta \qquad\qquad 3.1$$
$$z = q \sinh \xi \sin \eta.$$

The contour lines of constant ξ are confocal ellipses, and those of constant η as confocal hyperbolae as shown in Fig.

Fig. 3.1

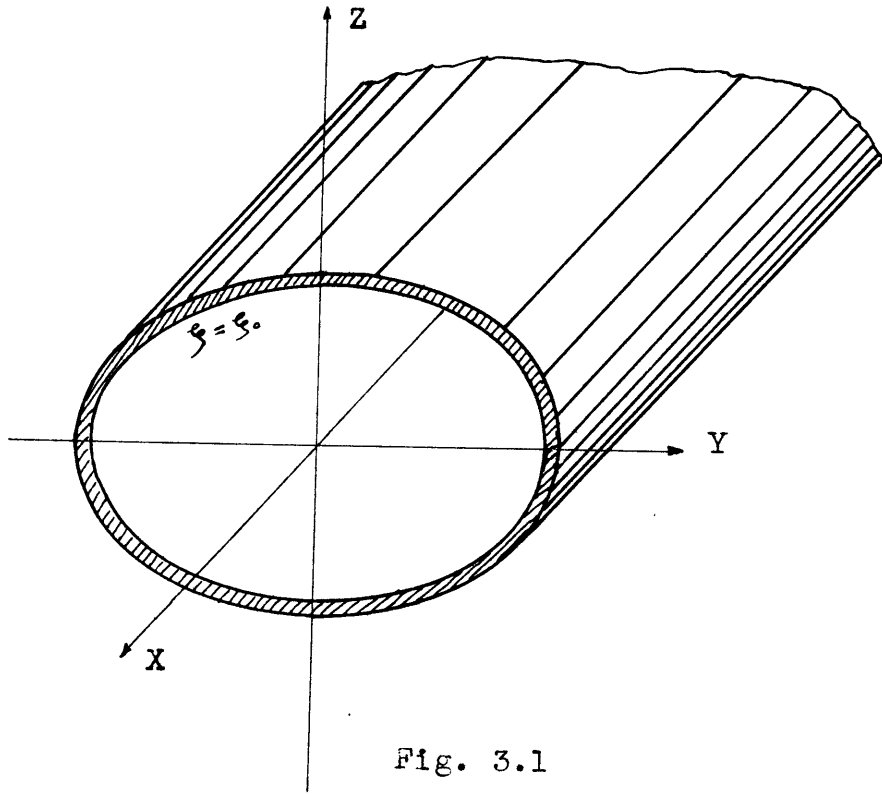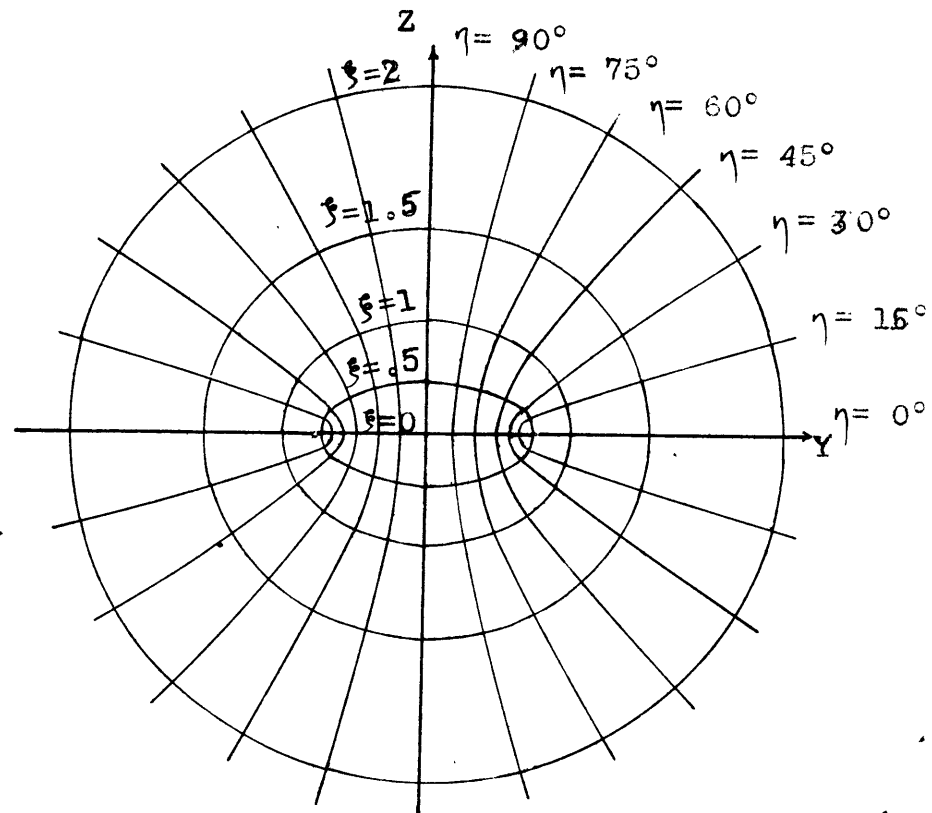
Fig. 3.2

3.2. The constants q is the one-half $\overset{\text{of}}{\wedge}$ the distance between the foci. For large values of ξ, $\cosh \xi \cong \sinh \xi$, the elliptical coordinates reduce to polar coordinates. For this reason, ξ may be referred to as the radial variable and η as the angular variable.

We may make one of the confocal ellipses coincide with the inner boundary of the elliptical pipe. At the boundary, $\xi = \xi_o$. The major axis of the boundary ellipse is $q\cosh \xi_o$ and the minor axis is $q \sinh \xi_o$. The eccentricity e of the boundary ellipse is defined as the reciprocal of $\cosh \xi_o$.

We shall confine our interest to waves having simple sinusoidal time variations and a propagation in the positive x-direction along the axis. In complex representation, the wave functions inside the pipe are multiplied by the factor $e^{i\omega t - hx}$. The propagation constant $h = \alpha + i\beta$ is to be determined from the boundary conditions.

The Maxwell equations in elliptical coordinates are as follows:

$$\nabla \times H = \frac{i_\xi}{q_1} \left[\frac{\partial H_x}{\partial \eta} + hq_1 H_\eta \right] - \frac{i_\eta}{q_1} \left(hq_1 H_\xi + \frac{\partial H_x}{\partial \xi} \right) + \frac{i_x}{q_1^2} \left[\frac{\partial (q_1 H_\eta)}{\partial \xi} - \frac{\partial (q_1 H_\xi)}{\partial \eta} \right]$$

$$= (i\omega\xi + \sigma) \left[i_\xi E_\xi + i_\eta E_\eta + i_x E_x \right] \qquad 3.2a$$

$$\nabla \times E = \frac{i_\xi}{q_1} \left[\frac{\partial H_x}{\partial \eta} + hq_1 E_\eta \right] - \frac{i_\eta}{q_1} \left(hq_1 E_\xi + \frac{\partial E_x}{\partial \xi} \right) + \frac{i_x}{q_1^2} \left[\frac{\partial (q_1 E_\eta)}{\partial \xi} - \frac{\partial (q_1 E_\xi)}{\partial \eta} \right]$$

$$= - i\omega\mu \left[i_\xi H_\xi + i_\eta H_\eta + i_x H_x \right] \qquad 3.2b$$

where i_ξ, i_η, and i_x are three orthogonal unit vectors in the direction of ξ, η and x. The variable q_1 is defined as:

$$q_1 = \frac{1_\xi}{grad\,\xi} = \frac{1_\eta}{grad\,\eta} = q\sqrt{\sinh^2\xi + \sin^2\eta} \ . \qquad 3.3$$

Equating the three vectorial components of the two equations gives the six equations:

$$(\sigma + i\omega\epsilon)E_\xi = \frac{1}{q_1}\frac{\partial H_x}{\partial \eta} + h H_\eta \qquad 3.4a$$

$$-(\sigma + i\omega\epsilon)E_\eta = \frac{1}{q_1}\frac{\partial H_x}{\partial \xi} + h H_\xi \qquad 3.4b$$

$$(\sigma + i\omega\epsilon)E_x = \frac{\partial(q_1 H_\eta)}{\partial \xi} - \frac{\partial(q_1 H_\xi)}{\partial \eta} \qquad 3.4c$$

$$-i\omega\mu H_\xi = \frac{1}{q_1}\frac{\partial E_x}{\partial \eta} + h E_\eta \qquad 3.4d$$

$$i\omega\mu H_\eta = \frac{1}{q_1}\frac{\partial E_x}{\partial \xi} + h E_\xi \qquad 3.4e$$

$$-i\omega\mu q_1^2 H_x = \frac{\partial(q_1 E_\eta)}{\partial \xi} - \frac{\partial(q_1 E_\xi)}{\partial \eta} \ . \qquad 3.4f$$

It is more convenient to solve for the transverse components E_ξ, E_η, H_ξ and H_η in terms of the longitudinal components, E_x and H_x. Thus in place of Eq. 3.4a, 3.4b, 3.4d and 3.4e, we have,

$$q_1(\kappa^2 + h^2)E_\xi = -h\frac{\partial E_x}{\partial \xi} - i\omega\mu\frac{\partial H_x}{\partial \eta} \qquad 3.4a'$$

$$q_1(\kappa^2 + h^2)E_\eta = -h\frac{\partial E_x}{\partial \eta} + i\omega\mu\frac{\partial H_x}{\partial \xi} \qquad 3.4b'$$

$$q_1(\kappa^2 + h^2)H_\xi = (\sigma + i\omega\epsilon)\frac{\partial E_x}{\partial \eta} - h\frac{\partial H_x}{\partial \xi} \qquad 3.4d'$$

$$q_1(\kappa^2 + h^2)H_\eta = -(\sigma + i\omega\epsilon)\frac{\partial E_x}{\partial \xi} - h\frac{\partial H_x}{\partial \eta} \ . \qquad 3.4e'$$

where k is the wave constant.

To find the wave equation for E_x, we take the partial derivative of Eq. 3.4d' and 3.4e' with respect to ξ and η respectively, and substitute the results into Eq. 3.4c. We have:

$$\left[\frac{\partial^2}{\partial \xi^2} + \frac{\partial^2}{\partial \eta^2} + (\kappa^2 + h^2)q_1^2 \right] E_x = 0 \ . \qquad 3.5a$$

Similarly, by manipulating Eq. 3.4a', 3.4b' and 3.4f, we have the wave equation for H_x:

$$\left[\frac{\partial^2}{\partial \xi^2} + \frac{\partial^2}{\partial \eta^2} + (\kappa^2 + h^2) q_1^2 \right] H_x = 0 \quad . \tag{3.5b}$$

The two wave equations for the longitudinal components of fields have the same form. The wave equations for the transverse field may be similarly obtained but have different forms. Solution of the equation requires a separation of the variables. Let

$$E_x = F (\xi) G (\eta) e^{i\omega t - hx} ,$$

and use the value of q_1 in Eq. 3.3. Substitute both into Eq. 3.5a, and separate the variables

$$\left[\frac{\partial^2}{\partial \xi^2} + (h^2 + \kappa^2) q^2 \sinh^2 \xi + g \right] F (\xi) = 0 \tag{3.6a}$$

$$\left[\frac{\partial^2}{\partial \eta^2} + (h^2 + \kappa^2) q^2 \sin^2 \eta - g \right] G (\eta) = 0 \tag{3.6b}$$

where g is the separation constant. Equation 3.6b is called the Mathieu Equation and Eq. 3.6a the associate Mathieu Equation; their solutions are known as Mathieu Functions. All the equations thus far derived are valid in the dielectric and in the conductor.

Waves in Non-dissipative Elliptical Pipes

If the conductor has perfect conductivity, no energy may penetrate the wall. The boundary conditions require simply that the electric field intensity tangential to the boundary must vanish at the boundary. Since the dielectric is assumed to be a perfect insulator, the waves propagates through the pipe without attenuation. Therefore the

real part of the propagation constant h is zero. The solutions
of the wave equations 3.5a and 3.5b are then as follows:

$$E_x = \left[B_1 Se_n(\eta) Re_n(\xi) + B_2 So_n(\eta) Ro_n(\xi) \right] e^{i\omega t - i\beta x} \qquad 3.7a$$

$$H_x = \left[B_1 Se_n(\eta) Re_n(\xi) + B_2 So_n(\eta) Ro_n(\xi) \right] e^{i\omega t - i\beta x} \qquad 3.7b$$

where B_1 and B_2 are constants, taking care of the phases and
amplitudes of the wave; Se_n and So_n are the even and odd an-
gular Mathieu Functions, Re_n and Ro_n are the radial Mathieu
Functions of the first kind and nth order, and n is a posi-
tive integer. Both Mathieu Functions are functions of $(k^2 - \beta^2) q^2$.

The longitudinal components E_x and H_x may exist
at the same time in the pipe, but we shall study the two
simple types: the H-wave, with only transverse electric
field and both longitudinal and transverse magnetic fields;
and the E-wave, with only transverse magnetic field and both
longitudinal and transverse electric fields.

H-wave

Under the condition that $E_x = 0$, the remaining
components may be obtained from Eq. 3.4a', 3.4b', 3.4d' and
3.4e':

$$H_x = B \frac{Se_n}{So_n}(\eta) \frac{Re_n}{Ro_n}(\xi) e^{i(\omega t - \beta x)}$$

$$H_\xi = B \frac{-h}{q_1(\kappa^2 - \beta^2)} \frac{Se_n}{So_n}(\eta) \frac{Re_n'}{Ro_n'}(\xi) e^{i(\omega t - \beta x)}$$

$$H_\eta = B \frac{-h}{q_1(\kappa^2 - \beta^2)} \frac{Se_n'}{So_n'}(\eta) \frac{Re_n}{Ro_n}(\xi) e^{i(\omega t - \beta x)} \qquad 3.8$$

$$E_\xi = B \frac{i\omega\mu}{q(\kappa^2 - \beta^2)} \frac{Se_n'}{So_n'}(\eta) \frac{Re_n}{Ro_n}(\xi) e^{i(\omega t - \beta x)}$$

$$E_\eta = B \frac{-i\omega\mu}{q(\kappa^2 - \beta^2)} \frac{Se_n}{So_n}(\eta) \frac{Re_n'}{Ro_n'}(\xi) e^{i(\omega t - \beta x)}$$

$$E_x = 0 .$$

The primed Mathieu Functions denote their derivative with respect to ξ or η. The boundary condition requires that the tangential component of electric field $E_\eta \big|_{\xi = \xi_0} = 0$, where ξ_0 is the value for the boundary ellipse. Thus,

$$\left. \begin{matrix} Re'_n \\ Ro'_n \end{matrix} \right\}(\xi_0) = 0 .$$

The Re'_n and Ro'_n are also functions of $q\sqrt{k^2 - \beta^2}$, which is a constant and may be determined from the zeros of the radial Mathieu Functions for a given type of wave in a given elliptical pipe. When the operating frequency is so low that the value qk is equal to the above constant, the phase constant β is zero. This frequency or wave length is defined as the critical frequency f_0 or wave length λ_0, and the corresponding wave constant is denoted by k_0. Hence, the phase constant β of the non-dissipative wave may be determined as:

$$\beta = i \sqrt{k^2 - k_0^2}$$

$$= i \frac{\omega}{c} \sqrt{1 - (\frac{\lambda}{\lambda_0})^2} . \qquad\qquad 3.9$$

For wave lengths shorter than λ_0, the propagation constant is imaginary, and the wave travels unattenuated. For wave length longer than λ_0, the propagation is purely dissipative and no travelling wave may exist inside the pipe. The Eq. 3.8 may be simplified by substituting k_0 for $\sqrt{k^2 - \beta^2}$.

Other propagation properties, such as the wave length in the tube, the phase velocity and the group velocity

are the same as they are for waves in pipes of circular or rectangular cross-section of the same critical wave length (Eq. 2.5).

Solutions with a zero radial component of the electric field in the dielectric are generally impossible in elliptical pipes; only when the cross-section degenerates. into a circle are such solutions possible. For the H-wave, ($E_x = 0$), if E_ξ is to be zero, Eq. 3.4a' requires that $\frac{\partial H_x}{\partial \eta} = 0$ or H_x is independent of η. If this were true, the second derivative in the wave equation would vanish and leave

$$\left[(k^2 + h^2)\, q^2 \sin^2 \eta - g\right] H_x = 0 .$$

Since g is a constant, namely the separation constant, the above equality is not true unless both q and g are zero. The same reasoning may be applied to prove that $H_\eta \neq 0$ unless the pipe is circular.

E-wave

By putting $H_x = 0$ in Eq. 3.4a', 3.4b', 3.4d', and 3.4e', the remaining five components of field intensities are:

$$E_x = B \quad \frac{Se_n(\eta)}{So_n} \frac{Re_n(\xi)}{Ro_n} e^{i(\omega t - \beta x)}$$

$$E_\xi = -B \frac{i\beta}{q(\kappa^2 - \beta^2)} \frac{Se_n(\eta)}{So_n} \frac{Re_n'(\xi)}{Ro_n'} e^{i(\omega t - \beta x)}$$

$$E_\eta = -B \frac{i\beta}{q(\kappa^2 - \beta^2)} \frac{Se_n'(\eta)}{So_n'} \frac{Re_n(\xi)}{Ro_n} e^{i(\omega t - \beta x)} \qquad 3.10$$

$$H_\xi = B \frac{i\omega\epsilon}{q(\kappa^2 - \beta^2)} \frac{Se_n'(\eta)}{So_n'} \frac{Re_n(\xi)}{Ro_n} e^{i(\omega t - \beta x)}$$

$$H_\eta = -B \frac{i\omega \xi}{q(\kappa^2 - \beta^2)} \frac{Se_n}{So_n}(\eta) \frac{Re'_n}{Ro_n}(\xi) \, e^{i(\omega t - \beta x)}$$

$$H_x = 0 \qquad .$$

To satisfy the boundary conditions that E_x and E_η vanish at $\xi = \xi_o$, we set

$$\left. \begin{matrix} Re_n \\ Ro_n \end{matrix} \right\}(\xi_o) = 0 \qquad .$$

From this relation we are able to solve for $\sqrt{k^2 - \beta^2}$ and determine the critical w⌒ave length in a way similar to that used for the H-wave. The phase constant is therefore,

$$\beta = i\sqrt{\kappa^2 - \kappa_o^2} = i \frac{\omega}{c}\sqrt{1 - (\frac{\lambda}{\lambda_o})^2} \qquad . \qquad\qquad 3.9$$

Other properties may be derived from the critical wave length, being discussed in the section of H-wave. By a similar procedure, we may prove that none of the five components of fields may vanish unless the cross-section is a circle,——— a degenerate ellipse. The Eq. 3.10 may be simplified by substituting k_o for $\sqrt{k^2 - \beta^2}$.

What we have discussed so far are the general E- and H-waves in elliptical pipes. An H- or E-wave is defined to be a nth even or odd wave according to whether the solution of the component field H_x or E_x is the even or odd Mathieu Function of nth order. A prescript $\underline{e}$ or $\underline{o}$ is used to indicate the even or odd wave and a subscript n to indicate the order of the wave. Thus, we have the eH_o-, eH_1-, oH_1-, eE_o-, eE_1-, and oE_1-waves (read as the "even-E-zero" wave, etc.). The oH_o- and the oE_o-waves do not exist, since there is no odd Mathieu Function of zero order. Only the six waves of the lowest orders will be studied. Our investigation will

also be confined to the first zero of the radial Mathieu
Function for the E-waves and the first zero of the deriva-
tives of the radial Mathieu Functions for the H-waves. No
additional subscript will therefore be used to indicate the
nature of the zeros.

Mathieu Functions

We shall now review the property of the Mathieu
Functions of the first kind, and of zero and first orders.
The functions in series form as given by Prof. P. M. Morse
in his unpublished tables are the following:

$$Se_0 \left(\frac{2\pi q}{\lambda_0} ; \eta \right) = \sum_{m=0} D_{2m}^0 \cos (2m\eta)$$

$$Se_1 \left(\frac{2\pi q}{\lambda_0} , \eta \right) = \sum_{m=0} D_{2m+1}^1 \cos (2m + 1)\eta$$

$$So_1 \left(\frac{2\pi q}{\lambda_0} , \eta \right) = \sum_{m=0} F_{2m+1}^1 \sin (2m + 1)\eta$$

$$Re_0 \left(\frac{2\pi q}{\lambda_0} , \xi \right) = \sqrt{\frac{\pi}{2}} \sum_{m=0} (-1)^m D_{2m}^0 \; J_{2m} \left(\frac{2\pi q}{\lambda_0} \cosh \xi \right)$$

$$Re_1 \left(\frac{2\pi q}{\lambda_0} , \xi \right) = \sqrt{\frac{\pi}{2}} \sum_{m=0} (-1)^m D_{2m+1}^1 \; J_{2m+1} \left(\frac{2\pi q}{\lambda_0} \cosh \xi \right)$$

$$Ro_1 \left(\frac{2\pi q}{\lambda_0} , \xi \right) = \sqrt{\frac{\pi}{2}} \tanh \xi \sum_{m=0} (-1)^m F_{2m+1}^1 \; J_{2m+1} \left(\frac{2\pi q}{\lambda_0} \cosh \xi \right) .$$

3.11

The e and o of Se and So indicate that they are even or odd
functions about $\eta = 0$. There is no zero odd Mathieu Functions.
When q approaches zero as a limit, the ellipse degenerates
into a circle——all D's vanish, except one with subscript
= n, and the angular Mathieu Functions become the following
trigonometric functions:

$$\lim_{q \to 0} Se_n \left(\frac{2\pi q}{\lambda_0} , \eta \right) = \cos n\eta \qquad 3.12$$

$$\lim_{q \to 0} So_n \left(\frac{2\pi q}{\lambda_o}, \eta \right) = \sin n \eta .$$ 3.12

The radial Mathieu Functions and the angular ones of equal order subscripts have the same separation constant. When q approaches zero, ξ must be large and $q \cosh \xi$ is the radial coordinate r of the polar coordinates; and $\tanh \xi = 1$. Therefore the degenerate forms of the radial Mathieu Functions are

$$\lim_{q \to 0} Re_n \left(\frac{2\pi q}{\lambda_o}, \xi \right) = \sqrt{\frac{\pi}{2}} J_n \left(\frac{2\pi}{\lambda_o} r \right)$$

$$\lim_{q \to 0} Ro_n \left(\frac{2\pi q}{\lambda_o}, \xi \right) = \sqrt{\frac{\pi}{2}} J_n \left(\frac{2\pi}{\lambda_o} r \right) .$$ 3.13

Referring to the solution of waves inside the pipes of circular cross-section, we may consider them as degenerate cases of elliptical pipe waves. The following table corelates the wave in pipes of elliptical and circulat cross-section.

Table 3.1

$$\left. \begin{array}{c} \text{Waves in} \\ \text{Elliptic Pipe} \end{array} \right\} \text{degenerated into} \left\{ \begin{array}{c} \text{Waves in} \\ \text{Circular Pipe} \end{array} \right.$$

eE_o	E_o
$\left. \begin{array}{c} eE_1 \\ oE_1 \end{array} \right\}$	E_1
eH_o	H_o
$\left. \begin{array}{c} eH_1 \\ oH_1 \end{array} \right\}$	H_1

That the E_o- and the H_o-waves in circular pipes have a circular symmetry is probably the reason why there is only one corresponding wave for each in pipes of elliptical cross-section. The higher order waves in circular pipe do not

have a circular symmetry. The deformation of the circle may occur along either one of the two axes of symmetry in the cross-section; therefore, there are two waves for each order higher than zero in elliptical pipes.

Zeroes of Mathieu Functions

In general, there are n zero between $\eta = 0$ and π for the angular Mathieu Function. The following table shows the location of the zeros of the angular Mathieu Functions as based upon the series representation.

Table 3.2

Zeros of Angular Mathieu Functions

Angular Mat. Func.	No. of Zeros between $\eta = 0$ to 2π	η
$Se_0(\eta)$	0	$-----$
$\frac{\partial}{\partial\eta} Se_0(\eta)$	4	$0, \frac{\pi}{2}, \pi, \frac{3\pi}{2}$
$Se_1(\eta)$	2	$\frac{\pi}{2}, \frac{3\pi}{2}$
$\frac{\partial}{\partial\eta} Se_1(\eta)$	2	$0, \pi$
$So_1(\eta)$	2	$0, \pi$
$\frac{\partial}{\partial\eta} So_1(\eta)$	2	$\frac{\pi}{2}, \frac{3\pi}{2}$

The determination of the critical wave length depends upon the zeros of radial Mathieu Function at $\xi \neq 0$. The functions Ro_1, $\frac{\partial}{\partial\xi} Re_0$ and $\frac{\partial}{\partial\xi} Re_1$ are equal to zero when $\xi = 0$. The radial Mathieu Functions are periodic. So

[1] S. Goldstein, Trans. Camb. Phil. Soc., Vol. 23, No. 11, p. 326, Oct. (1927).---Footnote to next page.

far, there is no rule for determining their zeros except for large values of the variable where the asymptotic expressions may be used? However, for ellipses of not too large eccentricity, the Bessel Function series (Eq. 3.11) converges rather rapidly, and it would not be too difficult to use cut-and-try methods and numerical computation. The value of ξ_o for the zeros depends upon the constant $\frac{2\pi q}{\lambda_o}$. In Prof. Morse's Table, sets of D's are given for constant values of $\frac{2\pi q}{\lambda_o}$. Hence a reverse process is required to determine the size and eccentricity of the elliptical pipe that would fit the values of q and λ_o. In Fig. 3.3 are plotted the eccentricities of ξ_o ellipse against $2\pi\frac{q\cosh\xi_o}{\lambda_o}$. The constant "$q\cosh\xi_o$" is the semi-major axis of the ellipse, and λ_o is the critical wave length. Hence the ratio is equivalent to $2\pi\frac{r_o}{\lambda_o}$ of circular pipe. For eccentricity $=\frac{1}{\cosh\xi} = 0$, the ordinates are the roots of the Bessel Functions or their derivatives.

If we reduce the length of the minor axis ($= 2q\sinh\xi_o$) of the boundary ellipse of an elliptical pipe gradually to zero, while keep the length of major axis ($=2q\cosh\xi_o$) constant, the Fig. 3.3 represents the variation of the critical frequency f_o with the eccentricity, (since $f_o \propto \frac{1}{\lambda_o}$). The critical frequencies of all waves, except those of the eH_1-wave, go to infinity as the ellipse degenerates into a straight line. The critical frequency of eH_1-wave remains
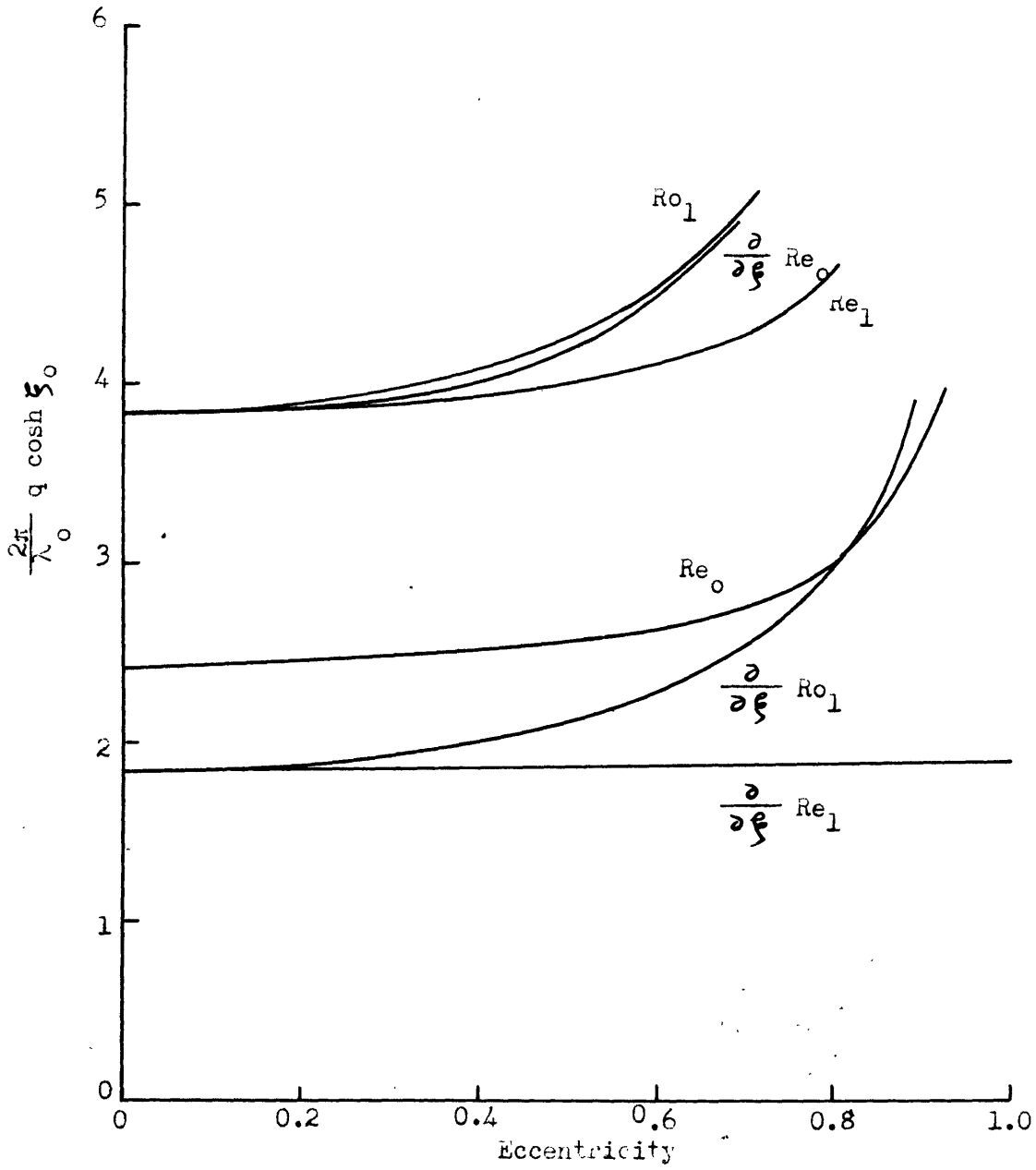
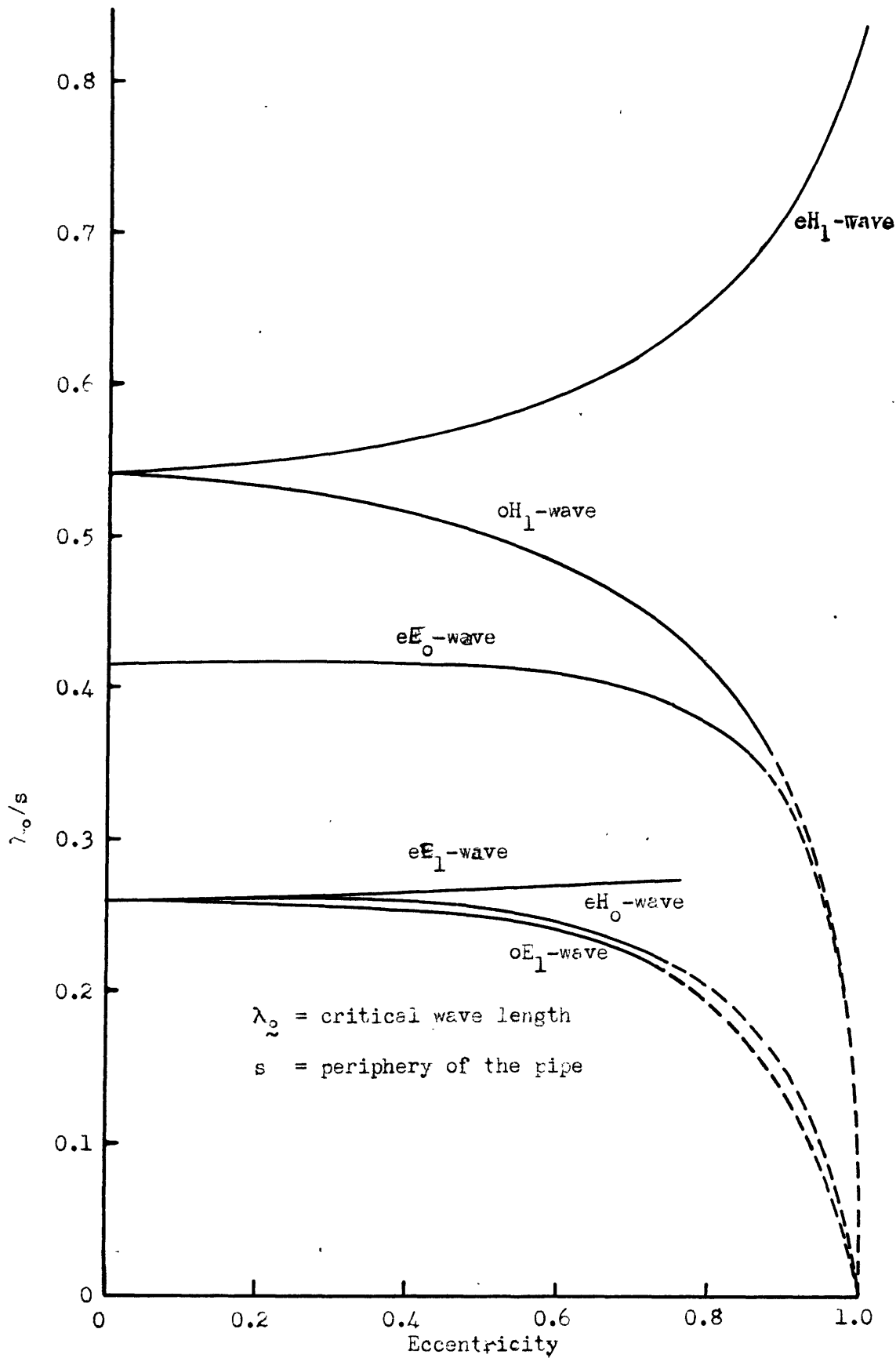Fig. 3.3 Zeros of Radial Mathieu Functions and Their Derivatives.

Fig. 3.4

fairly constant and approaches a finite value as the ellipse becomes a line. So far the critical frequency is concerned, this particular type of wave behaves exactly like the $H_{0,1}$-wave in rectangular pipes, when the dimension "a" is reduced to zero while the dimension "b" is kept constant.

It is probably fair to compare the critical wave length of waves in elliptical pipes of equal peripheries. Practically, this is the situation when a circle is deformed into ellipse by pressing the circle along one of the diameters. The periphery of an ellipse is:

$$s = \int_0^{2\pi} q_1 \, d\eta = \int_0^{2\pi} q \sqrt{\sinh^2 \xi_0 + \sin^2 \eta} \, d\eta$$

or

$$\frac{s}{q \cosh \xi_0} = \int_0^{2\pi} \sqrt{1 - \left(\frac{\cos \eta}{\cosh \xi_0}\right)^2} \, d\eta \, . \qquad 3.14$$

The left side of Eq. 3.14 is the ratio of the length of periphery to the length of the semi-major axis, and the right side is an Elliptical Integral, for which, tables are available. In Fig. 3.4 is plotted the ratio of $\frac{\lambda_0}{s}$ against the eccentricity $\frac{1}{\cosh \xi_0}$ of the boundary ellipse. All the curves drop to zero at eccentricity = 1, except the curve for eH_1-wave. The latter has a value of $\frac{\lambda_0}{s} = 0.84$. Under the similar condition, the ratio $\frac{\lambda_0}{s}$ of the $H_{0,1}$-wave in rectangular pipe is equal to unity.

Field Configuration

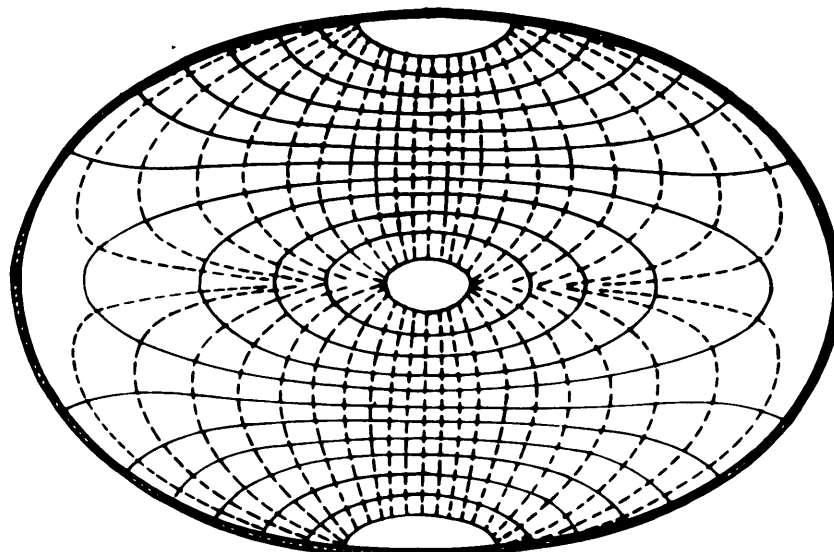In the cross-section of the elliptical pipe,

Fig. 3.5a
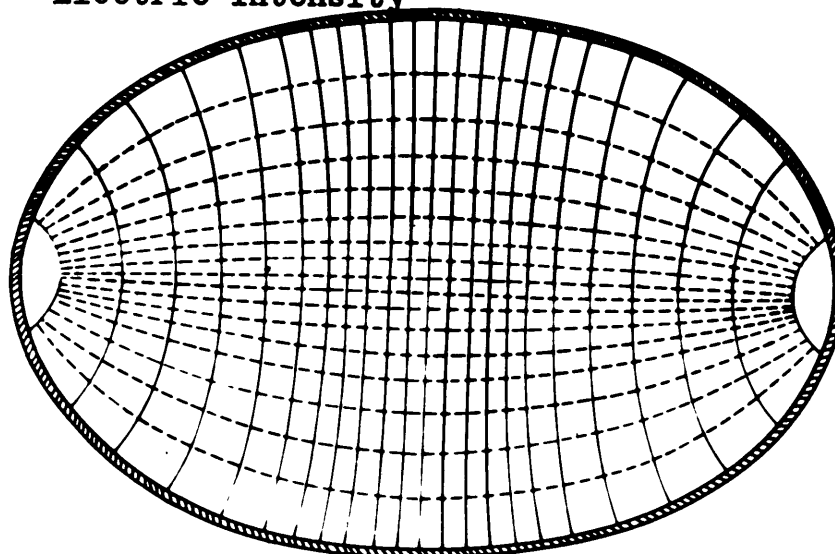eH$_0$-wave

----- Magnetic Intensity
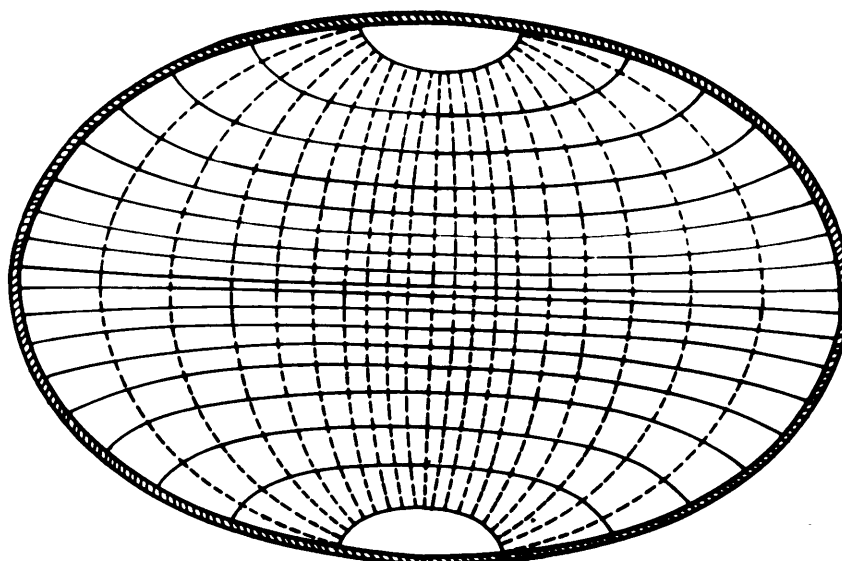——— Electric Intensity
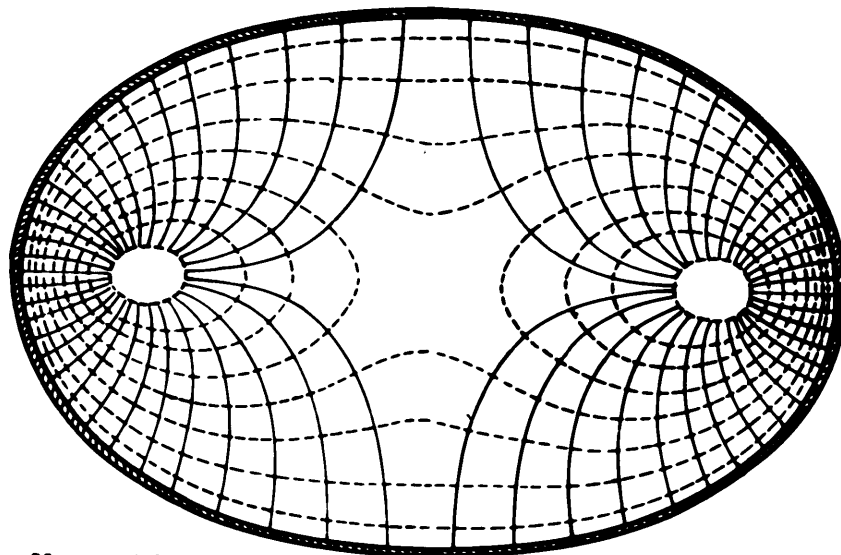
Fig. 3.5b
eH$_1$-wave

Fig. 3.5c
oH$_1$-wave

Fig. 3.6a
eE₀-wave

----- Magnetic Intensity
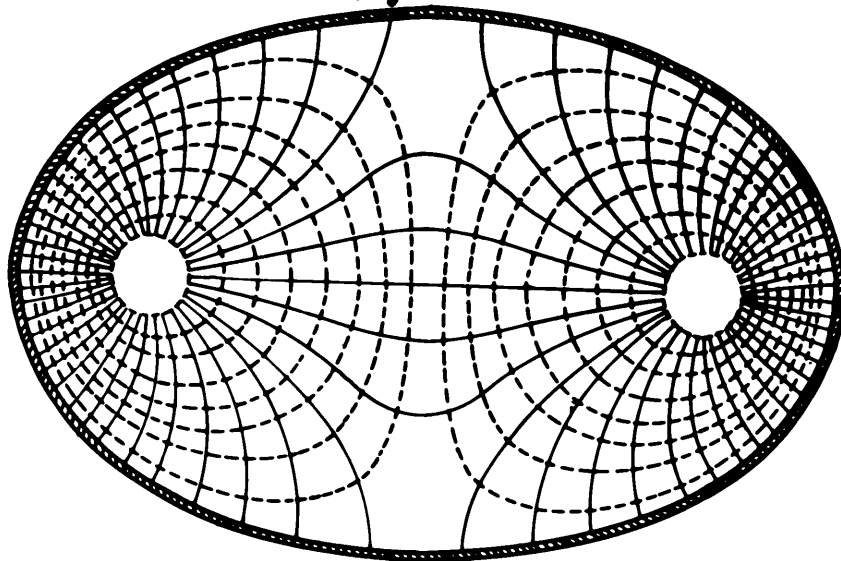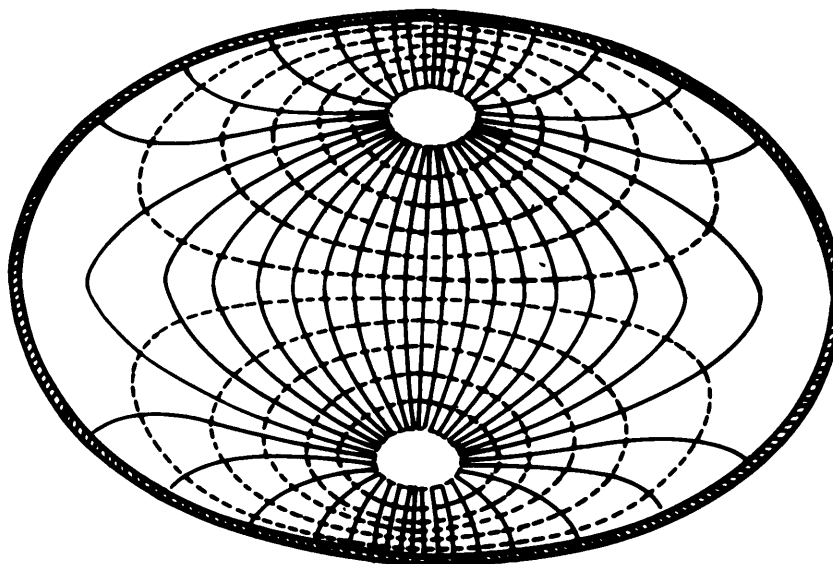—— Electric Intensity

Fig. 3.6b
eE₁-wave

Fig. 3.6c
oE₁-wave

the electric and magnetic field intensities are equal in time phase. For any one of the simple waves, we may find that

$$\left| \frac{E_\xi}{E_\eta} \right| = \left| \frac{H_\eta}{H_\xi} \right|$$

That is, the components of electric and magnetic field intensities in the cross-section are always normal to each other. Since there are longitudinal components of fields, the lines of force donot necessarily form closed|obe or terminate normal to the boundary. Ordinary method of flux plotting for two dimensional electrostatic or magnetic field by forming squares cannot be applied here.

In the present investigation, an arbitrary ellipse is chosen. From its semi-focal length q and the eccentricity e, the constant $\frac{2\pi q}{\lambda_o}$ may be determined from Fig. 3.4. Then, the zeros and the directions (whether positive or negative) of the transverse component fields may be determined and plotted in the ellipse on separate sheets. By adding these components vectorially, the approximate directions of the resultant fields must lie between E_ξ and E_η if both exist, or in the hyperbolic direction if E is zero and so on. Finally, smooth lines are drawn to link points with constant changing slope, under the rule that the electric and magnetic lines are normal to each others. The results are not as accurate as those for square pipes, but serve the purpose.

Fig. 3.5a to Fig. 3.6c show the field distributions of the first six waves in the cross-section obtained by

the above method. This particular ellipse has an eccentricity $\frac{1}{\cos \xi_o}$ = 0.75. A set of field distribution diagrams of waves in circular pipe shown in Southworth's paper may serve as the degenerate case of the present diagrams.

Referring to Fig. 1 of Southworth's paper, the so-called even or odd waves correspond to two types of deformation of a circular-pipe wave. If we lengthen the vertical diameter and shorten the horizontal diameter, the waves are deformed into the even waves. If the vertical diameter is shortened and the horizontal diameter lengthened, the results will be the odd waves. Since the H_o-wave or E_o-wave in a circular pipe has a perfectly symmetrical field distribution, there is only one type of deformed wave no matter along what diameter the cross-section is deformed into ellipse.

The field distribution of the eH_o-wave is shown in Fig. 3.5a. Part of the electric lines form con-center lobes, and the rest terminate on the boundary. As the eccentricity of the ellipse becomes less, the lobe portion looks more circular and less electric lines terminate on the boundary. At the same time, the curvatures of the magnetic lines are gradually straightened up. When the ellipse degenerates into a circle, all the electric lines become circular and the magnetic lines become straight radial lines. The vanishing of the electric field normal to the boundary is responsible for the ever-decreasing of attenuation with increasing

frequency.

For the eE_0-wave (Fig. 3.6a) the foci of the ellipse, in these cross-sectional diagrams, look something like sinks or sources of the electric lines. Part of the magnetic lines forms closed lobes around each focus. As the eccentricity increases, the length between the foci is shortened,and such magnetic lines find less space for themselves. Eventually, such lines vanishes for a circular pipe.

For the H_1-wave in a circular pipe, there are two corresponding waves in elliptical pipes; because the field distribution has two lines of symmetry instead of a single point of symmetry. The lines of forces of the H_1- wave of a circular pipe are almost parallel. This wave has the lowest cut-off frequency. In an elliptical pipe (Fig. 3,5b,c) the lines of forces become more parallel. For the eH_1-wave, the configuration of the magnetic lines become elongated, while for oH_1-wave, the electric lines become elongated. If we compare the eH_1- and the oH_1-waves with the $H_{0,1}$-wave ($\lambda_0 = 2b$) and the $H_{1,0}$-wave ($\lambda_0 = 2a$) in rectangular pipes ($a < b$), we may see why for ellipses of constant periphery, the critical wave length λ_0 of the eH_1-wave increases, and that of the oH_1-wave decreases with increasing eccentricity.

For large eccentricity, the magnetic lines of the eE_1-wave (Fig. 3.6b) form closed lobes around each focus. As the foci are moved nearer to the center, such lobes follow

along until the eccentricity is about 0.7. Then they stay
right there as the foci are moved closer, This phenomena may
be explained mathematically, in that a new zero of $Re\xi$ appears
between $\xi = 0$ and $\xi = \xi_o$ when the eccentricity is less than
0.7, which stops the shifting.

The field distribution of the oE_1-wave may be
obtained from the eE_1-wave by carrying out a ninety degree ro-
tation of the latter. Both waves have a close resemblance to
the E_o-wave of a circular pipe.

Attenuation of Waves in the Elliptical Pipes

Before calculating the attenuation of waves in
pipes of elliptical cross-section, let us see first what the
difficulties are, so as to justify the necessary approxima-
tions used hereafter. In the problems of circular and rec-
tangular pipes we have learned that, strictly speaking, no
simple E- or H-waves as defined heretofore may exist in a
finitely conducting metal pipe. Instead, all six components
of fields must be present. The same situation prevails in
the present problem. In addition to that, as in the case
of a rectangular pipe , an elliptical pipe does not possess
circular symmetry. The variations of the wave functions
along the two orthogonal coordinates in the cross-section of
the pipes are all dependent upon the constants of materials

used and the dimensions of the pipe. Therefore, if inside the pipe, there were a wave which might be represented by Mathieu Function of a single order, the wave outside would likely have to be represented by a infinite series of Mathieu Functions in order that the boundary conditions might be satisfied.

Fortunately, the conductivities of the ordinary commercial metals likely to be used for hollow pipes are so very large, though not infinite, that we are able to use the two following approximations: (1) The field inside the pipe is not appreciably effected by the imperfect conductivity, so that the fields inside the pipe remain essentially one of the types considered before, but very slightly modified. (2) In the conductor, the asymptotic forms of the wave functions for large values of ξ may be used.

Since the wave can only penetrate the conductor by an infinitesimal distance, we may limit our investigation to the region of the conductor in the immediate neighborhood of the boundary. The dielectric is assumed to be a perfect insulator. The metallic wall is assumed to be thick enough to dissipate all the energy penetrating from the interior.

An H-wave or an E-wave in a dissipative hollow pipe may be defined as one, which would degenerate into the H-wave or the E-wave of non-dissipative pipe, were the conductivity of the conducting wall to become infinitely large. Eq. 3.8 and 3.10 for the fields in the non-dissipative ellip-

tical pipe will be used with necessary modifications for the fields in the dielectric portion of the dissipative pipe.

The Maxwell equations and the wave equations for the longitudinal components of fields, $H_x^!$ and $E_x^!$, in the metal are as in Eq. 3.4 and 3.5. The constant $i\omega\epsilon'$ may be neglected. The wave functions and constants in the conductor are primed to differentiate them from those in the dielectric. Since the propagation constant h of all the waves in the X-direction must be the same in both the conductor and the dielectric, it is negligible as compared to the wave constant k' of the conductor. Hence

$$k'^2 + h^2 \cong k'^2.$$

The wave equations of $E_x^!$ or $H_x^!$, after separating the variables, become

$$[\tfrac{\partial^2}{\partial\xi^2} + (K'q \sinh\xi)^2 + g]\, H_x' = 0$$

$$[\tfrac{\partial^2}{\partial\eta^2} + (K'q \sin\eta)^2 - g]\, H_x' = 0.$$

3.15

The solution of $H_x^!$ or $E_x^!$ will be of the form

$$\sum_{m=0}^{\infty} A_m \, Re_m^4\,(K'q,\,\xi)\, Se_m(K'q,\eta)\, e^{i(\omega t - \beta x)}.$$

3.16

where Re_m^4 are the even radial Mathieu Functions of the fourth kind, and $i\beta$ is the approximate value of the propagation constant h. Of course, there is a similar solution of odd Mathieu Functions.

Prof. Stratton[1] has treated the radial Mathieu Functions of fourth kind, which for the even functions are defined as

$$Re_m^4 = Re_m^1 - iRe_m^2.$$

[1] J.A.Stratton, Proc. Nat. Acad. of Sciences, Vol.21, No.1, pp. 51-62, Jan. (1935), and No. 6, pp. 316-321, June (1935).

The exponentials denote the kinds of Mathieu Function. The asymptotic forms for large k'qcosh ξ are

$$Re_m^1 \cong (K'q \cosh \xi)^{-\frac{1}{2}} \cos(K'q\cosh\xi - \frac{2m+1}{4}\pi)$$

$$Re_m^2 \cong (K'q\cosh\xi)^{-\frac{1}{2}} \sin(K'q\cosh\xi - \frac{2m+1}{4}\pi)$$

and therefore,

$$Re_m^4 \cong (K'q\cosh\xi)^{-\frac{1}{2}} e^{-i(K'q\cosh\xi - \frac{2m+1}{4}\pi)} \qquad 3.17$$

Then H_x' or E_x' for the even waves are as following:

$$H_x' = (K'q\cosh\xi)^{-\frac{1}{2}} e^{i(\omega t - \beta x - K'q\cosh\xi)} \sum A_m e^{i(\frac{2m+1}{4}\pi)} Se_m(K'q,\eta)$$

$$= B'(K'q\cosh\xi)^{-\frac{1}{2}} e^{i(\omega t - \beta x - K'q\cosh\xi)} Te_n(K'q,\eta) \qquad 3.18$$

The factor $Te_n(k'q, \eta)$ represents the summation and is only a function of η and k'q. B' is a new constant.

H-wave

Inside a finitely conducting pipe, the electric fields tangential to the boundary no longer vanish at the boundary, but they have a very small amplitude. The tangential magnetic fields, H_η and H_x, which do not vanish at the boundary in the case of perfect conductivity, are not appreciably affected by the finite conductivity. Hence, we may select from Eq. 3.8, for the even H-waves:

$$H_x \cong B\, Re_n(\xi)\, Se_n(\eta)\, e^{i\omega t - i\beta x}$$

$$H_\eta \cong B\, \frac{-i\beta}{q_i K_o^2}\, Re_n(\xi)\, Se'(\eta)\, e^{i\omega t - i\beta x} \qquad 3.19$$

In the conductor, assume that,

$$H_x' = B'(K'q\cosh\xi)^{-\frac{1}{2}} e^{i(\omega t - \beta x - K'q\cosh\xi)} Te_n(\eta), \qquad 3.20$$

$$H'_\eta = C'(K'q\cosh\xi)^{-\frac{1}{2}} e^{i(\omega t - \beta x - K'q\cosh\xi)} Te'_n(K'q, \eta) \qquad 3.21$$

where Te'_n is the derivative of Te_n with respect to η. The H'_η in this form may be proven to satisfy its own wave equation.

Equate the H_x to H'_x, the tangential magnetic intensities at the boundary $\xi = \xi_o$, and solve for B':

$$B' = B\, Re_n(\xi_o)\sqrt{k'q\cosh\xi}\; e^{ik'q\cosh\xi_o} \frac{Se_n(\eta)}{Te_n(\eta)}.$$

Since $Se_n(\eta)$ and $Te_n(\eta)$ are only functions of η while the remaining factors are not, the ratio $\frac{Se_n(\eta)}{Te_n(\eta)}$ must be equal to a constant. We may arbitrary set the ratio equal to unity since the amplitude of $Te_n(\eta)$ so far is not definite. The angular Mathieu Function in the metal is the same as that in the dielectric. Consequently, $Te'_n(\eta) = Se'_n(\eta)$ and

$$B' = BRe_n(\xi_o)\sqrt{k'q\cosh\xi_o}\; e^{ik'q\cosh\xi_o} \qquad 3.22$$

Equate the H_η and H'_η, the tangential magnetic intensity at the boundary $\xi = \xi_o$, and solve for C':

$$C' = -B\frac{1}{q_1 k_o^2}\, Re_n(\xi_o)\sqrt{k'q\cosh\xi_o}\, e^{ik'q\cosh\xi_o} \qquad 3.23$$

With known H'_η and H'_x, the remaining tangential electric field in the metal may be found by Eq. 3.4a', b', c' and d'. The four tangential components of field in the metal near the boundary are as follows:

$$H'_x = B\, Re_n(\xi_o)\, Se_n(\eta)\sqrt{\frac{\cosh\xi_o}{\cosh\xi}}\; e^{i[\omega t - \beta x - K'q(\cosh\xi - \cosh\xi_o)]}$$

$$E'_x = B\frac{\omega\mu' i\beta}{K'q\sinh\xi\, K_o^2}\, Re_n(\xi_o)\, Se'_n(\eta)\sqrt{\frac{\cosh\xi_o}{\cosh\xi}}\; e^{i(\omega t - \beta x - K'q(\cosh\xi - \cosh\xi_o))}$$

$$H'_\eta = -B\frac{i\beta}{q_1 K_o^2}\, Re_n(\xi_o)\, Se'_n(\eta)\sqrt{\frac{\cosh\xi_o}{\cosh\xi}}\; e^{i[\omega t - \beta x - K'q(\cosh\xi - \cosh\xi_o)]} \qquad 3.24$$

$$E_\eta' = B \frac{\omega \mu' q \sinh \xi}{K' q_1} Re_n(\xi_o) Se_n(\eta) \sqrt{\frac{\cosh \xi_o}{\cosh \xi}} e^{i(\omega t - \beta x - Kq(\cosh \xi - \cosh \xi_o))} \Bigg]$$

.

At the boundary $\xi = \xi_o$.

$$H_x' = B \qquad Re_n(\xi_o) Se_n(\eta) e^{i(\omega t - \beta x)}$$

$$E_x' = B \frac{\omega \mu'}{K' q \sinh \xi_o K_o^2} \frac{i\beta}{} Re_n(\xi_o) Se_n'(\eta) e^{i(\omega t - \beta x)}$$

$$H_\eta' = -B \frac{i\beta}{q_1 K_o^2} \qquad Re_n(\xi_o) Se_n'(\eta) e^{i(\omega t - \beta x)} \qquad\qquad 3.25$$

$$E_\eta' = B \frac{\omega \mu' q \sinh \xi_o}{K' q_1} Re_n(\xi_o) Se_n(\eta) e^{i(\omega t - \beta x)}$$

.

The longitudinal component of electric intensity E_x' does not really vanish in the dissipative pipes.

The loss per unit area, dissipated into the metal at the boundary is:

$$= \frac{1}{2} \left[-E_x' H_\eta' + E_\eta' H_x' \right]_{real\ part}$$

$$= -\frac{1}{2\sqrt{2}} \sqrt{\frac{\omega \mu'}{\sigma'}} \frac{|B|^2}{q_1} \left[Re_n(\xi_o) \right]^2 \left\{ \frac{\beta^2 \left[Se_n'(\eta) \right]^2}{K_o^4 q \sinh \xi_o} + q \sinh \xi_o \left[Se_n(\eta) \right]^2 \right\}$$

.

Obtain the total power loss per unit length of the tube,

$$L = \int_o^1 \int_o^{2\pi} \left[loss/\ cm^2 \right] q_1\ d\eta\ dx$$

$$= -\frac{|B|^2}{2\sqrt{2}} \sqrt{\frac{\omega \mu'}{\sigma'}} \left[Re_n(\xi_o) \right]^2 \left[\frac{\beta^2}{K_o^4 q \sinh \xi_o} M_\eta + q \sinh \xi_o N_n \right] \qquad 3.26$$

where

$$M_n = \int_o^{2\pi} \left[Se_n'(\eta) \right]^2 d\eta$$

$$N_n = \int_o^{2\pi} \left[Se_n(\eta) \right]^2 d\eta \qquad\qquad 3.27a$$

The total power transmitted through the pipe:

$$S = \frac{1}{2} \int_o^{2\pi} \int_\xi^{\xi_o} \left[E_\xi H_\eta - E_\eta H_\xi \right] q_1^2\ d\xi\ d\eta$$

$$= \frac{1}{2} \frac{\omega \mu \beta |B|^2}{2 K_o^4} \int_o^{\xi_o} \left\{ \left[Re_n(\xi) \right]^2 M_n + \left[Re_n'(\xi) \right]^2 N_n \right\} d\eta \qquad 3.28$$

.

The attenuation constant is therefore,

$$\alpha = \frac{1}{2} \frac{L}{S}$$

$$= \sqrt{\frac{\pi \mu' \ell}{\sigma' \mu}} \frac{\sqrt{f_0}}{2q \sinh \xi_0} \left[1 - \left(\frac{f_0}{f}\right)^2 \right]^{-\frac{1}{2}} .$$

$$\frac{\left[\left(\frac{f}{f_0}\right)^{\frac{1}{2}} + \left(\frac{N_n}{M_n} K_0^2 q^2 \sinh^2 \xi_0 - 1\right)\left(\frac{f_0}{f}\right)^{\frac{3}{2}}\right] \left[Re_n(\xi_0)\right]^2}{\int_0^{\xi_0} \left[Re_n(\xi)\right]^2 d\xi + \frac{N_n}{M_n} \int_0^{\xi_0} \left[Re_n'(\xi)\right]^2 d\xi} \qquad \text{nepers per cm.} \qquad 3.29a$$

Similarly, we may prove that for the odd H_n-waves, the attenuation constant is

$$\alpha = \sqrt{\frac{\pi \mu' \ell}{\sigma' \mu}} \frac{\sqrt{f_0}}{2q \sinh \xi_0} \left[1 - \left(\frac{f_0}{f}\right)^2\right]^{-\frac{1}{2}} \frac{\left[\left(\frac{f}{f_0}\right)^{\frac{1}{2}} + \left\{\left(\frac{N_n'}{M_n'}\right) K_0^2 q^2 \sinh \xi_0 - 1\right\}\left(\frac{f_0}{f}\right)^{\frac{3}{2}}\right] \left[Ro_n(\xi_0)\right]^2}{\int_0^{\xi_0} \left[Ro_n(\xi)\right]^2 d\xi + \frac{N_n}{M_n} \int_0^{\xi_0} \left[Ro_n'(\xi)\right]^2 d\xi} \quad \text{nepers/cm.} \quad 3.29b$$

where

$$M_n' = \int_0^{2\pi} \left[So_n'(\eta)\right]^2 d\eta$$

$$N_n' = \int_0^{2\pi} \left[So_n(\eta)\right]^2 d\eta .$$

3.27b

E-wave

The attenuation of the E-wave may be calculated in a similar way as for the H-wave. The even wave will be considered first. The component fields for the non-dissipative case are given by Eq. 3.10. Out of the five components, there is only one tangential magnetic field H_η which does not vanish at the boundary. Since the magnitude and phase of H_η is only slightly affected by the finite conductivity, the boundary condition is that the H_η' in the conductor must be equal to it. From Eq. 3.10, for even waves, we have:

$$H_\eta = B \frac{-i\omega \ell}{q_1 k_0^2} Re_n'(\xi) Se_n(\eta) e^{i\omega t - i\beta x} . \qquad 3.10$$

Inside the metal, the longitudinal electric

field is:

$$E'_x = B' \, Te_n(\eta) \, \frac{1}{\sqrt{k' q \cosh \xi}} \, e^{i(\omega t - \beta x - K' q \cosh \xi)} \qquad 3.30a$$

The longitudinal magnetic field H'_x, if any, has a magnitude of infinitesimal order. From E'_x and by Eq. 3.4b', e', H'_η may be found as follows:

$$H'_\eta = B' \frac{\sigma'}{q_1 K'^2} \, Te_n(\eta) \frac{i K' q \sinh \xi}{\sqrt{K' q \cosh \xi}} \, e^{i(\omega t - \beta x - K' q \cosh \xi)} \qquad 3.30b$$

Equate H'_η and H_η at the boundary $\xi = \xi_0$, and solve for A':

$$B' = -B \frac{\omega \xi K'}{\sigma' K_0^2} \frac{Re'_n(\xi_0)}{q \sinh \xi_0} \sqrt{K' q \cosh \xi_0} \, e^{i K' q \cosh \xi_0} \frac{Se_n(\eta)}{Te_n(\eta)} \qquad 3.31$$

The ratio $\dfrac{Se_n(\eta)}{Te_n(\eta)}$ must be equal to a constant. Let it be equal to unity. Thus, $Se_n(\eta) = Te_n(\eta)$ and consequently, $Se'_n(\eta) = Te'_n(\eta)$.

In the metal and near the boundary:

$$E'_x = -B \frac{\omega \xi}{K_0^2} \sqrt{-\frac{i \omega \mu}{\sigma'}} \frac{Re'_n(\xi_0)}{q \sinh \xi_0} Se_n(\eta) \sqrt{\frac{\cosh \xi_0}{\cosh \xi}} \, e^{i[\omega t - \beta x - K' q(\cosh \xi - \cosh \xi_0)]}$$

$$\qquad 3.30$$

$$H'_\eta = -B \frac{i \omega \xi}{q_1 K_0^2} Re'_n(\xi_0) Se_n(\eta) \frac{\sinh \xi}{\sinh \xi_0} \sqrt{\frac{\cosh \xi_0}{\cosh \xi}} \, e^{i[\omega t - \beta x - K' q(\cosh \xi - \cosh \xi_0)]}$$

At the boundary:

$$E'_x = -B \frac{\omega \xi}{K_0^2} \sqrt{-\frac{i \omega \mu}{\sigma'}} \frac{Re'_n(\xi_0)}{q \sinh \xi_0} Se_n(\eta) e^{i(\omega t - \beta x)}$$

$$H'_\eta = -B \frac{i \omega \xi}{q_1 K_0^2} Re'_n(\xi_0) Se_n(\eta) e^{i(\omega t - \beta x)} \qquad 3.32$$

The loss per square centimeter into the conductor at its boundary is:

$$= -\frac{1}{2} E'_x H'_\eta$$

$$= -\frac{|B|^2}{2\sqrt{2}} \sqrt{\frac{\omega \mu}{\sigma'}} \frac{\omega^2 \xi^2}{K_0^4} \frac{[Re'_n(\xi_0) Se_n(\eta)]^2}{q_1 q \sinh \xi_0}$$

The total power loss into the metal per cm² of the tube:

$$L = \int_0^1 \int_0^{2\pi} [\text{loss}/\text{cm}^2] \, q_1 \, d\eta \, dx$$

$$= -\frac{|B|^2}{2\sqrt{2}} \sqrt{\frac{\omega\mu}{\sigma}} \left[\frac{\omega\xi}{k_0^2} Re_n'(\xi_0)\right]^2 \frac{N_n}{q \sinh \xi_0} \, . \qquad 3.33$$

The total power transmitted through the pipe is obtained by calculating the Poynting Vector in axial direction, using fields inside a non-dissipative pipe,

$$S = \frac{1}{2} \int_0^{2\pi} \int_0^{\xi_0} [E_\xi H_\eta - E_\eta H_\xi] \, q^2 \, d\xi \, d\eta$$

$$= |B|^2 \frac{\beta\omega\xi}{2k_0^4} \int_0^{\xi_0} [M_n \{Re_n(\xi)\}^2 + N_n \{Re_n'(\xi)\}^2] \, d\xi \qquad 3.34$$

The attenuation constant, in nepers per cm. is,

$$\alpha = \frac{1}{2} \frac{L}{S}$$

$$= \sqrt{\frac{\pi\mu\xi}{\sigma'\mu}} \frac{\sqrt{f_0}}{2q \sinh\xi_0} \frac{(f/f_0)^{1/2}}{\sqrt{1-(f_0/f)^2}} \frac{[Re_n'(\xi_0)]^2}{\frac{M_n}{N_n} \int_0^{\xi_0} [Re_n(\xi)]^2 d\xi + \int_0^{\xi_0} [Re_n'(\xi)]^2 d\xi} \qquad 3.35a$$

Similarly the attenuation constant of the odd E_n-wave may be found to be:

$$\alpha = \sqrt{\frac{\pi\mu\xi}{\sigma'\mu}} \frac{\sqrt{f_0}}{2q \sinh\xi_0} \frac{(f/f_0)^{1/2}}{\sqrt{1-(f_0/f)^2}} \frac{[Ro_n'(\xi_0)]^2}{\frac{M_n'}{N_n'} \int_0^{\xi_0} [Ro_n(\xi)]^2 d\xi + \int_0^{\xi_0} [Ro_n'(\xi)]^2 d\xi} \qquad 3.35b$$

The problem confronting us is how to evaluate these integrals, M_n, N_n, etc. The value of N_n and N_n' for different angular Mathieu Functions of various value of $k_0 q$ has been calculated by Prof. Morse in his Table. By differentiating the angular Mathieu Function in its series form, we have,

$$Se_0' \left(\frac{2\pi q}{\lambda_0}, \eta\right) = -\sum_{m=1} 2m \, D_{2m}^0 \sin(2m\eta) .$$

$$Se_1'(\frac{2\pi q}{\lambda_o}, \eta) = -\sum_{m=0} (2m+1) D_{2m+1}' \sin(2m+1)\eta$$

$$So_1'(\frac{2\pi q}{\lambda_o}, \eta) = \sum_{m=0} (2m+1) F_{2m+1}' \cos(2m+1)\eta .$$

3.36

The integral of their square from 0 to 2π or from π to $-\pi$ are therefore,

$$M_o = \int_o^{2\pi} [Se_o'(\eta)]^2 d\eta = \pi \sum_{m=1} (2m \, D_{2m})^2$$

$$M_1 = \int_o^{2\pi} [Se_1'(\eta)]^2 d\eta = \pi \sum_{m=0} [(2m+1) D_{2m+1}]^2$$

3.37

$$M_1' = \int_o^{2\pi} [So_1'(\eta)]^2 d\eta = \pi \sum_{m=0} [(2m+1) F_{2m+1}']^2 .$$

Based upon the above three series, M's are calculated. In Fig. 3.7, the ratio $\frac{M}{N}$'s are plotted. For a circle, q = 0, $\frac{M_o}{N_o}$ is zero and $\frac{M_1}{N_1} = \frac{M_1^*}{N_1^*}$ equal unity.

The square of the radial Mathieu Functions or their derivatives at the boundary $\xi = \xi$, may be calculated directly from Prof. Morse's Table. They are plotted in Fig. 3.8.

The analytic method for integration of the squares of the radial Mathieu Functions or their derivatives has not been developed yet. In the present investigation, attempts have been made trying to replace the Bessel Functions in Eq. 3.11 by hyperbolic functions and to develop the squares of these series into series of hyperbolic functions. The latter would be integrable, but a large number of terms would have to be used because the series converge slowly. Also, an integration of the square of Eq. 3.11 has been tried, but the products of Bessel Functions are not always integrable.

Finally, it was decided to use a graphical

Fig. 3.7

Integration of Square of
Angular Mathieu Functions

$\dfrac{M_1}{N_1}$

$\dfrac{M_1'}{N_1'}$

$\dfrac{M_0}{N_0}$

3.0

2.5

2.0

1.5

1.0

0.5

Odd function

Even function

4 3 2 1 0 1 2 3 4

$2\pi q/\lambda_0$

4

$10\times[\text{Re}_1(\xi_0)]^2$

$10\times[\text{Re}_1(\xi_0)]^2$

$[\frac{\partial}{\partial\xi}\text{Re}_1(\xi)]^2$

$[\frac{\partial}{\partial\xi}\text{Re}_1(\xi_0)]^2$

3

$[\frac{\partial}{\partial\xi}\text{Re}_0(\xi_0)]^2$

2

Fig. 3.8

Square of Radial Mathieu
Functions

$10\times[\text{Re}_0(\xi_0)]^2$

1

Odd Functions

Even Functions

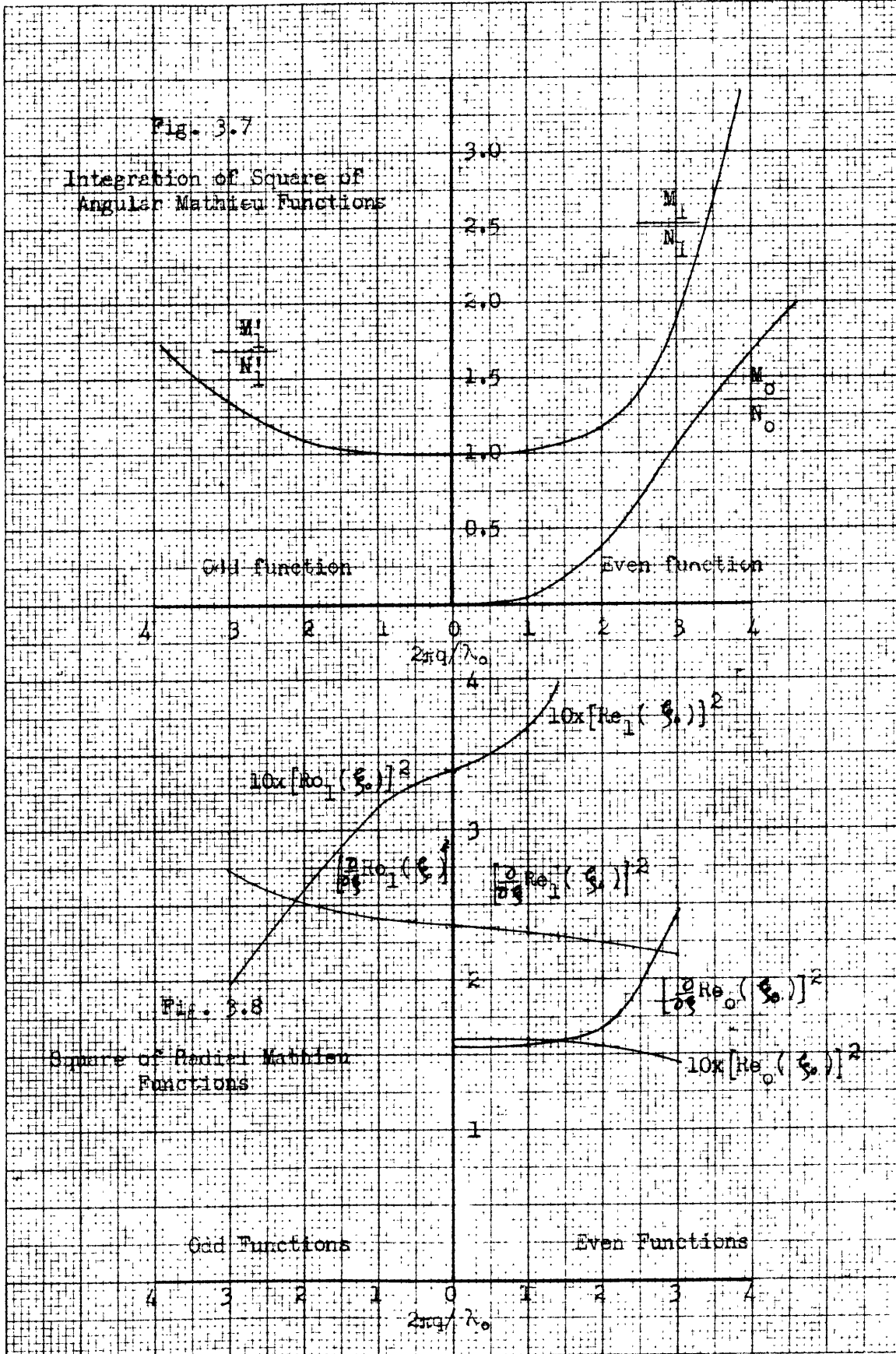4 3 2 1 0 1 2 3 4

$2\pi q/\lambda_0$

Table 3.3

Integration of Square of Radial Mathieu's

Functions and Their Derivatives

Wave	$\dfrac{2\pi q}{\lambda_0}$	ξ_0	$\dfrac{2}{\pi}\displaystyle\int_0^{\xi_0} R^2\, d\xi$	$\dfrac{2}{\pi}\displaystyle\int_0^{\xi_0} (\dfrac{dR}{d\xi})^2 d\xi$
eH_0	1	2.04	.753	1.163
	2	1.36	.2515	1.052
	3	1.01	.1042	.991
$e\,H_1$	1	1.23	.3364	.0458
	1.414	.78	.2865	.00645
oH_1	1	1.37	.1979	.2474
	2	.81	.1009	.3806
	3	.56	.0556	.4828
eE_0	1	1.57	.718	.745
	2	.915	.219	.638
	3	.596	.0791	.546
eE_1	1	2.03	.513	.712
	1.414	1.67	.494	.673
	2	1.315	.415	.640
oE_1	1	2.045	.315	.438
	2	1.37	.1803	.963
	3	1.02	.1049	.698

method. The square of the radial Mathieu Functions and
their derivatives were plotted against ξ . The areas under
the curves were measured in appropriate units. The results
thus obtained are fairly accurate. In Table 3.3, R represents
the even or odd radial Mathieu Functions.

Degeneration into Circular Pipes

When the ellipse degenerates into a circle, the
expressions for the attenuation constants are still valid.
However, they may be simplified by carrying out the integr-
ations. For a circle,

$$\eta = \phi$$

$$\text{qcosh } \xi = \text{qsinh } \xi = r$$

3.38

The ratio is
$$\frac{M_n}{N_n} = \frac{M_n'}{N_n'} = n^2$$

3.39

The integral,

$$\int_0^{\xi_0} \left\{ \frac{M_n}{N_n} \left[Re_n(\xi) \right]^2 + \left[Re_n'(\xi) \right]^2 \right\} d\xi$$

or
$$\int_0^{\xi_0} \left\{ \frac{M_n'}{N_n'} \left[Ro_n(\xi) \right]^2 + \left[Ro_n'(\xi) \right]^2 \right\} d\xi$$

3.40

appears in all the attenuation constants. By substituting
r for qcosh ξ and qsinh ξ , letting the radius of the circle
be r_0, and using the following equations:

$$d\xi = \frac{dr}{r}$$

$$Re_n(\xi) = Ro_n(\xi) = \sqrt{\frac{\pi}{2}} \, J_n(K_0 r)$$

$$\frac{\partial}{\partial\xi} Re_n(\xi) = \frac{\partial}{\partial\xi} Ro_n(\xi) = \sqrt{\frac{\pi}{2}} \, K_0 r \, J_n'(K_0 r) \; ,$$

where
$$J_n'(K_0 r) = \frac{\partial}{\partial(K_0 r)} J_n(K_0 r) \; ,$$

the Eq. 3.40 becomes,

$$\frac{\pi}{2} \int_0^{r_o} \left[n^2 J_n^2(K_o r) + K_o r J_n'^2(K_o r) \right] \frac{d(K_o r)}{K_o r}$$

$$= \frac{\pi}{2} \int_0^{r_o} \left\{ \left[n J_n(K_o r) + K_o r J_n'(K_o r) \right]^2 - 2n K_o r J_n(K_o r) J_n'(K_o r) \right\} \frac{d K_o r}{K_o r} .$$

3.41

The second term is simply equal to $-2n J_n^2 (k_o r) \Big|_0^{r_o}$. The first

term is equal to, (by Eq. 16, p.158 McLachlan)

$$\frac{\pi}{2} \int_0^{r_o} J_{n-1}^2(K_o r) K_o r\, d(K_o r)$$

$$= \frac{\pi}{4} (K_o r_o)^2 \left\{ J_{n-1}'^2(K_o r_o) + \left(1 - \frac{(n-1)^2}{K_o^2 r_o^2}\right) J_{n-1}^2(K_o r_o) \right\} .$$

3.42

This may be expressed in terms of $J_n(k_o r_o)$ and $J_n'(k_o r_o)$, and

combined with the second term of Exp. 3.41. The integral is

therefore as follows:

$$\frac{\pi}{4} \left[(K_o^2 r_o^2 - n^2) J_n^2(K_o r_o) + 2 K_o r_o J_n(K_o r_o) J_n'(K_o r_o) + K_o^2 r_o^2 J_n'^2(K_o r_o) \right]$$

3.43

Here, $k_o r_o$ is the root of $J_n(k_o r) = 0$ or $J_n'(k_o r) = 0$. For

the H-wave, $J_n'(k_o r_o) = 0$, and for E-wave, $J_n(k_o r_o) = 0$. The

attenuation constants of circular pipe are reduced to the

form:

H_n-wave:

$$\alpha = \sqrt{\frac{\pi \mu' \epsilon f_o}{\sigma' \mu}} \frac{1}{r} \left[1 - \left(\frac{f_o}{f}\right)^2 \right]^{-\frac{1}{2}} \left[\left(\frac{f_o}{f}\right)^{\frac{3}{2}} + \frac{n^2}{K_o^2 r^2 - n^2} \left(\frac{f}{f_o}\right)^{\frac{1}{2}} \right]$$

3.44

E_n-wave:

$$\alpha = \sqrt{\frac{\pi \mu' \epsilon f_o}{\sigma' \mu}} \frac{1}{r} \left(\frac{f}{f_o}\right)^{\frac{1}{2}} \left[1 - \left(\frac{f_o}{f}\right)^2 \right]^{-\frac{1}{2}} .$$

3.45

They are the same as given by Carson, Mead and Schelkunoff.

Discussion of Attenuation in Elliptical Pipes

Referring to Eq. 3.27a,b and Eq. 3.35a,b, the

attenuation constants of waves in elliptical pipes consists

of a number of factors; most of them are common to waves in

pipes of any geometrical shape. The factor $\dfrac{\sqrt{f_o}}{q\sinh \xi_o}$ plays an important part when the eccentricity of the ellipse approches unity. The $q\sinh \xi_o$ is the half length of the minor axis. The critical frequency f_o varies in the opposite way as the eccentricity except for the eH_1-wave, as shown in Fig. 3.4. Since the remaining factors do not approach zero at unit eccentricity, the attenuation always approaches infinity at unit eccentricity.

So far as the ratio $\dfrac{f}{f_o}$ is concerned, the attenuation constant may be divided into two terms, one proportional to $\sqrt{f/f_o}$ and the other proportional to $(\dfrac{f_o}{f})^{3/2}$ at high frequency. Both terms are equal to infinity at the critical frequency. At very high frequency, the two terms behave differently, one approaching infinity and the other approaching zero as a limit. Only the first terms are significant at high frequency. We may trace this term back and find that it is caused by the angular component of magnetic field, and never vanishes unless that component of field disappears. Only the H_o-wave in the circular pipes and the H-wave in a degenerated rectangular pipe (referred to II) satisfy this condition. The angular component of magnetic field always exists in an elliptical pipe. For eH_o-wave, this field varies as the eccentricity.

Except for the H_o-wave of a circular pipe, there is always a ratio f/f_o at which the attenuation of a given

elliptical pipe is minimum. The optimum ratio may be cal-
culated by setting the derivative of the attenuation constant
with respect to the frequency ratio $\frac{f}{f_o}$ equal to zero. Thus
for all types of E-wave, the optimum ratio is equal to $\sqrt{3}$.
For the H-wave, the optimum ratio is equal to

$$\frac{f}{f_o} = \frac{1}{\sqrt{2}} \ (3A + 3 + \sqrt{9A^2 + 14A + 9}\ )^{1/2}, \qquad 3.46$$

where $A = \frac{N_n}{M_n} \ K_o^2 q^2 \ \sinh \xi_o - 1$.

For eH_o-wave, this ratio gets smaller as the eccentricity in-
creases.

As a numerical illustration, let us take a set
of air-filled copper elliptical pipes of equal peripheries (s
= 40 cm.). The attenuation constants are expressed in deci-
bels per mile. Fig. 3.9a to Fig. 3.10c show the curves of
attenuation constants as functions of frequency. Various
curves in same sheet represent different eccentricities.
Unfortunately, all the calculations must be made in a reverse
way, so that the eccentricity is the last item obtained.
Thus, it is quite difficult to interprete these curves quan-
titatively. All the curves rise when the frequency exceeds
the optimum value, except the H_o-wave in a circular pipe.
The ecc. =0.256 curve of eH_o-wave does not rise again within
the range of the variable shown in the curves, but of course
it will do so for larger values of frequency.

In Fig. 3.11, the minimum attenuation constants
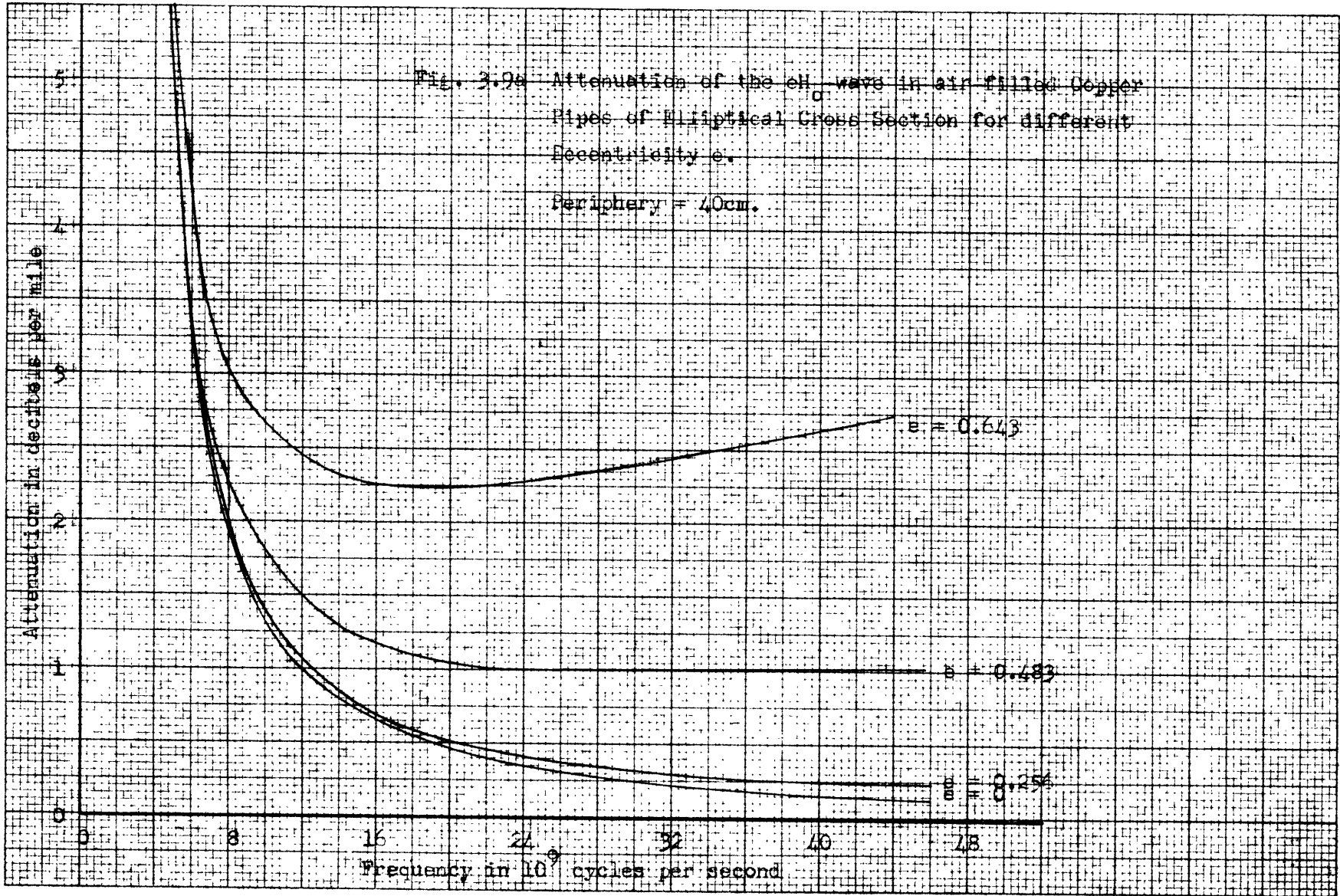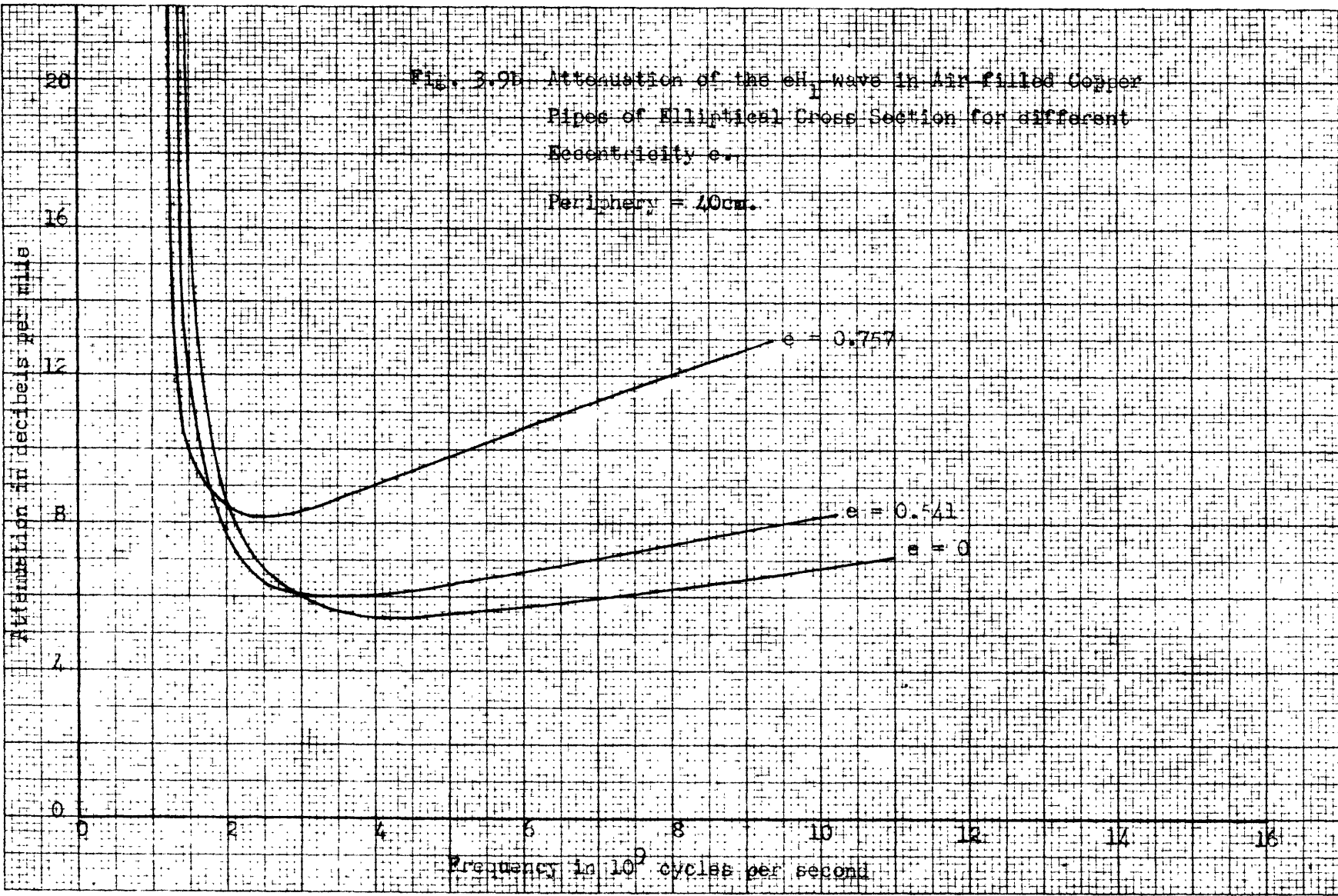of different waves are plotted as functions of eccentricity

Fig. 3.9a Attenuation of the eH_o wave in air filled copper
Pipes of Elliptical Cross Section for different
Eccentricity e.

Periphery = 40cm.

Fig. 3.9b Attenuation of the eH_1 wave in Air-filled Copper Pipes of Elliptical Cross Section for different Eccentricity e.

Periphery = 40cm.

Fig. 3.9c Attenuation of the $_0H_1$-wave in Air-filled Copper

Pipes of Elliptical Cross Section for different

Eccentricity e.

Periphery = 40cm.

$e = 0$ $e = 0.743$

$e = 0.477$ $e = 0.861$

$e = 0$

$e = 0.477$
$e = 0.743$
$e = 0.861$

Attenuation in decibels per mile

20

16

12

8

4

0

0   2   4   6   8   10   12   14   16

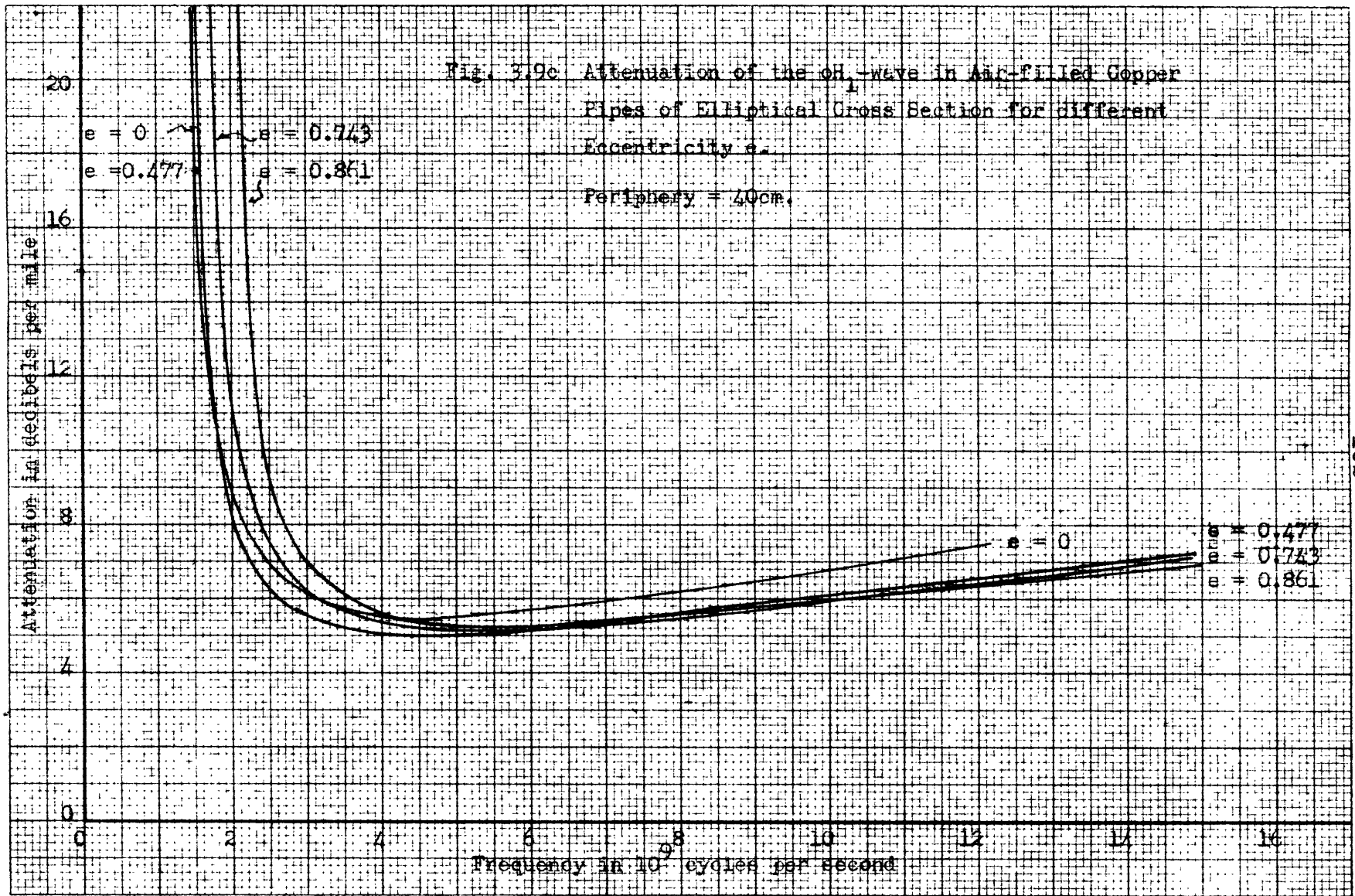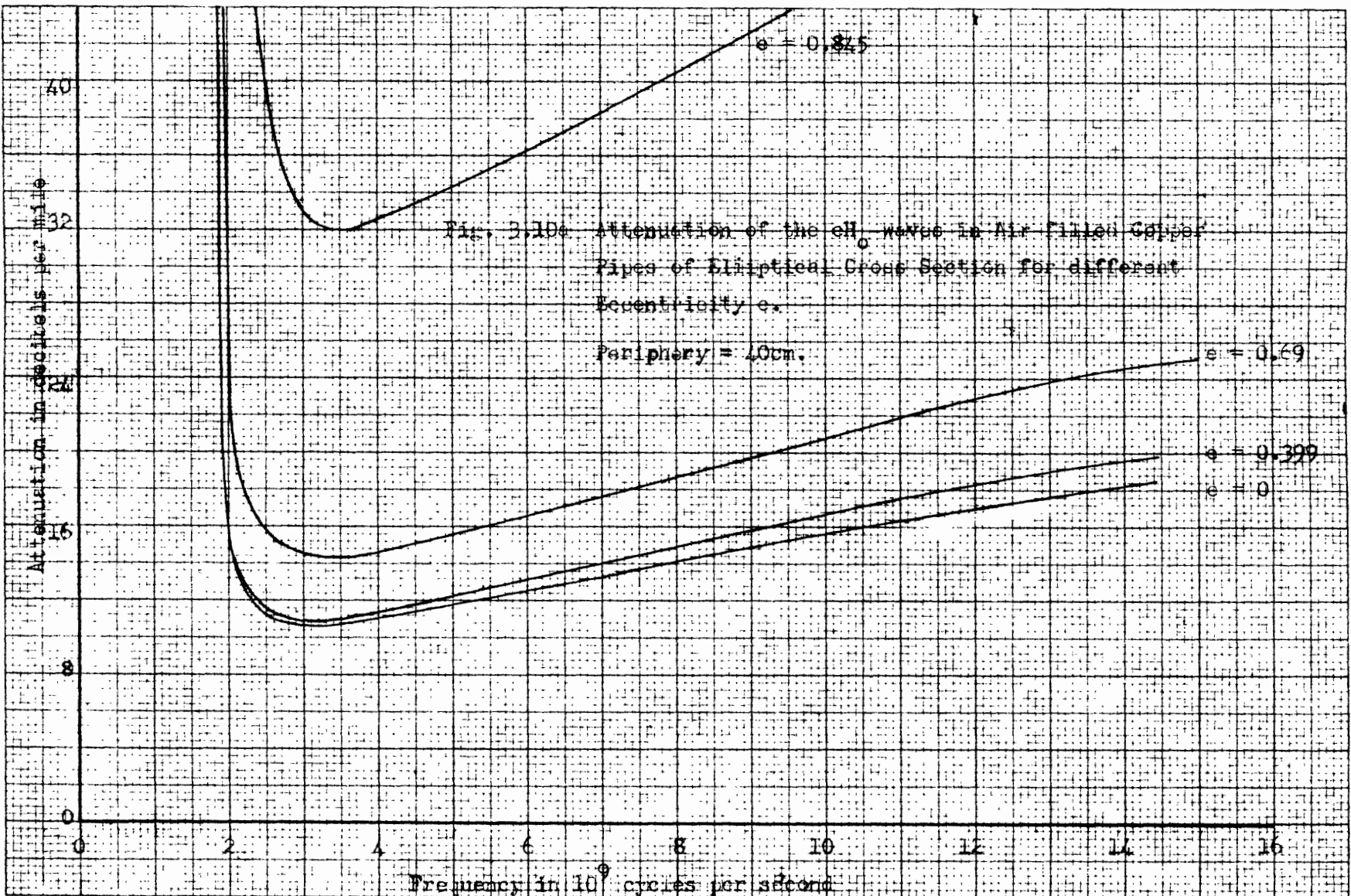Frequency in 10^9 cycles per second

FORM 47

Fig. 3.10c Attenuation of the eH_0 Waves in Air-Filled Copper Pipes of Elliptical Cross Section for different Eccentricity e.

Periphery = 40cm.

Fig. 2.10b Attenuation of the eB_1-wave in Air-filled Copper Pipe of Eliptical Cross Section for different Eccendity e.

Periphery = 40cm.
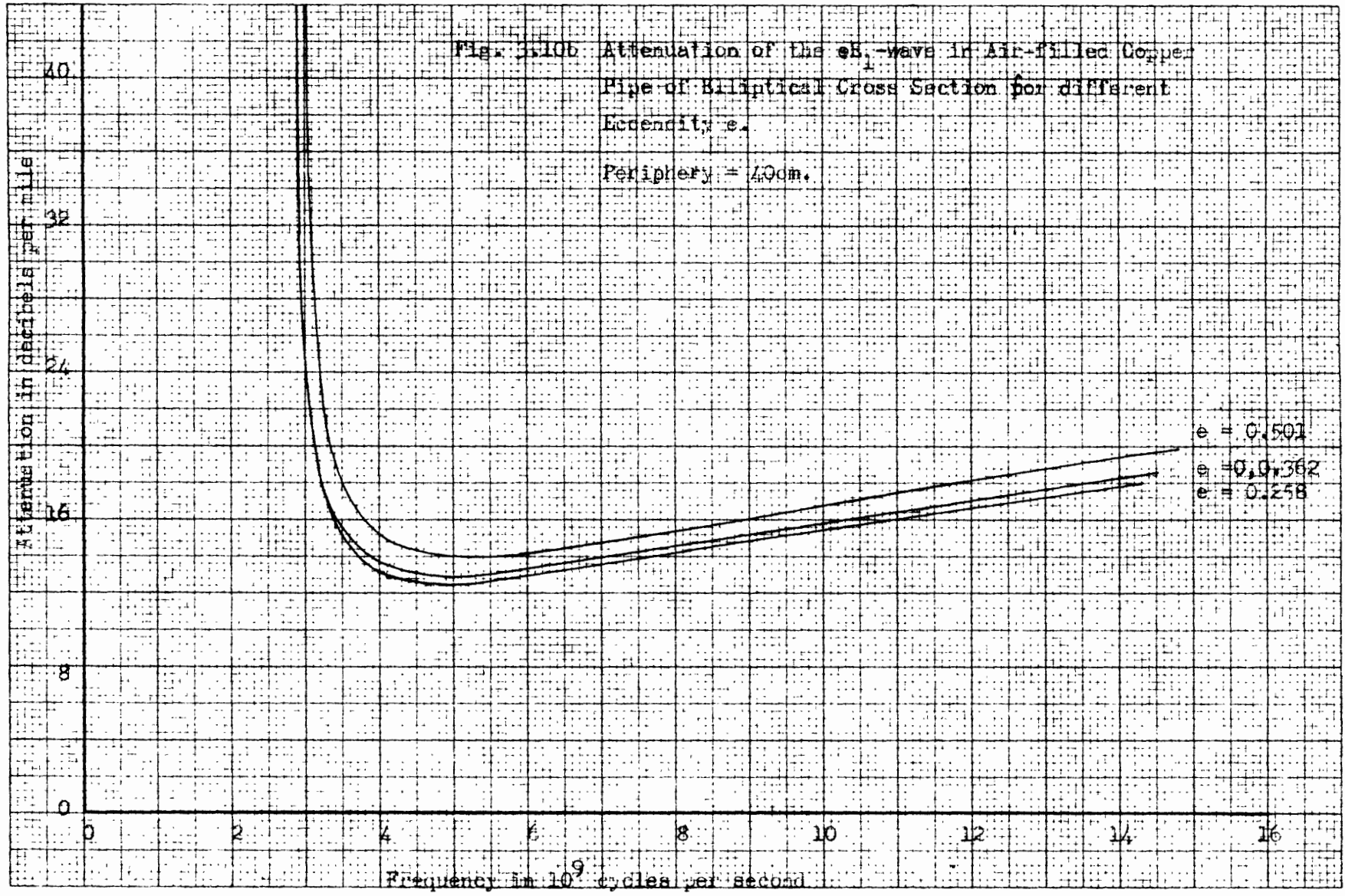
Fig. 3.10c Attenuation of the oE₁-wave in Air-filled Copper
Pipes of Elliptical Cross Section for different
Eccentricity e.

Periphery = 40cm.

e = 0.638

e = 0.477

e = 0.55

e = 0

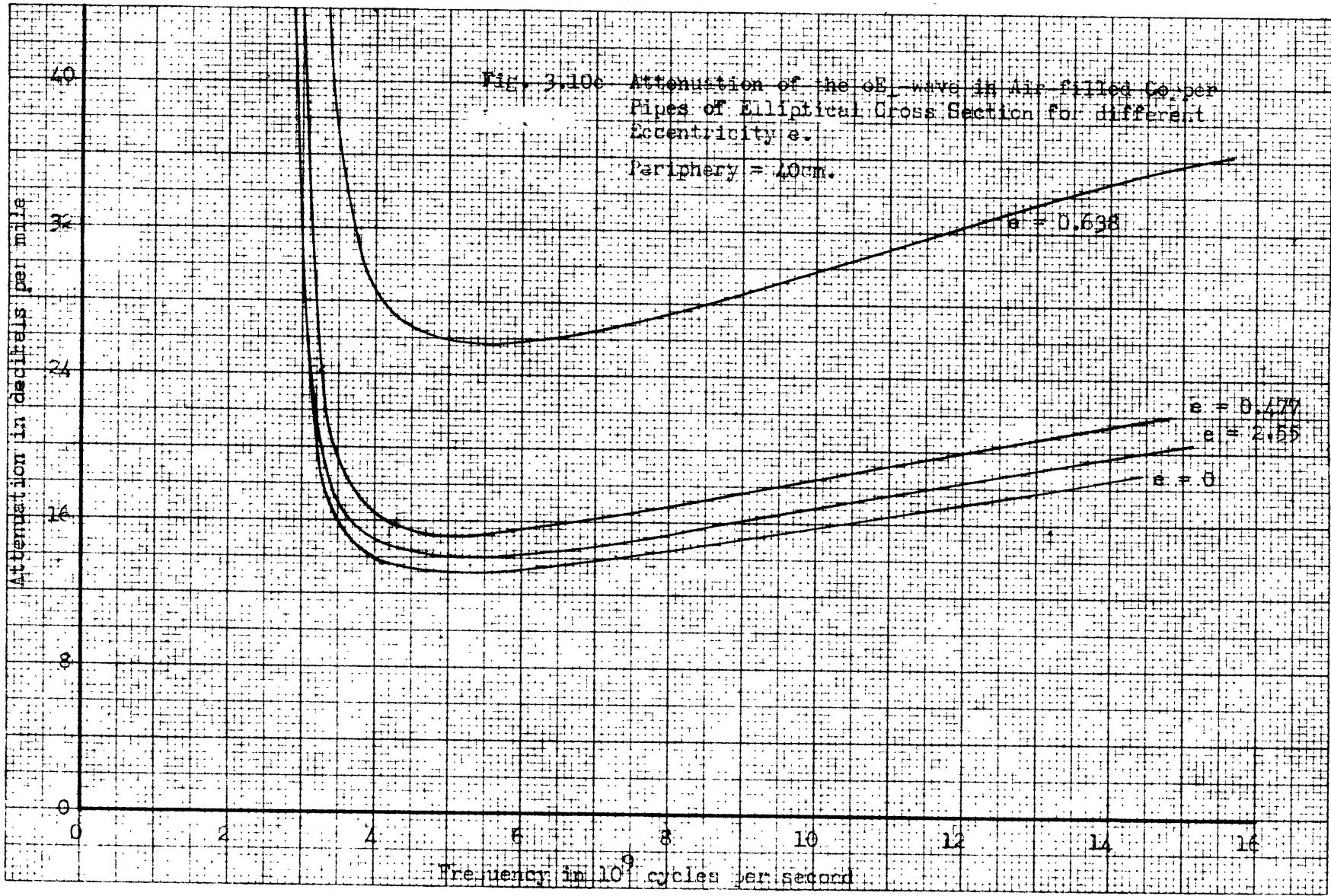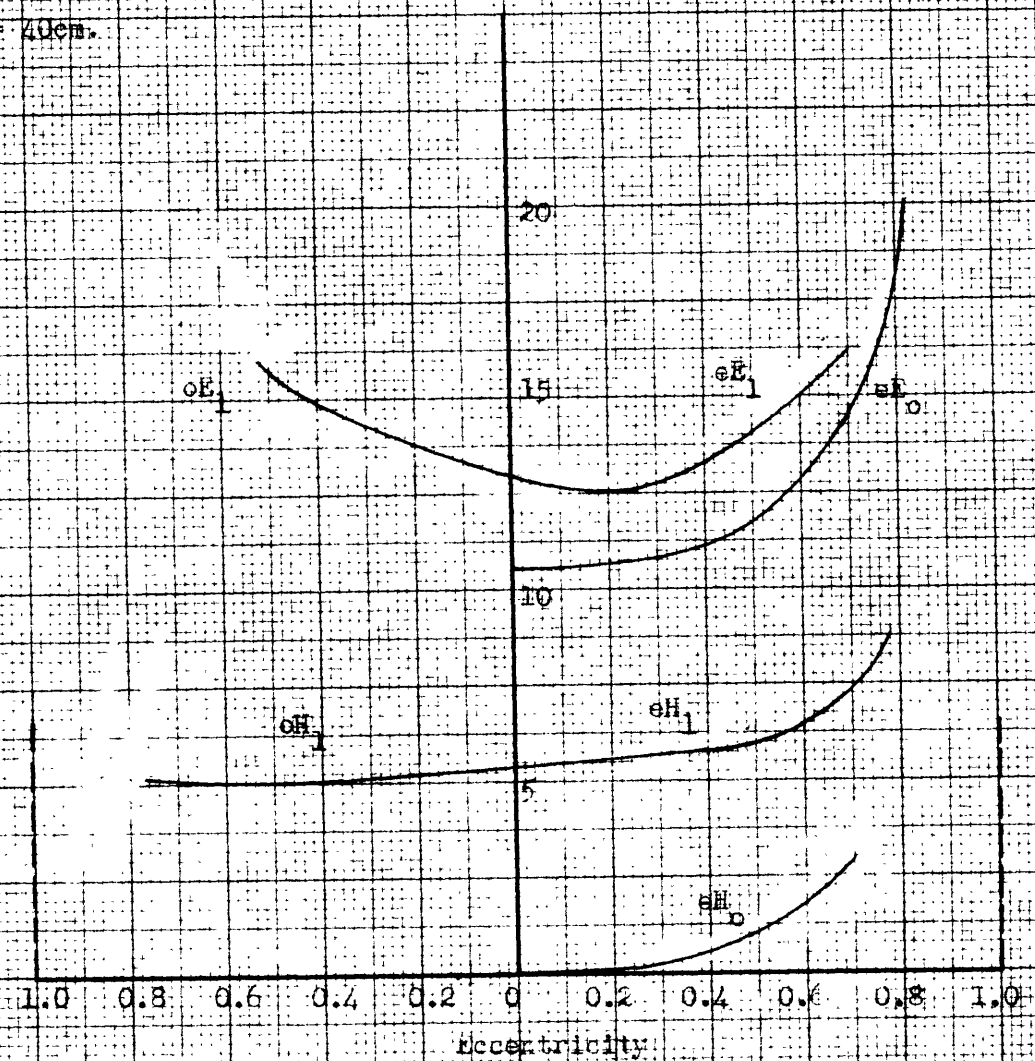Attenuation in decibels per statutory mile

Frequency in 10⁹ cycles per second

Fig. 3.11 Minimum Attenuation of waves in Air-filled Copper Pipes of elliptical Cross Section
Periph. = 40cm.

for the elliptical pipes of equal peripheries ($s = 40$ cms.)
regardless of the frequencies used to obtain such attenuation.
Curves for the even waves are plotted on the righthand side
and those for the odd waves on the lefthand side.

The eH_0-wave has no minimum attenuation when the
eccentricity is equal to zero. As the eccentricity increases,
the peculiar property of the decreasing attenuation with in-
creasing frequency disappears. The curve has a zero slope
and a zero attenuation at zero eccentricity. It means that
for this degenerate form of the elliptical pipe, the eH_0-wave
has a lower attenuation than waves in a pipe of any other geo-
metrical cross-section, though it must be operated at infi-
nitely high frequency. It also indicates that any deform-
ation to the cross-section of circular pipe increases the
attenuation.

The curve for the eE_0-wave has also zero slope
at the zero eccentricity, and the curve goes up as the eccen-
tricity. Therefore, it shows that a circular pipe is better
than an elliptical one for the transmission of the eE_0-wave.
The fields of both the H_0- and the E_0-waves have a circular
symmetry for $e = 0$. This is analogous to the fact that the
$H_{1,1}$-wave and the $E_{1,1}$-wave in a square pipe have lower at-
tenuations than the corresponding waves in a rectangular
pipe having the same periphery.

The eH_1- and the oH_1-waves both degenerate into

the H_1-wave in the circular pipe when the eccentricity be-
comes zero. It has been pointed out that this two waves can
be obtained by degenerating a circular pipe containing the
H_1-wave along two orthogonal diameters of symmetry. The
curve shows a continuous slope ($\neq 0$) at zero eccentricity.
It may be recalled that the $H_{0,1}$-wave in a rectangular pipe
with the ratio of the cross-sectional dimensions $\frac{a}{b} = 1.18$
has a lower attenuation than in a square pipe. Similarly,
the H_1-wave in a circular pipe does not have a circular sym-
metry and any deformation of the circular pipe may decrease
the attenuation. Thus, we find from the curve that the low-
est attenuation for this type of wave exists in pipes with
slight eccentricity, namely the oH_1-wave. The configuration
of the fields for the oH_1-wave shows that the electric line
is nearly parallel to the major axis. (For the $H_{0,1}$-wave
in rectangular pipe, the dimension"a" is parallel to the elec-
tric lines.)

The attenuation of the eE_1-wave and the oE_1-
wave behaves in a similar way. This time, however, the even
wave has a lower minimum attenuation. This phenomenon may
be similarly explained by the fact that the E_1-wave in a cir-
cular pipe does not have a circular symmetry.

Discussion of the Anomalous Attenuation Characteristics

All the waves, which we have investigated in the last two chapters and also in the appendix, have an atten-uation increasing with the frequency at sufficiently high frequencies, except for the H_0-wave in a circular pipe and the H-wave in a degenerate rectangular pipe (which is equivalent to the H_g-wave between two parallel planes). The anomalous attenuation characteristics of the H_0-wave and the H_g-wave may be explained physically by referring to the problem of light reflection by a finitely conducting material. But we must first observe that both the above-named waves do not have a transverse component of magnetic field tangential to the conducting surfaces.

Consider a light wave in a dielectric projected at an angle to the normal of the finitely but highly conductive metallic surface. The total energy is partly reflected back to the dielectric and partly absorbed by the conducting metal. The absorption coefficient of the metal depends upon the polarization of the light wave. The case that interested us is that in which the angle of incidence is at or about 90°, i.e., the grazing angle. For this angle of incidence, the absorption coefficient is zero when the wave is so polarized that the electric field is normal to the plane of incidence, that is to say, the wave has no transverse

magnetic field tangential to the surface. The absorption

coefficient is not zero when the wave is polarized to the

other way, i.e., the magnetic field is normal to/the plane

of incidence——a transverse field tangential to the surface.

Now let us turn to the hollow pipe waves again.

For a pipe of any cross-section, the phases constant may be

written in the form:

$$\beta = \frac{\omega}{c} \sqrt{1 - (\frac{f_o}{f})^2}$$

where f_o is the critical frequency of the hollow pipe waves.

At $f = \infty$, the phase constant β approaches the value $\frac{\omega}{c}$, which

incidentally is the phase constant of a plane wave. The long-

itudinal component fields for a non-dissipative pipe vanish

under this condition. That is to say, at infinitely high

frequencies, the hollow-pipe waves become transverse, tra-

veling in the longitudinal direction of the pipe and parallel

to the wall. If we take an infinitesinal longitudinal slice

of the wall, the situation is reduced to grazing angle case

of light reflection, which we have discussed above. On this

infinitesimal slice of surface, the hollow-pipe waves at in-

finitely high frequency may have a composite polarization or

a simple one. If there is a transverse magnetic field tan-

gential to/the surface, we may predict, in terms of light,

that the absorption eoefficient is not zero, i.e., the loss

into the wall cannot be eliminated. On the other hand, if

there is no transverse magnetic field tangential to the

surface, the absorption coefficient of the wall is zero, ie.,
there is no loss caused by the metallic wall.

Therefore, we may conclude that the attenuation
of a wave in any hollow pipe is zero at infinitely high
frequencies if there is no transverse component of magnetic
field tangential to any part of the wall or walls. So far
as we have discovered, only the H_o-wave in a circular pipe
and the H-wave in a degenerate rectangular pipe (by extending
the dimension 'b' to infinity) satisfy the necessary condition
of the above theorem. For the H_o-wave in a circular pipe, the
absence of that component field is possible on account
of the circular symmetry. For the H-waves in a rectangular
pipe, there are always transverse components of the magnetic
fields tangential to the metallic surfaces, but their effect
may be eliminated by extending the dimension 'b' to infinity.

Summary of Equations

Non-dissipative Case

Component fields of the eH_n- and oH_n-waves:

$$H_x = B \quad S_n(\eta) \, R_n(\xi) \, e^{i(\omega t - \beta x)}$$

$$H_\xi = -B \frac{i\beta}{q \cdot \kappa_o^2} \, S_n(\eta) \, R_n'(\xi) \, e^{i(\omega t - \beta x)}$$

$$H_\eta = -B \frac{i\beta}{q \cdot \kappa_o^2} \, S_n'(\eta) \, R_n(\xi) \, e^{i(\omega t - \beta x)} \qquad\qquad 3.8$$

$$E_\xi = B \frac{i\omega\mu}{q_1 K_o^2} S_n'(\eta) R_n(\xi) e^{i(\omega t - \beta x)}$$

$$E_\eta = -B \frac{i\omega\mu}{q_1 K^2} S_n(\eta) R'(\xi) e^{i(\omega t - \beta x)}$$

$$E_x = 0 \qquad \qquad .$$

3.8

where R represents Re and Ro, and S represents Se and So
for the even and the odd waves respectively.

Component fields of the eE_n- and oE_n-waves:

$$E_x = B \qquad S_n(\eta) R_n(\xi) e^{i(\omega t - \beta x)}$$

$$E_\xi = -B \frac{i\beta}{q_1 K_o^2} S_n(\eta) R_n'(\xi) e^{i(\omega t - \beta x)}$$

$$E_\eta = -B \frac{i\beta}{q_1 K_o^2} S_n'(\eta) R_n(\xi) e^{i(\omega t - \beta x)}$$

3.10

$$H_\xi = B \frac{i\omega\xi}{q_1 K^2} S_n'(\eta) R_n(\xi) e^{i(\omega t - \beta x)}$$

$$H_\eta = -B \frac{i\omega\xi}{q_1 K_o^2} S_n(\eta) R_n'(\xi) e^{i(\omega t - \beta x)}$$

$$H_x = 0$$

Dissipative Case

Attenuation constant of the eH_n- and the oH_n-
waves in an elliptical pipe:

$$\alpha = \sqrt{\frac{\pi\mu'\varepsilon}{\sigma'\mu}} \frac{\sqrt{f_o}}{2q \sinh \xi} \left[1 - \left(\frac{f_o}{f}\right)^2 \right]^{-\frac{1}{2}} \cdot$$

$$\frac{\left[\left(\frac{f}{f_o}\right)^{\frac{1}{2}} + \left(\frac{M_n}{N_n} K_o^2 q^2 \sinh^2\xi_o - 1\right)\left(\frac{f_o}{f}\right)^{\frac{3}{2}} \right] \left[R_n(\xi_o) \right]^2}{\int_0^{\xi_o} \left[R_n(\xi) \right]^2 d\xi + \frac{M_n}{N_n} \int_0^{\xi_o} \left[R_n'(\xi) \right]^2 d\xi}$$

3.29

where

$$M_n = \int_0^{2\pi} \left[S_n'(\eta) \right]^2 d\eta$$

3.27

$$N_n = \int_0^{2\pi} [S_n(\eta)]^2 \, d\eta \; .$$

<div align="right">3.27a</div>

For the H_n-wave in a circular pipe, the attenuation constant is:

$$\alpha = \sqrt{\frac{\pi \mu' \epsilon f_0}{\sigma' \mu}} \; \frac{1}{r} \left[1 - \left(\frac{f_0}{f}\right)^2 \right]^{-\frac{1}{2}} \cdot$$

$$\left[\left(\frac{f_0}{f}\right)^{\frac{3}{2}} + \frac{n^2}{k_0^2 r_0^2 - n^2} \left(\frac{f}{f_0}\right)^{\frac{1}{2}} \right]$$

<div align="right">3.44</div>

Attenuation constant of the eE_n- and the oE_n-wave in an elliptical pipe.

$$\alpha = \sqrt{\frac{\pi \mu' \epsilon}{\sigma' \mu}} \; \frac{\sqrt{f_0}}{2q \sinh \xi_0} \; \frac{\left(f/f_0\right)^{\frac{1}{2}}}{\sqrt{1 - (f/f_0)^2}} \; \frac{\left[R_n'(\xi_0) \right]^2}{\frac{M_n}{N_n} \int_0^{\xi_0} [R_n(\xi)]^2 \, d\xi + \int_0^{\xi_0} [R_n(\xi)]^2 \, d\xi}$$

<div align="right">3.35a</div>

For the E_n-wave in a circular pipe, the attenuation constant is:

$$\alpha = \sqrt{\frac{\pi \mu' \epsilon f_0}{\sigma' \mu}} \; \frac{1}{r} \left(\frac{f}{f_0}\right)^{\frac{1}{2}} \left[1 - \left(\frac{f_0}{f}\right)^2 \right]^{-\frac{1}{2}}$$

<div align="right">3.45</div>

IV. RADIATION FROM THE OPEN END
OF A RECTANGULAR PIPE

It is known that an electromagnetic wave with distributed charge and current density can be represented by a vector potential A and scalar potential ϕ, which are generally called Lorentz or retarded potentials. They may be started by the following expressions:

$$A = \frac{1}{4\pi} \int_v \frac{u(t-r/c)}{r} \, dv \qquad \qquad 4.1a$$

$$\phi = \frac{1}{4\pi} \int_v \frac{\rho(t-r/c)}{r} \, dv \qquad \qquad 4.1b$$

where u is the vector conduction current density and p is the charge density, both in complex representation. The electric and magnetic field intensities may be expressed in terms of the two potentials:

$$H = \text{curl } A$$

$$E = -\text{grad } \phi - i\omega\mu A \, . \qquad \qquad 4.1c$$

The two potentials are related to each other by

$$\text{div} \cdot A + i\omega\mu\,\phi = 0$$

with this functional relation, the scalar potential may be eliminated from the field expressions 4.1c.

$$H = \text{curl } A \qquad \qquad 4.2a$$

$$E = -i\omega\mu A + \frac{\text{grad div } A}{i\omega\xi} \, . \qquad \qquad 4.2b$$

Both A and ϕ satisfy the D'Alemberts equation, which for A is:

$$\nabla^2 A + \frac{\omega^2}{c^2} A = - \frac{u}{c} .$$

In a region free of conduction current, this equation reduces to the wave equation.

Inside a hollow pipe of any geometrical form and of sufficient length, if we set aside the problem of how waves of different types are produced, it is possible to choose a vector potential whose divergence is zero. The vector electric field intensity is thus reduced to the form

$$E = -i\omega\mu A . \qquad\qquad 4.3$$

The vector potential can then be calculated readily from the electric field vector of a hollow-pipe wave.

From Eq.4.3 and the definitions of the E-wave, and the H-wave, it is apparent that for the E-wave, the vector potential has both longitudinal and transverse components. For H-wave, on the other hand, the vector potential has only transverse component. The latter fact is particularly significant for the $H_{0,m}$-waves in rectangular pipes, which may be produced experimentally by placing an antenna perpendicular to the XZ-plane. The conduction current oscillates in the antenna, and from Eq. 4.1a, we would expect the vector potential to have the same vertical direction.

For the calculation of the radiation pattern from the open end of the pipe, it is convenient to represent the hollow-pipe waves by a single vector potential. From this vector potential, we are able to calculate the corresponding vector potential of the radiated wave in the surrounding free

space. The method which we shall use to calculate the
radiation is Huygens' Principle, often used in the calculation
of diffraction problems. The derivation may be found, for ex-
ample, in Försterling's "Lehrbuch der Optik" pp.224-227.
The general form of the expression is as following:

$$
A = -\int_{v} \frac{(\nabla^2 A - \frac{1}{c^2}\frac{\partial^2 A}{\partial t^2})_{(t-\frac{\rho}{c})}\, dv}{\rho} + \int_{s} \frac{1}{\rho}\left[\left\{\frac{1}{c}\left(\frac{\partial A}{\partial t}\right)_{(t-\frac{\rho}{c})} + \frac{A(t-\frac{\rho}{c})}{\rho}\right\}\cos(n,\rho) + \left(\frac{\partial A}{\partial n}\right)_{(t-\frac{\rho}{c})}\right]ds
$$

4.4

where A is the vector potential, the one on the left is the
quantity for the point where the fields are to be calculated,
and those on the right are the value over any enclosing sur-
face. The radial distance between the point of observation
and the surface is p, and n is the inner normal to the surface;
the time t is replaced by $(t-\frac{p}{c})$ to take care of the time
retardation. For a space free of charge and conduction cur-
rent, the volume integral is zero. Eq. 4.4 is only good for
A in Cartesian coordinates. The equation must be modified,
if A is expressed in some other orthogonal coordinate system
since it is a vector function.

We will assume a pipe of rectangular cross-sec-
tion of finite length. It is excited at one end to produce
one or more types of the hollow-pipe waves. The exciting
system is shielded to prevent the radiation of energy direct-
ly into space. The walls of the pipe are so thick that no
energy is able to penetrate them. The only radiation into the
external space is from the open end of the pipe. The pipe is

assumed to be of sufficient length for the use of the field
and potential functions calculated for a pipe of ideal ma-
terials and infinite length. It is also assumed that the fields
at the open end of the hollow pipe are not appreciably dis-
torted by end effects. (Refer to Fig. 4.1)

Since the vector potential of the hollow-pipe
wave is known, we may substitute it into Eq. 4.4 to calculate
the vector potential of the radiation field. From the latter
potential, the magnetic and electric field intensities of
the wave in free space may then be calculated by Eq. 4.2.

Eq. 4.2 may be simplified for the radiation field
by carrying out the vector operations. The vector potential
of the radiated wave will be first calculated in Cartesian
coordiantes:

$$A = 1_x A_x + 1_y A_y + 1_z A_z .$$

It can be expressed in spherical coordinates (R, θ, ζ) by

$$A = 1_R A_R + 1_\theta A_\theta + 1_\zeta A_\zeta$$

where 1_R, 1_θ, and 1_ζ are a set of orthogonal unit vectors.
The two expressions of A are related as following.

$$A_R = A_x \cos\theta + A_y \cos\zeta \sin\theta + A_z \sin\zeta \sin\theta$$

$$A_\theta = -A_x \sin\theta + A_y \cos\zeta \cos\theta + A_z \sin\zeta \cos\theta \qquad 4.5$$

$$A_\zeta = \qquad - A_y \sin\zeta \qquad + A_z \cos\zeta .$$

The wave function for any wave radiated from a single source
must be a function of R of the form $\frac{1}{R} e^{i\omega(t-R/c)}$. The
factor $(t - \frac{R}{c})$ in the exponential represents a wave travel-

ing radially from the source. Terms with higher power of R
than (-1) can not exist, if the function is to vanish at
inifinity, and terms with lower power of R than (-1) can
be neglected when R is sufficiently large. Hence we may
write

$$A = \left[i_R A_R' + i_\theta A_\theta' + i_\zeta A_\zeta' \right] \frac{e^{i\omega(t-R/c)}}{R}$$

where A_R' , A_θ' and A' are scalar functions of θ and ζ only.
By applying the vectorial operation to such a potential
for large value of R and using Eq. 4.2ab, the radiated elec-
tric and magnetic field intensities may be found as below.

$$E = -i\omega\mu(i_\theta A_\theta + i_\zeta A_\zeta) \qquad 4.6$$

$$H = curl\ A \qquad 4.7$$

$$= \frac{i\omega}{c}\ (i_\theta A_\zeta - i_\zeta A_\theta).$$

Both the electric and magnetic field intensities
thus derived have no radial components. This means that all
the fields are transverse to the direction of propagation,
a special characteristic of radiated waves in space. It
is obvious from the expression of E and H that

$$E_\theta = \sqrt{\frac{\mu}{\zeta}}\ H_\zeta$$

$$E_\zeta = -\sqrt{\frac{\mu}{\zeta}}\ H_\theta . \qquad 4.8$$

Both E and H satisfy the wave equation.

The Poynting's vector which represent the tran-
smission of energy per sq. cm. of area is always in the

radial direction, since the radial components of fields are zero:

$$S = \frac{1}{2} (E_\theta \hat{H}_\zeta - E_\zeta \hat{H}_\theta)$$

$$= \frac{1}{2} \sqrt{\frac{\mu}{\epsilon}} \left[|H_\theta|^2 + |H_\zeta|^2 \right]$$

$$= \frac{1}{2} (\frac{\omega}{c})^2 \sqrt{\frac{\mu}{\epsilon}} \left[|A_\theta|^2 + |A_\zeta|^2 \right] . \qquad 4.9$$

The power radiated in any solid angle is constant.

The radiation pattern may be defined as the curve expressing the relative magnitudes of electric or magnetic field intensity, radiated from a certain source, over a sphere of radius R with the source as center.

Radiation Patterns of the $H_{o,m}$-wave (m = odd)

The field expressions for $H_{o,m}$-wave with the X-axis at the center of the tube for m = odd are

$$H_x = B \frac{m\pi}{b} \sin (\frac{m\pi}{b}z) e^{i(\omega t - \beta x)}$$

$$H_z = -B i\beta \cos (\frac{m\pi}{b}z) e^{i(\omega t - \beta x)}$$

$$E_y = -B i\omega\mu \cos (\frac{m\pi}{b}z) e^{i(\omega t - \beta x)} .$$

The most important type of wave so far as radiation is considered is $H_{o,1}$-wave, in which the electric field intensity is parallel to the Y-axis, and has a sinusoidal variation with the maximum at the center. It will give a maximum radiation directly in front of the pipe. Higher orders of $H_{o,m}$-wave are interesting as they are apt to appear in the tube when the operating frequency

is sufficiently high. We shall first consider the m = odd
$H_{o,m}$-waves, in which the electric field is evenly symme-
trical with respect to the X Y plane. With a $H_{o,m}$-waves
in which m is even, the electric fields are zero at the
center and possess odd symmetry with respect to the X,Y-
plane. The radiation field of such types of waves will
have a zero directly to the front of the tube but it will
have symmetrical side lobes. Since the scalar potential
inside the pipe is zero, we have from Eq. 4.3

$$E = -i\omega\mu A .$$

The vector potential inside the pipe is as follows:

$$A_y = B \cos\left(\frac{m\pi}{b} z\right) e^{i(\omega t - \beta x)} \qquad\qquad 4.10a$$

$$A_x = A_z = 0 .$$

We assume this expression to be valid at the opening of
pipe, which coincides with the x = 0 plane. Let P be
any point in the space where field is to be calculated and
the distance to any point (x, y, z) on the opening be p.
Since inside the pipe, the wave function is a function of
x and t, of the form $e^{i\omega t - i\beta x}$ for all types of waves in rec-
tangular pipe the expression for Huygens'principle can be
further simplified. The volume integral is equal to zero,
and the remaining terms are

$$\frac{1}{c}\left(\frac{\partial A}{\partial t}\right)_{(t-\frac{p}{c})} = \frac{i\omega}{c} A e^{-i\omega\frac{p}{c}}$$

$$\frac{A_{(t-\frac{p}{c})}}{p} = \frac{1}{p} A e^{-i\omega\frac{p}{c}}$$

$$\cos(n,p) = \cos\theta$$

So

$$\left(\frac{\partial A}{\partial n}\right)_{(t-\frac{P}{C})} = -\left(\frac{\partial A}{\partial x}\right)_{(t-\frac{P}{C})} = i\beta A e^{-i\omega\frac{P}{C}}.$$

$$A = \iint \frac{1}{P}\left[\left(\frac{i\omega}{c} + \frac{1}{P}\right)\cos\theta + i\beta\right] A e^{-i\omega\frac{P}{C}} ds \quad 4.11$$

Put the value of Ay of Eq. 4.10a into the right-hand side of the expression and neglect the term proportional to $\frac{1}{P^2}$ and put x = 0. We have the vector potential in the external free space.

$$A_y = \int_{-\frac{b}{2}}^{\frac{b}{2}}\int_{-\frac{a}{2}}^{\frac{a}{2}} \frac{i\omega}{cP}\left[\cos\theta + \frac{\beta c}{\omega}\right] B \cos\left(\frac{m\pi}{b}z\right) e^{i\omega(t-\frac{P}{C})} ds \quad 4.22$$

As p is a large number, we may neglect its variation over the surface of integration and use an average value R so far as magnitude is concerned but introduce an approximation into the exponential (Fig. 4.1)

$$P = \sqrt{(R\sin\theta\cos\zeta - y)^2 + (R\sin\theta\sin\zeta - z)^2 + (R\cos\theta)^2}$$

$$\cong R - (y\cos\zeta + z\sin\zeta)\sin\theta$$

and the integral becomes:

$$A_y = \frac{i\omega}{cR} B \left[\cos\theta + \frac{\beta c}{\omega}\right] e^{i\omega(t-\frac{R}{C})} \int_{-\frac{a}{2}}^{\frac{a}{2}} e^{i\frac{\omega}{c}y\cos\zeta\sin\theta} dy \int_{-\frac{b}{2}}^{\frac{b}{2}} \cos\left(\frac{m\pi}{b}z\right) e^{i\frac{\omega}{c}z\sin\zeta\sin\theta} dz$$

$$= -\frac{i\lambda^2 m}{2b\pi R} B e^{i\omega(t-\frac{R}{C})}\left[\cos\theta + \sqrt{1-(\frac{\lambda}{\lambda_0})^2}\right] \frac{\sin\left(\frac{\pi a}{\lambda}\cos\zeta\sin\theta\right)\cos\left(\frac{\pi b}{\lambda}\sin\zeta\sin\theta\right)}{\cos\zeta\sin\theta\left[\sin^2\zeta\sin^2\theta - (\frac{\lambda}{\lambda_0})^2\right]}$$

$$A_z = A_x = 0$$

since

$$\lambda_0 = \frac{2b}{m}$$

$$\beta = \sqrt{\left(\frac{\omega}{c}\right)^2 - \left(\frac{m\pi}{b}\right)^2} \qquad\qquad 4.10b$$
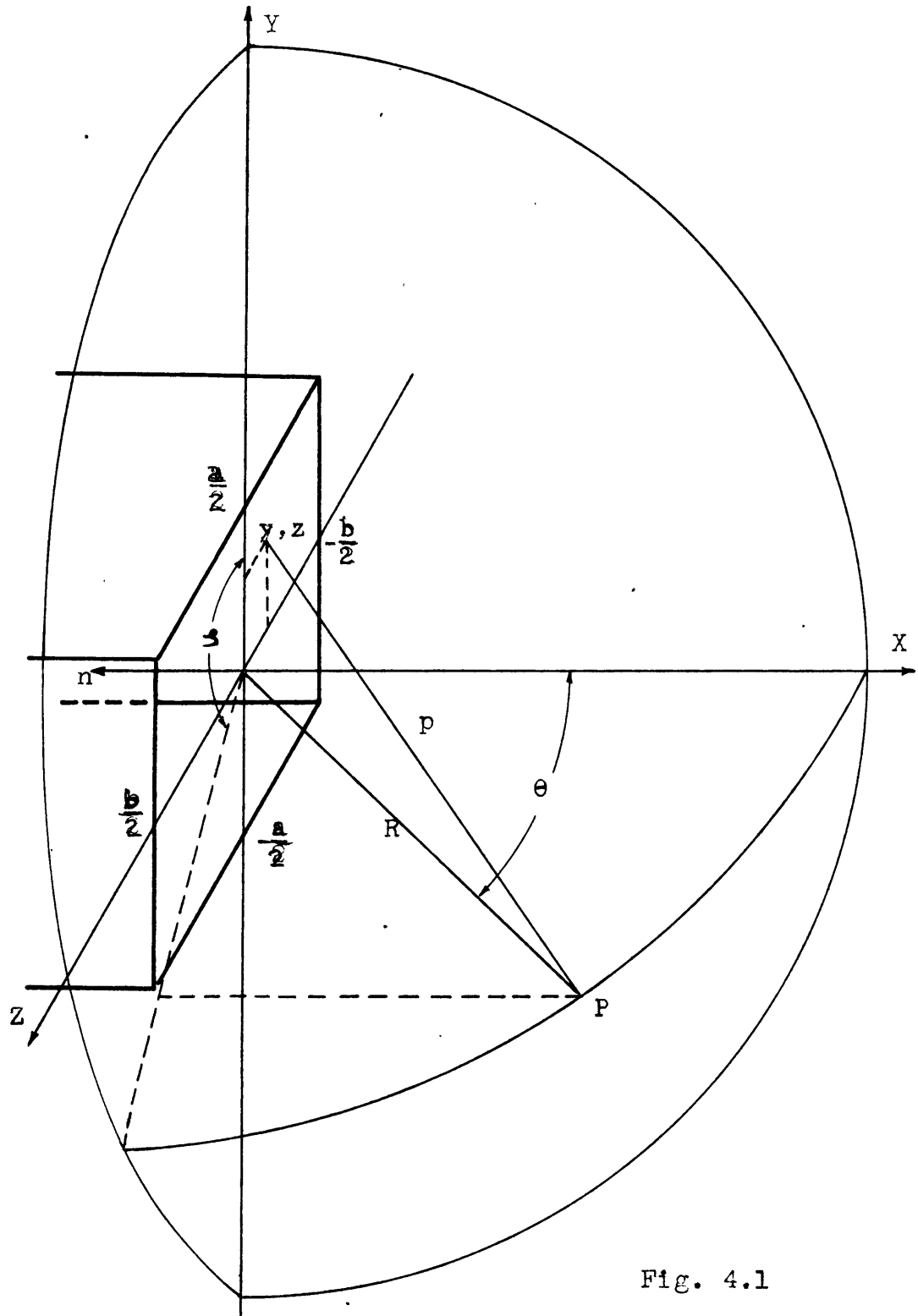
$$\frac{\omega}{c} = \frac{2\pi}{\lambda}$$

Fig. 4.1

Using expressions 4.5, we resolve A_y (Eq. 4.10b) into spherical coordinates

$$A_R = -\frac{i\lambda^2 m}{2\pi R b} B e^{i\omega(t-\frac{R}{c})}(\cos\theta + \sqrt{1-(\frac{\lambda}{\lambda_0})^2}) \frac{\sin(\frac{\pi a}{\lambda}\cos\zeta\sin\theta)\cos(\frac{\pi b}{\lambda}\sin\zeta\sin\theta)}{\sin^2\zeta\sin^2\theta - (\frac{\lambda}{\lambda_0})^2}$$

$$A_\theta = -\frac{i\lambda^2 m}{2\pi R b} B e^{i\omega(t-\frac{R}{c})}(\cos\theta + \sqrt{1-(\frac{\lambda}{\lambda_0})^2}) \frac{\sin(\frac{\pi a}{\lambda}\cos\zeta\sin\theta)\cos(\frac{\pi b}{\lambda}\sin\zeta\sin\theta)}{\sin^2\zeta\sin^2\theta - (\frac{\lambda}{\lambda_0})^2} \cot\theta$$

$$A_\zeta = \frac{i\lambda^2 m}{2\pi R b} B e^{i\omega(t-\frac{R}{c})}(\cos\theta + \sqrt{1-(\frac{\lambda}{\lambda_0})^2}) \frac{\sin(\frac{\pi a}{\lambda}\cos\zeta\sin\theta)\cos(\frac{\pi b}{\lambda}\sin\zeta\sin\theta)}{\sin^2\zeta\sin^2\theta - (\frac{\lambda}{\lambda_0})^2} \frac{\tan\zeta}{\sin\theta}$$

The magnetic and electric field intensities in the external space are

$$E_\theta = \sqrt{\frac{\mu}{\varepsilon}} H_\zeta = -i\omega\mu A_\theta = -\frac{i2\pi}{\lambda}\sqrt{\frac{\mu}{\varepsilon}} A_\theta$$

$$= -\frac{\lambda m}{b R}\sqrt{\frac{\mu}{\varepsilon}} B (\cos\theta + \sqrt{1-(\frac{\lambda}{\lambda_0})^2}) \frac{\sin(\frac{\pi a}{\lambda}\cos\zeta\sin\theta)\cos(\frac{\pi b}{\lambda}\sin\zeta\sin\theta)}{\sin^2\zeta\sin^2\theta - (\frac{\lambda}{\lambda_0})^2} \cot\theta \, e^{i\omega(t-\frac{R}{c})}$$

$$4.13$$

$$E_\zeta = -\sqrt{\frac{\mu}{\varepsilon}} H_\theta = -i\omega\mu A_\zeta = -\frac{i2\pi}{\lambda}\sqrt{\frac{\mu}{\varepsilon}} A_\zeta$$

$$= \frac{\lambda m}{b R}\sqrt{\frac{\mu}{\varepsilon}} B (\cos\theta + \sqrt{1-(\frac{\lambda}{\lambda_0})^2}) \frac{\sin(\frac{\pi a}{\lambda}\cos\zeta\sin\theta)\cos(\frac{\pi b}{\lambda}\sin\zeta\sin\theta)}{\sin^2\zeta\sin^2\theta - (\frac{\lambda}{\lambda_0})^2} \frac{\tan\zeta}{\sin\theta} e^{i\omega(t-\frac{R}{c})}$$

$$H_R = 0, \qquad\qquad E_R = 0$$

.

Poynting's vector (in radial direction) is given by

$$S = \frac{1}{2}|B|^2 \frac{\lambda^2 m^2}{b^2 R^2}\sqrt{\frac{\mu}{\varepsilon}} [\cos\theta + \sqrt{1-(\frac{\lambda}{\lambda_0})^2}]^2 \frac{\sin^2(\frac{\pi a}{\lambda}\cos\zeta\sin\theta)\cos^2(\frac{\pi b}{\lambda}\sin\zeta\sin\theta)}{[\sin^2\zeta\sin^2\theta - (\frac{\lambda}{\lambda_0})^2]^2}[\cot^2\theta + \frac{\tan^2\zeta}{\sin^2\theta}] \quad 4.14$$

.

The factor $\left[\cos\theta + \sqrt{1-(\frac{\lambda}{\lambda_0})^2}\right]$ contributes to the directivity of radiation by a relatively slow variation. For $(\frac{\lambda_0}{\lambda})$ equal or greater than 2, the expression is approximately equal to $[1+\cos\theta]$. It is maximum directly in front of the surface of integration and approaches zero behind the surface of integration. It would disappear if we use equivalent theorem[1] to introduce fictitious magnetic and electric current sheaths at the opening of the pipe.

The analysis of the remaining factor may be simplified if we confine our attention to two perpendicular planes X Y and X Z-planes:

Radiation Pattern in XY-plane

$$(\zeta = 0)$$

By putting ζ equal to zero, we find

$$E_\theta = \sqrt{\frac{\mu}{\epsilon}}\, H_\zeta = \frac{4b}{\lambda\mu R}\sqrt{\frac{\mu}{\epsilon}}\, B\, e^{i\omega(t-\frac{R}{c})}\left[\cos\theta + \sqrt{1-(\frac{\lambda}{\lambda_0})^2}\right]\sin(\frac{\pi a}{\lambda}\sin\theta)\cot\theta$$

4.15

$$E_\zeta , E_R , H_\theta , \text{ and } H_R = 0 .$$

Poynting's vector (in radial direction)

$$= \frac{8 b^2}{\lambda^2 m^2 R^2}\sqrt{\frac{\mu}{\epsilon}}\, |B|^2 \left[\cos\theta + \sqrt{1-(\frac{\lambda}{\lambda_0})^2}\right]^2 \sin^2(\frac{\pi a}{\lambda}\sin\theta)\cot^2\theta$$

4.16

Omitting constant factor for the present, we have three factors which effect the radiation pattern of the $H_{o,m}$ - waves. It is amusing to see that, except for the term $\sqrt{1-(\frac{\lambda}{\lambda_0})^2}$

1. S: A. Schekunoff, Bell Sys. Tech. Jour. Vol.XV pp 92-112 January 1936

which is approaching a constant at sufficiently high ratios

of $\frac{\lambda_0}{\lambda}$, all the three factors are independent of the criti-

cal wave length or the dimension b of the tube. This

is caused by the symmetry of field with respect to the

XY-plane at the opening of the pipe. Thus it is possible

to control the radiation pattern in this plane practically

adjusting the dimension a .

The order of harmonic, m, of the $H_{o,m}$ -wave

(m = odd) has little to do with the radiation pattern in

XY-plane, since the fields at the opening are independent of

y , regardless of the order of harmonics. It enters the expre-

ssion only in the critical wave length, and its effect on

the pattern in XY-plane is of minor importance.

The factor $\sin(\frac{\pi a}{\lambda}\sin\theta)/\sin\theta$ has its first zero at

$$\theta = \sin^{-1}\left(\frac{\lambda}{a}\right) . \qquad\qquad 4.17$$

It is apparent that the smaller the dimension a, the larger the

value θ, and the broader will be the main beam of radiation.

For large values of a, there will be a number of zeros or

lobes beyond the first one, the maximum amplitude of which

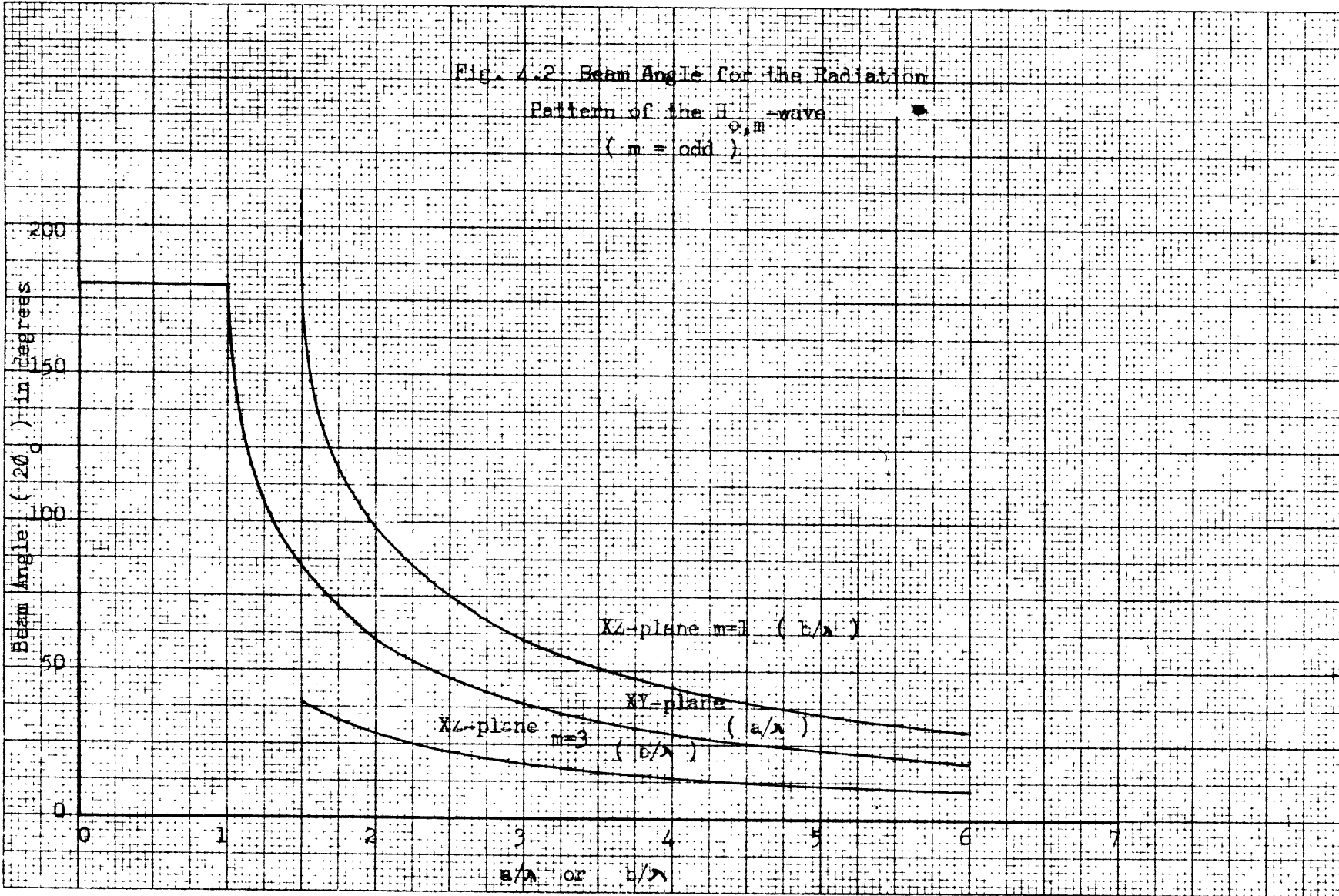varies inversely as $\sin\theta$.

The significance of the factor $\cos\theta$ can be

easily visualized if we refer to the solution for the

radiation field from a small oscillating dipole placed at

the origin and coinciding with the Y-axis. The same(and

only) angular function $\cos\theta$ appears in that solution.

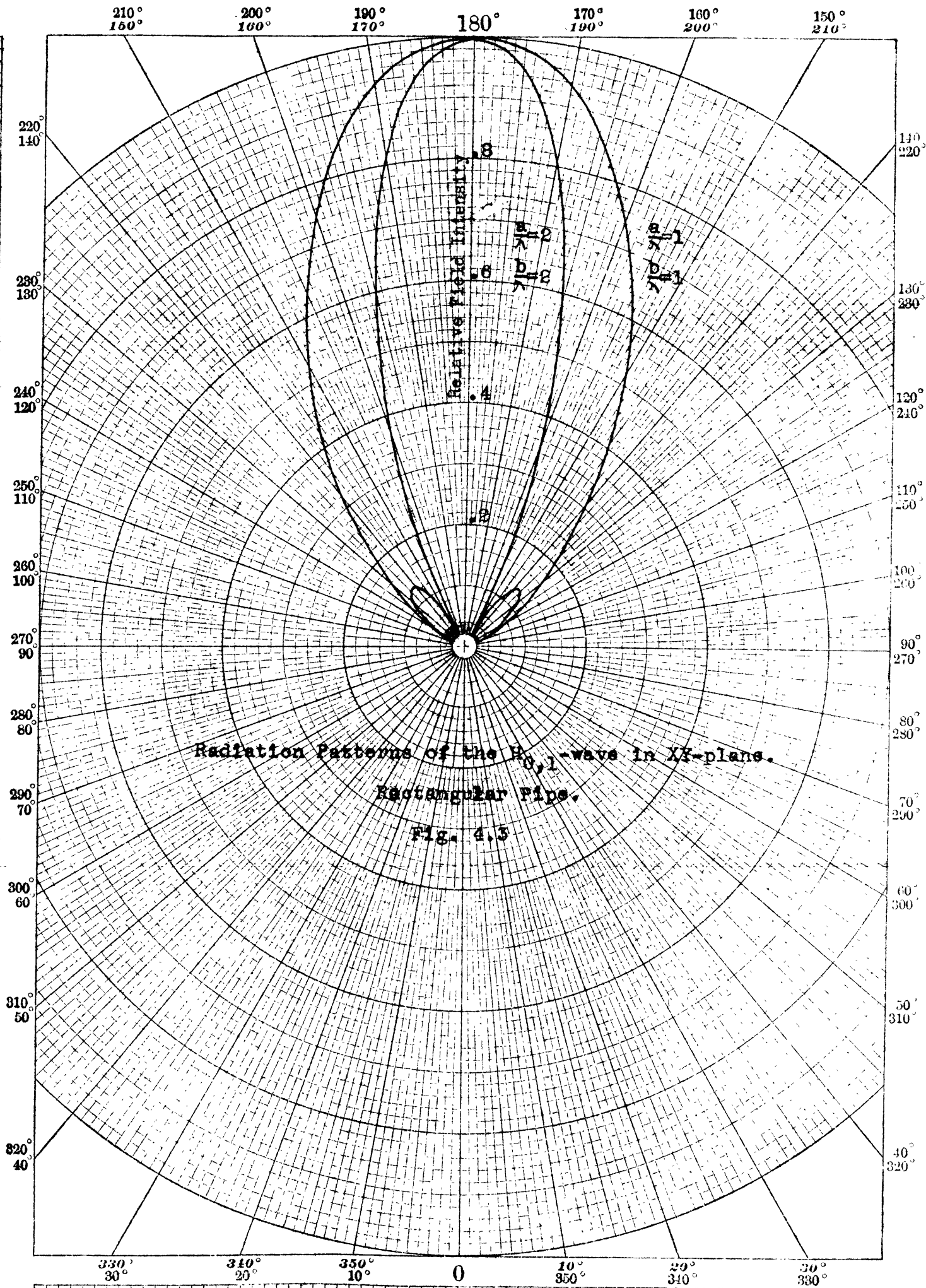The radiation field is identically zero at all points on

the prolongation of the axis of the dipole. In our case
we have an infinite number of displacement current elements
whose directions are all parallel to Y axis, consequently
there is no radiation along the $\pm$Y axis.

For the sake of convenience, the beam angle[1] is defined
as that including the main lobe of radiation. It is twice
the angle measured from the X-axis to the first zero of
the radiated field functions. Using the expression 4.17,
Fig. 4.2 is plotted with beam angle against the value of
$\frac{a}{\lambda}$ for radiation field of $H_{o,m}$-waves in XY-plane. The
discontinuity of the slope of the curve at $\frac{a}{\lambda} = 1$ is caused
by the coincidence of zeros of $\cos\theta$ and $\sin\left(\frac{\pi a}{\lambda}\sin\theta\right)/\sin\theta$

Fig 4.3 shows the radiation pattern of $H_{o,1}$-
wave in XY-plane. The calculation covers only the front half
of the sphere. Comparing the two curves, we see that the lar-
ger the dimension "a" the narrower the beams, and at the
same time, the larger the secondary lobe. The dimension "b"
has but little effect on the shape of the pattern. A curve
with $a/\lambda = 2$ and $b/\lambda = 1$ was calculated and discarded because
it lies too close to the curve ($a/\lambda = 2$, $b/\lambda = 2$). In fact,
the beam becomes slightly broader as the value of b/λ is
decreased. The radiation pattern of $H_{o,3}$ has essentially
the same form.

---

[1] The beam angle is not always defined in this way. It is
sometimes defined as the angle within which, the electric
or the magnetic field intensity is equal or greater than
one half of the maximum intensity of radiation. By this
definition, the lowest power density at the edges of the
beam is one-fourth of the maximum power density.

Fig. 4.2 Beam Angle for the Radiation
Pattern of the $H_{0,m}$ -wave
(m = odd)

Xz-plane m=1 (b/λ)

XY-plane (a/λ)

Xz-plane m=3 (b/λ)

Beam Angle ($2\theta_0$) (in degrees)

a/λ or b/λ

Radiation Patterns of the $H_{0,1}$-wave in XY-plane.
Rectangular Pipe.

Fig. 4.3

Radiation Pattern in XZ-plane

$$(\zeta = \frac{\pi}{2})$$

By putting $\zeta = \frac{\pi}{2}$ in Eq 13 and 14, the radiated field intensities are

$$E_s = -\sqrt{\frac{\mu}{\varepsilon}}\, H_\theta = \frac{m\pi a}{Rb}\sqrt{\frac{\mu}{\varepsilon}}\, B\, e^{i\omega(t-\frac{R}{c})}\left[\cos\theta + \sqrt{1-(\frac{\lambda}{\lambda_o})^2}\right] \frac{\cos(\frac{\pi b}{\lambda}\sin\theta)}{\sin^2\theta - (\frac{\lambda}{\lambda_o})^2} \qquad 4.18$$

$$E_\theta,\ E_R,\ H_\zeta,\ \text{and}\ H_R = 0 \qquad .$$

The Poynting's vector in radial direction:

$$= \frac{m^2\pi^2 a^2}{2R^2 b^2}\sqrt{\frac{\mu}{\varepsilon}}\, |B|^2\left[\cos\theta + \sqrt{1-(\frac{\lambda}{\lambda_o})^2}\right] \frac{\cos^2(\frac{\pi b}{\lambda}\sin\theta)}{[\sin^2\theta - (\frac{\lambda}{\lambda_o})^2]^2} \qquad 4.19$$

XZ-plane (y = 0) is the one which is perpendicular to the orientation of electric vector at the opening of the pipe. We would expect the result that the electric field intensity in this plane is everywhere parallel to the Y-axis. The field is not always zero at $\theta = \pm\frac{\pi}{2}$, points on the Z-axis. The field patern in the XZ-plane is independent of the dimension "a".

The same factor, $\cos\theta + \sqrt{1-(\frac{\lambda}{\lambda_o})^2}$, as in the XY-plane, appeard here also. The third factor has the form

$$\frac{\cos(\frac{\pi b}{\lambda}\sin\theta)}{\sin^2\theta - (\frac{m\lambda}{2b})^2} \qquad . \qquad 4.20$$

In Eq. 4.20 the factor $\cos(\frac{\pi b}{\lambda}\sin\theta)$ is zero for a series of values of θ, viz.,

$$\theta = \sin^{-1}\left(\frac{h\lambda}{2b}\right) , \qquad\qquad n = 1.\ 3,\ 5,\ \ldots \qquad 4.21a$$

but the denominator is zero for only one value:

$$\theta = \sin^{-1}\left(\frac{m\lambda}{2b}\right) \qquad\qquad 4.21b$$

where m denotes the order of harmonics. Thus, the first
zero of the fraction with m = 1 , i.e. for the $H_{o,1}$-wave,
occurs at

$$\theta = \sin^{-1} \left(\frac{3\lambda}{2b} \right) ,$$ 4.22a

while that for the $H_{o,3}$-wave is at

$$\theta = \sin^{-1} \left(\frac{\lambda}{2b} \right) .$$ 4.22b

The angle of the first zero determines the spread of the
main or center lobe. The beam angles are twice of this
angle, i.e. twice the values of θ corresponding to the
first zero, and are plotted in Fig. 4.2. The field pattern
of the $H_{o,1}$-wave (m = 1) in XZ-plane will not have any
zero if $\lambda \geq \frac{2}{3} b$ (except the zero in the negative X-
direction). The curve for the $H_{o,3}$-wave is also plotted
in Fig 4.2. Naturally, the curve does not extend beyond
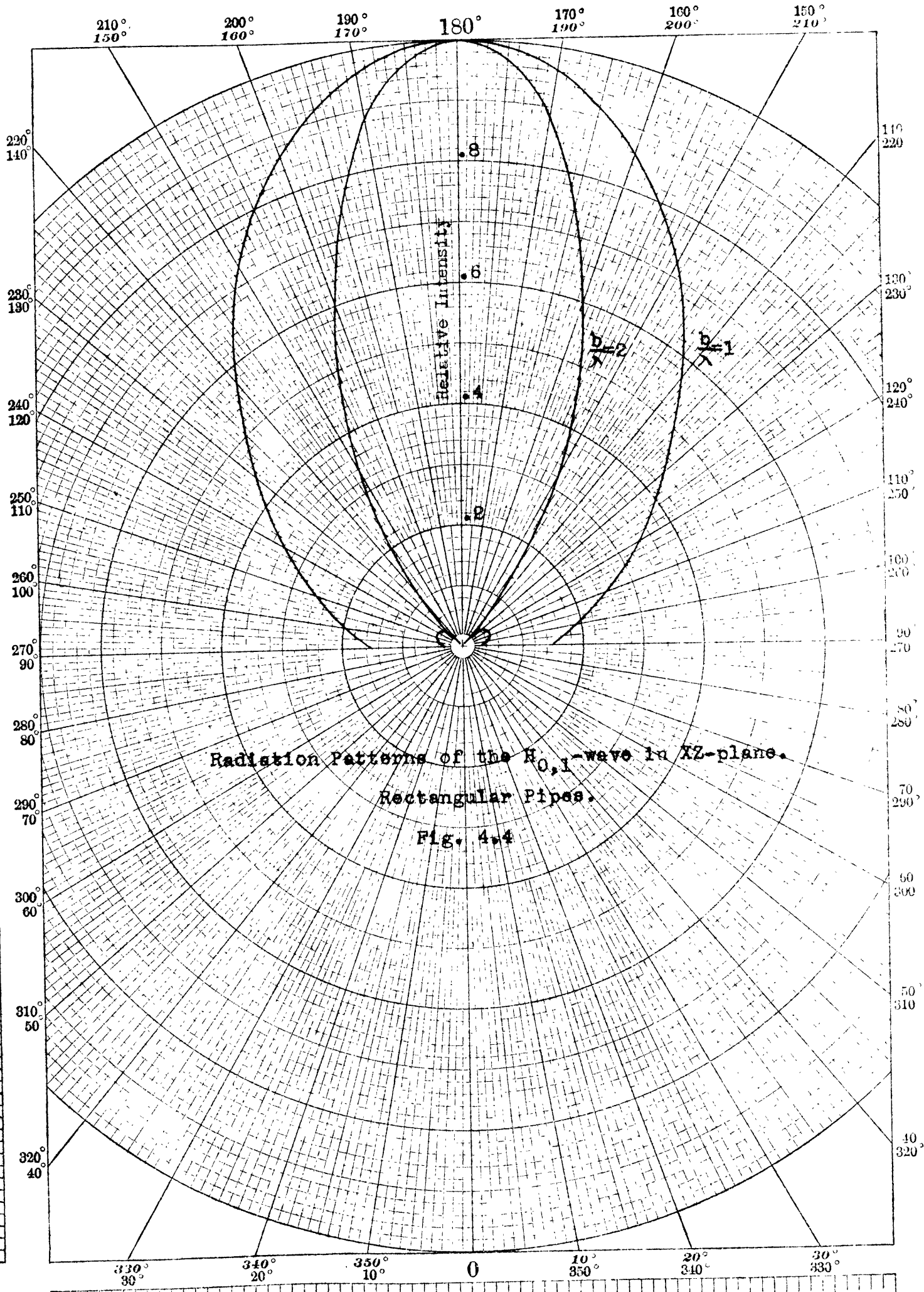the critical wave length for the particular wave type.

Consider the $H_{o,1}$-wave only, the beam angle
in XY-plane is always narrower than that in XZ-plane for
a square tube. If it is desired to have the same beam
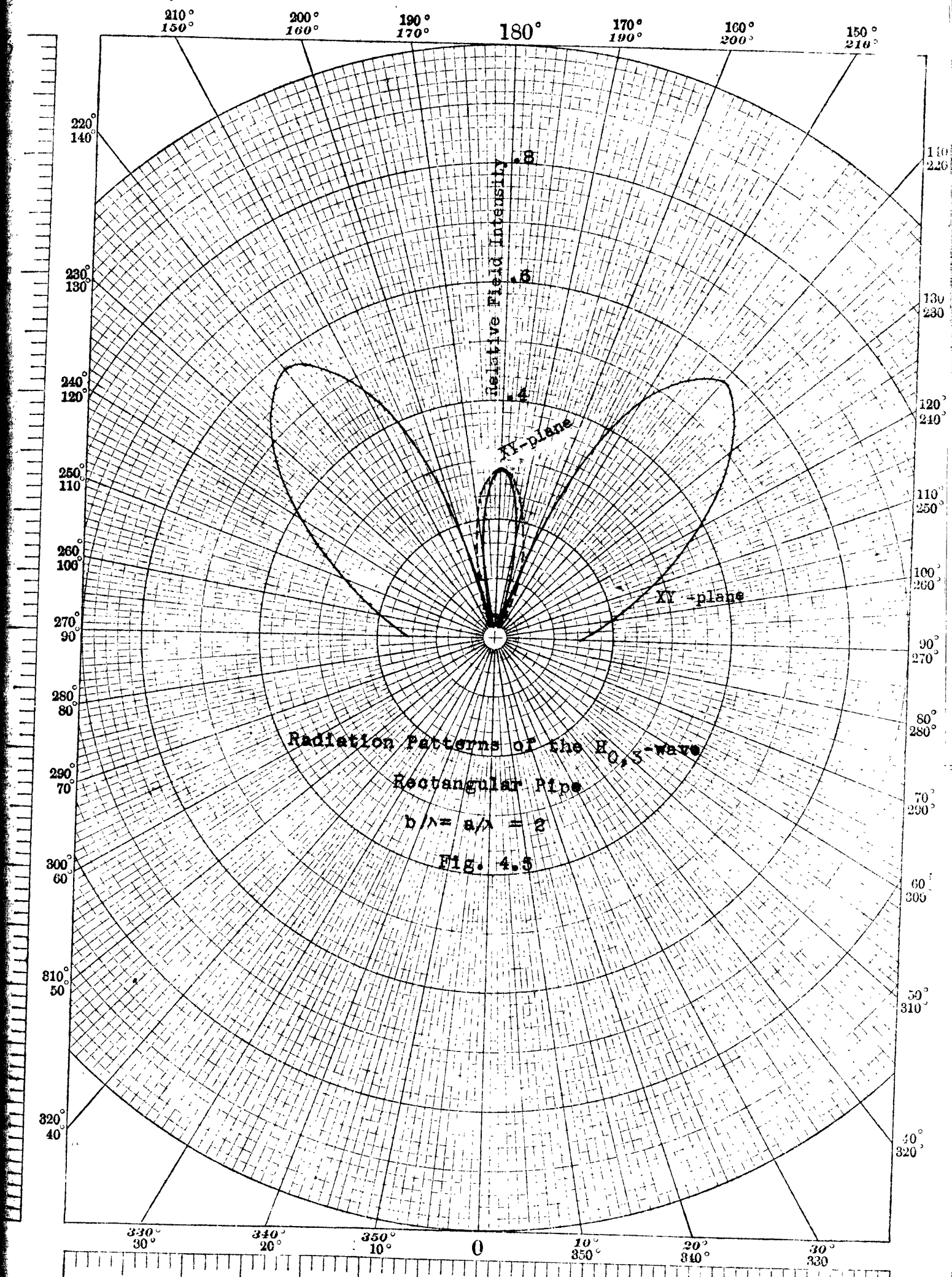angle in both planes we need a tube with a/b = 2/3 .

For the $H_{o,1}$-wave, besides the main or center
lobe, there will be side lobes when the ratio b/λ is above
3/2 . The narrower the main beam, the more the side lo-
bes appear. However the maximum magnitude of the side lobes
is small, compared to that of the main lobe. The denomi-
nator of Eq. 4.20 goes through zero within the main beam,
and therefore the main beam has the largest magnitude of all.

This is not so for the $H_{o,3}$-wave. There will always be side lobes when any $H_{o,3}$-wave is allowed to exist inside the pipe. The magnitude of the second lobe is always greater than that of the center lobe, because, for this wave, the denominator of Eq. 4.20 goes through zero within the second lobe of the beam.

Fig. 4.4 shows the radiation patterns of the $H_{o,1}$-wave in the XZ-plane, for ratio $b/\lambda = 1$ and 2. For $b/\lambda = 2$, the operating wave length is below the critical wave length of the $H_{o,3}$-wave. Let us assume there is a $H_{o,3}$-wave existing alone inside the pipe operating at $b/\lambda = 2$, and the maximum amplitude of its electric field intensity is equal to that of the $H_{o,1}$-wave used in the calculation of the curve ($b/\lambda = 2$), Fig. 4.4 . The radiation pattern of this $H_{o,3}$-wave in XZ-plane, plotted to the same scale as curve ($b/\lambda = 2$), Fig. 4.4 , is shown in Fig. 4.5 . Thus, by comparing the two curves, the amplitude at the center main lobe of $H_{o,3}$-wave is only 28.2% of that of the $H_{o,1}$-wave, while the amplitude at the center of the secondary lobe is 58% of the same. In Fig. 4.5 , the radiation pattern of the $H_{o,3}$-wave in the XY-plane is also shown in dotted line for ratio $a/\lambda = 2$.

The $H_{o,3}$-wave does not exist alone in a rectangular pipe practically, but is always accompanied by the $H_{o,1}$-wave since the critical wave length of the $H_{o,1}$-wave is three times longer than that of the $H_{o,3}$-wave. The phase velocity

Radiation Patterns of the $H_{0,1}$-wave in XZ-plane.
Rectangular Pipes.

Fig. 4.4

Radiation Patterns of the $H_{0,3}$-wave
Rectangular Pipe
$b/\lambda = a/\lambda = 2$
Fig. 4.5

of the two waves are different, and since the resultant
field distribution over a cross section of the pipe is
just the vector and complex sum of the fields of the two,
the resulatant field distribution inside the pipe varies
with the axial distance. Only the field distribution at
the opening is important for the radiation. The radiation
pattern of such composite wave is just the linear super-
position of the radiation patterns of the $H_{o,1}$ -wave and
the $H_{o,3}$ -wave, taking into consideration · · the relative
magnitude and phase difference of the two waves at the
opening.   In Fig. 4.6 , the inner curve shows the result-
ant radiation pattern, in XZ-plane, of an $H_{o,3}$-wave and an
$H_{o,3}$ -wave of 20% amplitude and equal phase., i.e. at the
opening, the resultant field distribution is as follows

$$E_y \propto \cos\left(\frac{\pi}{b} z\right) e^{i\omega t - i\beta_1 x} + 0.2 \cos\left(\frac{3\pi}{b} z\right) e^{i\omega t - i\beta_3 x} \qquad 4.23a$$

and the outer curve represents the radiation pattern of an
$H_{o,1}$ -wave and an $H_{o,3}$ -wave of 20% amplitude and opposite
in phase, i.e. at the opening, the resultant field distri-
bution is as follows.

$$E_y \propto \cos\left(\frac{\pi}{b} z\right) e^{i\omega t - i\beta_1 x} - 0.2 \cos\left(\frac{3\pi}{b} z\right) e^{i\omega t - i\beta_3 x} \qquad 4.23b$$

By comparing them with radiation pattern of
$H_{o,1}$ -wave (Fig. 4.4 inner curve), we see that the main lobe
is sharpened but the side lobe enlarged by introducing
an $H_{o,3}$ -wave in phase at the opening; the greater the am-
plitude of $H_{o,3}$ -wave, the sharper the beam and larger the

Radiation Patterns in XZ-plane, of
An H₀,₁-wave and An H₀,₃-wave of
20% Amplitude in Rectangular Pipe.

b/λ = 2

Fig. 4.6
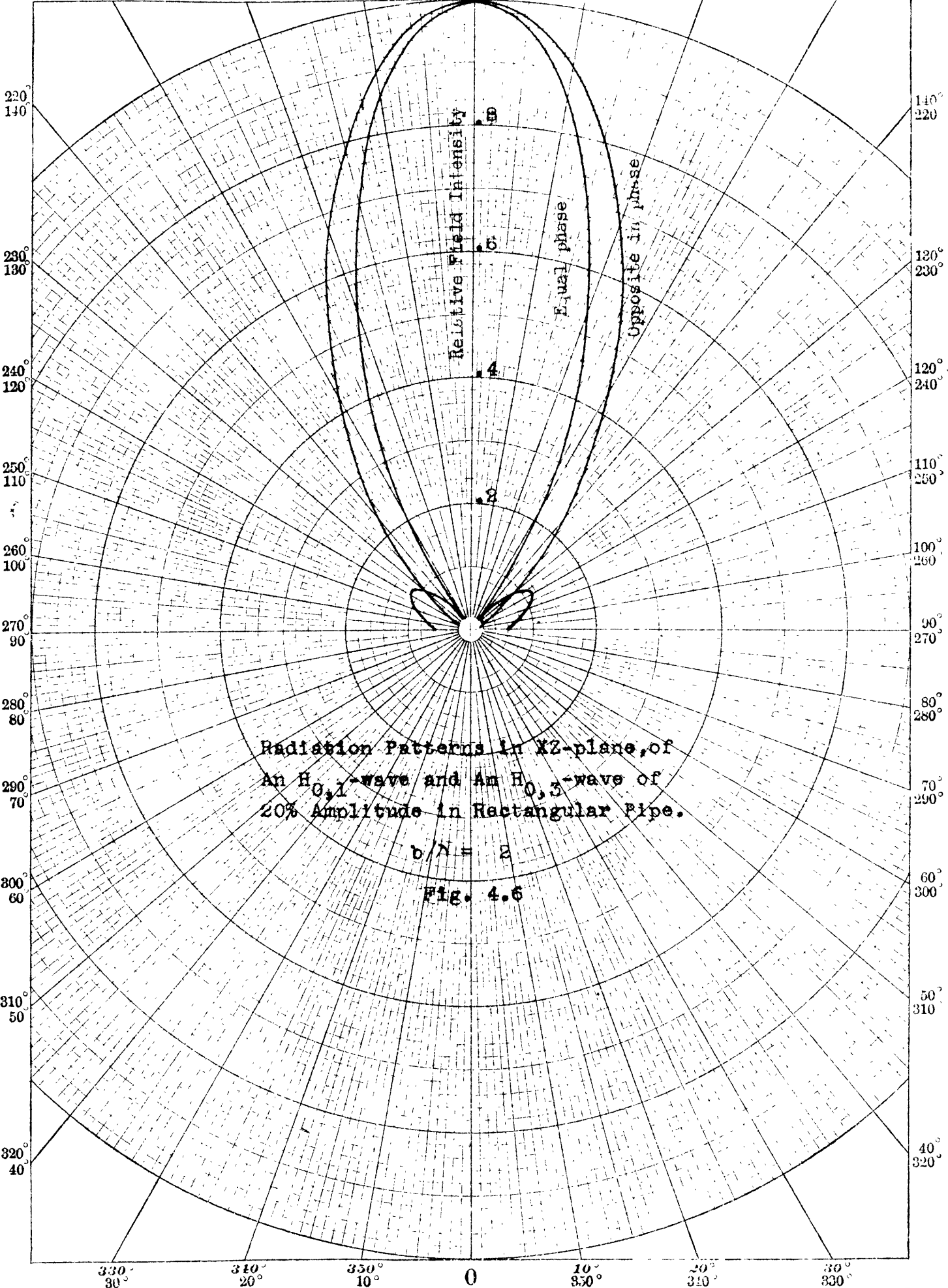
secondary lobe. The reverse is true when the $H_{o,1}$-wave

and $H_{o,3}$-wave are opposite in phase. Thus it is possible

by tuning the length of the pipe to sharpen the main beam

at the expense of larger secondary lobes.

Eq. 4.23a represents a sharpened sinusoidal dis-

tribution. and the radiation pattern from this distribution

is also sharper than the radiation pattern of the $H_{o,1}$-

wave. Eq. 4.23a represents a flattened sinusoidal distri-

bution, and the radiation pattern is also broader than the

radiation pattern of the $H_{o,1}$-wave.

From these fact we may conclude that a sharp

field distribution at the opening is favorable for the

single beam directional radiation.

One method of expressing the single beam dire-

ctivity of a certain wave is to compare the power which would

be needed to feed a non-directional wave from a dipole sour-

ce to the power actually needed to feed the directional wave

under consideration, such that, the maximum power densities

of the two cases at equal distances from the sources are equal.

This ratio is generally defined as power gain of the direction-

al system. Let us take a dipole, lying on the X-acis at the

origin, whose radiated power density on a given sphere of

radius R is $\sin\theta$. Thus the maximum radiated total density

on that sphere is unity. The total power radiated from

the dipole is the integration of radiated power density

over that sphere:

$$R^2 \int_0^{2\pi} \int_0^\pi \sin^2\theta \sin\theta \, d\theta \, d\zeta = \frac{8}{3}\pi R^2.$$

The maximum radiated power density if the $H_{0,1}$ -wave of a rectangular pipe is obtained by putting $\theta = 0$ in either expression 4.16 or 4.19:

$$\frac{8\pi^2 a^2 b^2}{\lambda^4 R^2} \sqrt{\frac{\mu}{\varepsilon}} \, |B|^2 \left[1 + \sqrt{1 - (\tfrac{\lambda}{\lambda_0})^2} \right]^2$$

when the dipole have the same maximum power density on the sphere of radius R, the power output from the dipole would be

$$\frac{8}{3}\pi R^2 \frac{8\pi^2 a^2 b^2}{\lambda^4 R^2} \sqrt{\frac{\mu}{\varepsilon}} \, |B|^2 \left[1 + \sqrt{1 + (\tfrac{\lambda}{\lambda_0})^2} \right]^2 \qquad 4.25$$

The actual power output from the rectangular pipe, is the energy transmitted along the tube, if we neglect the reflection, etc. caused by the end effects.

$$|B|^2 \frac{ab\pi}{\lambda^2} \sqrt{\frac{\mu}{\varepsilon}} \left[1 - (\tfrac{\lambda}{\lambda_0})^2 \right]^{\frac{1}{2}}. \qquad 4.26$$

Therefore the power gain Q as compared to a dipole is

$$\text{Power Gain} = \frac{16}{3}\pi^2 \frac{a}{b} (\tfrac{\lambda_0}{\lambda})^2 \frac{\left[1 + \sqrt{1 - (\tfrac{\lambda}{\lambda_0})^2} \right]}{\sqrt{1 - (\tfrac{\lambda}{\lambda_0})^2}} \qquad 4.27a$$

This expression does not tell the truth when the ratio $\frac{\lambda_0}{\lambda}$ is near unity since at critical wave length, no wave may possibly travel along the pipe. This ambiguity is caused by the assumption that a wave would exist at the end of the pipe, though it did not propagate at such wave length. Hence, if we exclude the region around $\frac{\lambda}{\lambda_0} = 1$, the power gain is expressed as

$$\text{Power Gain} = \frac{64}{3}\pi^2 \frac{a}{b}\left(\frac{\lambda_0}{\lambda}\right)^2 \qquad\qquad 4.27b$$

The power gain is proportional to the square of the ratio $\frac{\lambda_0}{\lambda}$ or $\frac{f}{f_0}$ at sufficiently high frequency.

Radiation pattern of Other types of Wave

The essential requirement for directive radiation is to have the flow of radiated energy concentrated within a sharp angle. Using a rectangular pipe as a radiation device, the point of maximum radiation energy usually lies on the axis of the cylinder, the X-axis, on account of the symmetrical field distribution over the cross section of the pipe about that axis. This is so for $H_{o,1}$ - wave, which has the electric field vector parallel to one side of the pipe. It has been shown also that the maximum of the central lobe of the radiated field for an $H_{o,m}$ - wave, where m is an odd integer, lies on the X-axis. No other type of wave in a rectangular pipe has this property. For the sake of simplicity, we shall proceed to prove that for all types of wave, except the $H_{o,m}$, m=odd, the fields and therefore the flow of energy at any point on the X-axis is zero, and therefore the production of a single beam of radiant energy is impossible. We shall also illustrate the general shape of a radiation pattern of this kind with a special example, viz., $H_{1,1}$ -wave.

Let us rewrite the expression of Huygens' principle for space free of charge and conduction current, and for radiation from a rectangular pipe (Eq. 4.11):

$$A = \int\int \frac{1}{\rho} \{ (\frac{i\omega}{c} + \frac{1}{\rho}) \cos\theta + i\beta \} A e^{-i\omega\frac{\rho}{c}} ds .$$

The $\frac{1}{\rho^2}$ term is to be neglected for the radiation field. Since θ is equal to zero at any point on the X-axis, it is obvious from Eq. 4.12 that the distance from that point to any point over the cross-section at the end of the pipe is constant and equal to R. Putting θ to zero and $\dot{p}$ to R , all factors under the integration become independent of y and z except the factor A. Thus

$$A = \frac{i\omega}{cR} (1 + \frac{\beta c}{\omega}) e^{-i\omega\frac{R}{c}} \int_s A \, ds .$$

4.28

We shall investigate the integral $\int_s A \, ds$ alone, because if we can show that it vanishes on the x-axis, there can be no radiation in this direction and our theorem will be proved.

$H_{o,m}$-wave (m = even)

The component fields of the $H_{o,m}$-wave for m = even with the center of the pipe coinciding with the x-axis are as follows:

$$E_y = i\omega\mu B \sin(\frac{m\pi}{b} z) e^{i(\omega t - \beta x)}$$

$$H_z = i\beta B \sin(\frac{m\pi}{b} z) e^{i(\omega t - \beta x)}$$

$$H_x = \frac{m\pi}{b} B \cos(\frac{m\pi}{b} z) e^{i(\omega t - \beta x)} .$$

4.29

Using Eq. 4.3, we have the vector potential at the opening of the pipe as below:

$$A_y = - B \sin \left(\frac{m\pi}{b} z \right) e^{i(\omega t - \beta x)}$$

$$A_x = A_z = 0 \qquad\qquad 4.30$$

The surface integral $\int_s A \, ds$ for A_y at any point on X-axis

$$- \int_{-\frac{a}{2}}^{\frac{a}{2}} dy \int_{-\frac{b}{2}}^{\frac{b}{2}} \sin \left(\frac{m\pi}{b} z \right) e^{i(\omega t - \beta x)} \, dz$$

$$= a \frac{b}{m\pi} e^{i(\omega t - \beta x)} \left[\cos \left(\frac{m\pi}{2} \right) - \cos \left(-\frac{m\pi}{2} \right) \right]$$

$$= 0$$

,

and since A_x and A_y are identically zero in all the space, the electric and magnetic field intensities vanish along that line.

We may similarly prove for the $H_{o,m}$-wave (m = even) that the radiated fields in the entire XY-plane is zero. It is because the vector potential of the $H_{o,m}$-wave (m = even) inside the pipe has an odd symmetry with the XY- plane.

$H_{n,m}$ -wave

For $H_{n,m}$-wave we place one corner instead of the central axis, of the rectangular pipe coincide with the X-axis, so that we may write a single set of field expressions for both even and odd values of n and m . (Refer to Fig. 2.2c , field diagram of $H_{1,1}$ -wave.) The expressions of fields are given in Eq. 2.1. The components of the vector potential inside the tube are consequently

$$A_y = -B \frac{\frac{m\pi}{b}}{\kappa^2 - \beta^2} \cos\left(\frac{n\pi}{a} y\right) \sin\left(\frac{m\pi}{b} z\right) e^{i(\omega t - \beta x)}$$

$$A_z = B \frac{\frac{n\pi}{a}}{\kappa^2 - \beta^2} \sin\left(\frac{n\pi}{a} y\right) \cos\left(\frac{m\pi}{b} z\right) e^{i(\omega t - \beta x)} \qquad 4.31$$

$$A_x = 0$$

The component A_y at any point on the X-axis in the space is proportional to the integral, omit the comstant coefficient,

$$\int_0^b \int_0^a \cos\left(\frac{n\pi}{a} y\right) \sin\left(\frac{m\pi}{b} z\right) dy \, dz$$

$$= -\frac{a}{n\pi} \frac{b}{m\pi} \left[\sin(m\pi) - 0 \right] \left[\cos(m\pi) - 1 \right] = 0$$

Similarly, the surface integral of A_z is zero. Therefore the radiation fields of $H_{n,m}$-wave along X-axis are equal to zero.

$E_{n,m}$-wave

By placing one corner of the rectangular pipe coincide with the X-axis, the fields for the $E_{n,m}$-wave inside the pipe are given in Eq. 2.4. The vector potential inside the pipe is

$$A_x = -\frac{B}{i\omega\mu} \sin\left(\frac{n\pi}{a} y\right) \sin\left(\frac{m\pi}{b} z\right) e^{i\omega t - i\beta x}$$

$$A_y = \frac{B}{i\omega\mu} \frac{i\beta}{\kappa^2 - \beta^2} \frac{n\pi}{a} \cos\left(\frac{n\pi}{a} y\right) \sin\left(\frac{m\pi}{b} z\right) e^{i\omega t - i\beta x}$$

$$A_z = \frac{B}{i\omega\mu} \frac{i\beta}{\kappa^2 - \beta^2} \frac{m\pi}{b} \sin\left(\frac{n\pi}{a} y\right) \cos\left(\frac{m\pi}{b} z\right) e^{i\omega t - i\beta x} \qquad 4.32$$

Comparing the above A_y and A_z with the A_z and A_y of the $H_{n,m}$-wave (Eq. 4.31) respectively, we conclude that the components of vector potential A_y and A_z along the X-axis are zero.

Along the X-axis, x is equal to R, and A_x is the radial component A_R of the vector potential. It is shown in Eq. 4.6 and 4.7 that both E and H are independent of A_R . Therefore, both the fields and flow of energy along X-axis are zero.

We have mathematically proven that all types have of waves in retangular pipes do not single beam radiation pattern except for the $H_{o,m}$-wave (m = odd). The $H_{o,m}$-(m=even) wave has zero fields in the XY-plane.

Whether a type of wave in a hollow pipe yields directional radiation pattern or not may be visualized from its diagram of electric field distribution over the cross-section at the mouth. Each area element over the cross-section is occupied by a displacement current element, which, in a way, behaves as a dipole. Since the current element is proportional to the time derivative of electric field intensity, it is represented by the same distribution diagram. Referring to Fig. 2.2 , it is observed that for any type of wave, the displacement current elements located at two points diametrically symmetrical about the center of the cross-section, are always vectorially parallel. If their vector sense is the same, their

radiation fields at points along the X-axis are cumulative,
and we obtain a case of directional radiation in a single
beam. On the other hand, if their vector senses are oppo-
site, their radiation fields at points along the X-axis
cancel each other, and give zero fields at those points.
A check of the field distribution diagrams reveals that the
$H_{1,1}$-, $E_{1,1}$-, and $H_{0,m}$- (m is an even integer) waves do not
give directional radiation. Since the diagrams of the $H_{n,m}$-
and $E_{n,m}$-waves can be constructed by piling n times m number
of the diagrams of the $H_{1,1}$- and the $E_{1,1}$-waves together in
one pipe, they also do not give directional radiation. Only
the $H_{0,m}$-waves, where m is odd integer, have a radiation
pattern possessing a central lobe.

Similar analysis may be applied to the radiation
patterns of waves inside pipes of circular cross section.
Referring to the field distribution diagrams of waves in
circular pipes[1], we see that only the H_1-wave and probably
the E_1-wave of the four simplest types, possess the pro-
perty of directional radiation. The H_1-wave is similar to
the $H_{0,1}$-wave in rectangular pipe, since the electric
fields over the cross section are all nearly parallel.
Therefore, it will have a radiation pattern possessing
large central lobe. Although the radiation pattern of the

---

[1] G. C. Southworth, Bell Sys. Tech. Jour. Vol. 15 , April
issue, Fig. 1, (1936)

E_1-wave may probably have a central lobe, the side lobes will have much larger amplitude.

Radiation Pattern of the $H_{1,1}$-wave

Let us pick up the $H_{1,1}$-wave as a special case of those types of waves, whose radiation patterns do not have central lobes. With the axis of the pipe coinciding with the X-axis, the field expressions of $H_{1,1}$-waves inside the pipe may be written as

$$H_x = B \quad \sin\left(\tfrac{\pi}{a}y\right)\sin\left(\tfrac{\pi}{b}z\right) e^{i(\omega t - \beta x)}$$

$$H_y = -\tfrac{\beta}{\omega\mu}E_z = B \frac{i\beta\pi/a}{\left(\tfrac{\pi}{a}\right)^2+\left(\tfrac{\pi}{b}\right)^2} \cos\left(\tfrac{\pi}{a}y\right)\sin\left(\tfrac{\pi}{b}z\right) e^{i(\omega t - \beta x)} \qquad 4.33$$

$$H_z = \tfrac{\beta}{\omega\mu}E_y = B \frac{i\beta\pi/b}{\left(\tfrac{\pi}{a}\right)^2+\left(\tfrac{\pi}{b}\right)^2} \sin\left(\tfrac{\pi}{a}y\right)\cos\left(\tfrac{\pi}{b}z\right) e^{i(\omega t - \beta x)}$$

The vector potential inside the pipe is

$$A_y = B \frac{\pi/b}{\left(\tfrac{\pi}{a}\right)^2+\left(\tfrac{\pi}{b}\right)^2} \sin\left(\tfrac{\pi}{a}y\right)\cos\left(\tfrac{\pi}{b}z\right) e^{i(\omega t - \beta x)}$$

$$A_z = B \frac{\pi/a}{\left(\tfrac{\pi}{a}\right)^2+\left(\tfrac{\pi}{b}\right)^2} \cos\left(\tfrac{\pi}{a}y\right)\sin\left(\tfrac{\pi}{b}z\right) e^{i(\omega t - \beta x)}$$

$$\qquad 4.34$$

$$A_x = 0$$

Substitute these two components of vector potential into Eq. 4.11 , and carry out the integration. The results are

$$A_y = B \frac{\lambda^2}{b^2 R} \frac{\cos\theta + \sqrt{1-(\frac{\lambda}{\lambda_o})^2}}{(\frac{\pi}{a})^2 + (\frac{\pi}{b})^2} \frac{\cos\zeta\sin\theta \cos[\frac{\pi a}{\lambda}\cos\zeta\sin\theta]\cos[\frac{\pi b}{\lambda}\sin\zeta\sin\theta] e^{i\omega(t-\frac{R}{c})}}{[(\cos\zeta\sin\theta)^2 - (\frac{\lambda}{2a})^2][(\sin\zeta\sin\theta)^2 - (\frac{\lambda}{2b})^2]}$$

$$A_z = -B \frac{\lambda^2}{a^2 R} \frac{\cos\theta + \sqrt{1-(\frac{\lambda}{\lambda_o})^2}}{(\frac{\pi}{a})^2 + (\frac{\pi}{b})^2} \frac{\sin\zeta\sin\theta \cos[\frac{\pi a}{\lambda}\cos\zeta\sin\theta]\cos[\frac{\pi b}{\lambda}\sin\zeta\sin\theta] e^{i\omega(t-\frac{R}{c})}}{[(\cos\zeta\sin\theta)^2 - (\frac{\lambda}{2a})^2][(\sin\zeta\sin\theta)^2 - (\frac{\lambda}{2b})^2]} \qquad 4.35$$

By resolving A into spherical coordinates and calculating the field intensities of radiation, we have the radiated field as follows

$$H_\theta = -\sqrt{\frac{\varepsilon}{\mu}} E_\zeta = B \frac{i2\lambda}{\pi R}[\cos\theta + \sqrt{1-(\frac{\lambda}{\lambda_o})^2}] \frac{\sin\zeta\sin\theta \cos[\frac{\pi a}{\lambda}\cos\zeta\sin\theta]\cos[\frac{\pi b}{\lambda}\sin\zeta\sin\theta] e^{i\omega(t-\frac{R}{c})}}{[(\cos\zeta\sin\theta)^2 - (\frac{\lambda}{2a})^2][(\sin\zeta\sin\theta)^2 - (\frac{\lambda}{2a})^2]}$$

$$H_\zeta = \sqrt{\frac{\varepsilon}{\mu}} E_\theta = B \frac{i2\lambda}{\pi R} \frac{[\cos\theta + \sqrt{1-(\frac{\lambda}{\lambda_o})^2}]\{a^2\cos^2\zeta - b^2\sin\zeta\}}{a^2 + b^2}$$
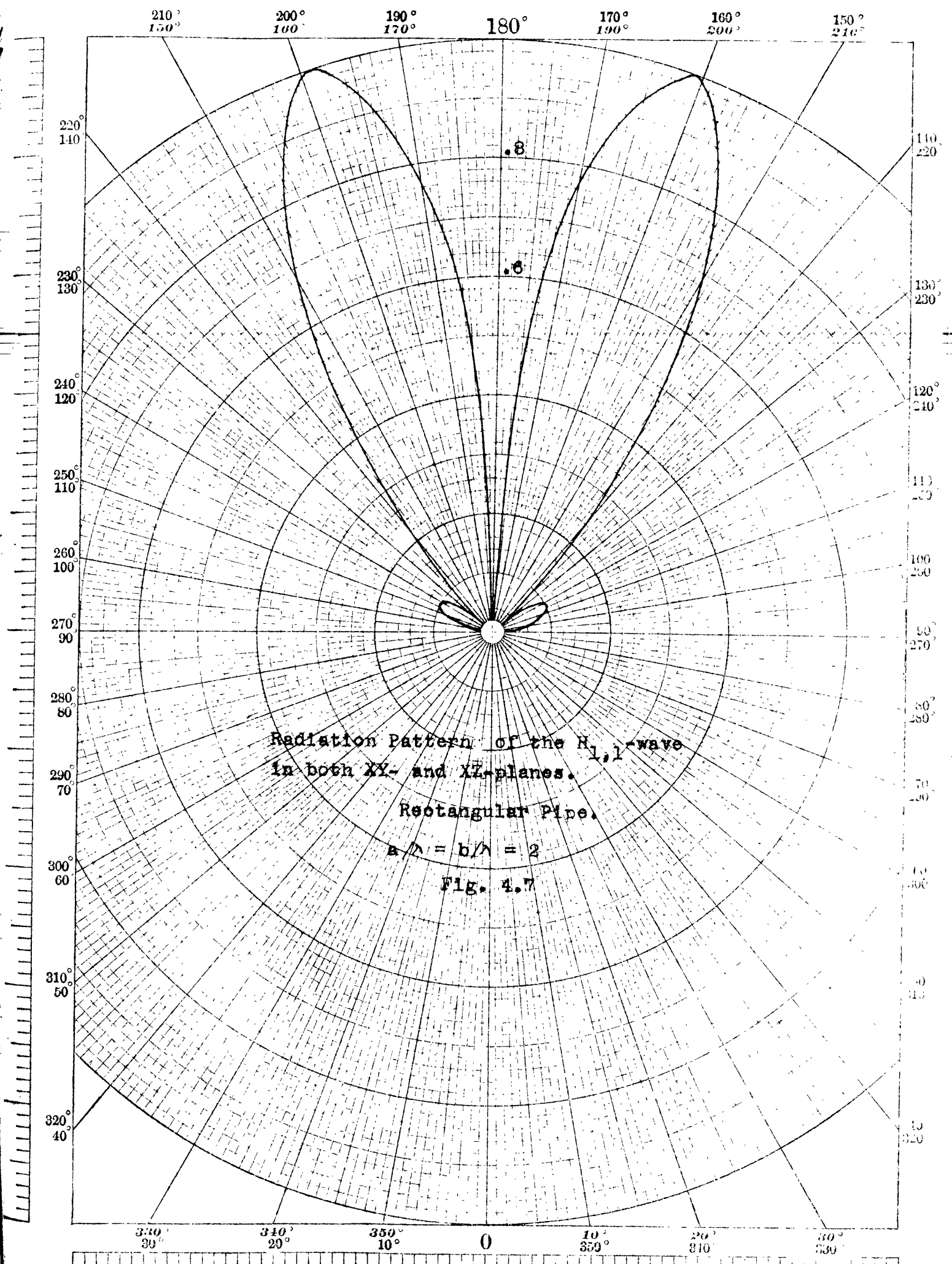
$$\times \frac{\cos\theta\sin\theta \cos[\frac{\pi a}{\lambda}\cos\zeta\sin\theta]\cos[\frac{\pi b}{\lambda}\sin\zeta\sin\theta] e^{i\omega(t-\frac{R}{c})}}{[(\cos\zeta\sin\theta)^2 - (\frac{\lambda}{2a})^2][(\sin\zeta\sin\theta)^2 - (\frac{\lambda}{2a})^2]} \qquad 4.36$$

$$H_R = 0 , \qquad E_R = 0$$

In the XY-plane, ($\zeta = 0$)

$$H_\zeta = \sqrt{\frac{\varepsilon}{\mu}} E_\zeta = -B \frac{i8a^4}{\pi R\lambda} \frac{[\cos\theta + \sqrt{1-(\frac{\lambda}{\lambda_o})^2}]}{a^2+b^2} \frac{\cos\theta\sin\theta \cos[\frac{\pi a}{\lambda}\sin\theta]}{\sin^2\theta - (\frac{\lambda}{2a})^2} e^{i\omega(t-\frac{R}{c})}$$

$$4.37$$

$$H_\theta , H_R , E_\zeta , \text{ and } E_R = 0$$

Radiation Pattern of the $H_{1,1}$-wave
in both XY- and XZ-planes.

Rectangular Pipe.

$a/\lambda = b/\lambda = 2$

Fig. 4.7

In XZ-plane ($\zeta = \dfrac{\pi}{2}$)

$$H_\zeta = \sqrt{\tfrac{\varepsilon}{\mu}}\, E_\theta = B\,\frac{i 8 b^4}{\pi R \lambda}\,\frac{[\cos\theta + \sqrt{1-(\tfrac{\lambda}{\lambda_o})^2}]}{a^2 + b^2}\,\frac{\cos\theta \sin\theta \cos[\tfrac{\pi b}{\lambda}\sin\theta]}{\sin^2\theta - (\tfrac{\lambda}{2b})^2}\,e^{\,i\omega(t-\tfrac{R}{c})}$$

$$H_\theta,\; H_R,\; E_\zeta \;\; \text{and}\;\; E_R = 0 \qquad\qquad 4.39$$

The radiation field distributions in XY-and XZ-planes have the same function except the reverse role of a and b . In Fig. 7 is plotted the radiation pattern in both planes for a square tube of a = b = 2 .

Summary:

The $H_{o,m}$-waves (m = odd)

Vector potential inside the pipe:

$$A_y = B\cos\left(\tfrac{m\pi}{b}z\right)e^{\,i(\omega t - \beta x)}$$

$$A_x = A_z = 0 \qquad\qquad 4.10a$$

Radiation Patern in XY-plane

$$E_\theta = \sqrt{\tfrac{\mu}{\varepsilon}}\,H_\zeta = \frac{4b}{\lambda \mu R}\sqrt{\tfrac{\mu}{\varepsilon}}\,B\,e^{\,i\omega(t-\tfrac{R}{c})}[\cos\theta + \sqrt{1-(\tfrac{\lambda}{\lambda_o})^2}]\sin\left(\tfrac{\pi a}{\lambda}\sin\theta\right)\cot\theta$$

$$E_\zeta,\; E_R,\; H_\theta \;\; \text{and}\;\; H_R = 0 \qquad\qquad 4.15$$

Beam angle

$$2\theta = 2\sin^{-1} \lambda/a$$

Radiation Patern in XZ-plane

$$E_\zeta = -\sqrt{\tfrac{\mu}{\varepsilon}}\ H_\theta = \frac{m\pi a}{Rb}\sqrt{\tfrac{\mu}{\varepsilon}}\ B\,e^{i\omega(t-\frac{R}{c})}\left[\cos\theta + \sqrt{1-(\tfrac{\lambda}{\lambda_0})^2}\right]\frac{\cos(\tfrac{\pi b}{\lambda}\sin\theta)}{\sin^2\theta - (\tfrac{\lambda}{\lambda_0})^2}$$

$$E_\theta,\ E_R,\ H_\zeta\ \text{and}\ H_R = 0 \qquad\qquad\qquad 4.18$$

Beam angle

$$2\theta = 2\sin^{-1}\left(\frac{3\lambda}{2b}\right)\ \text{for}\ H_{0,1}\text{-wave} \qquad\qquad 4.21$$

$$2\theta = 2\sin^{-1}\left(\frac{\lambda}{2b}\right)\ \text{for}\ H_{0,3}\text{-wave}\,. \qquad\qquad 4.22$$

Power Gain of the $H_{0,1}$-wave:

$$\text{Power Gain} = \frac{16}{3}\ \pi^2\ \frac{a}{b}\ \left(\frac{\lambda_0}{\lambda}\right)^2 \qquad\qquad 4.27b$$

Other Types of Waves

Other types of waves, the $H_{0,m}$- (m=even) the $H_{n,m}$-, and the $E_{n,m}$-waves, do not have single beam radiation patterns. For example:

The $H_{1,1}$-wave

Radiation pattern in XY-plane

$$H_\zeta = \sqrt{\tfrac{\varepsilon}{\mu}}\ E_\theta = -B\,\frac{i8a^4}{\pi R\lambda}\ \frac{\cos\theta + \sqrt{1-(\tfrac{\lambda}{\lambda_0})^2}}{a^2+b^2}\ \frac{\cos\theta\sin\theta\cos\left[\tfrac{\pi a}{\lambda}\sin\theta\right]}{\sin^2\theta - (\tfrac{\lambda}{2a})^2}\,e^{i\omega(t-\frac{R}{c})} \qquad 4.37$$

$$H_\theta,\ H_R, E_\zeta,\ \text{and}\ E_R = 0$$

Radiation pattern in XZ-plane

$$H_\zeta = \sqrt{\tfrac{\varepsilon}{\mu}}\, E_\theta = B\, \frac{i 8 b^4}{\pi R \lambda}\, \frac{\left[\cos\theta + \sqrt{1-(\tfrac{\lambda}{\lambda_0})^2}\,\right]}{a^2+b^2}\, \frac{\cos\theta \sin\theta \cos\left[\tfrac{\pi b}{\lambda}\sin\theta\right]}{\sin^2\theta - (\tfrac{\lambda}{2b})^2}\, e^{\,i\omega(t-\tfrac{R}{c})}$$

<div style="text-align:right">4.39</div>

H_θ, H_R, E, and $E_R = 0$

V. SECTORAL HORN

We have studied in the last chapter, the radiation characteristics of various types of waves within a pipe of rectangular cross-section. Only one type of wave, the $H_{o,m}$-wave, gives a single beam radiation pattern. The beam angle of the radiated wave depends upon the ratio of the linear dimensions of the cross-section to the wave length. The larger is the ratio, the narrower is the beam. The $H_{o,1}$-wave is characterized by the property that the electric field intensity is everywhere parallel to one pair of opposite sides. If we increase the cross-sectional area of the pipe in order to obtain a sharper beam, we need a proportionally longer pipe for the formation of this wave. These results might naturally sug est the idea of forming an electromagnetic horn with its smaller end attached to a rectangular pipe or some other forms of excitation systems. In this chapter, the properties and the radiation characteristics of the simplest geometrical construction will be investigated.

The shape of the horn now considered is illustrated in Fig. 5.1. It is generated by revolving a rectangular surface, with one side parallel to the Y-axis, about the Y-axis through an angle $2\phi_o$ less than $180°$. The top and bottom of the horn are bounded by two parallel conducting
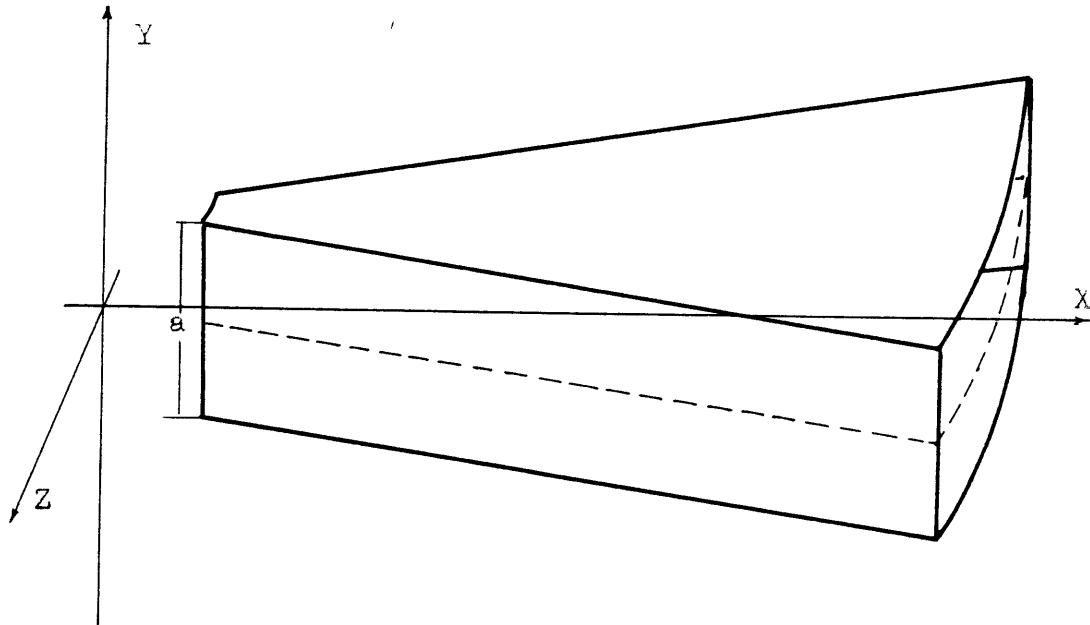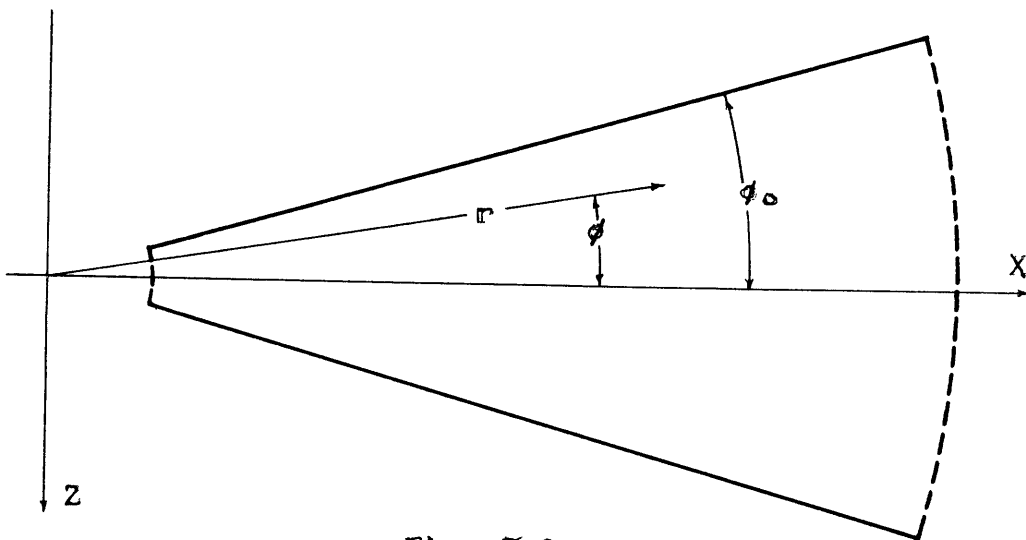
Fig. 5.1

Fig. 5.2

planes, "a" cms. apart. The two remaining sides are bound-
ed by conducting planes, which, if extended, would pass thru
the Y-axis. The volume around the Y-axis will be excluded
from this analysis, since it is a singular point mathematic-
ally. The horn is assumed to be extended to infinity in the
radial direction, so that the wave inside the horn may be
investigated. The end-effect for a horn of finite length
will not be considered. The conductor is assumed to have
infinitely great conductivity. We may define it as a sec-
toral horn because of its geometric shape.

Waves Inside the Horn

Inside a horn of this kind, the wave propagates
in the radial direction.[1] It is possible to have waves whose
field intensities and potentials vary both angularly and
vertically, i.e., with ϕ and with y. It is also possible
to have two types of waves, corresponding to the E- and H-
waves inside a hollow pipe, one without a radial component
of magnetic field intensity and the other without a radial
component of electric field intensity. Since we are princi-
pally interested in those types of waves which give single-

---

[1]The mathematical background of this chapter may be found in:
Slater, J.C. and Frank, N.H. :"An Introduction to Theo-
retical Physics"
Watson, G.N. :"Theory of Bessel Functions"
Jahnke, E. and Emde, F. :"Tables of Functions"

beam radiation patterns, we will limit our attention to the type of wave corresponding to the $H_{o,m}$-wave inside a rectangular pipe. This wave has wave functions independent of the coordinate y, and the electric field intensities are all parallel to the y-axis, i.e., perpendicular to the top and bottom boundary surfaces. The problem of obtaining the fields inside the horn is then reduced to a two dimensional one. Fig. 2 shows the horizontal cross-section, in which, the several functions vary.

The Maxwell equations, expressed in cylindrical coordinates (y,r,ϕ) for space free of conduction currents or charges, with a time variation $e^{i\omega t}$ are:

$$i\omega\varepsilon r\ E_y = \frac{\partial}{\partial r}(rH_\phi) - \frac{\partial}{\partial \phi}\ H_r \qquad\qquad 5.1\ a$$

$$i\omega\varepsilon r\ E_r = \frac{\partial}{\partial \phi}H_y - \frac{\partial}{\partial y}\ rH_\phi \ . \qquad\qquad 5.1\ b$$

$$i\omega\varepsilon\ E_\phi = \frac{\partial}{\partial y}\ H_r - \frac{\partial}{\partial r}\ H_y \qquad\qquad 5.1\ c$$

$$-i\omega\mu r\ H_y = \frac{\partial}{\partial r}\ rE_\phi - \frac{\partial}{\partial \phi}E_r \qquad\qquad 5.1\ d$$

$$-i\omega\mu r\ H_r = \frac{\partial}{\partial \phi}\ E_y - \frac{\partial}{\partial y}rE_\phi \qquad\qquad 5.1\ e$$

$$-i\omega\mu\ H_\phi = \frac{\partial}{\partial y}\ E_r - \frac{\partial}{\partial r}\ E_y \qquad\qquad 5.1\ f$$

$$\text{div } E = 0 \qquad\qquad 5.1\ g$$

$$\text{div } H = 0\ . \qquad\qquad 5.1\ h$$

Let us impose the conditions that the radial component of electric field intensity E_r is zero and the wave functions are independent of y. Under these two conditions, Eq. 5.1-b shows that H_y is also equal to zero, and incident-

ally, from Eq. 5.1-c or 5.1-d, $E_\emptyset$ is also zero. Thus, out of the first six equations, there remain only the following group of three:

$$i\omega\epsilon r \, E_y = \frac{\partial}{\partial r} \, rH_\emptyset - \frac{\partial}{\partial \phi} \, H_r \qquad \text{5.2a}$$

$$-i\omega\mu r \, H_r = \frac{\partial}{\partial \phi} \, E_y \qquad \text{5.2b}$$

$$i\omega\mu H_\emptyset = \frac{\partial}{\partial r} \, E_y \quad . \qquad \text{5.2c}$$

This type of wave has an electric field intensity parallel to the Y-axis, and a magnetic field intensity lying entirely in planes y= constant. The components of magnetic field intensity has components $H_\emptyset$ and H_r as given by Eq. 5.2b,c in terms of E_y. By eliminating $H_\emptyset$ and H_r, we have the two dimensional wave equation for E_y:

$$\frac{\partial^2 E_y}{\partial r^2} + \frac{1}{r} \frac{\partial E_y}{\partial r} + \frac{1}{r^2} \frac{\partial^2 E_y}{\partial \phi} + \frac{\omega^2}{c^2} E_y = 0 \qquad \text{5.3}$$

The general solution of this equation is

$$E_y = \left[A \sin(n\nu\phi) + B \cos(n\nu\phi) \right]\left[C J_{n\nu}\left(\frac{\omega}{c} r\right) + D Y_{n\nu}\left(\frac{\omega}{c} r\right) \right] e^{i\omega t},$$

where A, B, C, and D are arbitrary complex constants, n is a positive integer, ν is a real constant to be determined from the boundary conditions, and $J_{n\nu}$ and $Y_{n\nu}$ are Bessel functions of the first and second kind respectively. This solution is similar in two respects to that of the $H_{0,m}$- wave in rectangular pipes. First, in a pipe there is a sinusoidal variation in the Z-direction, and in a sectoral horn there is a sinusoidal variation in the $\emptyset$-direction, i.e., along an arc. Second, in a pipe the wave is propagated in

the X-direction in exponential form, and in the horn, it is propagated in the radial direction in the form of a Bessel function. Since solutions having odd symmetry about the line $\phi = 0$ do not give single-beam radiation patterns, we will retain the cosine term alone. We note also that as a practical matter, the sine terms do not exist if the horn is excited by an antenna placed vertically in the $\phi = 0$ plane. As we desire a wave traveling outward in the radial direction having a time function $e^{i\omega t}$, we may put C = 1 and D = -i. The solution is thus reduced to the form:

$$ E_y = B \cos(n\nu\phi) \, K_{n\nu}(\tfrac{\omega}{c}r) \, e^{i\omega t}, \qquad 5.4a $$

where K is the second Bessel function of third kind or Hankel function[1], usually written as $H^{(2)}$. It is:

$$ K_{n\nu} = J_{n\nu} - iY_{n\nu}. \qquad 5.5 $$

From Eq. 5.2b and 5.2c, we have H_r and H_ϕ:

$$ H_r = \frac{B n\nu}{i\omega\mu r} \sin(n\nu\phi) \, K_{n\nu}(\tfrac{\omega}{c}r) \, e^{i\omega t} \qquad 5.4b $$

$$ H_\phi = -i B \sqrt{\tfrac{\varepsilon}{\mu}} \cos(n\nu\phi) \, K'_{n\nu}(\tfrac{\omega}{c}r) \, e^{i\omega t} \qquad 5.4c $$

$$ E_x = E_\phi = H_y = 0 . $$

where K' is a derivative of K with respect to its variable $(\tfrac{\omega}{c}r)$.

This wave can be represented by a single vector potential whose divergence is equal to zero. By using Eq. 4.2b, we have,

$$ A_y = - \frac{B}{i\omega\mu} \cos(n\nu\phi) \, K_{n\nu}(\tfrac{\omega}{c}r) \, e^{i\omega t} \qquad 5.6 $$

This function will be useful in the calculation of radiation

[1] Watson, G.N. : "Theory of Bessel Functions" pp 73

field.

The boundary condition is that the tangential component of electric field intensity is equal to zero on the surface of the conductor. Therefore, at the two side where $\phi = \pm \phi_0$, E_y must equal zero, which requires that:

$$\cos (n \nu \phi_0) = 0$$

and

$$n \nu \phi_0 = \frac{m \pi}{2}$$

where m is an odd integer. Since n is an undefined integer, we may set n = m and therefore the constant ν becomes

$$\nu = \frac{\pi}{2 \phi_0} . \qquad 5.7$$

The integer n is now limited to be an odd one. It specifies the order of harmonic of the wave. Thus when n = 1, it is the fundamental wave, having a half-period sinusoidal variation along the arc between the two sides. When n = 3, it is the third harmonic wave, having three half-period sinusoidal variation along the same and so on. The order of Hankel's function is nν and equals ν for the fundamental wave; it is inversely proportional to the angle betwwen the two sides. A sectoral horn approaches a pipe of rectangular cross-section, as ϕ_0 becomes vanishingly small, and a sectoral horn of 2 ϕ_0 = 180° represents a single reflecting plane. The useful range as a horn is somewhere between, say, 2 ϕ_0 = 20° to 90°. The value of ν changes correspondingly from 9 to 2, not necessary an integer.

Before we go on the discussion of the charac-
teristic properties of the wave, let us review the general
behavior of the Hankel function. We have excluded the point
at the origin of the coordinate, since it is a singular point
for Neumann's function. For small value of the variable (
$\frac{2\pi}{\lambda} r$), the real part of the Hankel function (i.e., Bessel
function of the first kind) is nearly zero and the imaginary
part (Neumann's function) is very large, being infinity when
the variable is zero. So, as a whole, the absolute magnitude
of the Hankel function is very large, and decreases with an
increase of the variable. The phase remains almost constant.
For large value of variable, both the real part and imaginary
part of the Hankel function vary periodically; their magnitudes
are approximately inversely proportional to the square root
of the variable. They differ by a quarter a period in phase.
With a time function $e^{i\omega t}$, the Hankel function represents a
wave propagated radially outward. We shall hereafter call
the regions of small values of the variable and of large
values the "attenuation" and "transmission" regions, respect-
ively, of the Hankel function for reasons explained later on.
The boundary betweem these two regions is not definite. How-
ever, we may roughly define it as the point at which the Neu-
mann's function passes through its first zero.

Fig. 53 is plotted with values from Jahnke and

Fig. 5.3 First Zeros of Bessel Functions
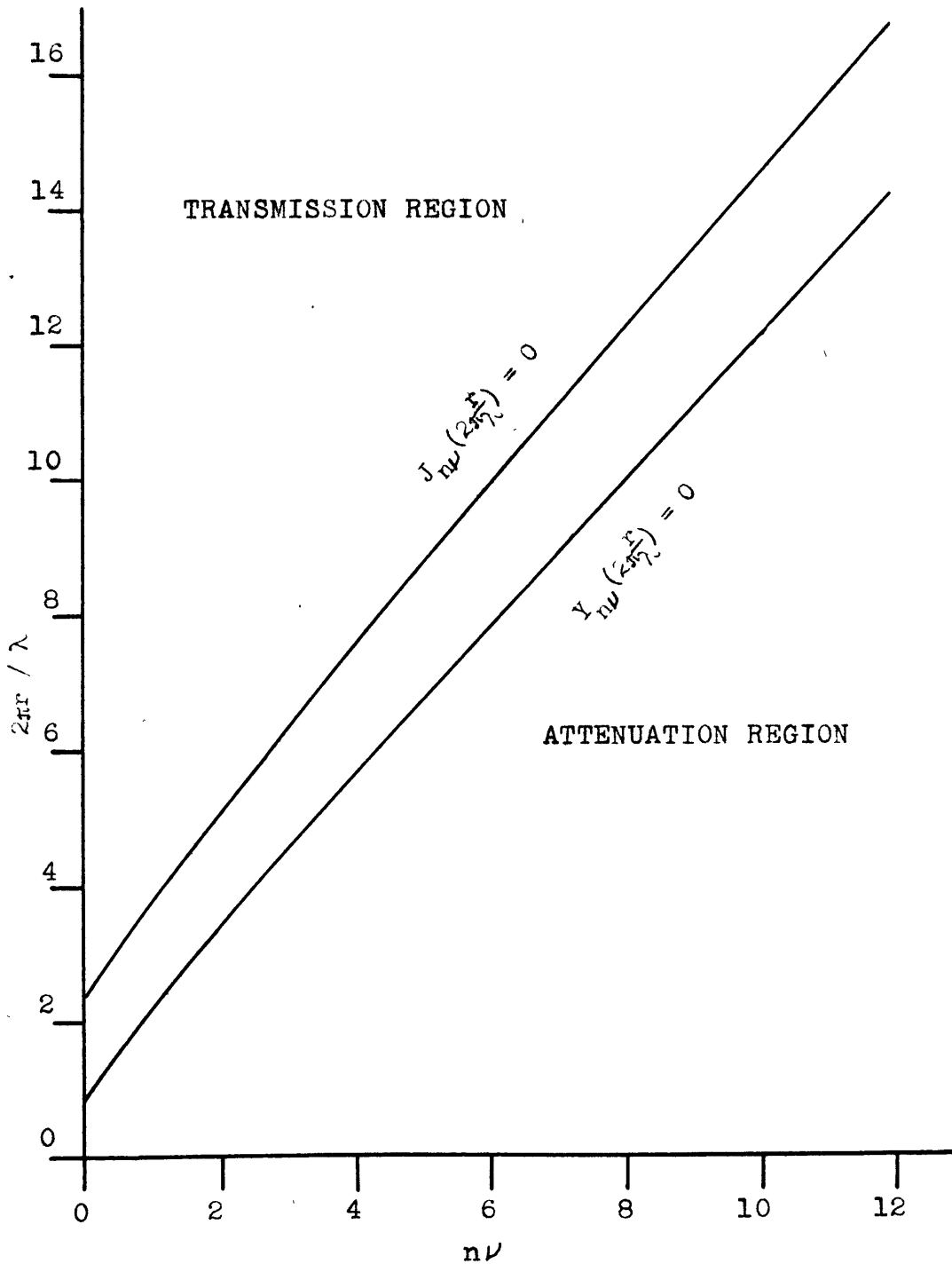
Emde: "Tables of Functions". It shows the variation of the
first zeros with the order for Bessel functions of the first
and second kinds. We note that the value of the variable
that gives the first zero of the function is nearly propor-
tional to the order . The larger is the order, the wider the
attenuation region of the Hankel function.

The asymptotic expansion of the Hankel function
in the tra:nsmission region is the complex sum of the asymp-
totic expansions of its two components. For the Bessel func-
tion of the first and second kinds, they are as follows:

$$J_{n\nu}(x) = \frac{1}{\sqrt{\frac{1}{2}\pi x}} \cos\left(x - \frac{2n\nu+1}{4}\pi\right)$$

$$Y_{n\nu}(x) = \frac{1}{\sqrt{\frac{1}{2}\pi x}} \sin\left(x - \frac{2n\nu+1}{4}\pi\right)$$

for large x .

Thus the asymptotic expansion of the Hankel function is

$$K_{n\nu}(x) = \frac{1}{\sqrt{\frac{1}{2}\pi x}} e^{-i\left(x - \frac{2n\nu+1}{4}\pi\right)} .$$
5.8

Phase Constant and the Phase Velocity

The wave functions in a horn do not appear ex-
plicitly as an exponential function. The phase constant,
therefore, can not be obtained in the conventional way. How-
ever, we may define the phase constant by analogy with the
plane wave as the imaginary part of the ratio $\frac{\partial E_y}{\partial r}/E_y$.
This expression gives the correct phase constants for hollow
pipe waves or plane waves.

Substituting into the ratio, we have,

$$-i\beta = \left[\frac{\frac{\partial}{\partial r} K_{n\nu}\left(\frac{\omega}{c}r\right)}{K_{n\nu}\left(\frac{\omega}{c}r\right)}\right]_{\text{imag. part}} .$$
5.9

For the sake of simplicity of discussion, let us limit $n\nu$ to a positive integer for the present. In the transmission region, where the ratio $\frac{r}{\lambda}$ is large, we may use the asymptotic expansion (Eq. 5.8). Substitute Eq. 5.8 into Eq. 5.9:

$$-i\beta \cong -i\frac{\omega}{c} \text{ , or } \beta = \frac{\omega}{c} \text{ .}$$

For values of $2\pi\frac{r}{\lambda} << 1$, and integer orders of the Hankel function, the approximate formulae for the Hankel function is

$$K_{n\nu}(x) = \frac{x^{n\nu}}{(n\nu)!\,2^{n\nu}} + \frac{i\,(n\nu-1)!}{\pi}\left(\frac{2}{x}\right)^{n\nu}$$

$$\cong +i\frac{(n\nu-1)!}{\pi}\left(\frac{2}{x}\right)^{n\nu} \text{ .} \qquad\qquad 5.10$$

Using this expression, we find,

$$-i\beta \doteq 0 \text{ ,}$$

With this value of phase constant, the general trend of its variation may be found. The phase constant increases with the ratio $\frac{r}{\lambda}$ from zero at $\frac{r}{\lambda} = 0$ and approaches the value $\frac{\omega}{c}$ asymptotically for large values of $\frac{r}{\lambda}$.

The wave length in the horn is equal to $\frac{2\pi}{\beta}$. Therefore, it decreases with the increase of ratio $\frac{r}{\lambda}$ from infinity at $\frac{r}{\lambda} = 0$ and approaches the value λ ——wave length in free space——asymptotically for large value of $\frac{r}{\lambda}$. The phase velocity has the same form of variation as that of the wave length, and approaches asymptotically the light velocity. It depends upon the order of harmonic of the wave; the higher the harmonic, the larger the phase velocity. For sufficiently large value of $\frac{r}{\lambda}$, the phase velocity approaches the
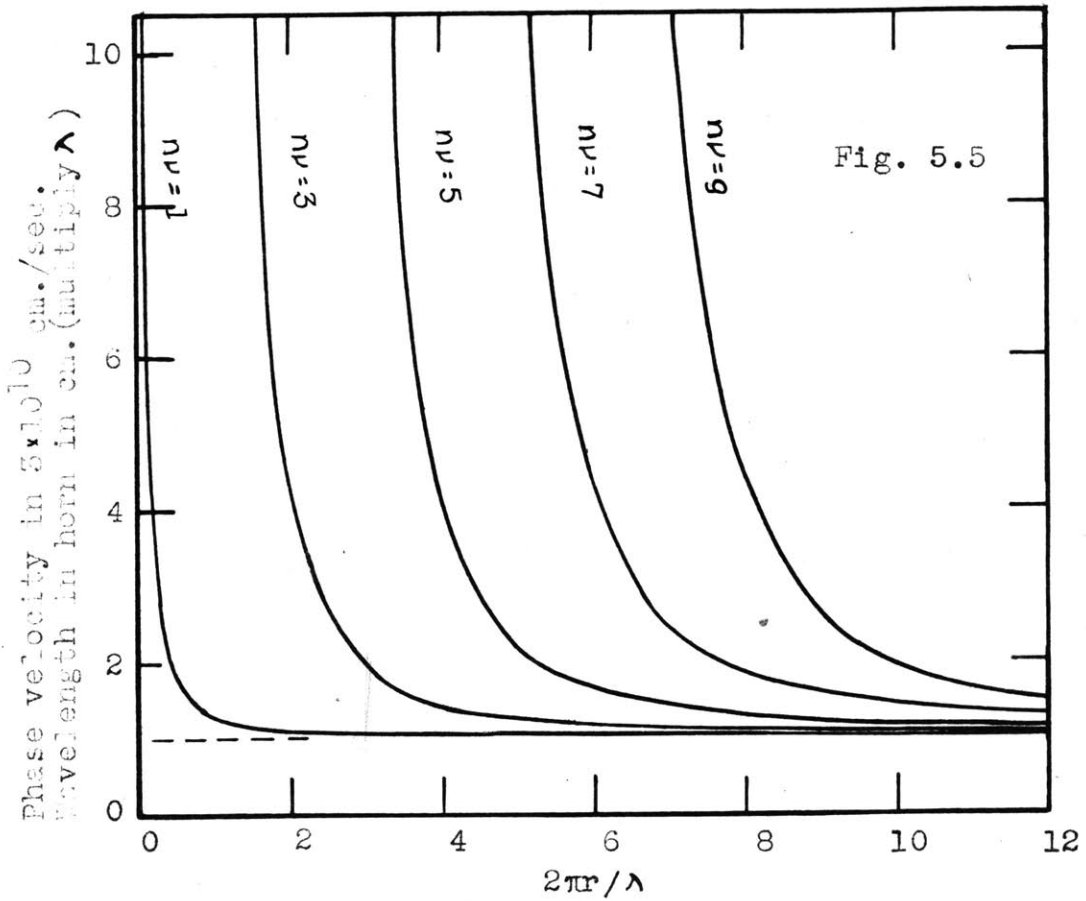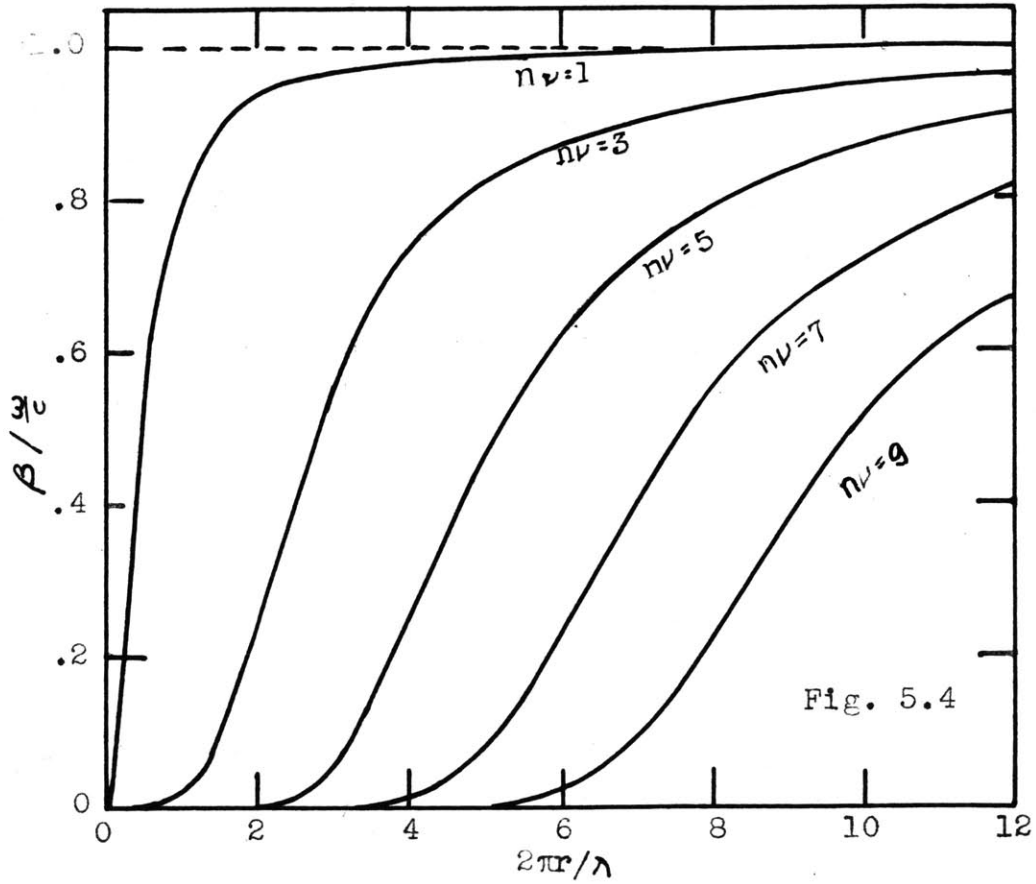
same velocity, viz., the velocity of light, regardless of the order of harmonic. Thus, the third harmonic will travel faster than the fundamental, but both will be slowed down gradually to the same speed. The resultant field, along an arc, being linearly superposible, changes constantly with the radial distance and finally takes on a constant pattern.

Fig. 5.4 and 5.5 are sketches showing the variations of phase constant, phase velocity and wave length in the horn with the radial distance. The dotted lines are the asymptotic values to which the functions approaches for large value of $\frac{r}{\lambda}$.

Attenuation

The horn is assumed to have a conductive boundary of perfect conductivity while the dielectric inside it is assumed to be a perfect insulator. The word "attenuation" here applies to the decreasing of the magnitudes of field intensities as r increases. Since there is no transfer of energy between planes parallel to the top and bottom of the horn, if the total power along an arc transmitted in the radial direction were constant, the magnitude of the field intensity should be proportional to $\frac{1}{\sqrt{r}}$. Dissipation of energy is represented by field intensity which decreases more rapidly than the above.

In the transmission range, for large values of

Fig. 5.4

$\beta/\frac{w}{c}$ versus $2\pi r/\lambda$

$n\nu=1$
$n\nu=3$
$n\nu=5$
$n\nu=7$
$n\nu=9$

Fig. 5.5

Phase velocity in 5×10^{10} cm./sec.
wavelength in horn in cm. (multiply λ)

$n\nu=1$
$n\nu=3$
$n\nu=5$
$n\nu=7$
$n\nu=9$

$2\pi r/\lambda$

$\frac{r}{\lambda}$, using the asymptotic expansion, we have,

$$E_y \propto [\bar{K}_{n\nu}(\tfrac{\omega}{c}r)]$$

$$\propto \frac{1}{\sqrt{r}}$$

and

$$H_\phi \propto [\bar{K}'_{n\nu}(\tfrac{\omega}{c}r)]$$

$$\propto \frac{1}{\sqrt{r}} \, .$$

$$5.11a$$

It shows that there is nearly no dissipation of energy during transmission in that part of horn. In the attenuation region, for $2\pi\frac{r}{\lambda} << 1$, using approximate Eq. 5.10, the fields are

$$E_y \propto \frac{1}{r^{n\nu}}$$

$$H_\phi \propto \frac{1}{r^{n\nu+1}} \, .$$

$$5.11b$$

The constant ν is always greater than 2 for a horn having $2\phi_0$ $< 90°$. Thus the region near the origin is highly dissipative. The narrower the horn, or the higher the order of harmonic, the greater is the dissipation of energy. This is the reason why the two regions of Hankel function have been here named the attenuation and transmission regions respectively. The curves in Fig. 5.3 indicate the approximate boundary of the two regions. Suppose the horn is excited at the converging end at a wave length λ such that the ratio $2\pi\frac{r}{\lambda}$ near that end falls within the first region: then only a very small part of the energy is able to be transmitted radially forward. This loss of energy can only be eliminated by either decreasing the wave length or shortening the horn at its converging end.

In Fig. 5.6, the absolute magnitude of Hankel

Fig. 5.6
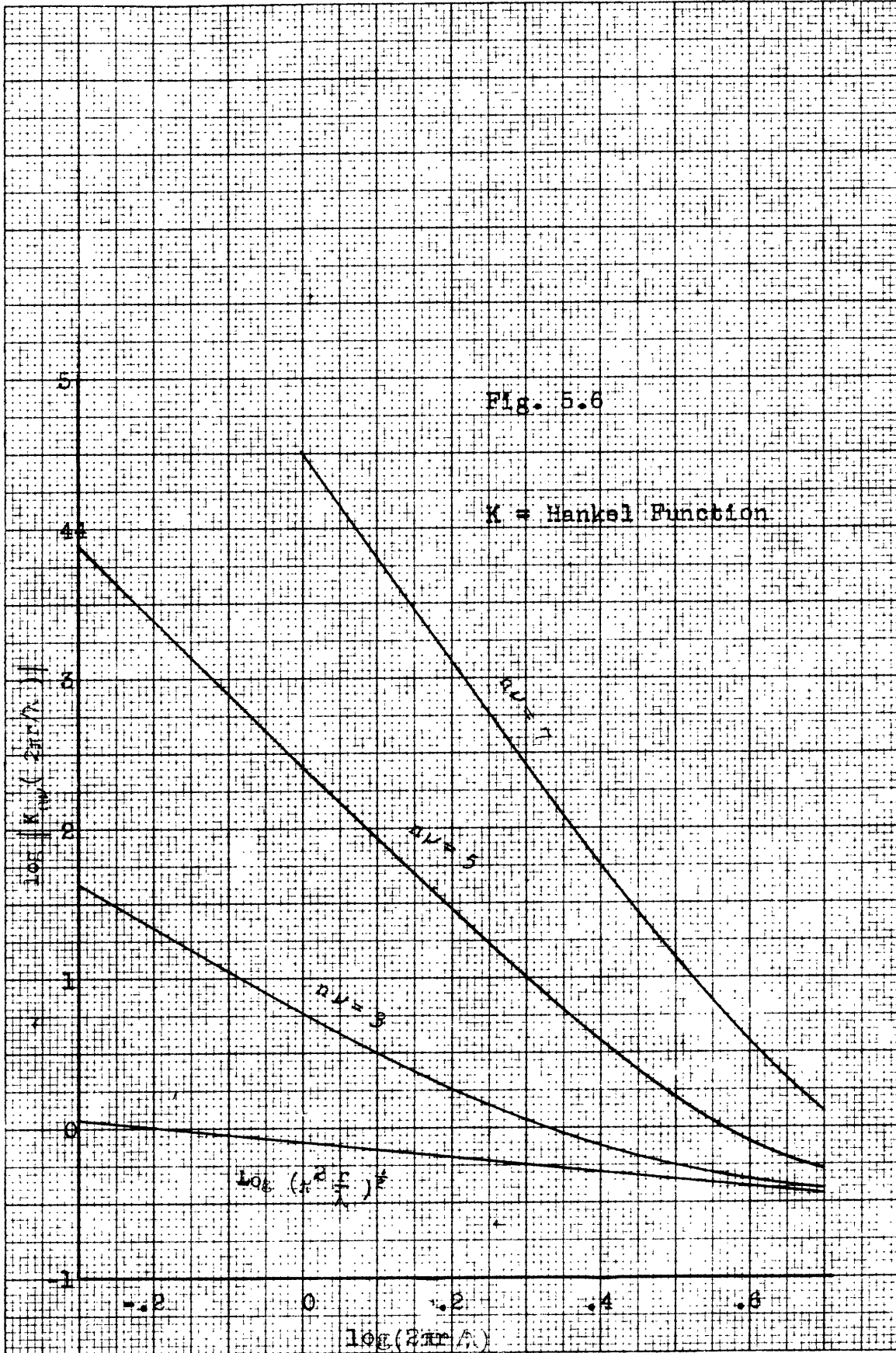
K = Hankel Function

function is plotted against its variable in logarithmic scale
for three different values of $n\nu$ ——the order of the Hankel
function. The magnitude of the asymptotic value $(\frac{\pi^2}{\lambda}r)^{-\frac{1}{2}}$
of Hankel function is also plotted to the same scale. The
latter is a straight line with slope $= -1/2$. The differen-
ce of the ordinate of the asymptotic line and that of the
Hankel function line, is proportional to the attenuation of
the Hankel function. Thus, we see graphically that the
higher the order of Hankel function, the larger the atten-
uation, and consequently the wider the attenuation region.

The dissipative property of the horn may be used
for the suppression of higher harmonics. It has been shown
that the value of $2\pi\frac{r}{\lambda}$ at the above-mentioned boundary is
roughly proportional to the order of the Hankel function $n\nu$,
where n indicates the order of harmonic of the wave. For ex-
ample, if the attenuation region of the fundamental wave for
a given wave length extends to the value $r = r_1$, then the
attenuation region for the third harmonic will extend about
three times as far or to $3r_1$. Now, if we want to transmit
only the fundamental wave, we may cut off the horn between
$r = r_1$ and $r = 3r_1$ and set the excitation system there. Be-
yond the region $r = 3r_1$, only a trace of the third harmonic
wave will be left, while the fundamental wave is almost un-
altered. A similar procedure may be used to suppress the
fifth and higher harmonics.

Field Distribution Inside the Horn

The field distribution of the fundamental wave
and the third harmonic wave is sketched in Fig. 5.7a,b. It
is not drawn to scale but rather symbolically. At the con-
verging end, the wave length in the horn is very large, and
the crowded magnetic lines represent the great magnitudes
of the field intensities in the attenuation region. In this
attenuation region, the magnetic lines do not form closed
loops. Beyond the open field lines, the wave enters the
transmission region. The wave length in the horn decreases
gradually, as also does the concentration of the lines.
The radial component of the magnetic field intensity is still
considerable. At the remote end of the horn, $(\frac{r}{\lambda} >>> 1)$, the
radial component of the magnetic field intensity is negligible
since it is proportional to $\frac{1}{r} \cdot \frac{1}{\sqrt{r}}$, and the closed magnetic
lines are broken up. As the electric field intensity is al-
ways normal to the direction of propagation, the wave behaves
precisely as a plane wave with transverse electric and mag-
netic field intensities.

The field distribution of the third and higher
harmonics may be similarly sketched. Instead of a single set
of closed magnetic lines along the arc between two sides,
there will be three or more sets equally spaced. The first
group of closed magnetic lines will occur at a larger radial
distance from the origin. The field distribution of the

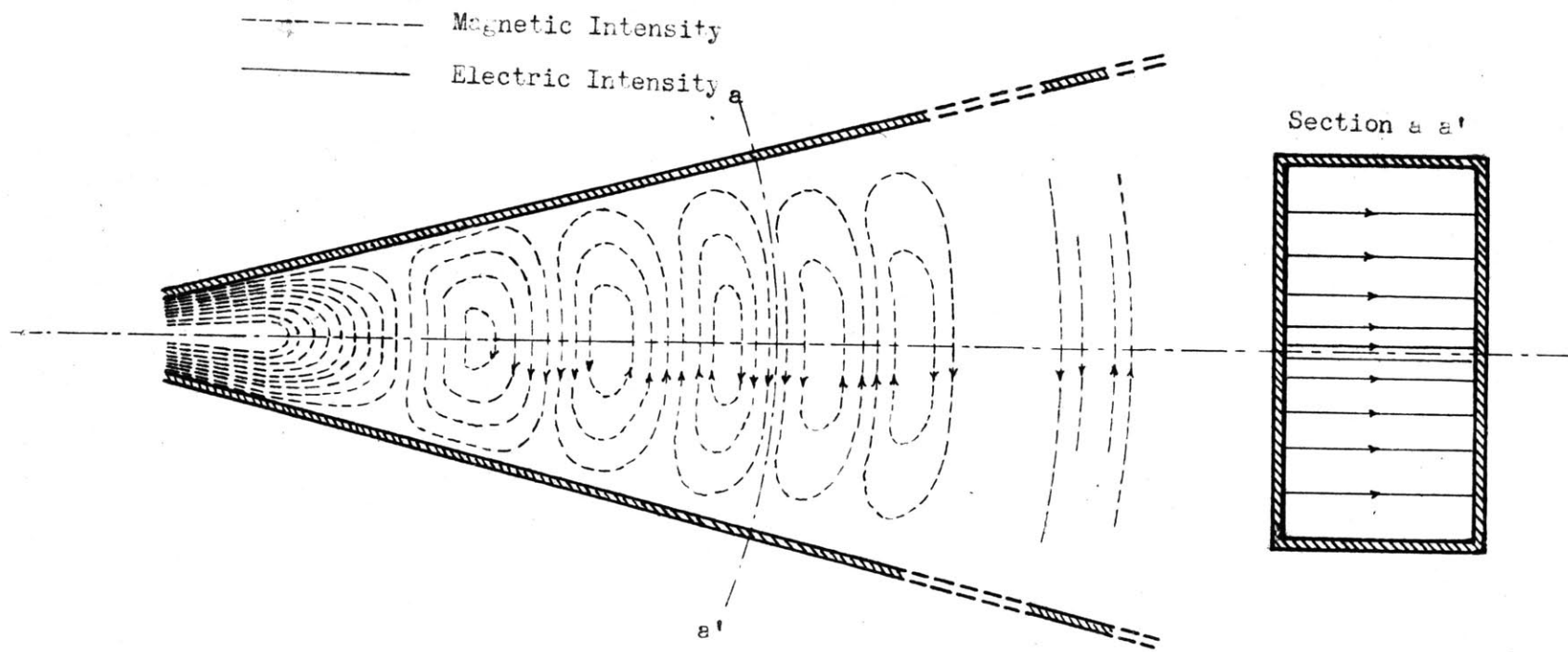Fig. 5.7a Field distribution of Fundamental
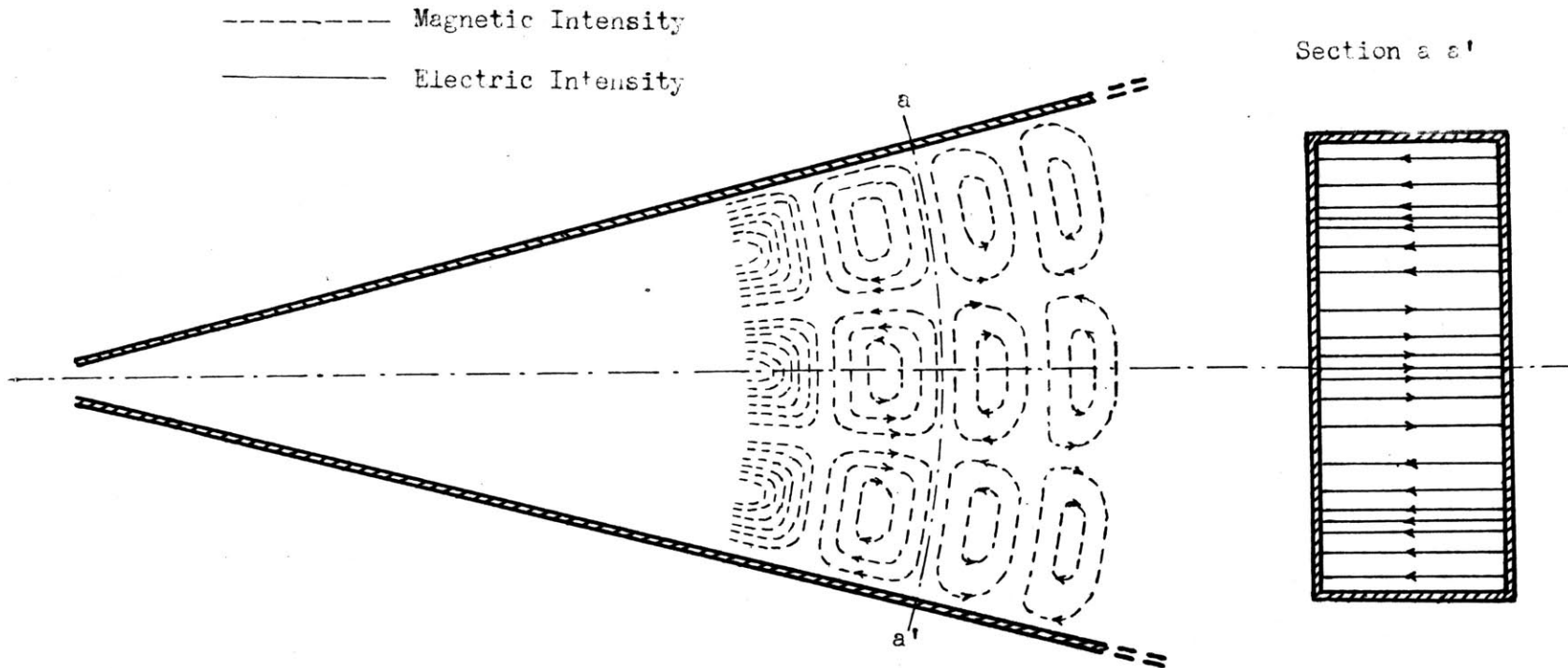Wave in Sectoral Horn

Fig. 5.7b Field distribution of Third
Harmonic Wave in Sectional Horn

------- Magnetic Intensity

————— Electric Intensity

Section a a'

third harmonic wave is shown in Fig. 5.7b.

The behavior of waves in a sectoral horn bear several striking similarity to that of waves in hollow pipes, especially the $H_{o,m}$-wave of rectangular pipe. The arc length $2\phi_o r$ corresponds to the dimension b of the rectangular pipe, and the variation of the fields is sinusoidal along both these dimensions. While the $H_{o,1}$-wave has a definite cut-off wave length, depending upon $\frac{b}{\lambda}$, the corresponding wave in a sectoral horn, too, has a kind of cut-off wave length that depends upon the ratio $\frac{r}{\lambda}$. The shapes of the curve of β vs. $\frac{b}{\lambda}$ and that of β vs. $\frac{r}{\lambda}$ are similar. A horn is therefore in a way, a rectangular pipe with an ever linearly increasing cross-section. It may be considered as a tapered hollow pipe transmission line.

Radiation Patterns of Horn

The transmission characteristics of waves in horn thus far discussed has been limited to horns that extended to infinity in the radial direction. We are not able to treat rigorously a horn of finite length. However, if the angle made by the two sides of the horn is not too large $(2\phi_o < 90°)$, and the length of the horn is above several wave length, any type of wave that is impressed at the throat end of the horn will be able to transform itself into sectoral-

horn-wave. Furthermore, if the horn is long enough, the end
effects will not distort the field distribution too much.
Therefore, we will assume that the radiation pattern of a
finite horn can be calculated from the field distribution
appropriate to an infinite horn.

The vector potential of the sectoral horn wave
is $$A_y = -\frac{B}{i\omega\mu} \cos(n\nu \phi) K_{n\nu} (\frac{\omega}{c}r) e^{i\omega t} \qquad 5.6$$
Let us cut off the horn at a circular cross-section $r = r_1$.
A cross-section of the finite length horn looks like the sket-
ch of Fig. 5.8. We also assume that the horn is excited
at its throat so that only one harmonic or a number of har-
monics are able to transmit through the horn. The throat and
source is taken as shielded. As we have discussed before,
the radiation pattern in the XY-plane depends roughly only on
the dimension "a" for the $H_{o,m}$-wave in a rectangular pipe.
Now, the field distribution of a sectoral horn wave in the
XY-plane is exactly the same as that of $H_{o,m}$-wave of rectangu-
lar pipe. Therefore, it is reasonable to assume that the ra-
diation pattern in the XY-plane has the same form as that of
the $H_{o,m}$-wave of rectangular pipes, (refer to Fig. 4.3).
For this reason only the radiation patterns in XZ-plane will
be considered.

In the expression 4.4, the surface integration
is carried out over the outer surface of the metallic boundary
and the open end along the sector of the cylindrical surface.
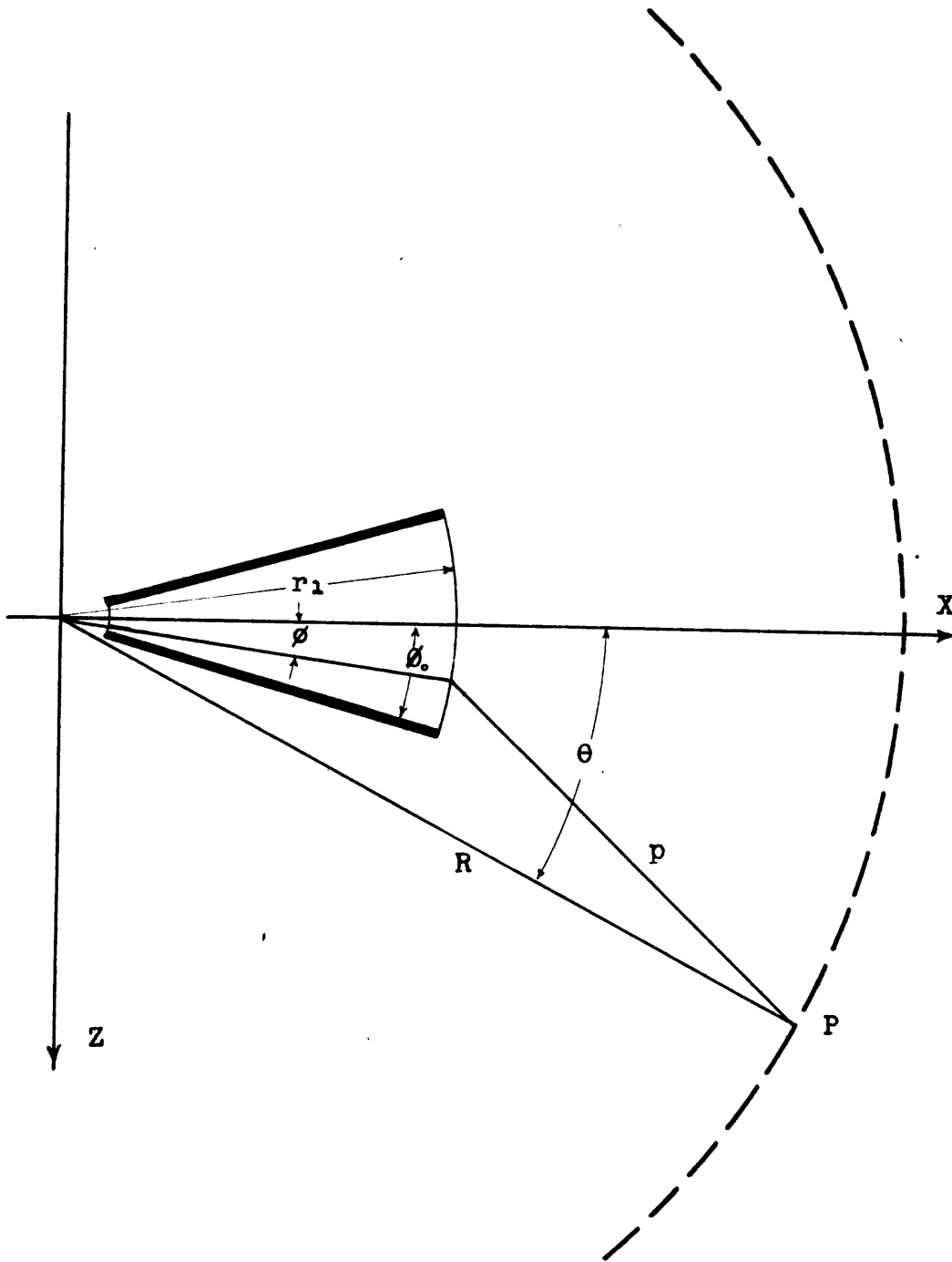
Fig. 5.8

Since it is assumed that no energy penetrates the boundary surface, the integration over that surface is zero. By Huygens' Principle, the vector potential at any point P (R , θ) in the XZ-plane is

$$A = \int \int \frac{1}{p} \Big[\frac{1}{c} \Big(\frac{\partial A}{\partial t} \Big)_{(t- \frac{p}{c})} \cos\ (n,p) + \Big(\frac{\partial A}{\partial n} \Big)_{(t- \frac{p}{c})} \Big]\ ds.$$

Substituting A_y into the right hand side gives,

$$A_y = - \frac{B}{i\omega\mu} \int_{-\frac{a}{2}}^{\frac{a}{2}} \int_{-\phi_o}^{\phi_o} \frac{i\omega}{pc} \Big[K_{n\nu} \Big(\frac{\omega}{c} r_i \Big) \cos\ (\phi - \theta) + i K'_{n\nu} \Big(\frac{\omega}{c} r_i \Big) \Big] \cos (n\nu\phi)\ e^{i\omega(t - \frac{p}{c})} r_i d\phi\ dy.$$

5.11

If the angle between the two sides is small, the factor in the square bracket has a slow variation compared to the remaining factors. Let us use the mean value of $\phi - \theta \cong \theta$ over the surface, and bring the square bracket out of the integral. We shall use the asymptotic form of $K_{n\nu}$ and $K'_{n\nu}$ so as to be consistant with the above approximation. These approximations are not essential in the following process of derivation, but help to simplify the result.

The variable p is the distance from P to a point on the surface of integration. Since P is in XZ-plane,

$$p = \sqrt{R^2 - r_1^2 - 2Rr_1 \cos (\phi - \theta)}$$
$$\cong R - r_1 \cos (\phi - \theta)$$

for large values of R. Substituting this value for p into the integral, it becomes:

$$A_y = - \frac{Ba}{i\omega\mu} \frac{i\omega}{Rc} \frac{1}{\sqrt{\frac{\pi\omega}{2c} r_i}} [1 + \cos\theta]\ e^{i\omega(t - \frac{r_i + R}{c})}$$
$$\int_{-\phi_o}^{\phi_o} \cos(n\nu\phi)\ e^{i \frac{\omega}{c} r_i \cos(\phi - \theta)}\ d\phi$$

5.12

Consider the integral

$$\int_{-\phi_o}^{\phi_o} \cos (n\nu\phi)\ e^{i\frac{\omega}{c} r_1 \cos (\phi - \theta)}\ d\phi \qquad\qquad 5.13$$

It is an integral with cosine in the exponential. It is possible to expand the exponential into Bessel-Fourier series and perform the integration term by term. However, as $\frac{\omega}{c} r_1$ is much greater than unity, such series converge very slowly and will be useless in actual calculation. We have to use some other means of integration.

It is known that the cosine may be expressed as the infinite product:

$$\cos x = \left[1 - (\tfrac{2x}{\pi})^2\right]\left[1 - (\tfrac{2x}{3\pi})^2\right]\left[1 - (\tfrac{2x}{5\pi})^2\right] \cdots\cdots$$

For values of x within $\pm\frac{\pi}{2}$, all except the first factor are nearly unity. By expanding the product of the first two factors, and neglecting the terms of fourth power of x, we have the approximate value of $\cos (\phi - \theta)$:

$$\cos (\phi - \theta) \cong 1 - \frac{10}{9}(\tfrac{2}{\pi})^2\ (\phi - \theta)^2$$

$$\text{for}\qquad\qquad (\phi - \theta)^2 \leqq (\tfrac{\pi}{2})^2$$

This is equivalent to replacing the cosine by a parabola. Split $\cos (n\nu\phi)$ into two exponentials,

$$\cos(n\nu\phi) = \frac{1}{2}(e^{in\nu\phi} + e^{-in\nu\phi})\ .$$

The integral 5.13 becomes,

$$\frac{1}{2}\int_{-\phi_o}^{\phi_o} e^{i\frac{\omega}{c} r_1 (1 - \frac{40}{9\pi^2}\theta^2 - \frac{40}{9\pi^2}\phi^2 + \frac{80}{9\pi^2}\theta\phi) \pm in\nu\phi}\ d\phi\ , \qquad\qquad 5.14$$

It consists of two terms corresponding to the upper and lower signs in the exponential. Bring the constant factor out of the integral:

$$\frac{1}{2} e^{i2\pi\frac{r}{c}\cdot(1-\frac{40}{9\pi^2}\theta^2)} \int_{-\phi_0}^{\phi_0} e^{-i\frac{80}{9\pi}\frac{r}{\lambda}[\phi^2-2\theta\phi \mp n\nu\frac{9\pi\lambda}{80r}\phi]} d\phi$$

5.15

Since

$$\phi^2 - 2\theta\phi \mp n\nu\frac{9\pi\lambda}{80r_1}\phi = [\phi - \theta \mp n\nu\frac{9\pi\lambda}{160r_1}]^2 + [\theta \pm n\nu\frac{9\pi\lambda}{160r_1}]^2$$

the integral 5.13 becomes

$$\frac{1}{2} e^{i[2\pi\frac{r}{\lambda} \pm n\nu\theta + \frac{9\pi\lambda}{320r_1}(n\nu)^2]} \int_{-\phi_0}^{\phi_0} e^{-i\frac{80r_1}{9\pi\lambda}[\phi - \theta \mp n\nu\frac{9\pi\lambda}{160r_1}]^2} d\phi .$$

5.16

It has been reduced to the form of Fresnel's integral. Detailed discussions of this integral appear in Slater and Frank's "An Introduction to Theoretical Physics" and Watson's "A Treatise of the Theory of Bessel Functions". Let

$$v = \frac{80\,r_1}{9\,\pi\lambda}[\phi - \theta_1 \mp n\nu\frac{9\,\pi\lambda}{160\,r_1}]^2$$

5.17

and

$$d\theta = \sqrt{\frac{9\pi\lambda}{80r_1}}\frac{dv}{2\sqrt{v}} = \frac{3\pi}{4}\sqrt{\frac{\lambda}{10r_1}}\frac{dv}{\sqrt{2\pi v}} .$$

The integral part of 5.16 becomes (omit the coefficient outside the integral),

$$= \frac{3\pi}{4}\sqrt{\frac{\lambda}{10r_1}}\int_{v_1}^{v_2}[\cos v - i\sin v]\frac{dv}{\sqrt{2\pi v}}$$

$$= \frac{3\pi}{4}\sqrt{\frac{\lambda}{10r_1}}\int_{v_1}^{v_2}\frac{1}{2}[J_{-\frac{1}{2}}(v) - iJ_{\frac{1}{2}}(v)]\,dv .$$

5.18

Either the real or the imaginary terms turns out to be an infinite series of Bessel functions of half orders, and is called Fresnel Integral. Numerical values for a range of v from 0 to 50 have been tabulated in Watson or Jahnke and Emde.

The complete expression of radiation vector potential A_y is : $-B\frac{3a\lambda}{8Rr_1}\sqrt{\frac{\epsilon}{10\mu}}e^{i(\omega t - 2\pi\frac{R}{\lambda} + \frac{9\pi\lambda}{320r_1}(n\nu)^2)} \times [1 + \cos\theta]$

$$[e^{in\nu\theta}\int_{v_1}^{v_2}\frac{1}{2}\{J_{-\frac{1}{2}}(v) - iJ_{\frac{1}{2}}(v)\}dv + e^{-in\nu\theta}\int_{v_3}^{v_4}\frac{1}{2}\{J_{-\frac{1}{2}}(v) - iJ_{\frac{1}{2}}(v)\}dv]$$

5.19

$$\begin{cases} v_2 = [\phi_0 - \theta - n\nu\frac{9\pi\lambda}{160r_1}]^2\frac{80r_1}{9\pi\lambda} \\ v_1 = [-\phi_0 - \theta - n\nu\frac{9\pi\lambda}{160r_1}]^2\frac{80r_1}{9\pi\lambda} \end{cases} \qquad \begin{cases} v_4 = [\phi_0 - \theta + n\nu\frac{9\pi\lambda}{160r_1}]^2\frac{80r_1}{9\pi\lambda} \\ v_3 = [-\phi_0 - \theta + n\nu\frac{9\pi\lambda}{160r_1}]^2\frac{80r_1}{9\pi\lambda} \end{cases}$$

This above value is true only for points in the XZ-plane.
The magnetic and electric field intensities are:

$$H_\theta = - \frac{i\omega}{c} A_y$$

$$E_\zeta(= -E_y) = i\omega\mu A_y$$

$$H_x = H_\zeta = E_x = E_\theta = 0 \; ,$$

5.20

Fig. 5.9 is a reproduction of a three dimensional plot of Fresnel Integral taken from Jahnke and Emde's "Tables of Functions", p.111. The variable and functions are

$$u = \sqrt{\frac{2}{\pi}} \, v$$

$$C_s = \int_b^v \frac{1}{2} J_{-\frac{1}{2}}(v) \, dv$$

$$S_s = \int_b^v \frac{1}{2} J_{\frac{1}{2}}(v) \, dv$$

Both C_s and S_s are periodic functions. The projection of this curve on $u = 0$ plane is called Cornu's Spiral. Both the real and imaginary parts oscillate about the asymptotic value 0.5. This three dimensional curve is actually extended into the diagonally opposite rectangular box of the space, one eighth of which is represented in this figure, for negative value of u. In terms of the limits of integration, the absolute magnitude of the integral is the projection on $u = 0$ plane of a straight line joining two points on the curve cut by $u = u_1$ and $u = u_2$ planes. Thus, when u_1 and u_2 are of opposite sign, the two planes cut through the straight-line portion of the curve, the integral will have its maximum amplitude. This somehow determines the beam angle of the radiation pattern.

As an illustration to the above result, a series
of radiation patterns in the XZ-plane are plotted under dif-
ferent conditions. These patterns are for the ratio $\frac{r_1}{\lambda} \rightleftharpoons 8$,
r_1 is the distance from the hypothetical center to the end
of the horn. So far as the fundamental wave is concerned, the
wave has travelled five or six cycles beyond the attenuation
region,and it is quite safe to use the asymptotic form of
Hankel function. Calculations are made only for v up to 50,
corresponding to the value of θ from 50 to 60 degrees. Be-
yond that value, the table of Fresnel Integral is not readi-
ly available. Fortunately, the plotted portion of the pat-
terns covers the main lobe of radiation; the maximum ampli-
tudes of the side lobes is estimated to be not over 10% of
that of the main lobe on a field intensity scale.

From Fig. 5.9 to Fig. 5.13, a fundamental wave
is assumed to exist alone inside the horn. Since it is the
least attenuated wave, it plays a dominant part in the problem
of directional radiation. Other harmonics are usually pre-
sent in small magnitude. The distribution of electric field
intensity or vector potential along the arc at the opening
of the horn is $\cos \left(\frac{\pi \phi}{2 \phi_0} \right)$.

Fig. 5.9 to 5.11 are plotted with horns with con-
stant ratio $\frac{r_1}{\lambda} = 8$ but of different opening angles, $2\phi_0 = 30°$,
40, and 50°. It shows that by increasing the angle from
small value, the beam angle is sharpened steadily up to cer-
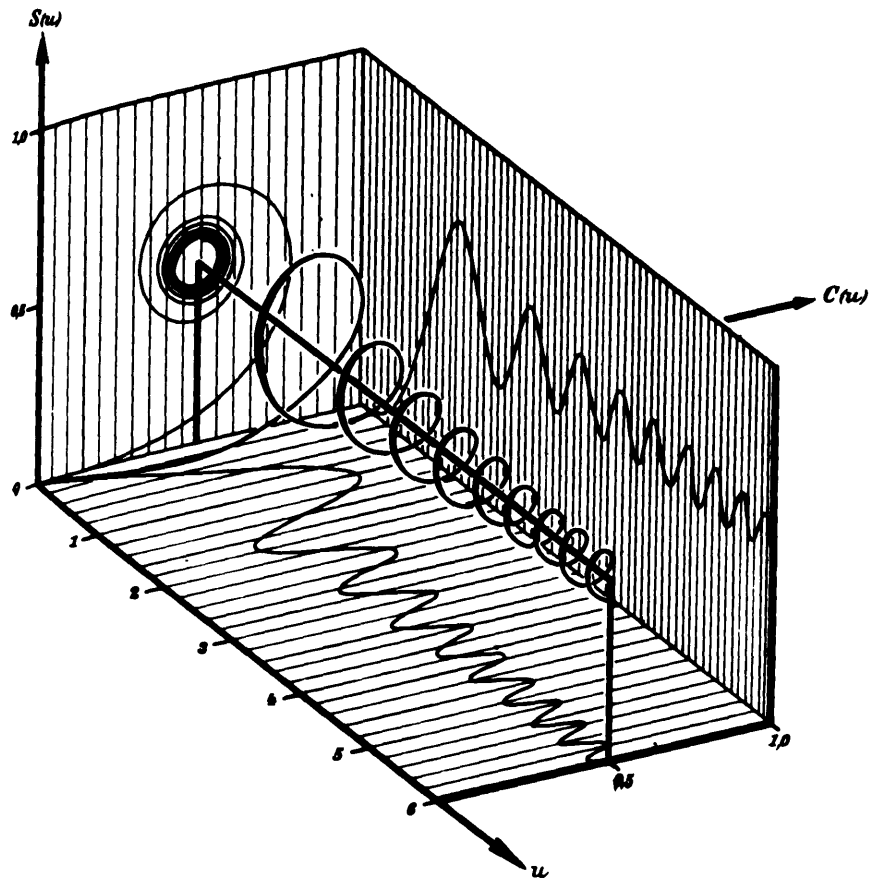
Fig. 5.9' Fresnel's Integrals

(From Jahnke-Emde:"Tables of Functions" p.111.)

Radiation Pattern of Sectoral Horn

Fundamental Wave

$r/\lambda = 8$

$2\phi_0 = 30°$

XZ-plane

Fig. 5.9

Relative Field Intensity

Radiation Pattern of Sectoral Horn

Fundamental Wave

$r / \lambda = 8$

$2\phi_0 = 40°$

XZ-plane

Fig. 5.10

Radiation Pattern of Sectoral Horn

Fundamental Wave

$r/h = 8$

$2\phi_0 = 50°$

XZ-plane

Fig. 5.11

Radiation Pattern of Sectoral Horn

Fundamental Wave

$r/\lambda = 10$

$2\phi_0 = 40°$

XZ-plane

Fig. 5.12

Radiation Pattern of Sectoral Horn

Fundamental Wave

r/λ = 12

2Φ₀ = 40°

XZ-plane

Fig. 5.13

Radiation Pattern of Sectoral Horn

Third Harmonic Wave

$r/\lambda = 8$

$2\phi_0 = 40°$

XZ-plane

Fig. 5.14

Fig. 5.15 Radiation Patterns of Fundamental and Third Harmonic
Waves Equal in Amplitude and Phase at Mouth of Horn

$$\frac{r}{\lambda} = 8 \; , \; 2\emptyset_{o} = 40^{\circ}$$
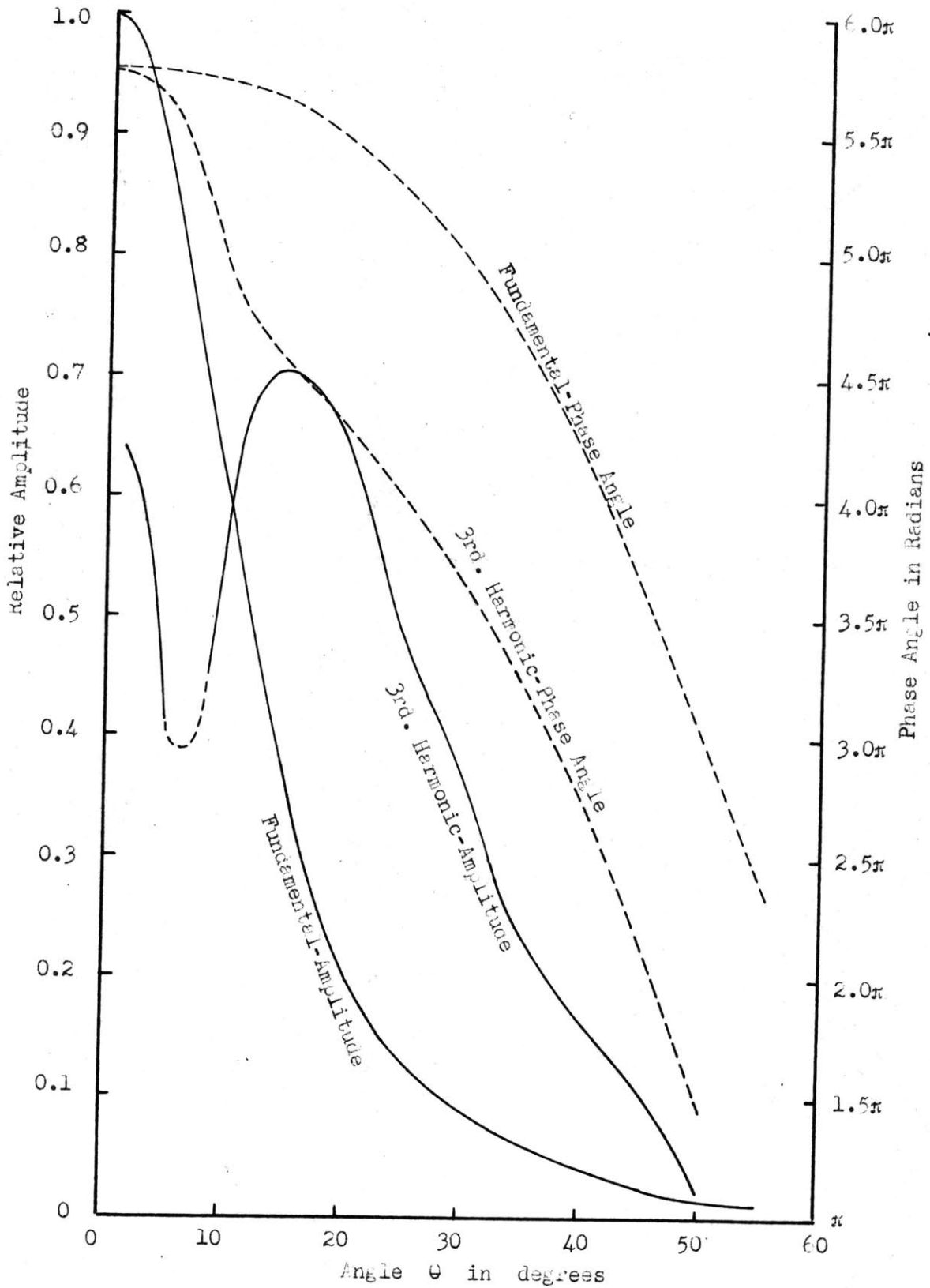
Fig. 5.16 Composite Waves Consisting of Fundamental and Third Harmonic.

Field Distributions at the Mouth of Horn

$$E_y \sim \cos\left(\frac{\pi}{2}\;\frac{\phi}{\phi_o}\right) + W\cos\left(\frac{3\pi}{2}\;\frac{\phi}{\phi_o}\right)$$

Relative Field Intensity

(A) W = -1/3

(B) W = -1/5

(C) W = +1/5

(D) W = + 1/3

ϕ in degrees

Radiation Patterns of Sectoral Horn

Composite Wave

Field Distribution at Mouth of Horn :

$$E_y \sim \cos\left(\frac{\pi\Phi}{2\Phi_0}\right) + w\cos\left(\frac{3\pi\Phi}{2\Phi_0}\right)$$

$r/\lambda = 8$

$2\Phi_0 = 40°$

XZ-plane

Fig. 5.17

Radiation Patterns of Sectoral Horn

Composite Wave

Field Distribution at Mouth of Horn:

$$E_y = \cos\left(\frac{\pi\varnothing}{2\varnothing_o}\right) + w\cos\left(\frac{3\pi\varnothing}{2\varnothing_o}\right)$$

$$B/\lambda = 8$$

$$2\varnothing_o = 40°$$

XZ-plane

Fig. 5.18
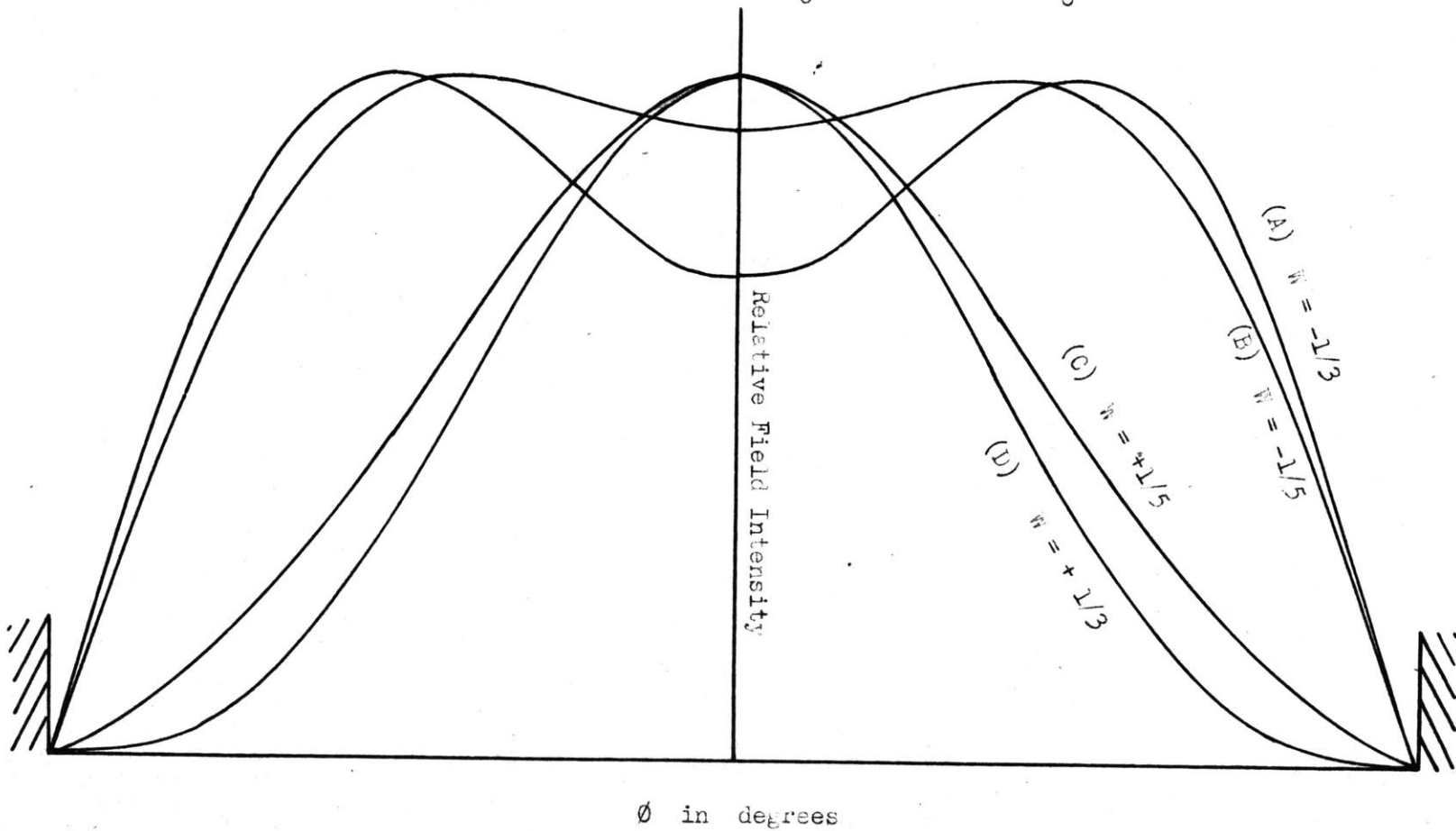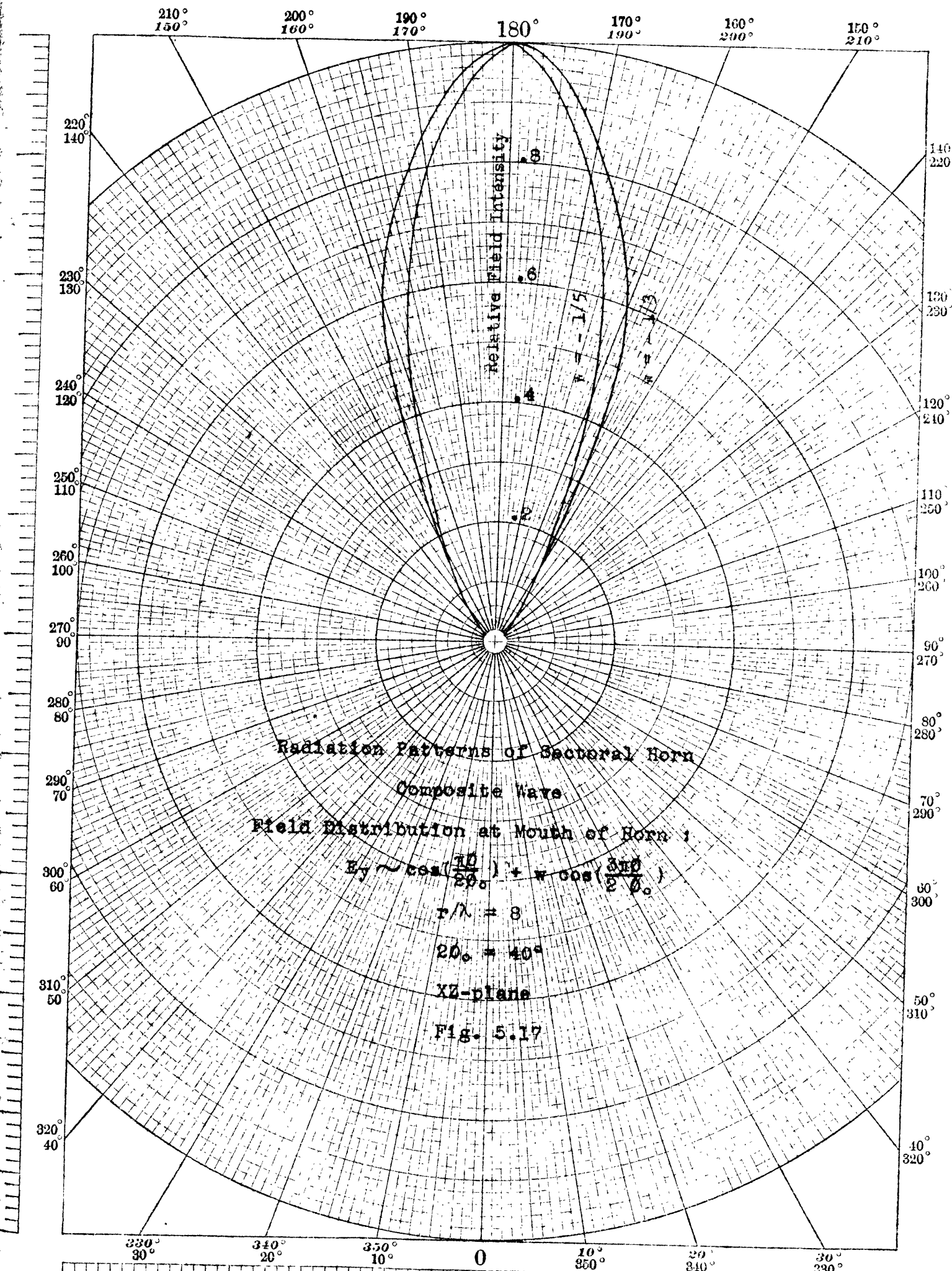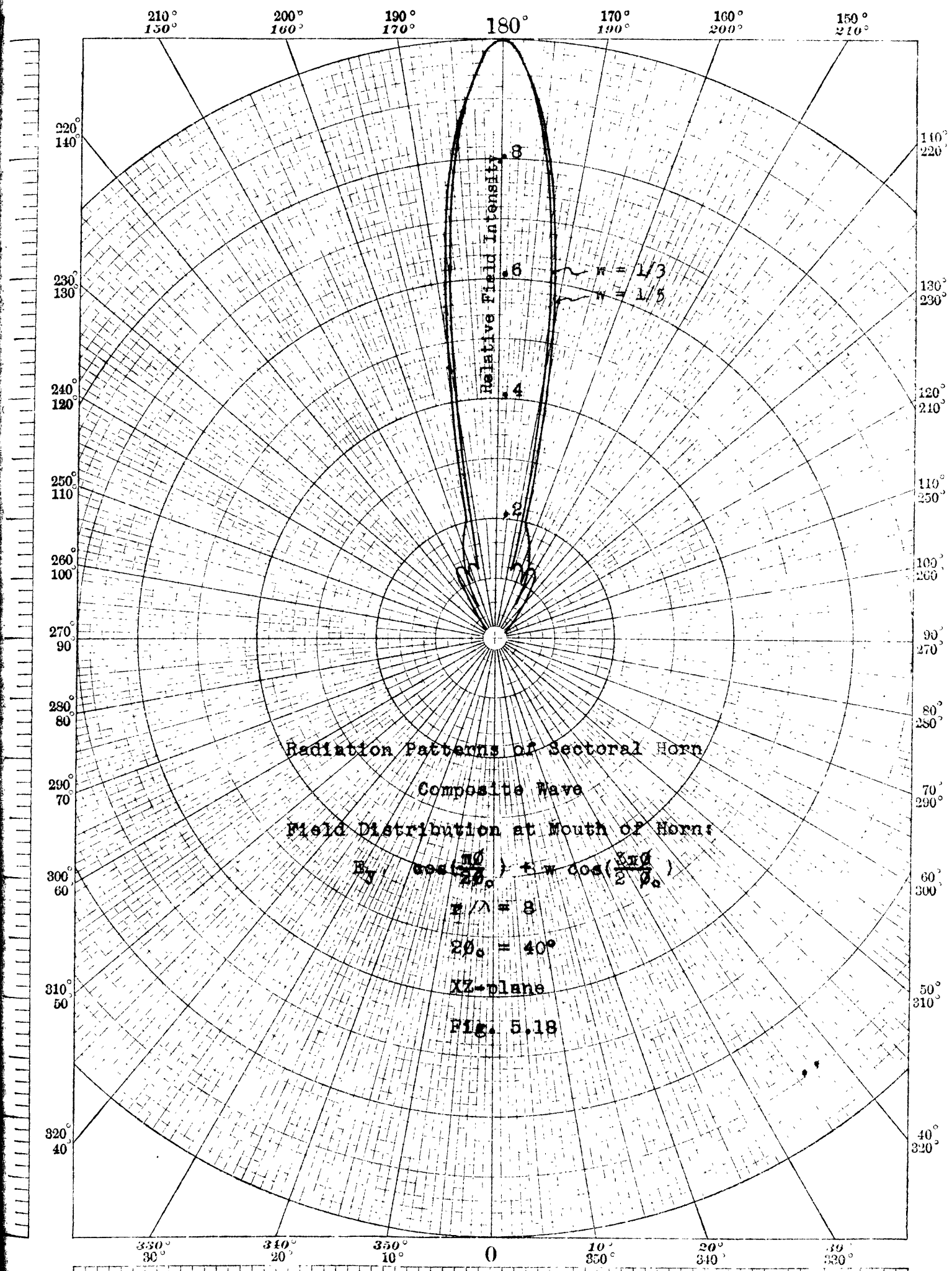
tain value and broadened again. The opening angle giving min-
imum beam angle is about $2\phi_0 = 40°$.

The broadening of the radiation pattern by either
increasing or decreasing the opening angle from its optimum
value is not surprising. We learned from the radiation prob-
lem of rectangular pipe that the sharpness of beam angle de-
pends upon the dimension "b" of the pipe. When the opening
angle of a sectoral horn is small, the two sides are almost
parallel to each other, and therefore it must behave subs-
tantially like a rectangular pipe. On the other hand, if
the opening angle of the horn is too great, it is evident that
it will lose control of the wave even inside the horn, since
there is almost no guiding action by the sides of the horn.
It may be recalled that a sectoral horn of $2\phi_0 = 180°$ is no-
thing other than a reflecting plane surface, which is ob-
viously not very effective in the problem of directional
radiation.

With the optimum value of opening angle $2\phi_0 =$
40°, another set of radiation pattern is plotted for several
horns of different radial lengths ($\frac{r_\perp}{\lambda} = 8$, 10 and 12). With-
in this range, there seems no appreciable variation in the
forms of the patterns. The beam angles are almost constant.
Such a range of $\frac{r_\perp}{\lambda}$ has practical importance. It is neither
too short to hinder the formation of horn waves within the
horn, nor too long to make its construction impracticable.

Let us see what happens if the radial length of the horn is very large. The length of the arc at the mouth of the horn is a great number of wave lengths. We may perform the integration of Eq. 5.12 in a simple approximate way known as Fresnel's zone. The process is illustrated on p.308, Slater and Frank, and it will not be repeated here. The radiation field in XZ-plane of such a horn would have the form

$$\frac{1}{\sqrt{R}} \cos\left(\frac{\pi\theta}{2\phi_o}\right) e^{i\omega\left(t - \frac{R}{c}\right)} .$$

That is, the pattern is same as that exists inside the long horn. As a matter of fact, it is none the better than a short horn of optimum beam angle.

The fumdamental wave does not exist alone inside a horn. For a horn ($2\phi_o = 40°$), it is possible to have an appreciable amount of third harmonic wave at the radiating end. Higher order of harmonics may exist but their magnitudes will be so small as to be neglected without much error.

The radiation pattern of third harmonic wave is plotted in Fig. 5.14. The horn has $\frac{r_1}{\lambda} = 8$ and $2\phi_o = 40°$. Its magnitude is so related to Fig. 5.10——radiation pattern of fundamental wave——that the two have equal amplitude of electric field intensity or vector potential at the opening of the horn. Namely,

$$\left| B_1 K_\nu\left(\frac{\omega}{c} r_1\right) \cos\nu\phi \right|_{\substack{\text{absolute} \\ \text{max. value}}} = \left| B_3 K_{3\nu}\left(\frac{\omega}{c} r_1\right) \cos 3\nu\phi \right|_{\text{a.m.v.}} .$$

It shows a central lobe with two side lobes of greater magni-

tude. The shape is quite similar to the corresponding one
for a rectangular pipe.

Since the fields and potentials are linearly
superposible, we are able to construct the composite pattern
from Fig. 5.10 and Fig. 5.14 with appropriate magnitude and
phase angle. Fig. 5.10 and Fig. 5.14 are repeated but in
Cartesian's coordinates in Fig. 5.15. Besides the magnitude,
the relative phase angles are also plotted. It is understood
that the two waves at the opening are equal in phase. The
phase difference is almost $z$ero within the first lobe of
third harmonic wave. Then it suddenly increases to approxi-
mately $180°$ at the beginning of the second lobe. This
means a change of sign of the third harmonic.

The composite radiation patterns are shown in
Fig. 5.17 and 5.18. In Fig. 5.17, the third harmonic is
taken as opposite in phase to the fundamental at the opening
of horns. The presence of third harmonic serves to broad-
en the pattern. The larger is the third harmonic, the flatter
is the pattern. The field distributions at the opening are
represented by Curves 1 and 2 of Fig. 5.16. In Fig. 5.18,
the third harmonic is taken as in phase to the fundamental
at the opening of horns. Its role is now the reverse to that
above. The larger is the third harmonic, the sharper is the
pattern. The corresponding field distribution at the open-
ing are represented by Curves 3 and 4 of Fig. 5.16. Thus,

we may conclude that a sharp field distribution at the opening of the horn produces sharp radiation pattern, and a flat one produces a broad radiation pattern.

The fundamental and the third harmonic waves do not travel at the same speed unless $\frac{r}{\lambda}$ is very large. Thus, in a real horn, we are able to adjust the phase difference by either shifting the position of the exciting system or turning the length of the horn. We may recall that the $H_{0,3}$-wave in a rectangular pipe has the same effect on the resultant radiation pattern, and the method of tuning is nearly the same.

The experimental work of sectoral horn has been carried on by Prof. W.L.Barrow and Messrs. F. M. Green[1] and F. D. Lewis at M. I. T. The sectoral horn is fed with the $H_{0,1}$-wave from a rectangular pipe. The field distributions measured inside the horn reveal the presence of high order harmonic whose magnitudes decrease with the decreasing angle of the horn. For $2\phi_0 = 20°$, only the fundamental and the third harmonic are present. The variations of the radiation pattern with the ratio $\frac{r}{\lambda}$ and $2\phi_0$, also checks with the present theoretical work. A horn of $2\phi_0 = 40°$ gives the sharpest beam angle obtained in the measurement.

_____

[1] E. E. Thesis, 1937, by Mr. F. M. Green.

Summary and Conclusions

The transmission and radiation characteristics of a sectoral horn may be summarized as follows. Only waves which are independent of the variable y and whose electric fields have an even sysmmetry about the $\phi = 0$ axis, are studied. They have a sinusoidal variation along any arc of the horn. The space inside the horn is divided into two regions:——(1) the attenuation region to the small end of the horn, where waves are highly attenuated and their phase constant is nearly zero, and (2) the transmission region to the large end of the horn, where waves are free to propagate along the radial direction. The boundary between the two regions is not definite. For a given harmonic, the attenuation region increases with decreasing horn angle ($2\phi_o$). For a given horn angle ($2\phi_o$), the range of the attenuation region is nearly proportional to the order of harmonic of the wave. Therefore, if it is desired to suppress the third and higher order harmonics, the small end of the horn must be cut off beyond the attenuation region of the fundamental and within the attenuation region of the third and higher order harmonic waves. Waves of different order of harmonics do not travel with the same speed except at a great distance away from their respective attenuation region.

The radiation patterns from the sectoral horn

depend upon the radial length and the angle of the horn, and also the order of harmonic and frequency of the wave. Consider there is only a fundamental wave inside the horn. A long horn (large $\frac{r_1}{\lambda}$) does not give the sharpest beam. A too short horn does not allow the complete transformation of wave from exciting system to horn-wave. The most suitable one is about $\frac{r_1}{\lambda} = 8$, r_1 being measured from the hypothetic line of intersection of the two side planes to the mouth of the horn. The radiation pattern does not change appreciably if the length is increased by 50%. The optimum angle of the horn, which gives the sharpest beam is about $2\phi_o = 40°$. The presence of the third harmonic wave distorts the resultant radiation pattern. Whether the resultant radiation pattern of the fundamental depends upon the phase difference of the fundamental and third harmonic waves at the mouth of the horn. A sharp resultant electric field distribution is favorable for the purpose of single beam directive radiation. Only the main center lobes of the radiation pattern of the horn waves have been studied. The side lobes, if any, are estimated to be not over 10% in magnitude.

VI. CONCLUSIONS

The results so far obtained will be briefly reviewed here.

Hollow-pipe Waves

In a pipe of rectangular cross section, the wave which is most conveniently handled is the $H_{o,1}$-wave. It has a lower critical frequency than any other type of waves in rectangular pipes. It has all the electric fields parallel to one of the walls, and consequently, the configurations of the fields are not symmetrical in the y and z directions, the two linear coordinates of the cross section. Rectangular pipes whose ratio of cross sectional dimensions a/b equals 1.18 have lower minimum attenuation than pipes of equal peripheries but different ratios of a/b. However, the attenuation of a square pipe is not very much greater than that for the optimum a/b ratio and would probably be as good for most practical purposes.

Other types of waves have higher critical frequencies, depending upon the orders of the wave and the linear dimensions of the cross-section. No wave whose attenuation decreases with increases with increasing frequency are possible in a realizable rectangular pipe. However, if the dimension "b" were to be increased indefi-

nitely, all the H-waves with finite values of n and m
would degenerate into a type of wave which possesses an
anamolous attenuation characteristic. This is made possi-
ble by reducing the effects caused by the transverse com-
ponent of magnetic field tangential to the walls of the
pipes.

We have used the resolution method to calculate
the attenuation of waves in rectangular pipe. It must be
pointed out here that such resolution is only possible in
a sufficiently long and uniform pipe, and can not be relied
upon to explain the phenomena associated with the analysis
of a non-uniform rectangular pipe like the terminal or the
joint of the pipe. For a plane wave with a small ratio of
the width of the wave (that is, the distance measured along
the wave front) to the wave length, the plane wave does
not follow a straight forward path but spreads side-wise.
The method of construction of waves in rectangular pipes
by directing a plane wave from outside into an open end of
the pipe, as illustrated by Léon Brillouin, are for an
idealized case, and are not practically realizable.

The effect of the deformation of a circular
pipe into an elliptical one depends upon the type of the
wave and the axis along which the pipe is deformed. For
waves whose fields have a circular sysmetry, both the
critical frequency and the attenuation are increased by
the deformation. For waves whose fields do not have the cir-
cular symmetry, there is no reason why a circular pipe

should be better than pipes of other eccentricities. The
eH_1-wave and the oH_1-wave are similar to the $H_{o,1}$-wave,
corresponding to the cases $a/b < 1$ and $a/b > 1$ repectively
in a rectangular pipe with sides a and b. Therefore, one
is not surprised to find that the eH_1-wave has a lower
critical frequency and the oH_1-wave has a lower attenuation
for a small value of eccentricity, than they do in a circu-
lar pipes of equal peripheries. Anologously, the eE_1-wave
has a lower attenuation than the E_1-wave in a circular pipe
of equal peripheries. For large eccentricity, the attenua-
tions of all types of waves increase and approach infinity
when the eccentricity is unity.

No waves inside a dissipative non-degenerate
elliptical pipe may have a decreasing attenuation with
increasing frequency. This is explained by the fact that
the transverse electric fields tangential to the boundary
do not vanish at the boundary.

The exact nature of the anomalous characteristic
of attenuation of the H_o-wave in circular pipe may be explain-
ed by the absorption coefficient of the metal; because,
when a light beam is directed on to a plane surface of
finite conductivity at grazing incidence the absorption
coefficient is zero when the light wave is so polarized that
the electric field is transverse to the plane of incidence.
There is no transverse magnetic field tangential to the

boundary for the H_o-wave. The deformation of a circular

pipe into a elliptical one produces a new angular magnetic

field for the eH_o-wave and the anomalous characteristic

of the attenuation disappears.

Radiation from Open End of rectanfular Pipes and Horns.

The $H_{o,1}$-wave in a rectangular pipe gives a more

effective single beam radiation pattern than all other types

of hollow-pipe waves. The beam angle of the radiation

patterns depends upon the ratio of the linear dimensions

of the cross-section of the rectangular pipe to the wave length.

Large ratios are desirable when a sharp beam is required. The

$H_{o,m}$-waves (m = odd) for m $\neq$ 1, have radiation patterns with

a small central lobe but a number of large side lobes. The

radiation patterns of other types of waves have zero fields

directly in front of the rectangular pipes.

In a non-dissipative sectoral horn, which can

be considered as a " tapered hollow pipe transmission line",

the waves are attenuated in a way similar to that in the

hollow pipes. However, the boundary between the attenuation

region and the transmission region is not definite. In

general, this boundary is farther from the hypothetical

center of the sector for higher order harmonic waves.

Hence it is possible to suppress the high order harmonic

waves for radiation purpose. Horns having an angle

$2\phi_o = 40°$ and of several wave lengths long give a very sharp beam of radiation for the fundamental wave and substantially suppress the higher order waves. A narrower horn has a too small opening and is not as effective a means for producing a single beam directive radiation. A much wider horn is not advisable since it loses control of the direction of the waves even inside the horn. The presence of the third harmonic wave may sharpen or broaden the main beams, depending upon whether the third harmonic wave is in equal or in opposite phase with the fundamental wave.

Other Problems Associated with Hollow-pipes and Horns.

Most of the theoretical work concerning the hollow-pipe system has been confined to the study of the fundamental nature of the waves in the pipe. Little has been done about the related problems of the system. The study of horns in this thesis has also been confined to one type having a special geometrical form. The following outline includes some problems of immediate importance concerning the applications of the hollow-pipe system and the electro-magnetic horns.

Terminal, joint, and branch devices:- The waves inside a hollow-pipe are subjected to distorsion and reflec-tion wherever the conditions are different from that of an infinitely long and straight pipe. Some forms of terminal

devices have been suggested to generate various types of
waves in hollow-pipes[1,2]. The joints, branches, and curved
portions of the pipes are unavoidable in practical case.
Some of the simple forms might be analytically investigated.

Resonant chamber:- A problem which has the same
physical and mathematical background, and one that has been
suggested for practical use is the hollow cavity resonator[2]
or resonant chamber[3], an elementary form of which is simply
a short section of rectangular or circular pipe closed by
a conducting sheet at both ends. The method and analysis
used in Chapter II might also be applied in this problem.

Dielectrics:- The use of dielectric of high
dielectric constant is always a temptation to those interest-
ed in hollow tube transmission. Apparently, the operating
frequency can be greatly reduced because of the decrease
of light velocity in dielectric. However, the attenuation
constant is higher for materials of large dielectric con-
stant. It is worthwhile to study the range of frequencies
within which, dielectrics may be used to advantage.

Horns:- The sectoral horns, heretofore inves-
tigated can only control the beam in one dimension. It may
be possible mathematically to treat a horn with all the four

[1]G.C.Southworth, Eng.Jour.(Canada)Vol.20,No.4.(1937)
[2]W.L.Barrow,Proc.I.R.E.Vol.24,No.1,pp 1324(1936)
[3]G.C.Southworth,Bell Sys.Tech.Jour.Vol.15,pp 300.(1936)

sides making an angle with respect to a reference axis, or a conical horn. Such horns have the possibility of radiating sharp two dimensional beams, i.e., confining the radiated energy within a small solid angle of the space.

APPENDIX

ATTENUATION OF WAVES BETWEEN PARALLEL CONDUCTING PLANES

Consider a piece of dielectric of $\sigma = 0$ extending to infinity both in x and y directions and bounded by two parallel conducting planes at $z = \pm \frac{d}{2}$ (Fig. A.1) The conductor has a large but finite conductivity and sufficient thickness that no energy from the dielectric may penetrate it. Let the waves of sinusoidal time variation travel along the X direction. The wave functions will be independent of y but will be functions of x and z; the latter comes in on account of finite thickness of dielectric in that direction.

Waves traveling in the x direction are functions of x and t in the form of $e^{i\omega t - h_g x}$; h_g being the peopogation constant in x direction. Owing to the absence of y, the Maxwell equations may be divided into two independent groups:

$$
\left.
\begin{aligned}
(\sigma + i\omega\varepsilon)\, E_y &= h_g H_z + \frac{\partial H_x}{\partial z} \\[2mm]
- i\omega\mu\, H_x &= - \frac{\partial E_y}{\partial z} \\[2mm]
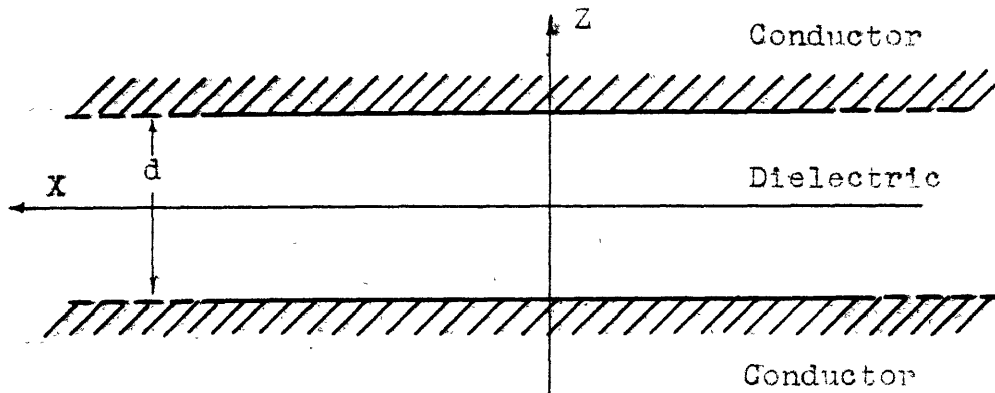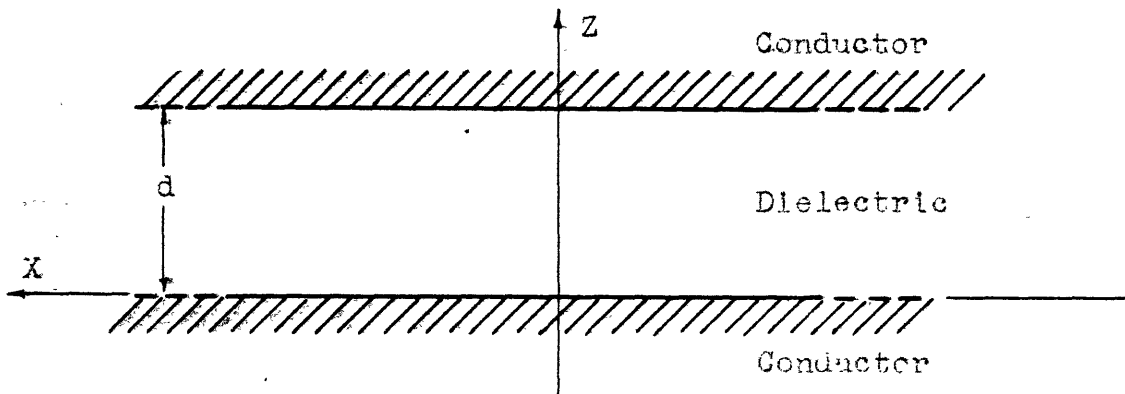- i\omega\mu\, H_z &= - h_g E_y
\end{aligned}
\right\}
\qquad A.1
$$

Fig. A-1

Fig. A-2

$$- i\omega\mu \, H_y = h_g E_z + \frac{\partial E_x}{\partial z}$$

$$(\sigma + i\omega\epsilon) \, E_x = - \frac{\partial H_y}{\partial z} \qquad\qquad\qquad \Big\}\qquad A.2$$

$$(\sigma + i\omega\epsilon) \, E_z = - h_g H_y$$

The first group involves only E_y , H_x and H_z , and the second group involves only H_y , E_x and E_z . We may define these two as the H_g -wave and the E_g -wave respectively in accordance with the definitions of the hollow-pipe waves. The subscript g is used to specify the waves between two parallel conducting planes, or parallel-plane waves. These two groups of equations are applicable in both the dielectric and the conductor. Letters without primes are used for the dielectric, while those with primes are for the conductor.

H_g -wave

By eliminating H_x and H_z from Eq. A.1 , the wave equation of E_y is

$$\frac{\partial^2 E_y}{\partial z^2} + (\kappa^2 + h_g^2) \, E_y = 0 \qquad\qquad A.3$$

where $\qquad \kappa^2 = - i\omega\mu \, (\sigma + i\omega\epsilon)$

$$\kappa^2 = \omega^2 \epsilon\mu \qquad\qquad\qquad \text{for dielectric}$$
$$\kappa^2 = - i\omega\mu'\sigma' \qquad\qquad \text{for conductor} \qquad \Big\} \quad A.4$$

The solutions in the dielectric are

$$E_y = B_g \cos(r_g z) e^{i\omega t - h_g x}$$

and

$$E_y = B_g \sin(r_g z) e^{i\omega t - h_g x} .$$

As will be shown later, in the real part of $r_g = \dfrac{m\pi}{d}$,
m is an $\wedge$odd (integer) for the first solution and even for the second
one. The wave is called an even or odd harmonic according
to the value of m.

Odd harmonics (m = odd) H_g-wave

By Eq. A.1 the three component fields in the
dielectric are:

$$E_y = B_g \cos(r_g z) e^{i\omega t - h_g x}$$

$$H_z = B_g \frac{h_g}{i\omega\mu} \cos(r_g z) e^{i\omega t - h_g x} \qquad \text{A.5}$$

$$H_x = -B_g \frac{r_g}{i\omega\mu} \sin(r_g z) e^{i\omega t - h_g x} .$$

where h_g is the propagation constant of the wave along
the X-axis. Inside the metal, since the waves are symme-
trical about the z = 0 plane, we will only consider the
upper half ($z \geqq \dfrac{d}{2}$). The field E_y' is chosen as

$$E_y' = B_g' e^{i\omega t - h_g x - r_g' z} ,$$

and from Eq. A.1

$$H_z' = \frac{h_g}{i\omega\mu'} B_g' e^{i\omega t - h_g x - r_g' z} \qquad \text{A.6}$$

$$H_x' = -\frac{r_g'}{i\omega\mu'} B_g' e^{i\omega t - h_g x - r_g' z}$$

The propagation constant h_g in the x direction must be the same in both the conductor and the dielectric if the wave travels with same velocity in the two mediums. The propagation constant in the Z-direction is denoted by r_g'. Eq. A.6 represents a wave traveling in both the x and z directions. If we substitute Eq. A.5a and A.6a into Eq. A.3, r_g and r_g' are found to be

$$r_g^2 = \omega^2 \varepsilon \mu + h_g^2 \qquad \text{A.7a}$$

$$r_g'^2 = i\omega\mu'\sigma' - h_g^2 \qquad \text{A.7b}$$

Since h_g^2 is of the order $\omega^2 \varepsilon \mu$, it is neglegible as compared to $i\omega\mu'r'$. Hence

$$r_g'^2 = i\omega\mu'\sigma' \qquad \text{A.8}$$

At the surface of the conductor of $z = \frac{d}{2}$, the tangential components of the fields in the dielectric and in the conductor are equal. Equating Eq. A.5a to Eq. A.6a and Eq. A.5c to A.6c respectively and simplifying, we have

$$B_g \cos\left(r_g \frac{d}{2}\right) = B_g' e^{-r_g' \frac{d}{2}}$$

$$\frac{r_g}{\mu} B_g \sin\left(r_g \frac{d}{2}\right) = \frac{r_g'}{\mu'} B_g' e^{-r_g' \frac{d}{2}} \qquad \text{A.9}$$

We may solve from these two equations for the values of r_g and B_g' if B_g is known. Take the quotient of the two equations:

$$\cot\left(r_g \frac{d}{2}\right) = \frac{r_g \mu'}{r_g' \mu} \qquad \text{A.10}$$

as

$$\cot\left(r_g \frac{d}{2}\right) = \tan\left(\frac{m\pi}{2} - r_g \frac{d}{2}\right)$$

$$\cong \frac{m\pi}{2} - r_g \frac{d}{2} \qquad (m = \text{positive integer})$$

for values of $r_g \frac{d}{2}$ near $\frac{m\pi}{2}$. Use this value of $\cot\left(r_g \frac{d}{2}\right)$ and solve Eq. A.10 for r_g,

$$r_g = \frac{m\pi}{d + \frac{2\mu'}{r_g' \mu}} \qquad \text{A.11}$$

The approximate value of r_g' is known (Eq. A.7b). The expression r_g may be further simplified on account of the fact that σ' is a quite large number:

$$r_g \doteq \frac{m\pi}{d} + i \frac{m\pi}{d\mu}\sqrt{\frac{2\mu'}{\omega\sigma'}} \qquad \text{A.12}$$

since

$$K^2 + h^2 - r_g^2 = 0 \qquad \text{A.7a}$$

$$h = \left\{\left[\left(\frac{m\pi}{d} + i \frac{m\pi}{d^2\mu}\sqrt{\frac{2\mu'}{\omega\sigma'}}\right)\right]^2 - \omega^2 \varepsilon\mu\right\}^{\frac{1}{2}}$$

$$\doteq i\sqrt{\omega^2\varepsilon\mu - \left(\frac{m\pi}{d}\right)^2} + \frac{\frac{m^2\pi^2}{d^3\mu}\sqrt{\frac{2\mu'}{\omega\sigma'}}}{\sqrt{\omega^2\varepsilon\mu - \left(\frac{m\pi}{d}\right)^2}}$$

The phase constant β_g and attenuation constant α_g of the wave inside the dielectric are

$$\beta_g = \sqrt{\omega^2 \varepsilon \mu - \left(\frac{m\pi}{d}\right)^2} \qquad\qquad \text{A.13a}$$

$$\alpha_g = \sqrt{\frac{2\mu'}{\omega\sigma'}} \left(\frac{m^2 \pi^2}{\beta_g d^3 \mu}\right) . \qquad\qquad \text{A.13b}$$

The above expressions are not exact enough for conductors having very low conductivity. For metals of perfect conductivity, the attenuation constant is zero.

The phase constant β_g would be imaginary if

$$\omega^2 \varepsilon \mu < \left(\frac{m\pi}{d}\right)^2 .$$

No wave can travel in the dielectric under such condition. The cut off or critical frequency f_0 is therefore

$$\frac{2\pi f_0}{c} = \frac{m\pi}{d}$$

$$f_0 = \frac{mc}{2d} . \qquad\qquad \text{A.14}$$

With this notation, α_g and β_g may be written as

$$\beta_g = \frac{2\pi f}{c} \sqrt{1 - (f_0/f)^2} \qquad\qquad \text{A.15a}$$

$$\alpha_g = \sqrt{\frac{2\pi\mu'\varepsilon c}{\sigma'\mu}} \; \frac{m^{\frac{1}{2}}}{d^{\frac{3}{2}}} \left(\frac{f_0}{f}\right)^{\frac{3}{2}} \left[1 - \left(\frac{f_0}{f}\right)^2\right]^{-\frac{1}{2}} \quad \text{A.15b}$$

By eliminating the sine and cosine in Eq.A.9, the constant β'_g may be obtained in terms of β_g.

$$B_g' \cong \pm B_g \frac{r_g}{\mu} \sqrt{\frac{\mu'}{i\omega\sigma'}} \; e^{r_g' \frac{d}{2}}$$
.

The sigh is positive or negative if m is divisible or
nondivisible by 4.

The fields in the donductor at $z \geqq \frac{d}{2}$ are

$$E_y' = \pm B_g \frac{m\pi\mu'}{d\mu\sqrt{i\omega\mu'\sigma'}} \; e^{i\omega t - h_g x - r_g'(z - \frac{d}{2})}$$

$$H_z' = \pm B_g \frac{\beta m\pi}{\omega\mu d \sqrt{i\mu'\omega\sigma'}} \; e^{i\omega t - h_g x - r_g'(z - \frac{d}{2})}$$

A.16

$$H_x' = \mp B_g \frac{r_g}{i\omega\mu} \; e^{i\omega t - h_g x - r_g'(z - \frac{d}{2})}$$
.

The loss per sq. cm. into the conductor at
the boundary is

$$\frac{1}{2} E_y' H_x' = + \frac{1}{2} |B_g|^2 \left(\frac{m\pi}{d\mu}\right)^2 \frac{1}{\omega} \sqrt{\frac{\mu'}{2\omega\sigma'}}$$
.

A.17

Even Harmonic (m = even) H_g-wave

The three component fields in the dielectric
are

$$E_y = B_g \sin(r_g z) \; e^{i\omega t - h_g x}$$

$$H_z = \frac{h_g}{i\omega\mu} B_g \sin(r_g z) \; e^{i\omega t - h_g x}$$

A.18

$$H_x = \frac{r_g}{i\omega\mu} B_g \cos(r_g z) \; e^{i\omega t - h_g x}$$
.

The fields in the metal for $z \geq \dfrac{d}{2}$ are same as Eq. A.6

The boundary conditions require

$$B_g \sin\left(r_g \frac{d}{2}\right) = B_g' \, e^{-r_g' \frac{d}{2}}$$

$$\frac{r_g}{\mu} B_g \cos\left(r_g \frac{d}{2}\right) = -\frac{r_g'}{\mu'} B_g' \, e^{-r_g' \frac{d}{2}}$$

A.18

Take the quotient

$$\tan\left(r_g \frac{d}{2}\right) = -\frac{r_g \mu'}{r_g' \mu}$$

A.19

since

$$\tan\left(r_g \frac{d}{2}\right) = \tan\left(r_g \frac{d}{2} - \frac{m\pi}{2}\right)$$

$$\cong r_g \frac{d}{2} - \frac{m\pi}{2}$$

(m = even integer)

$$r_g = \frac{m\pi}{d + \dfrac{2\mu'}{r_g' \mu}}$$

A.11a

This is the same expression as that for odd harmonic waves except that m is even integer(Eq. A.11). The expressions for the phase constant β_g, the attenuation constant and the cut-off frequency f_o are given by Eq. A.14, and Eq. A.15ab. The constant B_g' may be similarly obtained

$$B_g' = \pm B_g \, \frac{r_g}{\mu} \sqrt{\frac{\mu'}{2\omega\sigma'}} \, e^{r_g' \frac{d}{2}}$$

If m is divisible by 4 the lower sign is used and if not, the upper sign is used. The expressions for the fields in the conductor at $z \gtreqless \frac{d}{2}$ are the same as Eq. A.16, with appropriate positive or negative sign. Also the loss per sq. cm. into the metal is given by Eq. A.17 with appropriate signs.

If $m = 0$, Eq. A.19 becomes indeterminant. It means that the H_g-wave for $m = 0$, does not exist.

E_g- wave

From Eq. A.2, we have the wave equation for H_y

$$\frac{\partial^2 H_y}{\partial z^2} + (\kappa^2 + h_g^2) H_y = 0 \qquad\qquad \text{A.20}$$

The two solutions of H_y in the dielectric are

$$H_y = B_g \sin (r_g z) e^{i\omega t - h_g x}$$

$$H_y = B_g \cos (r_g z) e^{i\omega t - h_g x}$$

The former is the solution which has an odd number of half-period sinusoidal variation in the z direction (odd harmonic). The latter is the even harmonic solution.

Odd Harmonic (m = odd) E_g-wave

Here, we have, by Eq. A.2

$$H_y = B_g \quad \sin(r_g z)\, e^{i\omega t - h_g x}$$

$$E_x = -B_g \frac{r_g}{i\omega\varepsilon} \cos(r_g z)\, e^{i\omega t - h_g x} \qquad \text{A.21}$$

$$E_z = -B_g \frac{h_g}{i\omega\varepsilon} \sin(r_g z)\, e^{i\omega t - h_g x} \quad .$$

In the metal ($z \geq \frac{d}{2}$), we choose the exponential solution of the wave equation for H'_y and by Eq. A.2, we have

$$H'_y = B'_g \quad e^{i\omega t - h_g x - r'_g z}$$

$$E'_x = B'_g \frac{r'_g}{\sigma'} e^{i\omega t - h_g x - r'_g z} \qquad \text{A.22}$$

$$E'_z = -B'_g \frac{h_g}{\sigma'} e^{i\omega t - h_g x - r'_g z} \quad .$$

By substituting Eq. A.21a and A.22a into Eq. A20, we have

$$K^2 + h_g^2 - r_g^2 = 0 \qquad \text{A.23a}$$

$$K'^2 + h_g^2 + r'^2_g = 0 \quad . \qquad \text{A.23b}$$

At the boundary $z = \frac{d}{2}$, the two tangential fields are continuous. Equating H_y and E_x to H'_y to E'_x respectively, and simplifying, we have

$$B_g \sin(r_g \tfrac{d}{2}) = B'_g \quad e^{-r'_g \frac{d}{2}}$$

$$-B_g \frac{r_g}{i\omega\varepsilon} \cos(r_g \tfrac{d}{2}) = B'_g \frac{r'_g}{\sigma'} e^{-r'_g \frac{d}{2}} \qquad \text{A.24}$$

Take the quotient of the two equations

$$\cot(r_g \tfrac{d}{2}) = -\frac{r'_g \, i\omega\varepsilon}{r_g \, \sigma'} \quad . \qquad \text{A.25}$$

The real part of $r_g \frac{d}{2}$ is approximately $\frac{m\pi}{2}$, where m = odd integer.

$$\cot\left(r_g \frac{d}{2}\right) = \tan\left(\frac{m\pi}{2} - r_g \frac{d}{2}\right) \cong \frac{m\pi}{2} - r_g \frac{d}{2}.$$

With the approximate value of $r_g' = \sqrt{i\omega\mu'\sigma'}$ (from Eq. A.23b), Eq. A.25 becomes

$$r_g^2 - \frac{m\pi}{d} r_g + \frac{2}{d}\sqrt{\frac{\omega\mu'}{i\sigma'}} \, \omega\epsilon = 0 \quad ; \qquad \text{A.26b}$$

solving for r_g ,

$$r_g = \frac{m\pi}{2d} + \frac{1}{2}\sqrt{\left(\frac{m\pi}{d}\right)^2 - 8\sqrt{\frac{\omega\mu'}{i\sigma'}}\,\frac{\omega\epsilon}{d}} \qquad \text{A.26b}$$

This may be simplified by applying the Binomial Theorem to the square root and neglecting the high order terms of $\frac{1}{\sqrt{\sigma'}}$.

$$r_g = \frac{m\pi}{d} + i\frac{\omega\epsilon}{m\pi}\sqrt{\frac{2\omega\mu'}{\sigma'}} \,, \qquad \sigma^{-1} \qquad \text{A.27}$$

since $\quad K^2 + h_g^2 - r_g^2 = 0 \quad$ and $\quad h_g = \alpha_g + i\beta_g,$

$$\omega^2\epsilon\mu - \left[\frac{m\pi}{d} + \frac{i\omega\epsilon}{m\pi}\sqrt{\frac{2\omega\mu'}{\sigma'}}\right]^2 = -\left[\alpha_g + i\beta_g\right]^2.$$

Equate the real and imaginary parts respectively, we have

$$\beta_g = \sqrt{\omega^2\epsilon\mu - \left(\frac{m\pi}{d}\right)^2} \qquad \text{A.28a}$$

$$\alpha_g = \frac{\omega\epsilon}{d}\sqrt{\frac{\omega\mu'}{2\sigma'}}\left[\omega^2\epsilon\mu - \frac{m\pi}{d}\right]^{-\frac{1}{2}} \qquad \text{A.28b}$$

By setting the phase constant equal to zero, the cut off frequency is found to be

$$f_o = \frac{mc}{2d} \; .$$
<div align="right">A.29</div>

With this notation, the phase and attenuation constants may be weitten as

$$\beta_g = \frac{2\pi f}{c} \sqrt{1 - (\frac{f_o}{f})^2}$$
<div align="right">A.30a</div>

$$\alpha_g = \sqrt{\frac{\pi \mu' \varepsilon c}{2\sigma'\mu}} \; \frac{m^{\frac{1}{2}}}{d^{3/2}} (\frac{f}{f_o})^{\frac{1}{2}} [1 - (\frac{f_o}{f})^2]^{-\frac{1}{2}} \; .$$
<div align="right">A.30b</div>

By elimination the sine and cosine in Eq. A. 24 , the constant B'_g may be obtained in terms of B_g

$$B'_g \cong \pm B_g \; e^{r'_g \frac{d}{2}} \; .$$

The upper sign is used for m = 1 , 5 , 9 ,......, and the lower for m = 3, 7 , 11 , ... The fields in the metal (z $\frac{d}{2}$) are therefore

$$H'_y = \pm B_g \; e^{i\omega t - h_g x - r'_g (z - \frac{d}{2})}$$

$$E'_x = \pm B_g \; \frac{r'_g}{\sigma'} e^{i\omega t - h_g x - r'_g (z - \frac{d}{2})}$$

$$E'_z = \mp B_g \; \frac{h_g}{\sigma'} e^{i\omega t - h_g x - r'_g (z - \frac{d}{2})} \; ;$$

where
$$r'_g = \sqrt{i \omega \mu' \sigma'}$$

The power loss into per sq. cm. of the metal is:

$$\frac{1}{2} E'_x H'_y = \frac{1}{2} (B_g)^2 \sqrt{\frac{\omega \mu'}{2\sigma'}} \; .$$

Even Harmonic (m = even) E_g-wave

In the diàlectric the solution for the fields are:

$$H_y = B_g \quad \cos(r_g z) e^{i\omega t - h_g x}$$

$$E_x = B_g \frac{r_g}{i\omega\varepsilon} \sin(r_g z) e^{i\omega t - h_g x} \qquad \cdot \text{ A.33}$$

$$E_z = -B_g \frac{h_g}{i\omega\varepsilon} \cos(r_g z) e^{i\omega t - h_g x} .$$

The field expressions in the metal are the same as those for odd harmonic waves. (Eq. A.22) At the boundary, the tangential components of fields are equal, and so we have

$$B_g \cos(r_g \frac{d}{2}) = B_g' \quad e^{-r_g' \frac{d}{2}}$$

$$\text{A.34}$$

$$B_g \frac{r_g}{i\omega\varepsilon} \sin(r_g \frac{d}{2}) = B_g' \frac{r_g'}{\sigma'} e^{-r_g' \frac{d}{2}} .$$

By eliminating B_g and B_g' , we have

$$\tan(r_g \frac{d}{2}) = \frac{i\omega\varepsilon r_g'}{\sigma' r_g} \qquad \text{A.35a}$$

The real part of $r_g \frac{d}{2}$ is around $\frac{m\pi}{2}$ when m = even integer so

$$\tan(r_g \frac{d}{2}) = \tan(r_g \frac{d}{2} - \frac{m\pi}{2}) \cong r_g \frac{d}{2} - \frac{m\pi}{2} ,$$

With the approximate value of r_g' , Eq. A.35 becomes

$$r_g'^2 - \frac{m\pi}{d} r_g + \frac{2}{d} \omega\varepsilon \sqrt{\frac{\omega\mu'}{i\sigma'}} = 0 , \qquad \text{A.35b}$$

This is the same as Eq. A. 26a . Hence the results for odd harmonic Eg waves also apply for the even harmonic E_g-waves.

The constant B_g' may be solved in terms of B_g

$$B_g' = \mp B_g \, e^{r_g \frac{d}{2}}$$
.

The upper sign is for m = 2 , 6 , 10 , ... and the lower sign is for m = 4 , 8 , ... The expressions for the fields in the conductor ($z \geqq \frac{d}{2}$) and the power loss into the conductor per unit area are the same as Eq. A.31 and A.32.

For m = 0 , Eq. A.35b becomes

$$r_g^2 = - \frac{2\omega\varepsilon}{d} \sqrt{\frac{\omega\mu'}{i\sigma'}}$$

$$h_g = i \sqrt{\omega^2 \varepsilon\mu - r_g^2}$$

$$= i \sqrt{\omega^2 \varepsilon\mu + \frac{2\omega\varepsilon}{d}\sqrt{\frac{\omega\mu'}{i\sigma'}}}$$

$$\cong i \left\{ \frac{\omega}{c} + \frac{1}{d}\sqrt{\frac{\omega\mu'\varepsilon}{2\sigma'\mu}} \right\} + \frac{1}{d}\sqrt{\frac{\omega\mu'\varepsilon}{2\sigma'\mu}}$$

$$= \alpha_g + i\beta_g$$
.

Hence

$$\beta_g \doteq \frac{\omega}{c}$$

$$\alpha_g = \frac{1}{d}\sqrt{\frac{\omega\mu'\varepsilon}{2\sigma'\mu}} = \frac{1}{d}\sqrt{\frac{\pi\mu'\varepsilon}{\sigma'\mu}}\sqrt{f}$$
.

Both β_g and α_g may be derived from Eq. A.30. The expression for power loss also applies to the m = 0 case.

For the H_g- or E_g-wave, the expressions for thr losses and attenuation constants are identical. As judged from the value of h_g and Υ_g for both waves, the field distributions inside a dissipative pipe do not differ appreciably from the non-dissipative case unless the conductivity of the conductor is too small. By setting the conductivity equal to infinity, and shifting the center plane of the system to the $z = 0$ plane, the field expressions in the diälectric Eq. A.5, A.18, A.21 and A.33 may be simplified : (Refer to Fig A.2)

H_g-wave, $m = 1$, 2 , $\ldots$ nondissipative case

$$E_y = B_g \, \sin \left(\frac{m\pi}{d} z \right) e^{i(\omega t - \beta_j x)}$$

$$H_x = B_g \frac{m\pi}{i\omega\mu d} \cos \left(\frac{m\pi}{d} z \right) e^{i(\omega t - \beta x)} \qquad\qquad A.36$$

$$H_z = B_g \frac{\beta_g}{\omega\mu} \sin \left(\frac{m\pi}{d} z \right) e^{i(\omega t - \beta x)} .$$

E_g-wave, $m = 0$, 1 , 2 ,$\ldots$nondissipative case

$$H_y = B_g \, \cos \left(\frac{m\pi}{d} z \right) e^{i(\omega t - \beta x)}$$

$$E_x = B_g \frac{m\pi}{i\omega\varepsilon d} \sin \left(\frac{m\pi}{d} z \right) e^{i(\omega t - \beta_j x)} \qquad\qquad A.37$$

$$E_z = -B_g \frac{\beta_g}{\omega\varepsilon} \cos \left(\frac{m\pi}{d} z \right) e^{i(\omega t - \beta_j x)} .$$

Waves between parallel conducting planes are of a very simple types and their attenuation constants may be calculated directly from boundary conditions.

Other method available are rather synthetic. The results obtained here are simple examples of the general attenuation characteristics of guided waves. We note that at sufficiently short wave lengths the H_g-wave has an attenuation constant proportional to the three-half power of the operating wave length, while the E_g-wave has attenuation constant inversely proportional to the square root of operating wave length. That is to say, when the operating wave length is nearly zero, the attenuation of H_g-wave is zero and that of E_g-wave approaches infinity. We may recall that in a circular pipe, the H -wave has an attenuation characteristic simialr to that of the H_g-wave.

Summary

Summarize the results for parallel-plane waves:

H_g-wave

Fields in the dielectric (Fig. A.2)

$$E_y = B_g \quad \sin\left(\frac{m\pi}{d} z\right) e^{i\omega t - i\beta_g x}$$

$$H_x = B_g \frac{m\pi}{i\omega\mu d} \cos\left(\frac{m\pi}{d} z\right) e^{i\omega t - i\beta_g x} \tag{A.36}$$

$$H_z = B_g \frac{\beta_g}{\omega\mu} \sin\left(\frac{m\pi}{d} z\right) e^{i\omega t - i\beta_g x}$$

$$m = 1 , 2 , 3 , \ldots\ldots$$

The critical frequency

$$f_o = \frac{mc}{2d} \tag{A.14}$$

Phase constant

$$\beta = \frac{2\pi f}{c} \sqrt{1 - (\frac{f_0}{f})^2} .$$

A.15a

Attentuation constant

$$\alpha = \sqrt{\frac{2\pi\mu'\xi c}{\sigma'\mu}} \frac{\sqrt{m}}{d^{3/2}} (\frac{f_0}{f})^{3/2} [1 - (\frac{f_0}{f})^2]^{-\frac{1}{2}}$$

A.15b

The power loss per sq. cm. into the conductor at the boundary

$$= \frac{1}{2} |B_3|^2 (\frac{m\pi}{d\mu})^2 \frac{1}{\omega} \sqrt{\frac{\mu'}{2\omega\sigma'}} ,$$

A.17

E_g-wave

Fields in the dielectric (Fig. A.2)

$$H_y = B_3 \cos(\frac{m\pi}{d} z) e^{i\omega t - i\beta_3 x}$$

$$E_x = B_3 \frac{m\pi}{i\omega\xi d} \sin(\frac{m\pi}{d} z) e^{i\omega t - i\beta_3 x}$$

A.37

$$E_z = -B_3 \frac{\beta_3}{\omega\xi} \cos(\frac{m\pi}{d} z) e^{i\omega t - i\beta_3 x}$$

$$m = 0, 1, 2, 3, \ldots .$$

The critical frequency,

$$f_0 = \frac{mc}{2d} .$$

A.29

The phase constant,

$$\beta_3 = \frac{2\pi f}{c} \sqrt{1 - (\frac{f_0}{f})^2} .$$

A.30a

The attenuation constant

$$\alpha = \sqrt{\frac{\pi \mu' \xi \epsilon}{2 \sigma' \mu}} \; \frac{\sqrt{m}}{d^{3/2}} \; \left(\frac{f}{f_0}\right)^{\frac{1}{2}} \left[1 - \left(\frac{f_0}{f}\right)^{2} \right]^{-\frac{1}{2}} \qquad\qquad A.30b$$

The power loss per sq. cm. into the conductor at the boundary

$$= \frac{1}{2} \left| B_g \right|^{2} \sqrt{\frac{\omega \mu'}{2 \sigma'}} \; . \qquad\qquad A.32$$

BIBLIOGRAPHY

References on Hollow-pipe Waves:

Lord Rayleigh: "Scientific Papers" Vol. IV
    pp. 227-280. (1897)
R. C. Maclaurin, Cambridge Philosophical
    Transactions. Vol. XVII Part I. pp. 5-
    100. (1898)
D. Hondros and P. Debye, Ann. d. Phys. Vol.
    32, pp. 465 - 476. (1910)
S. A. Schelkunoff, Bell Sys. Tech. Jour.
    Vol. 13, pp. 533. (1934)
W. L. Barrow, Proc. I. R. E. Vol. 24, No. 10,
    pp. 1298 - 1328. (1936)
G. C. Southworth, Bell Sys. Tech. Jour. Vol.
    15, pp. 284 - 309. (1936)
J. R. Carson, S. P. Mead and S. A. Schelkunoff,
    Bell Sys. Tech. Jour. Vol. 15, pp. 310 -
    333. (1936)
Leon Brillouin, Revue Generale de E'lectricite,
    Vol. XL, pp. 227- 239. (1936)
L. Page and N. I. Adams Jr., Phy. Rev. Vol. 52,
    pp. 647 - 651. (1937)
S. A. Schelkunoff, Proc. I. R. E. Vol. 25,
    pp. 1457 - 1493. (1937)
G. C. Southworth, Eng. Jour. (Canada), Vol.
    20, No. 4 (1937)
W. L. Barrow and L. J. Chu, "Electromagnetic
    Waves in Hollow Metal Tubes of Rectangular
    Section ", paper submitted to the Institute
    of Radio Engineers for consideration for
    publication in their Journal.

References on Radiation:

K. Försterling, Lehrbuch der Optik. (1928)
J. C. Slater and N. H. Frank, "An Introduction
    to Theoretical Physics"
Bergmann and Kruegel, Ann. d. Phys. Vol. 21
    pp. 113 - 138. (1934)
S. A. Schelkunoff, Bell Sys. Tech. Jour.
    Vol. 15, pp. 92 - 112. (1936)
F. M. Green, E. E. Thesis, M. I. T. (1937)

Mathematical Reference:

    P. Frank and R. Mises, die Differentials
       und Integral-gleichungen, pp. 876
       (1935)

    G. N. Watson, A Treatise of the Theory of Bes-
       sel Functions.

    E. Jahnke and F. Emde, Tables of Functions.

    G. N. Watson and E. T. Whittaker, A Course of
       Modern Analysis, (1927).

    S. Goldstein, Trans, Camb. Phil. Soc. Vol. 23
       No. 11 (1927)

    J. A. Stratton, Proc. of the National Academy
       of Sciences, Vol. 21, No. 1,pp.51-62,
       and No. 6, pp. 316-321, (1935).

    P. M. Morse, Tables of Mathieu Functions,
       (manuscripts)

    N. W. McLachlan, Bessel Function for Engineers.
       (1934)

BIOGRAPHICAL SKETCH

Born at Hwei-ying, Kiangsu, China, on August
24, 1913. Admitted to Chiao-tung University,
Shanghai in 1930. Awarded the degree of
Bachelor of Science in Electrical Engineering,
July, 1934. Admitted to the Graduate School
of Massachusetts Institute of Technology in
September, 1934. Awarded the degree of
Master of Science in Electrical Engineering,
June, 1935. Associate Member of the Society
of Sigma Xi, April, 1936.